T. Putnam

LA-3253-MS

C.3

LOS ALAMOS SCIENTIFIC LABORATORY

OF THE UNIVERSITY OF CALIFORNIA o LOS ALAMOS NEW MEXICO

REVIEW OF CONTROLLED THERMONUCLEAR RESEARCH AT LOS ALAMOS 1965

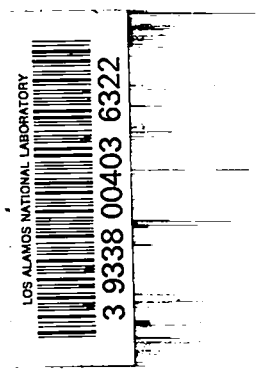

LEGAL NOTICE

LA-3253-MS
CONTROLLED THERMONUCLEAR
PROCESSES
Special Distribution

LOS ALAMOS SCIENTIFIC LABORATORY
OF THE UNIVERSITY OF CALIFORNIA LOS ALAMOS NEW MEXICO

REPORT WRITTEN: March 3, 1965

REPORT DISTRIBUTED: March 5, 1965

REVIEW OF CONTROLLED THERMONUCLEAR RESEARCH AT LOS ALAMOS 1965

Contract W-7405-ENG. 36 with the U. S. Atomic Energy Commission

CONTENTS

A REVIEW OF LOS ALAMOS FUSION RESEARCH*

J. L. Tuck

* Work performed under the auspices of the U. S. Atomic Energy Commission

CONTENTS

In this review, I present a case for pulsed high density high β plasmas as one route to power producing thermonuclear reactions. The testimony given before the JCAE in March, 1964 on Los Alamos Sherwood activity, is given in part as an appendix.

The review starts with a recapitulation of the characteristics of a power producing thermonuclear reaction. These are well known but lost sight of from time to time. We then discuss obstacles to the achievement of a power producing thermonuclear reaction - the immediate obstacle being of course instabilities of many types, hydromagnetic, electrostatic, micro , universal, (and many more yet to be discovered) which limit the duration of plasma confinement. Lying in wait beyond the instability obstacle, there are other obstacles not yet encountered in full strength, e.g. magnetic radiation, radiation damage to material of the reactor, plasma contamination, etc. These later obstacles are probably very real - but not so completely dominating to the design as the first one.

Briefly, my case for pulsed dense plasma is statistical:

(1) A confined plasma has a vast spectrum of instabilities, not all of which will be eliminable. By striving for reactors with the shortest possible plasma duration, τ, one decreases the chance of being struck down by an instability.

(2) The one process <u>contributing</u> to a thermonuclear reactor is binary, and consequently increasing with the square of the density, while of the several processes <u>subtracting</u>, some are binary, some not. Hence increasing the density tends to maximize the ratio gain/loss.

I try to identify two likely breakthrough points in the τ (or n) spectrum, one with a τ as short as the strength of materials will reasonably allow (about 1 - 20 msec), and another, which by-passes the strength of materials difficulty altogether by using a z-pinch, but which <u>may</u> have to live with the fast hydromagnetic kink instability and so be forced to very short times (0.1 - 10 μsec) and therefore heroic extremes of pulse power.

Reviewing next the thermonuclear plasma achievements at Los Alamos, we have achieved:

(1) The first controlled thermonuclear reaction.

(2) The strongest thermonuclear reaction, i.e., having the nearest approaches to reactor $n\tau s$, 2×10^{11} ion cm^{-3} sec in the world. In an unconfirmed thermonuclear reaction, we have an even larger $n\tau$ of 2×10^{12}.

These achievements are acknowledged abroad. So it seems that the pulsed dense plasma philosophy has justified itself.

We have never (until the last year) been impeded by lack of funds; our budget, which has consumed no more than one-tenth of the AEC CTR total, being usually underspent.

Looking ahead, a number of attractive avenues of research are opening up; by an advance down the main avenue - achievement of an $n\tau$ with one-tenth of that for a reactor looks feasible. But the next advance cannot be done so cheaply. We shall have nearly to double in size and expenditure to make good use of the position we are now in.

REACTOR PLASMA PROPERTIES

The Ideal Ignition Temperature is the first central quantity one encounters in describing a power producing thermonuclear reaction. First put forward by Fermi in his lectures on Thermonuclear Reactions in Los Alamos in 1944 - the concept is that the thermonuclear energy production rate must exceed the bremsstrahlung loss rate. Since both are binary processes, the Ideal Ignition Temperature is independent of density. Complications follow when one decomposes the thermonuclear energy into locally deposited (charged particle) and remotely deposited (neutron). Clearly for a reactor we had better be far above the Ideal Ignition Temperature which is 40 keV for DD, 5 keV for DT.

The Lawson criterion comes from the basic requirement that the net thermonuclear energy yield of a plasma, must at least repay the energy cost of preparing and maintaining the plasma. The criterion turns out

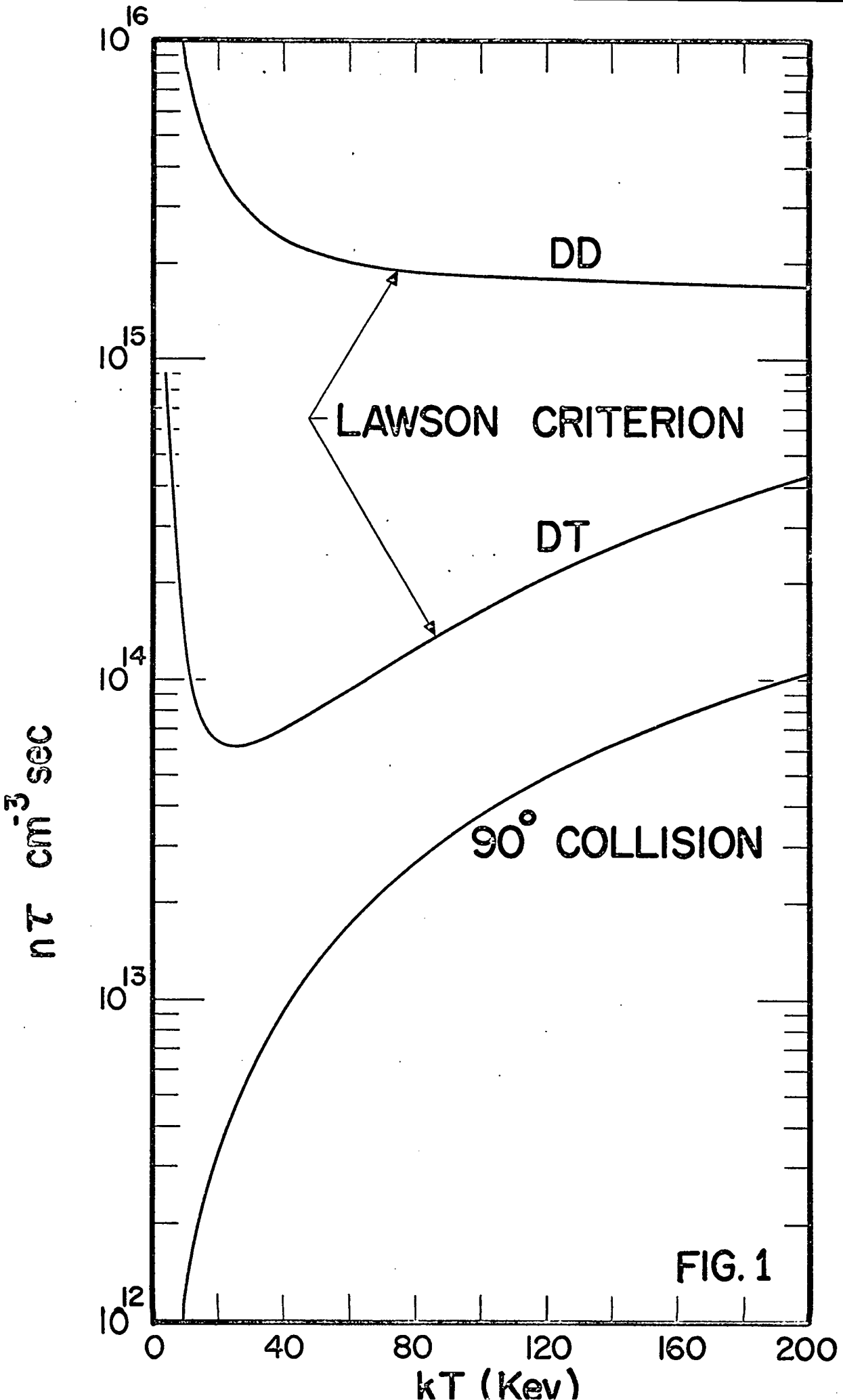
10^{16}
10^{15}
10^{14}
10^{13}
10^{12}
$n\tau$ cm^{-3} sec
DD
LAWSON CRITERION
DT
90° COLLISION
0
40
80
120
160
200
kT (Kev)

FIG. 1

to be the product $n\tau$, density $\times$ time.

This is derived by equating the total energy recoverable from a plasma, which has been burning thermonuclearly for a time τ, via a heat engine of efficiency ϵ, with the energy it took to create the plasma. We have

$$\epsilon \left[3\,nkT + \tfrac{1}{4} n^2 \langle \sigma v \rangle Q\, \tau + \text{magnetic rad.} \times \tau + \text{bremsstrahlung} \times \tau + \text{any other losses} \right]$$

$$= (3\,nkT + \text{magnetic rad.} \times \tau + \text{bremsstrahlung} \times \tau + \text{other loss.}$$

Leaving aside magnetic radiation and other losses and assuming that $T \gg IIT$ so that bremsstrahlung can be neglected, this simplifies to

$$n\tau = \frac{(1 - \epsilon)\ 12\ nkT}{\epsilon Q \langle \sigma v \rangle}$$

using $\epsilon = 1/3$, we get the values given in Fig. 1. We see a minimum for DT at about $n\tau = 6.10^{13}$ ion cm^{-3} sec, T = 24 keV and much higher values for DD, $n\tau > 10^{15}$, T = 60 - 100 keV.

Now clearly this is not a firm value - we have left out many factors, and it may be very hard to get an ϵ of 1/3 in real life with neutron heating of superconductors, etc., e.g. in the worked out example of a power producing reactor given below by Ribe, the $n\tau$ breakeven point turns out to be nearly 10 times higher than Lawson's in one case, and equal to it in another. But the Lawson criterion lies squarely athwart the path to a reactor and nobody will get there without doing at least as well as this. So it is a valid lower limit and a point to strive for. Once this point is settled, we are at liberty to look at the properties of the thermonuclear plasmas it prescribes.

At any given temperature, the number of collisions is a function of $n\tau$. So we can compute the number of ion-ion collisions and DT reacting collisions that occur in a Lawson criterion plasma as a function of T. The curve labeled 90^o collisions (Fig. 1) gives the $n\tau$ for a 90^o ion deflection, including distant small interactions. The ratio of the ordinates of the curves, gives the number of ion-ion 90^o deflections per

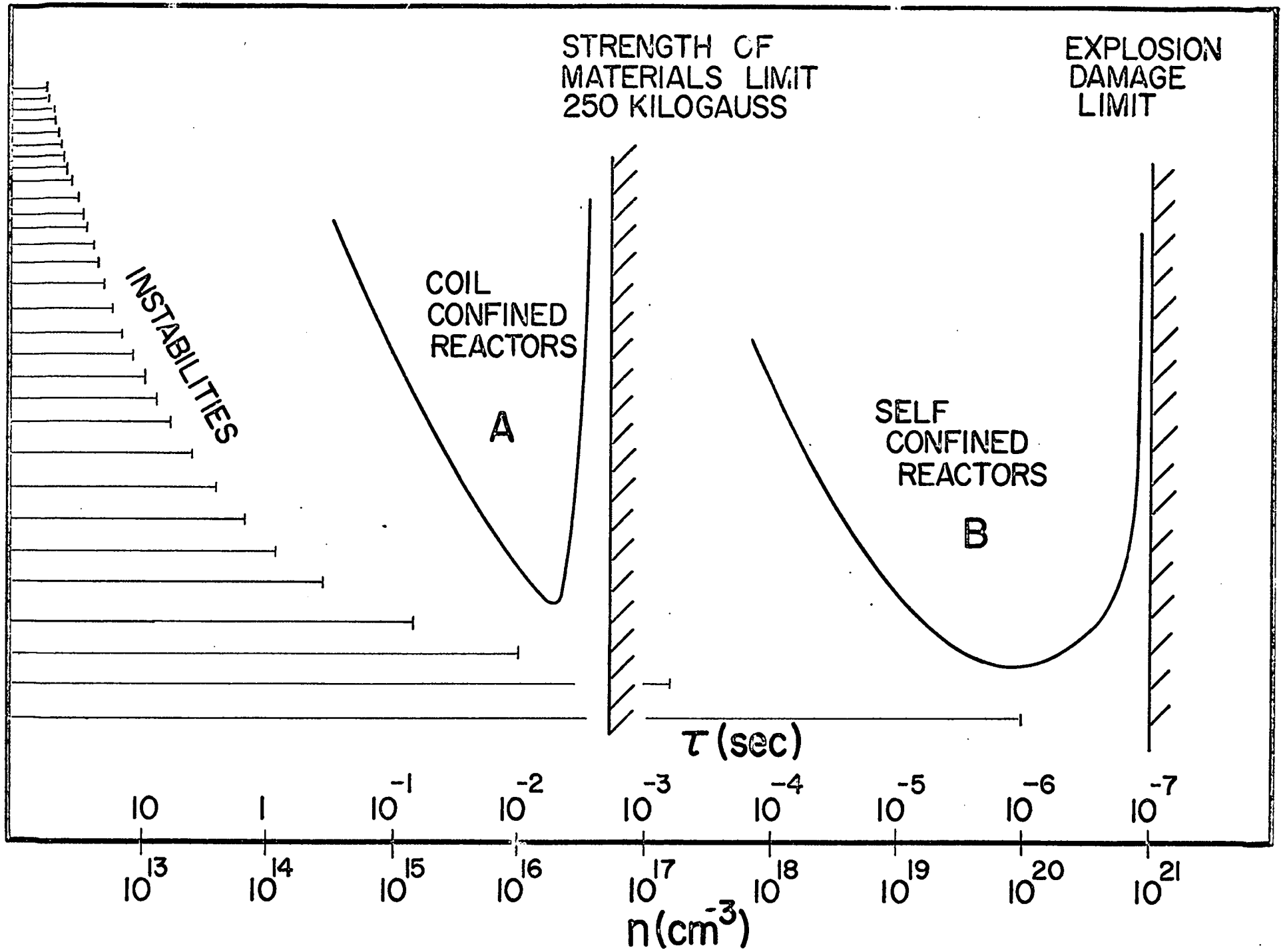
STRENGTH OF
MATERIALS LIMIT
250 KILOGAUSS
EXPLOSION
DAMAGE
LIMIT
INSTABILITIES
COIL
CONFINED
REACTORS
A
SELF
CONFINED
REACTORS
B
τ (sec)
10
1
10^-1
10^-2
10^-3
10^-4
10^-5
10^-6
10^-7
10^13
10^14
10^15
10^16
10^17
10^18
10^19
10^20
10^21
n(cm^-3)

FIG. 2

lifetime as a function of temperature. We see the average ion makes twelve 90^9 deflections in its lifetime at the optimum 24 keV temperature in DT and four at 200 keV. So such plasmas must spend most of their time randomized in velocity and direction and must be without orderly bundles of orbits. For DD, the number of collisions is an order of magnitude higher. These collision numbers are instructive in another sense; they show how scattering dominates over reactions.

Since n and τ are reciprocally related, it is interesting to examine the τ at which the confining pressure $p = B^2/8\pi$ becomes too high to be supported statically by the strength of materials. There is no absolute mathematical limit on this, (autofrettage, etc.,) but practically one encounters logarithmically increasing engineering difficulty, once the extrusion pressure of stiff solids is approached. So a reasonable upper limit of p is about 100,000 psi which turns out to be equivalent to $n = 10^{17}$ ion/cm^3 $\tau = 10^{-3}$ sec (Fig. 2). So τ less than this must be ruled out for reactors in which the magnetic confining field of the plasma tends to burst the coils of the machine. Not all systems do: Force free coils experience only volume compression forces; self-pinched plasma (z-pinches) hardly press on the walls at all. These exceptions provide ways of circumventing the strength of material limit we shall discuss later.

The region far to the long-time (lefthand side) of the τ diagram is greatly to be preferred both from the engineering point of view of working pressures, and also from that of having a smoother flow of power. Thus a steady state plasma maintained by particles fed in and bled out with sojourn time τ would be ideal. This region has been the target for most of the AEC supported CTR laboratories - to the extent that it has absorbed 3/4 to 9/10 of the expenditures to date. And it is at this point that we at Los Alamos diverge from them.

In order to explain why we prefer the difficult regions marked A and B in Fig. 2, we first glance at the final state of a plasma confinement system. A static magnetic bottle with plasma relaxes to a uniform plasma resting on and in temperature equilibrium with a wall,

with the magnetic field at its vacuum value. This is the state of maximum entropy, and minimum free energy. In parenthesis, the plasma need not rest on a wall if it experiences force describable by a potential e.g. electric or gravitational fields - so that, surprisingly enough a z-pinch could exist permanently in vacuo, in presence of diffusion, (instabilities permitting).[1]

Thus in general, a magnetically confined plasma is not in equilibrium; furthermore it is an exceedingly complex system with of order n^2 modes by which it may relax. A catalogue of already classified types of waves in it would fill several pages. We can gain some sense of what will happen in the future on this problem by looking at the past history of controlled fusion research.

At first, theory was of the simplest, i.e., infinite conductivity hydromagnetics. Nevertheless, naively, rather large laboratories and projects were founded on it - which have swallowed a large fraction of the total funds, and continue to do so. The measures to inhibit hydromagnetic instability, such as magnetic shear, incorporated in magnetic bottles of those days were easily evaded by real plasma which executes maneuvers prohibited by infinite conductivity hydromagnetics. The addition of finite conductivity to the theory was able to account i.e., by tearing, buckling, modes, for the new effects. It then became clear that even with finite plasma conductivity, hydromagnetic stability could still be got by going back to the first principles, cf Rosenbluth and Longmire[2] (1957) in the form of bottles with magnetic walls <u>everywhere</u> convex to the plasma. Topologically, this forces one to open-ended systems, and at first approach, to systems with magnetic field zeros (cusped geometries, picket fences). Fig. 3. These are far from out of the running these days - but the nonadiabaticity of field zeros is hard to work with and these systems find fusion reactor application solely in the pulsed high density region. More refined application and rereading of the literature revealed geometries with everywhere convex curvatures which, while still open-ended have no zeros. These are the currently highly topical nonzero absolute

EVOLUTION OF FLUTE STABLE SYSTEMS

FIG. 3

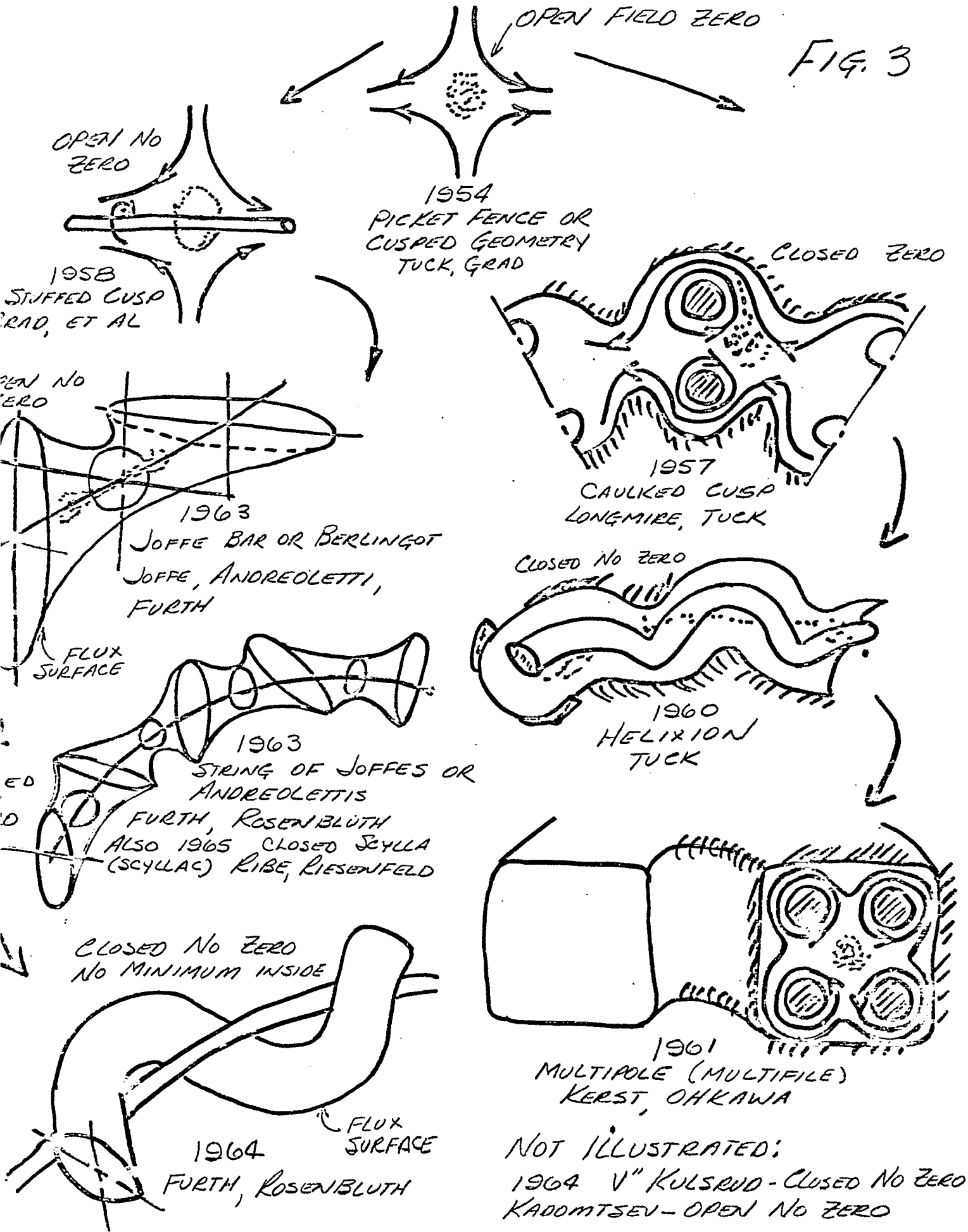

NOT ILLUSTRATED:

1964 V" KULSRUD - CLOSED NO ZERO

KADOMTSEV - OPEN NO ZERO

minimum bottles (magnetic dimples, wells, hybrid traps, minimum B). So these systems can be both adiabatic and flute stable. Experimentally in some cases, a large ~ 100 - 1000 fold increase in confinement time results from their use (Joffe) but only to bring to light (this result is not confirmed) another slower instability.

The next improvement (still mentioned in the original Rosenbluth-Longmire paper of 1957, is the possibility of closing off the open ends of flute stable convex-walled bottles, by very strong concave fields. Since the criterion for amount of instability is $\delta \int \frac{dl}{B}$ (or V'') for a particle sampling all regions on a closed line round the system, which have B in the denominator, it should be possible to more than compensate the flute inducing drift in the unstable strong B concave part by the stabilizing drift in the stable lower B one. Actually the first such system was the caulked cusp, proposed by the writer and Longmire in 1957 and this idea has now become highly topical with Helixions, Multipoles, toroidal strings of Andreoletti systems (Furth and Rosenbluth, negative V'' machines and several more shown in Fig. 3. They should be greatly superior to open low β systems since they have no mirror losses. The sampling procedure introduces a risk, however, so that the merit of closed flute stable systems will be related to the closeness of intercommunications of the good and bad regions. This is the reason for preferring the caulked cusp to the helixion at Los Alamos.

It seems that there are several measures that can be taken against hydromagnetic instability - in addition to shaping the magnetic field. Experimentally and as predicted theoretically, finite Larmor radius (high ion temperature) seems to have a stabilizing effect, essentially by smearing out the space charge which drives the flutes. On the whole, it seems that the outlook for hydromagnetic stability in systems with closed averaged $\int \frac{dl}{B}$ increasing backed up by finite Larmor radius stabilization is quite good.

Turning to the electrostatic (or micro) instability problem. Consider the state and development of a confined plasma meant to produce power:

1. The plasma ion and electron temperatures T_i and T_e will probably be different depending on the mode of generation of the plasma.
2. The distributions of ion and electron energies are unlikely to be quite Maxwellian from birth.
3. Plasma density falls from n to 0 in moving from plasma to field.
4. Field rises by a factor of $1/\beta$ in moving from plasma to field.
5. Since the plasma is confined, currents of oppositely directed electrons and ions flow in the transition region.
6. In a steady state device, there must be some point where the stream of diffusion to the wall is intercepted and disposed of. So plasma must flow along lines to the disposal point.
7. If the bottle has a region where magnetic lines leave the system, (magnetic mirror) the ions and electrons may have different loss rates, so that the plasma acquires a net electric charge.
8. Such an electric charge would be expected to set the plasma into rotation in systems with cylindrical symmetry.
9. The turning points of ions and electrons at the magnetic mirror may be different, causing compensating electric fields parallel to magnetic lines to develop.
10. In the plasma we have a large selection of possible waves including Alfven, ion cyclotron, electron accoustic, ion acoustic modes, moving in various directions.
11. Some of these can be expected to form standing waves with the plasma dimensions, i.e., cavity resonances. This means greater wave amplitudes with increased effects from non-linearity.
12. The great range of plasma density and magnetic field variation from center to wall maximizes the possibility of coincidence between wave singularities and resonances of different wave species.

13. Electrons in the sheath radiate at harmonics of the electron cyclotron frequency in a direction normal to the magnetic field. If the electrons are hot, the radiation (and absorption) can be strong, such that the mean free path of the radiation is short and the radiation is black body at the harmonics. This may alter the electron temperature in the sheath, creating a temperature gradient. The outgoing radiation will be reflected at the wall, entering the plasma at some other point with a direction not perpendicular to the magnetic field. The possibility of stimulated emission, by the radiation of otherwise non radiating electrons exists. Resonances should occur with reflecting walls producing standing electron cyclotron waves.

And so on, the list could be continued.

We now can expect to find in this plasma: unequal T_e, T_i, non-Maxwellian distributions $v_{\parallel} \neq v_{\perp}$, temperature gradients, currents along magnetic lines, density gradients, flows along magnetic lines, centrifugal forces, etc., everyone of which have been shown to drive one or another growing wave already classified in current plasma theory. But current plasma theory is by no means exact: it is usually linearized and therefore approximate: nonlinear-finite amplitude theory, second order effects like interactions between modal systems are yet to come.

I conclude therefore that:

1. A great number of kinds of instability are possible in a confined plasma.
2. Theory is quite incomplete.
3. Plasma theory should be heard with attention when it predicts an instability.
4. Plasma theory should be treated with reserve if it predicts stability for any particular combination of plasma parameters n, T_e, T_i, f, etc.

Nevertheless, although vast numbers of instabilities seem possible, there seem to be excellent chances that some whole classes of wave instabilities can be stabilized - for example finite Larmor radius may again be effective in smearing out wave disturbances. But more than this, it seems very likely to me that the net bad effect of instability - enhanced motion across the magnetic confining field may be diminished by dynamic methods, e.g. alternating and rotating magnetic fields - for these can have a continual restoring and reshaping effect on a magnetic boundary, and can even reverse the direction of the flow of diffusion. Dynamic confinement methods should therefore be an important item for laboratories aiming at steady state confinement. However for the next few years, it seems very unlikely that all or even a large fraction of possible instabilities will be stabilizable.

So I conclude that the safest approach must be a statistical one - the most likely route to a reactor is that least likely to encounter a killing instability. Now clearly, if instabilities were predominantly favored by large n, there would be a systematic clustering of instabilities to the small τ large n end of the spectrum, leaving the large τ steady state end clear and my argument for pulsed reactors would be invalidated. This is certainly not the case with hydromagnetic instabilities or Alfven waves which are largely independent of n. The electrostatic and wave instabilities are too numerous and varied to generalize. There will doubtless be some instabilities among them which are favored at high n, but not all.

We next observe that if we have an irreducible residue of instabilities which produce a randomly distributed set of effective loss times $\tau_i \ldots \tau_n$, then each τ_k cancels out all plasma confinement systems with τ greater than τ_k. Thus the largest possible confinement time for a reactor must be the shortest τ in the distribution.

Hence the reactor least likely to be killed by an instability is that with the smallest effective confinement time.

Once this important point is accepted, the optimum breakthrough points to get to a reactor are those with the smallest τs, i.e. region A

in Fig. 2, as close to the strength of materials limit $\tau \sim 1$ msec, as seems engineeringly practicable, and Region B in the microsecond region for z-pinches, limited only to keeping the energy release from being too explosive, and the electromagnetic power requirements too extreme.

PAST HISTORY AND PRESENT STATUS OF THE LOS ALAMOS SCIENTIFIC LABORATORY PROGRAM

The Scylla θ-Pinch Experiment

The original concept of this experiment in 1957-1958 was to heat a preionized plasma in two stages, first to a few eV by a strong radial shock produced by an E_θ field, and secondly by adiabatic compression by the rising B_z field to kilovolt temperatures. The first experiments were done with short ~ 10-cm long coils of 7-cm diameter shaped to produce magnetic mirrors, with magnetic fields rising to 50 kG in times of about 1.25 μsec.

The device produced neutrons from the start, though only on the second half cycle of the oscillating magnetic field. It was soon found that these neutrons were produced from a small ellipsoidal region at the center of the coil, and that these neutrons were quite different in energy distribution from the so-called phony neutrons that had been widely obtained from z-pinches, undoubtedly produced by instability mechanisms and not thermonuclear. The extent and number of interlocking and differing diagnostic experiments that have been made on the Scylla plasmas over the last eight years are rarely realized. The list in the main article on Scylla in this report should be read. Elaborate diagnostic experiments showed that the plasma depended for its high temperature on annihilation of the reversed magnetic field left over from the previous half cycle; that the reversed magnetic field played some more fundamental role than being merely a residue from the previous half cycle was first shown by Kolb at NRL.[3]

A hypothesis for the reversed field heating mechanism may be of interest. After the magnetic field reversal, an intense current sheath sweeps inward, preceded by a shock. This heats the plasma enough to trap the magnetic field inside left over from the previous half cycle. The magnetic compression proceeds but an internal magnetic dipole field reversed in

sign with respect to an external field is highly unstable with respect to flipping over the internal dipole. So this occurs. A rigid ring would continue to turn, end over end, the initial configurational energy periodically becoming all kinetic, A non-rigid plasma can never recover its original configuration, so a fluctuating, at every point increasingly tangled configuration results, the thermal energy still being divided equally on the average between configurational and kinetic. The tangling or knotting increases to the point where motion becomes indistinguishable from thermal. The compression by the external field, after the above has damped out, proceeds to pressure balance.

There are now many θ-pinches throughout the world. They differ greatly in their construction and phenomena. In some, the reversed magnetic field persists, and some produce hollow plasmas with the reversed magnetic field down the axis. It has been shown that axial compression contributes heating in some of them, and some show breakup into plasma rings, twin rotating filaments, etc. The plasma in some Scylla models develops into a single rotating filament with exponentially growing drift to the wall - i.e., an instability. Scylla has a higher effective voltage than most θ-pinches, in accordance with the initial philosophy of shock heating, makes more neutrons and is hotter. The Scylla plasma is not unique however. There exists one θ-pinch,[4,5] that at General Electric (Schenectady) which followed the Scylla prescriptions quite closely, which duplicated the Scylla results and extended them. The General Electric group discovered that by resorting to very strong preionization in the presence of a low bias magnetic field and lower pressures, operation would be obtained without reversed magnetic field heating. The Los Alamos Scylla IV adopted this technique - which amounts to achievement of the original concept of the experiment - with great improvements in impurity content, temperature, and especially stability.

By 1960, evidence for a thermonuclear (but not Maxwellized) origin for the Scylla neutrons (10^7 - 10^8 or more per shot) had piled up to a point where it must be regarded as confirmed. It would be churlish to deny the part that luck played in this achievement of the first laboratory

thermonuclear reaction. Without the reversed field heating which was not part of the original design, the experiment would not have developed thermonuclear temperatures as it then was and might have been abandoned.

The properties of the Scylla plasma are discussed more fully later in the paper below. I shall content myself with certain special questions which might arise. The Scylla thermonuclear reaction is quite strong (100 W for 3 μsec), but:

(1) Is it really a confined plasma?

(2) Could it be grossly unstable but last too brief a time to show it?

The present low density regime Scylla IV plasma has the following properties:

T_e (Maxwellized) - 300 eV.

T_i (largely monoenergetic) - 8 keV.

τ to half neutron yield - 3 μsec.

$n = 3 \times 10^{16}$ ion cm^{-3}.

Volume - 50 cc.

Total neutron yield - 5×10^8 per pulse.

Neutron rate - 1.7×10^{14}.

Configuration ellipsoid - 0.63-cm minor dia, 80-cm major dia.

Number of 90° ion-ion collisions per ion per pulse ~ 1.

Plasma pressure - 324 atmospheres.

Magnetic field - external - 90,000 G.

Magnetic field - internal - very small.

Path length per ion per pulse 870 cm.

Impurity content - $< 0.1\%$.

Gross thermonuclear power during the pulse - 95 W.

The plasma presents a picture of a field free region, with ions executing straight line paths and being reflected from the magnetic walls, the motion being predominantly radial. A radially directed ion would make 1400 reflections from the wall in its lifetime - so it is a confined plasma. So the answer to question one is "yes"; to question two, "in such hot plasma, flute growth velocity can be very high - approximately 50 cm per microsecond." Although the observed confinement lasts perhaps five flute instability e-folding times, no flutes are seen. Nevertheless when the conditions are changed significantly to lower temperatures and a shorter coil, in the same magnetic cycle time, major wall losses occur and strong flutes develop. The higher temperatures and longer length effects on stability are both indications that some finite Larmor radius stabilization is being obtained.

In the earlier high pressure regime, $T_i \sim 2.0$ keV, a wave of plasma impurities can be seen (from the Mach-Zehnder figures) to form at the wall and move inward. One of the most encouraging features of the low pressure regime is the absence of such wall effects. See Fig. 4.

Two hypotheses, which as yet we cannot distinguish, can be proposed to explain this: (a) the high pressure regime has more impurities and radiates more (about 40 times classical bremsstrahlung). This radiation may heat the wall and evaporate it; (b) the low pressure regime shows no radial diffusion whatever, whereas the high pressure regime diffuses somewhat. We may then have sufficient Bohm diffusion by microinstability in the latter, similarly to heat the wall. Absolute measurements of the bremsstrahlung rate from the low pressure Scylla plasma now show that the bremsstrahlung rate is only twice classical. This is a very low value indeed. Radiation from earlier Scylla plasmas has been as much as 200 times classical, and in the rare cases that such absolute measurements have been obtained from laboratory plasmas elsewhere the observed bremsstrahlung rate has been similarly larger than theory. This low radiation rate has important consequences for the future extension of the Scylla machine to longer times and closed systems. Until now, the influx of wall impurities in the high pressure regime had made it seem

Compressed plasma of the Los Alamos - Scylla IV θ-pinch as shown by Mach-Zehnder interferogram at λ = 6943 Å. This is near peak compression in the new low pressure, higher temperature regime without reverse magnetic field heating. $P_{initial} = 15\ \mu\ D_2$. B applied 90 kGauss. Time 1.6 μsec. Plasma mean length 70 cm. 1 fringe $\equiv 3.10^{17}$ electron/cm^2. Mean ion energy (calc) 7.3 keV (equivalent to 4.9 keV ion temperature for Maxwellized ion energies). Electron temperature 300 eV. Mean neutron yield 6×10^8 per discharge. Note absence of wall impurities.

Work performed under the auspices of the U. S. Atomic Energy Commission.

Fig 4

pointless to attempt longer confinement by going to a closed geometry Scylla.

Plasma Guns, Plasma Injection, and Trapping Studies

The hydromagnetic coaxial plasma gun developed in this laboratory provides a directed burst of dense plasma (10^{17} - 10^{18} ions total) with energy adjustable from 2 - 10 keV. The operation of the gun is considerably embarrassed by a later emission of slower cooler plasma. This gun, now in wide use around the world makes enough hot plasma that, once injected and captured into a static magnetic bottle, significant plasma physics experiments can be made. The operation of the gun is not clearly understood: It does not function by the simple-minded sweeping out of plasma by a j x B current magnetic field piston. The energies observed are many times too high for that. Probably some terminal acceleration process is involved. The plasma slug from the gun exerts dynamic pressures $1/2\ n\ m\ \bar{v}^2$ large enough to deform multi-kilogauss magnetic fields. Much interesting work is being done on the conduction of this gun plasma down magnetic ducts. A first requirement for effective application of these gun plasmas is to be able to control them magnetically, i.e., stop them, steer them round corners and so on. It is a surprising thing after nearly 15 years of plasma research throughout the world, that no one has succeeded in steering a slug of hot plasma round a 90° curve with more than 10 - 20% efficiency. In the laboratory, such plasmas act in ways that would not be predicted. This is because actual situations turn out to be more complicated than can reasonably be foreseen. Certain very interesting trapping possibilities exist, by virtue of the polarization charges which develop when gun plasmas cross magnetic fields. For example a gun plasma is directed across a magnetic field, lines of which are continuous, but reversed in direction from, magnetic lines traversed earlier by the plasma. When the fast plasma penetrating the field reaches this region, a large current of polarization elections can travel along the magnetic lines between the two regions to cancel the polarization, thus

halting the plasma automatically. This was one of the rare cases when observations on polarization and conduction led to a purposeful change in the magnetic field configuration - which functioned in the way predicted.

It may be noteworthy that the 1964 United States exchange delegation, on their tour of the USSR fusion installations in 1964, reported a large increase in Soviet work with plasma guns, ducts and trapping, very much on the lines of that at Los Alamos.

Plasma Focus Experiment

In 1960 some studies were made on coaxial guns in an effort to understand how they worked and thereby improve them. To determine the angular distribution of the ejected plasma, the DD neutrons generated when the plasma slug impinged on a distant D_2O ice target were plotted. This led to the observation that some neutrons were produced at the gun itself. Further exploration and optimization including working with a static deuterium filling, resulted in an apparatus which forms a plasma focus with extraordinary properties.

The focus has a volume of a few cubic mm. It generates a burst of neutrons lasting 0.1 to 0.2 μsec numbering up to 10^{11}. This is a very large number, and since mistakes have been made about neutrons before, the methods of detection and margin of error will be discussed. The yield is not measured by proton recoil in a scintillator, and is therefore not subject to confusion with γ ray Compton electrons. The yield is measured by the activation of silver in a standardized moderator-counter system. Such a method is not subject to intensity or pile-up errors - the only errors being:

(1) reflection of neutrons from the environment, and
(2) error in calibration or malfunction of the scaling equipment.

The environment errors should be small here - possibly 5 - 10%. The equipment is a standard piece of apparatus, known to be in fair adjustment.

However, in order to make more sure and increase accuracy, recalibration against a standardized DD neutron source is in progress. In the discussion below, we will assume pessimistically that the yield is 5×10^{10}.

Knowledge of the nature of the plasma focus is so far quite incomplete. The shape of the plasma focus is known, the electron temperature is known by differential absorber measurements on the bremsstrahlung, and it is known that the neutrons are close to isotropic. A Mach-Zehnder interferometer with great field magnification is being set up which should yield electron line density directly, as was used so effectively for the Scylla IV plasma. The Los Alamos extension of the Ashby-Jephcot He-Ne laser beam is also to be applied. This gives a continuous record of electron density along a very narrow pencil beam.

To produce so large a neutron rate from so small a volume by thermonuclear reaction, requires a density of about 10^{19} ion/cm^3, and a temperature of about 10 keV, since the duration of the neutron burst exceeds the Maxwellized.

The obvious deduction from the experimental arrangement is that a sheath sweeps down the space between the inner and outer coaxial electrodes, and contracts into a z-pinch when it runs off the end.

However, z-pinches (Columbus I - V) were studied extensively at Los Alamos in earlier years - 1953 onwards. Although these devices produced neutrons, it was shown that these neutrons were anisotropic and in fact must have been produced by acceleration in the strong electric fields of M = 0 (neck or pinch off) instabilities.

The ion temperatures in such z-pinches were probably quite low. However, an instability explanation for a yield of $5 - 10 \times 10^{10}$ neutrons from a few cubic mm of plasma is difficult for two reasons:

(1) The current of 10-keV deuterons required to pass through a cubic mm of deuterium of density 10^{19}/cm^3 is 5×10^8 amperes, which far exceeds the total current flowing in the apparatus ($\sim 10^6$ amperes).

(2) The neutrons are isotropic.

Another curious inconsistency, is that the calculated pinch-off time for an M = 0 instability is much less than the observed 0.2 μsec neutron

emission period. The suspicion is that we have here, for the first time, a hot z-pinch, so hot that we are getting some finite Larmor radius stabilization.

If this possible thermonuclear reaction becomes confirmed, which will need much further study, the $n\tau$ value of 2×10^{12} becomes the largest known, exceeding the previous Scylla record of 2×10^{11}.

There is a close similarity between the plasma focus and one reported by Filippov, et al.[6] Their neutron yield was less, and ours was reached by a different route (stumbled on in fact). The intensity of the DD reactions in the few cubic mm of the plasma focus would perhaps best be appreciated by calculating how long all the plasmas of the world's machines, would have to run on deuterium, to yield 5×10^{10} neutrons. It is simpler to calculate the running time of one of the largest steady state machines - OGRA. This is credited with 80,000 liters volume of plasma (of density 10^7 ion/cm^3 at mean energy 100 keV. If filled with deuterium this gives a total yield rate $Y = \frac{1}{2} n^2 \langle \sigma v \rangle V$ of 2×10^4 neutrons/sec. It would take about twenty-five days continuous operation of the whole machine to equal one pulse from the plasma focus.

A Sketch of Future Plans and Problems

Opening up before us are numerous attractive lines of research which as little as a year ago were hidden from view.

1. As we have seen, the Scylla IV plasma is dense and hot. For the present 3 μsec durations it is also stable so that it does not cross the compression field to any detectable extent but runs quite rapidly out of the open ends. We need to know how long it would last if the ends were closed. We do not expect it to remain stable for the classical diffusion time of course, but it becomes practically mandatory to find out what the confinement time for a $\beta = 1$ plasma dense enough and nearly hot enough for a reactor, would be.

The problem of a $\beta = 1$ plasma in a torus is that of combatting the outward force on the diamagnetic body - the so-called gross stability - in the magnetic field gradient of a torus. The solution to this force problem, by placing alternating Joffe bars on the outside of the torus is given in the Scylla papers below. It turns out that the confining system derived by Furth and Rosenbluth can also be applied (with some modification) to compensating the outward drift in a torus while maintaining $\int dl/B$ stability.

The plans for such a closed Scylla (Scyllac) are given. This will require a new building of total floor space comparable with our present total.

2. The ~ 0.6 cm dia 50 cm long hot plasma ellipsoid of Scylla IV makes a natural starting point for a z-pinch.

3. To complicate the situation further, Scylla turns out to have very good reactor possibilities. This is unexpected. It was planned as a plasma physics experiment - just to make a thermonuclearly reacting plasma in the laboratory - with no claims to being a prototype reactor. And it must be admitted, when in the company of enthusiasts disputing whether their machines would make thermonuclear power for $72.00 or $85.00 per kilowatt, the chances that the Scylla plasma at 100 watts for 3 μsec could ever

repay the megawatt expended in the compression coil seemed remote. We have examined the feasibility of two examples of pulsed high-density reactors (summarized in the Scylla section below), including multiplying blanket, heat transfer, and stresses. It turns out to be more straightforward to make a power producing reactor than was previously believed. The extrapolation beyond present plasma behavior is far less than "engineering concepts" for thermonuclear reactors have usually had to make.

4. The fast plasmas generated by our hydromagnetic guns make possible fundamental plasma physical studies of the way anisotropic plasmas, plasma winds, etc., react with magnetic walls in a way that it does not seem possible to reach any other way. The gun plasmas are a vital component of the plasma trapping methods (entropy, polarization) for getting gun plasma into magnetic bottles suddenly. If the confinement time of the closed flute-stable bottles at realistic reactor type densities turns out to be milliseconds - what other method is going to be available for filling them? So a start on a closed flute stable bottle with walls of magnetic field thick and strong enough to hold gun plasmas seems strongly indicated. The problem is which bottle is safest from the point of view of stability, and most economical to build. Our top priority effort over the last six months has been on this problem. It seems fairly clear now that safety and economy are incompatible - the helixion[7] is magnetically more economical than the multipole. But the magnetic lines joining different regions are long and complicated in the helixion and connect positive and negative curvature regions very directly in the multipole. Plans for a multipolar machine powered by a 10 MJ energy storage system are advanced but not complete.

5. The concept of a z-pinch so strong as to yield a positive thermonuclear power balance before the fast hydromagnetic kink instability can take it apart is an old one. Under the title Columbus X concept, it is discussed in my previous review of Los Alamos fusion research for the Atoms For Peace Conference, Geneva, 1958[8]. The term inertial confinement, is sometimes used (wrongly) to mean fast z-pinch. A z-pinch, in fact, gives some confinement over and above that for a straight implosion, which has

the minimum possible confinement. This concept now comes back strongly for the following reasons: (a) Straight z-pinches were extensively studied at Los Alamos in the years 1952-1957. Z-pinches have a special advantage over all other magnetic confinement systems in one respect - they provide more confinement pressure per unit of magnetic energy than any other system. They provided excellent, contracted, very brief condensations of plasma (See Fig. 5) but such plasmas were never hot - merely cold plasma traversed by a few fast ions. Increase of contraction velocity by increasing the voltage was also ineffective, plasma sheaths remaining attached to the wall with rapid emission of pressureless impurity plasma. So we have no knowledge of what a hot z-pinch is like. (b) Now we can make hot plasmas by other methods - Scylla or hydromagnetic guns. The experiment of taking the long 8-keV Scylla IV ellipsoid, which floats in vacuo away from all walls, as the starting point for a z-pinch looks very attractive. (c) Furthermore, the snowplow theory of z-pinches, which has been most serviceable, stops off before the interesting stage when the pinch has contracted to a radius and is at such a temperature, that it is narrower than the snowplow sheath thickness allows. Such a plasma might even be stable to M = 0 necking off modes. So this old problem needs to be taken up again theoretically and by computers. (d) In the early 1950's no methods for measuring the density in z-pinches were available: the density was too high to be measured by microwaves, and the laser had not yet been invented. Such pinches are now ideal subjects for our Mach-Zehnder technique, which has worked so well for Scylla. The He-Ne narrow beam laser should similarly work well. (e) The Columbus X type reactor needs very large currents and voltages if the disassembly time is given by pinch radius/sound velocity. Finite Larmor radius stabilization as a possibility for the z-pinch had certainly not occurred to me previously. But now we even have evidence that stabilization of some kind is occurring in the plasma focus - since the duration is otherwise about one hundred times too long. If this should turn out to be true - we can start thinking of a Columbus X type reactor with deuterium. It would be worth a great deal not to have the monstrous inconvenience of a multiplying blanket and attendant tritium recovery plant over all the other problems of a thermonuclear reactor.

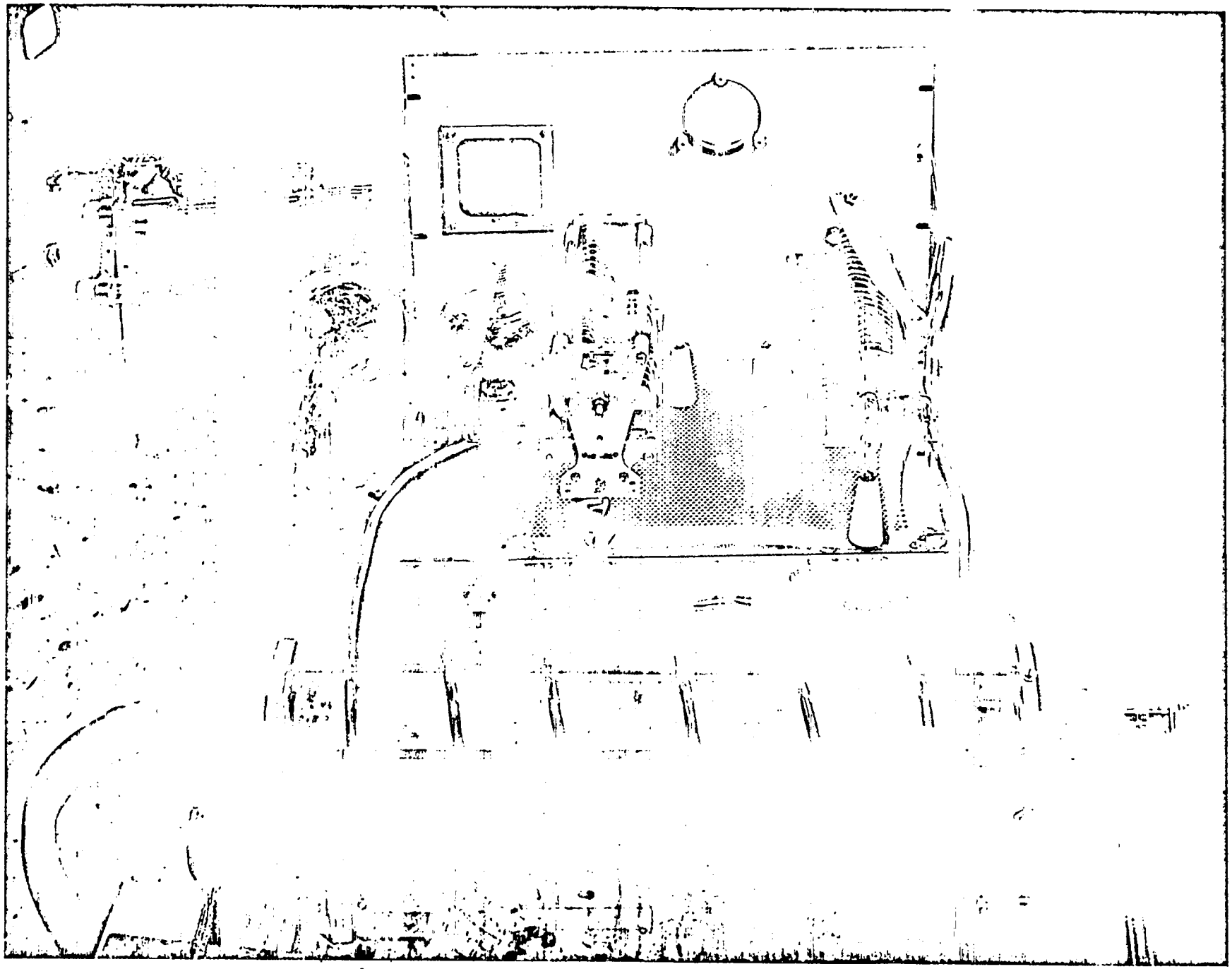

Fig. 5. 50,000 Ampere z-Pinch in Argon. LASL 1952-1953.

REFERENCES

1. C. L. Longmire, Proceedings of the Second United Nations Conference on the Peaceful Uses of Atomic Energy (United Nations, Geneva, 1958), Vol. 31, p. 84.

2. M. N. Rosenbluth and C. L. Longmire, Ann. Phys. 1, 120 (1957).

3. H. P. Furth and M. N. Rosenbluth, Phys. Fluids 7, 764 (1964).

4. A. C. Kolb, C. B. Dobbie, and H. R. Griem, Phys. Rev. Letters 3, 5 (1959).

5. L. M. Goldman, H. C. Pollock, J. A. Reynolds, and W. F. Westendorp, Phys. Rev. Letters 9, 361 (1962).
   L. M. Goldman, R. W. Kilb, and H. C. Pollock, Phys. Fluids 7, 1005 (1964).

6. N. V. Filippov, T. I. Filippova, and V. P. Vinogradov, Nuclear Fusion Suppl., Pt 2, 577 (1962).

7. J. L. Tuck, Nature 187, 863 (1960).
   J. L. Tuck, Proceedings of the Second United Nations Conference on the Peaceful Uses of Atomic Energy (United Nations, Geneva, 1958). Vol. 32, p. 22.

Dr. TUCK. First, speaking to the question in pursuing Project Sherwood, "Are we flogging a dead horse?" In my opinion fusion power is one of the really noble worthwhile projects of the present time. The world will soon have to depend on nuclear power; for this, fusion power is much more acceptable than fission. The reason for this is not because deuterium is more plentiful or cheaper than uranium, the fuel cost is a negligible part of nuclear power cost, the real reason is that fusion is safer, it won't blow up, and it doesn't leave behind long-lived poisonous fission products. Furthermore, though I do not consider this important compared with the above, some considerable time after fusion power is an accepted fact, it logically offers the means for high specific impulse space navigation, by comparison, with which all other methods including fission reactor rockets are lame. The trouble is that the achievement of controlled fusion is a difficult and subtle matter enormously much more so than fission.

But the very magnificence of the goal of Project Sherwood led its followers into trouble. For example, some enthusiasts oversold the AEC in the first days of the project on its immediacy so that there was too much money. We Sherwood scientists were inexperienced in this new subject, and truth to tell, naive, and some of us had new laboratories to create. Everything that popped into our heads was built and everyone was hired who could be caught. So there are, let's face it, many highly respected physicists who scowl at the word Sherwood. As I will try to show, this is unjustified, in fact there is nothing wrong with the Sherwood horse, it merely had a wild and misspent youth. Other countries suffered in the same way, the Zeta pinch in England cost $5 or $10 million of hard-earned money. It got the same results as our Los Alamos Perhapsatron which cost only $40,000 and neither were thermonuclear. We don't know about the early Russian mistakes except the time when they believed the early Zeta claims and crash built a duplicate which they called Alpha.

Considering now the LASL participation in fusion. We got into this very early, perhaps the first in the United States. We decided to take the rather down-to-earth approach of trying to make a thermonuclear reaction, something which had never been done before in the laboratory, by whatever means we could and however brief it might be, and not bother too much about reactors. We succeeded at the second attempt in 1958. Our first attempt was the Perhapsatron which used the simple pinch effect, for which we were the first in (1951), and seeing that it wasn't going to work, the first out. The pinch effect was prime favorite in those days, and some European laboratories, after arduous work were just getting moving on it, when we dropped it at LASL. It caused a sensation.

All the time we resisted the temptation to build huge machines or hire large staffs. The net result is that we have spent only one-tenth of the total Sherwood costs and are by far the smallest in size of the four AEC laboratories. This sounds very virtuous, but I have now come to realize that it was suicidal. Representative Cannon, chairman of the powerful Appropriations Committee has demanded very reasonably that "some concepts be cut out, you ought to know enough by now to weed out the unpromising ones" and funds for Sherwood are now being restricted.

How is the AEC to take account of these effects? Two months ago we discussed in Washington the proposal to cut out Los Alamos fusion completely, the logic being that after all it represents the smallest capital investment, and is therefore the most economical way of obeying senatorial instructions. Crazy logic of course, like throwing out the baby with the bath water. It didn't happen but it has frightened us and now the cuts are being parceled out among the four laboratories essentially in the ratio of their size, 4, 4, 2, and 1.

Returning to the LASL story: In 1957 we then turned to the θ-pinch. Scylla apparatus which seemed to give a thermonuclear reaction from the very beginning. This machine was exhibited in operation at the Atoms for Peace Conference in Geneva, Switzerland, in 1958 with the clear understanding that it was probably thermonuclear but that that still had to be proved. We have passed through four models of this device and we are now quite certain beyond a shadow of a doubt, that we had then and now have a stronger true but brief thermonuclear reaction. The yardstick which measured progress in this field toward a reactor is $n\tau$, density $\times$ time, and in this respect our small Scylla apparatus stands among the highest in the world. There are now many θ-inches in fusion laboratories, so much so that Academician Artsimovich was moved to say in his summary of controlled thermonuclear research progress at the last international conference in Austria, "Soon no housewife will be without one" but he went on, "but what a feeble thermonuclear reaction, only enough to give one neutron to each inhabitant of Austria. We must do better than that." Well, we have: We now make 1 billion neutrons per shot, enough to give everyone in the world half a neutron apiece. Our thermonuclear conclusions have been confirmed and extended in a scaled-up Scylla-like device which the General Electric Co. have built with their own funds. It will be exhibited at the New York World's Fair.

It is surprising to us how little prestige the AEC made out of this very real achievement of the first laboratory thermonuclear reaction.

Here, we had an achievement—not just a promise. No doubt, if the AEC had not had the uncomfortable task of holding the balance among the four competing AEC fusion laboratories, and we had not been so much smaller, it would have been easier for them.

There have been two reviews by outside scientific authorities of the overall Sherwood effort and both times, the Los Alamos work was picked out for favorable comment. The last review of the General Advisory Panel recommended an increase of staff for LASL and we propose, if given the chance, to increase from 50 to 54 people. Our present budget is approximately $2 million per annum. We are at last beginning to see how to make an intelligent but prudent expansion of our work. This is mainly in the direction of closed pulsed systems called caulked cusps but also involves making longer duration Scyllas.

Our philosophy is to concentrate on pulsed devices for fusion. The reason for this is not that we wouldn't prefer to have a steady running fusion reactor such as the other laboratories concentrate on—but that nature has plenty of surprises in store for us all yet. There are some quite likely ones (instabilities) which could kill steady running fusion reactor concepts dead but still leave pulsed concepts alive. It is safer, therefore, to stay with pulsed concepts and let the steady running, if nature lets us, come later. It is ironic that just when we see how money might at last be spent wisely on fusion, the money that we refused in the early days is no longer available.

I do not know the answer to the problems of growing up. I suspect there will always be some waste associated with vigorous new growth and vitality. Certainly if the U.S. effort hadn't started the way it did, we would now be tremendously behind in the subject vis-a-vis the rest of the world. So in a sense, the United States is indebted to the early superenthusiasts.

But there is still a problem—an organizational one for which I do offer a solution. Clearly—de minimis non curat lex—the law does not occupy itself with trifles—and for you, as representative of the United States, the relative survival of one laboratory versus another is a trifle—what matters is whether the job is done. I think the job will be less well done if Los Alamos gets pinched out.

As for the difficulty of finding the right level at which to support fusion, I propose that we express it in terms of what we spend on fission—some small fraction—say 5 percent and peg it there for awhile. Surely, this is logical—both are trying to provide nuclear power but fission is the more advanced.

Mr. CONWAY. Except they are cutting back on the fission program.

Dr. TUCK. But 5 percent would still leave us in clover.

Thank you.

Representative WESTLAND. I was just going to say in response to your de minimis non curat lex that this is a case of res ipsa loquitur.

Dr. MCDANIEL. Mr. Chairman, I note from the last speaker that there is no absence of enthusiasm for our project.

Representative WESTLAND. I would like to say that as long as you gentlemen can keep your sense of humor as exhibited by Dr. Tuck, things will probably be in pretty good shape in your field. We have the same problem in the job we have.

Dr. MCDANIEL. I think I would like to call on Dr. Allen Kolb from the Naval Research Laboratory who has a few words to say before we close.

Dr. KOLB. After the last presentation, I more or less changed the direction of what I would like to say. Actually, I share Dr. Tuck's enthusiasm for his Scylla-like machine and it might be interesting just to say that we spend a substantial sum of money in the Navy to establish that what he considers to be a fact is a fact.

Representative WESTLAND. I was wondering if I might interrupt here. Dr. Tuck, was it Scylla that blew up?

Mr. CONWAY. Some years ago, Dr. Tuck, about 5 years ago, I revisited your laboratory with Senator Hickenlooper, the day after you had some sort of explosion. It was right under Dr. Bradbury's office, as I remember.

Dr. TUCK. Actually I always think it is always nice to have a little change of pace. When we switched the machine on one of the capacitors blew up and caught fire. It made a tremendous flame. So whenever I show the people the thing working I always show the burst of flame.

Mr. CONWAY. I think of that in connection with your reference to fusion advantages compared to fission. You didn't wish to imply that the fission reactors that have been built today are in any way dangerous?

Representative WESTLAND. A shaking of the head cannot be picked up by the recorder. I want the record to show that Dr. Tuck shook his head in a manner to indicate a "no" answer.

I. PERSONNEL AND FINANCIAL HISTORY OF THE LOS ALAMOS SHERWOOD PROGRAM

E. L. Kemp

The Sherwood program began at Los Alamos in January, 1952 with a group of about five scientists and an annual budget around $100,000. In the following thirteen years the annual personnel never exceeded sixty-five people with a maximum annual budget near three million. Figures 1 and 2 show the personnel and operating expenses for each year. These curves show that the cost per man-year has remained fairly constant near $40,000 for the last ten years. The total expense budget at Los Alamos over the whole operation period amounts to approximately $21 million.

In years past it was fairly common for Los Alamos to return some of its appropriation for use by other Sherwood laboratories. However, during the past two fiscal years, the Los Alamos Scientific Laboratory Sherwood staff has increased from 47 to 55 which is the limit permitted by the present Sherwood budget. Dr. N. E. Bradbury, the director of the Los Alamos Scientific Laboratory has authorized continued expansion of Los Alamos Scientific Sherwood personnel to the extent permitted by funds made available in the future. Planned expansion is shown dotted on Fig. 1 in accordance with the increased funding shown dotted on Fig. 2. The cost per man-year is roughly constant at $40,000.

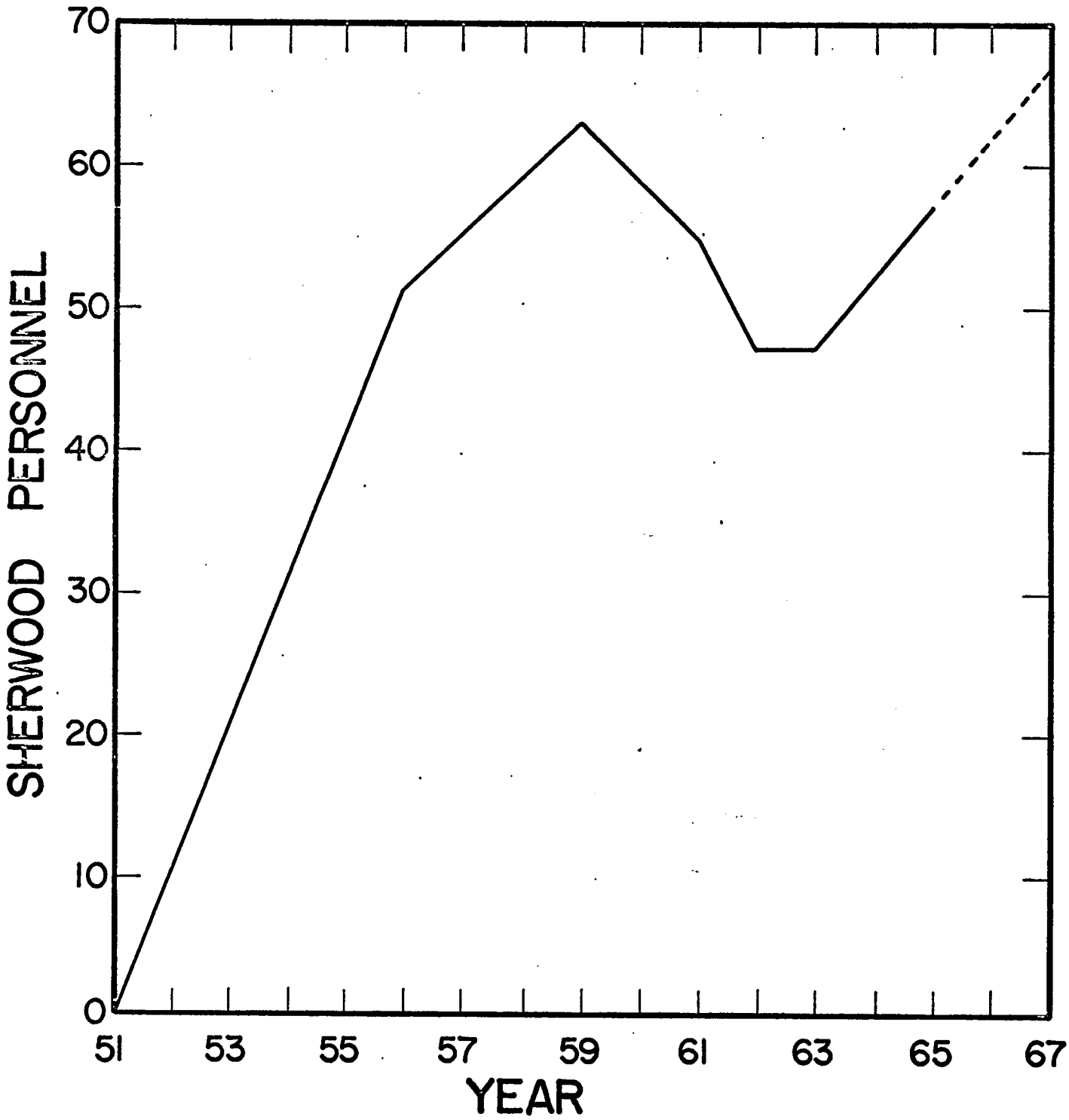
70
60
50
40
30
20
10
0
SHERWOOD PERSONNEL
51
53
55
57
59
61
63
65
67
YEAR

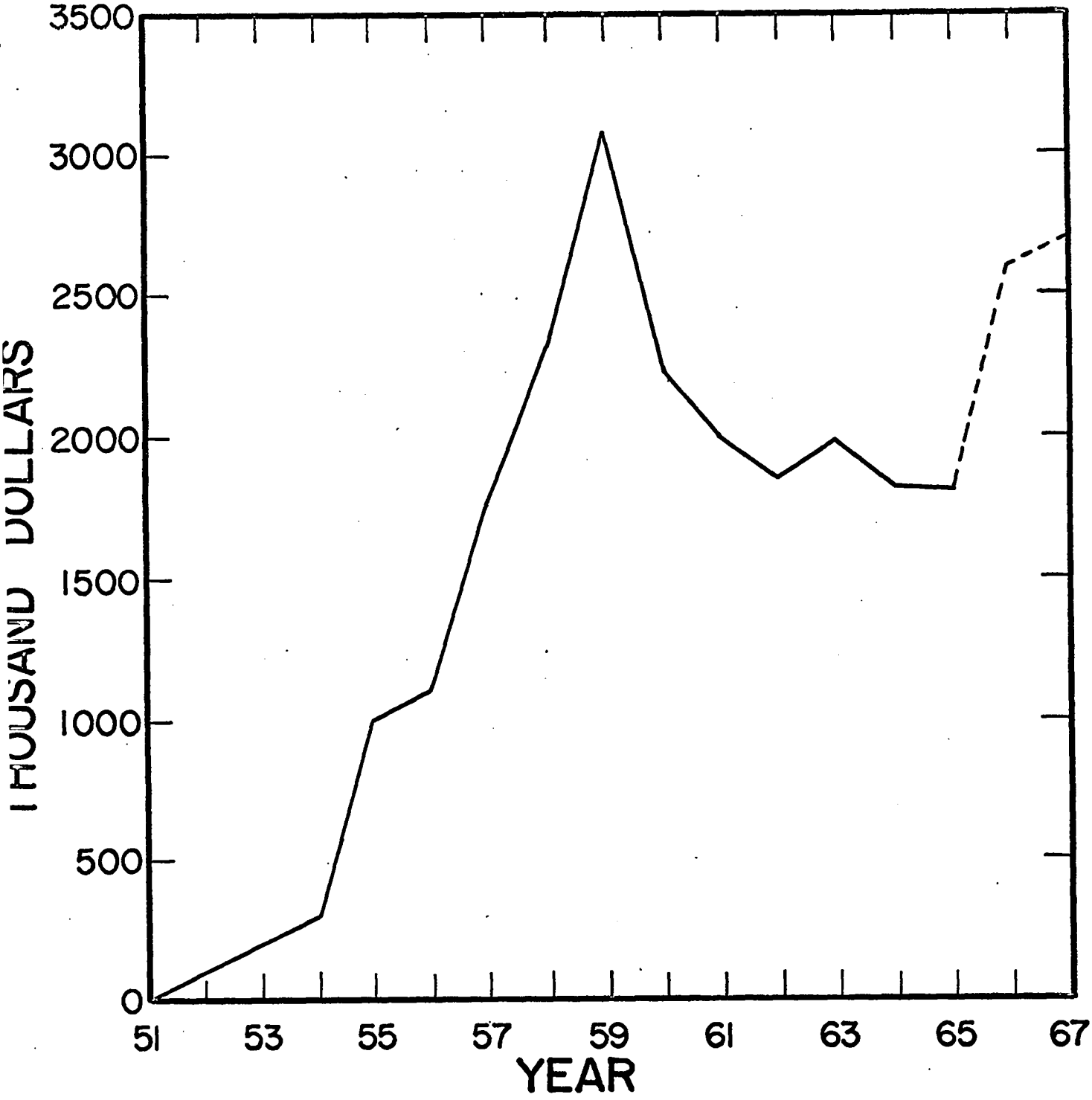
3500
3000
2500
2000
1500
1000
500
0
THOUSAND DOLLARS
51
53
55
57
59
61
63
65
67
YEAR

THE SCYLLA Θ-PINCH EXPERIMENTS:

STATUS, PLANS, AND PROPOSAL

FOR A SCYLLA V TORUS*

W. E. Quinn, F. L. Ribe, W. B. Riesenfeld, G. A. Sawyer,
and J. L. Tuck

* Work performed under the auspices of the U. S. Atomic Energy Commission

CONTENTS

I. INTRODUCTION

The essential processes by which the thermonuclear plasma in a θ-pinch is produced and contained are illustrated in Fig. 1. A massive, single-turn coil is rapidly filled with magnetic field as a capacitor bank is suddenly switched on. The inrushing magnetic field surrounds deuterium plasma inside the coil but cannot penetrate it because of the plasma's high electrical conductivity. Therefore a large magnetic pressure is built up between the outside of the plasma and the coil wall. This pressure drives the outer surface of the plasma rapidly inward [Fig. 1(a)]. During this early dynamic phase, a shock wave runs into the plasma to convert inward plasma motion to heat, producing temperatures of a few hundred electron volts. This dynamical process occurs before the capacitor has lost a great deal of its energy, i.e., long before the energy of the magnetic field in the coil has built up to its final value. As the magnetic field increases, it contains the heated plasma from the dynamic phase and slowly (adiabatically) compresses it during the quiescent phase of the discharge [Fig. 1(b)]. Finally when all the electrostatic energy has left the capacitor bank and been converted to magnetic energy in the coil, there is a long, ellipsoidal plasma held by the magnetic field away from the wall.

The 100,000-gauss magnetic field of Scylla IV is representative of those found in θ-pinches. The magnetic field is furnished by 10,000,000 amperes of current spread over the inner surface of the coil and flowing in a circle around it. The initial voltage to which the Scylla IV capacitor bank is charged is 50,000 volts and the electrostatic and magnetic energy is about 600,000 joules.

The Scylla experiments at Los Alamos differ from those carried out in many other laboratories in that the capacitor voltage is large and that a large fraction of the voltage is transferred to the compression coil through the inductance L_c of the external circuit. It is this high voltage (per unit circumference of the coil inner surface) that determines the speed of the initial dynamic phase and the heating by

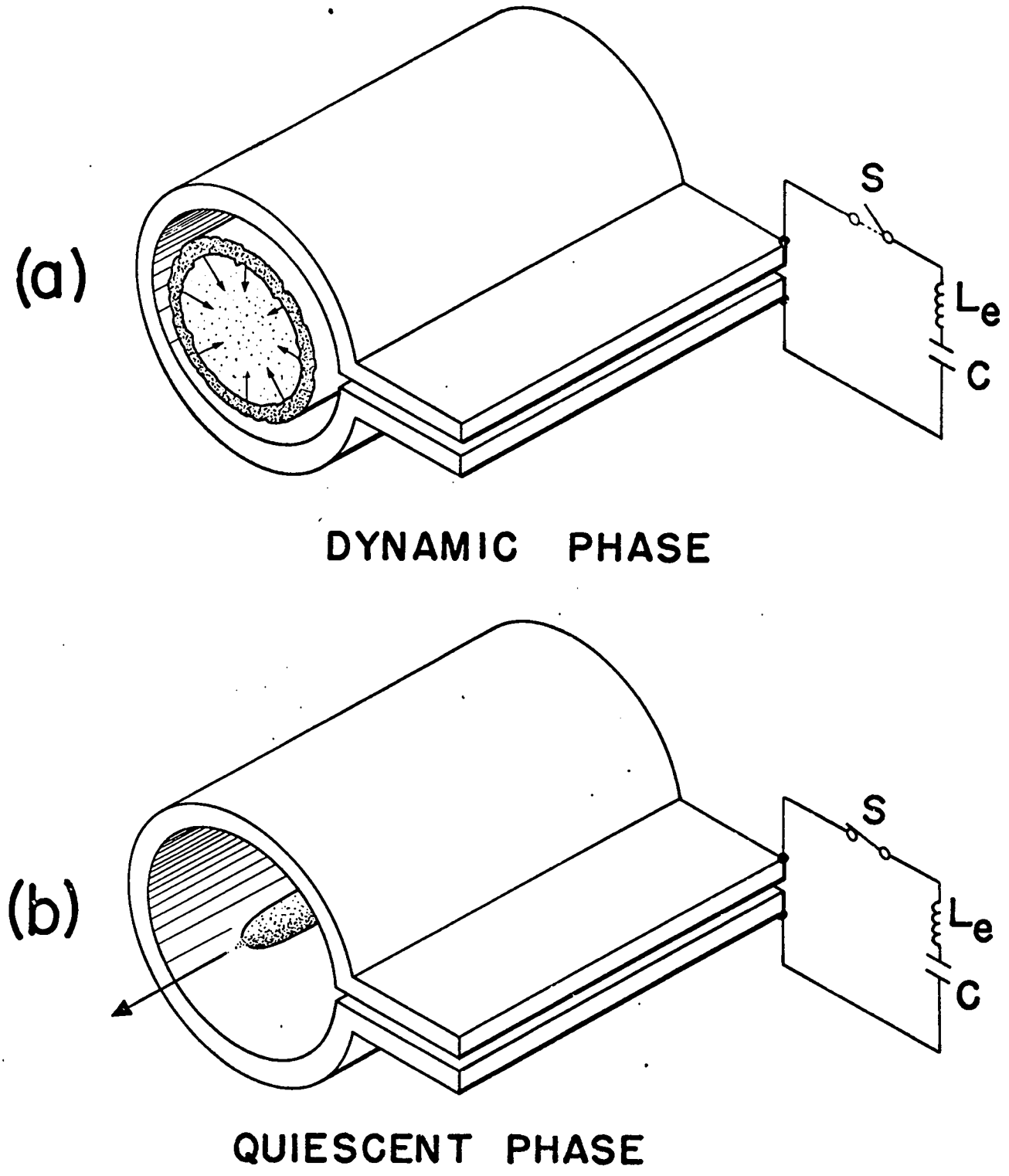

Fig. 1 Simplified schematic view of a theta pinch.

the shock wave. Figure 1, while correctly illustrating principles, is greatly over-simplified. The plasma is contained inside an evacuated cylindrical discharge tube made of refractory alumina ceramic (99% Al_2O_3) which is fitted closely inside the compression coil. The tube is evacuated to 5×10^{-7} torr (1 torr is approximately one thousandth atmospheric pressure) before the admission of deuterium gas to a pressure of 0.01 to 0.1 torr for producing the plasma. The switch S which allows current to flow from the capacitor bank actually consists of many parallel spark gaps, each feeding many parallel cables which carry the millions of amperes that flow in the coil. The current collector which feeds the coil slot is a pair of thick (3-in) aluminum plates, bolted and clamped together to withstand the large magnetic forces from the currents flowing between them.

A. Properties of the Plasma

The plasma of the quiescent phase of Fig. 1 is pictured with reasonable correctness. It consists of deuterium ions and electrons from which the magnetic field is almost completely excluded, and there is a relatively sharp (~1-mm thick) boundary separating plasma and magnetic field radially. The pressure of the plasma is balanced by that of the containing magnetic field and both are about 400 atmospheres. The plasma pressure is made up by equal numbers of ions and electrons at a number density of 3×10^{-16} cm^{-3} (about 1/1000 of atmospheric air density) at temperatures which are about 100,000 times room temperature. Specifically the ion temperature is about 5000 eV (55,000,000°K) and the electron temperature about 300 eV (3,300,000°K). The two temperatures are different because the ions obtain more energy during the initial dynamic phase. They are unable to communicate this energy to the electrons during the time, 3 μs (millionths of a second), during which the plasma exists, owing to the fact that collisions between the two at these elevated temperatures are very infrequent. In future devices in which the containment time will be longer, the electrons and ions can be expected to approach the same temperature. The fraction of impurity ions

in the discharge from wall materials and other sources is about one part in 1000. This means that the energy lost from the plasma in radiation exceeds the irreducible bremsstrahlung loss by about a factor of two. (The bremsstrahlung radiation is that emitted when plasma electrons collide with plasma ions).

B. Plasma Containment

At the present stage of research, the containment of the plasma is limited by the time during which the containing magnetic field is applied to it (7μsec). However, it is possible to give some idea of the containment to be anticipated with magnetic fields which last longer. The present Scylla experiments demonstrate that there is no appreciable diffusion across the magnetic field and that hydromagnetic instabilities which allow the plasma to push its way outward radially between magnetic lines instead of diffusing across them are slow. The limiting factor on the containment at present appears to be plasma streaming out the ends along magnetic field lines as indicated by the arrow in Fig. 1. This is an inevitable effect in an "open ended" geometry such as a linear θ-pinch, and the exact rate of loss depends on the length of the plasma, the thermal speed of its ions, and the size of the hole at the end of the plasma through which the plasma escapes parallel to the magnetic lines. Our present measurements indicate the hole area to be about 1/6 the cross-sectional area of the plasma.

C. Laboratory Astrophysics

The θ-pinch plasma is presently the only laboratory plasma whose electron temperature duplicates that of the solar corona. It therefore provides a means of doing experiments in astrophysical spectroscopy under convenient laboratory conditions. Considerable work has already been done to compare the results of solar rocket spectroscopy with θ-pinch work.

D. θ-Pinch Program for the Next Two Years

Scylla IV development over the next two years will be along several lines, all intended to answer questions important to the design of eventual pulsed fusion reactors where thermonuclear energy production overcomes the energy losses.

A major effort for the next year or so will be to measure the plasma properties at the higher fields (180,000 gauss) and extended times (50 μs) made available by applying a capacitor bank of much greater energy to the present θ-pinch experiments. Loss of plasma out the end of the discharge tube has emerged as an important factor in the present experiments, and it is expected that further study will show the need for an endless closed geometry for future θ-pinches. Operation with the capacitor bank of increased energy (power crowbar) will also show whether the Scylla plasma is stable over longer periods of time. Since it is believed that end losses will dictate a toroidal geometry, having no ends, in future Scyllas, studies will begin with curved sectors of tori to test the necessary stabilizing techniques for overcoming the outward drift of the plasma.

In addition to these developments aimed at longer plasma containment a difficult light scattering experiment will be attempted. The experiment involves the measurement of the scattering of ruby laser light from the plasma, and it is difficult primarily because of the extremely small portion of the incident light which is scattered. However, it is a potentially powerful technique for making a direct measurement of the deuteron ion energies in Scylla plasmas, a quantity which must now be derived indirectly from fusion reaction measurements and the pressure balance relationship.

E. Toroidal θ-Pinch (Scylla V)

It will be demonstrated in Section VIII of this report that pulsed systems such as Scylla are feasible for use in an eventual fusion reactor, provided of course that the basic plasma physics problems of confinement and heating can be solved. The Scylla IV plasma has already achieved approximately the necessary temperatures and densities for a

pulsed reactor, but its plasma confinement times are about a factor of 50,000 too short for a power-producing reactor. The principal effort must now be concentrated on problems of stability and long-time confinement.

A new θ-pinch experiment, Scylla V, is proposed in order to work toward these goals. Scylla V is conceived as a toroidal device of approximately 4 meters major diameter and 12.5 cm bore. The toroidal design eliminates the end-loss problem and permits detailed study of stable confinement in toroidal geometry hitherto untried in θ-pinches.

The experiment will have a fast primary capacitor bank to provide about 70,000 gauss of magnetic field with a period of about 15 μsec and a slower secondary capacitor bank to provide a magnetic field of about 120,000 gauss with a period of 150 μsec. The planned magnetic field is slightly less than that in Scylla IV because extremely large magnetic fields are not required for study of plasma confinement and stability. The primary capacitor bank will have approximately 5 MJ (megajoule) energy storage and the secondary bank about 20 MJ.

Additional smaller capacitor banks will provide bias magnetic field, preionization, and power for stabilizing windings.

Scylla V, if successful in confining a plasma for the order of 100 microseconds, will give confinement times perhaps a factor of 10 longer than those expected for Scylla IV with the power crowbar and will also give experience with the problems involved in the "closed" toroidal geometry which is most favorable to a fusion reactor.

A program of the magnitude described here will require approximately 3 to 5 years before meaningful conclusions can be derived.

F. Content of this Report

The next few sections of this report will summarize the experiments which have led to the production of the present plasma and to a knowledge of the properties just described as well as mathematical work to correlate experiment with theory. The relationship of the Los Alamos θ-pinch experiments to those in other parts of the world will also be

discussed. In addition the relation of physical measurements of the θ-pinch plasma to those of solar astrophysics will be summarized. Following these we outline plans for further research and its relationship to the production of a reactor having a balance between thermonuclear energy production and the electrical and other energy losses connected with the magnetic containment of the plasma.

A bibliography of published work on the Scylla θ-pinch experiments is included in the references at the end of the report. The first fourteen references document the main developments up to the present time. The secondary references provide related material on the Los Alamos θ-pinch experiments.

II. EXPERIMENTAL DEVELOPMENT OF THE THETA PINCH

A. Summary of Theta Pinch Development

Previous measurements on the Scylla plasmas have been extensive and include the following:

a) Effect on the plasma properties of variation of initial gas density, mirror ratio, coil length, magnetic field strength, operating voltage and initial bias magnetic field.[3,9]

b) Establishment of shape and position of the neutron emitting fireball by a scanning neutron telescope.[3]

c) Establishment that the neutrons emitted are not characteristic of those produced by a high energy deuteron component in the radial direction (i.e., from instabilities or direct acceleration) by measurement of the neutron energy distribution from nuclear emulsion techniques.[3]

d) Establishment of a similar conclusion in the axial direction by precise measurement of the center of mass axial velocity distribution of the DD reactions from momentum analysis of the emitted protons and tritons.[6]

e) Identification of a bremsstrahlung emitting region coincident with the fireball.[4]

f) Measurement of the approximate electron temperature by differential absorption in the soft x-ray region.[4]

g) Precise measurement of the electron temperature by separating the continuum radiation from impurity line radiation by crystal diffraction in the soft x-ray region (5 - 20 Å).[5,10]

h) Measurement of the electron (and therefore ion) density in the fireball by absolute bremsstrahlung intensity measurement in the visible.[4]

i) Determination of the magnetic field in the fireball at early times by internal magnetic probes and at late times by external magnetic probes.[8,9]

j) Determination of a low value upper limit to possible trapped magnetic field in the fireball by Zeeman splitting of impurity line radiation in the ultraviolet.[7]

k) Observation that the interchange instability (rotating flute), which is observed in the high pressure plasma regime with reversed bias magnetic fields in short (10 to 30cm) compression coils, does not occur in long (~ 1m) coils.[13]

l) Measurement of plasma electron density, shape and stability with a Mach-Zehnder interferometer.[13,14]

m) Measurement of a thin sheath region separating the plasma from the confining magnetic field with Schlieren techniques.[13]

n) Operation of Scylla IV in a new low pressure regime resulting in extreme freedom from wall contamination.[14]

o) Operation in the low-density regime showing end losses to be the predominant loss mechanism. Interchange instability observed in the high-density regime is absent.[14]

For some years now, the sum total of this evidence has been that Scylla θ-pinch plasmas have characteristic values: density, 6×10^{16} ion/cm^3; electron temperature, 400 - 1200 eV according to impurity level; mean ion energies, 2 - 3.8 keV (corresponding to temperatures in Maxwellized distributions of 1.3 to 2.6 keV); and β close to unity. Neutron yields range from 5×10^6 per pulse (Scylla I) to 2×10^9 per pulse (Scylla IV) with mean neutron rates of 2 to 6×10^{12} cm^{-3} sec^{-1}. During the 2 - 3 μsec neutron emitting lifetime of the fireball, an ion characteristically makes several hundred reflections from the magnetic wall in the radial direction and an average of one to two ion-ion collisions. It can thus be classed as a confined, strongly thermonuclear reacting plasma but is not necessarily Maxwellized.

More recently Scylla IV has been operated in an entirely new low pressure regime without bias magnetic field. Interferograms taken in this low pressure, zero B_o regime, show a plasma density lower than that for the high pressure with B_o operation and reduced plasma volume. Pressure balance measurements place the mean ion energy in the 3 - 10 keV region. The low pressure operation corresponds to the original conception of Scylla behavior. The plasma parameters, in particular the remarkable temperature, are predictable from classical shock and compression considerations. Characteristic values are: density, 2×10^{16} ion/cm^3; electron temperature, 300 eV; mean ion energies, 3 to 8 keV; and β close to unity.

A more detailed review of Scylla development follows in the next sections.

B. Scylla I

The earliest Los Alamos θ-pinch device, reported first in 1958[1,2], and shown that year at the Second Geneva Conference on the Peaceful Uses of Atomic Energy, consists essentially of a 10-cm-long brass compression coil, with a ceramic discharge tube, driven by a 30-kJ capacitor bank charged to 85 kV. A cross-section of the compression coil and alumina discharge tube is shown in Fig. 2(a). The time scale of the discharge is shown by the oscillograms of Fig. 2(b). The sinusoidal current of the L-C circuit has a rise time (quarter-cycle) of 1.25 μsec and produces a maximum in-phase, magnetic field of 55 kG.

The primary means of measuring the behavior of the plasma were the neutrons and other fusion reaction products emitted by the interacting hot deuterons, and the soft x-rays, uv, and visible radiation emitted by the electrons. The lower oscillograms of Fig. 2(b) show the neutron and soft x-ray emission signals. It is seen that both emissions occur on the second half cycle of the magnetic field. This is characteristic of the high-density regime of θ-pinch operation in which the deuterium gas is weakly preionized. Fig. 3 illustrates the operation. In the first half cycle the magnetic field penetrates the weakly ionized plasma (Fig. 3(a). The plasma becomes fully ionized at the end of the first

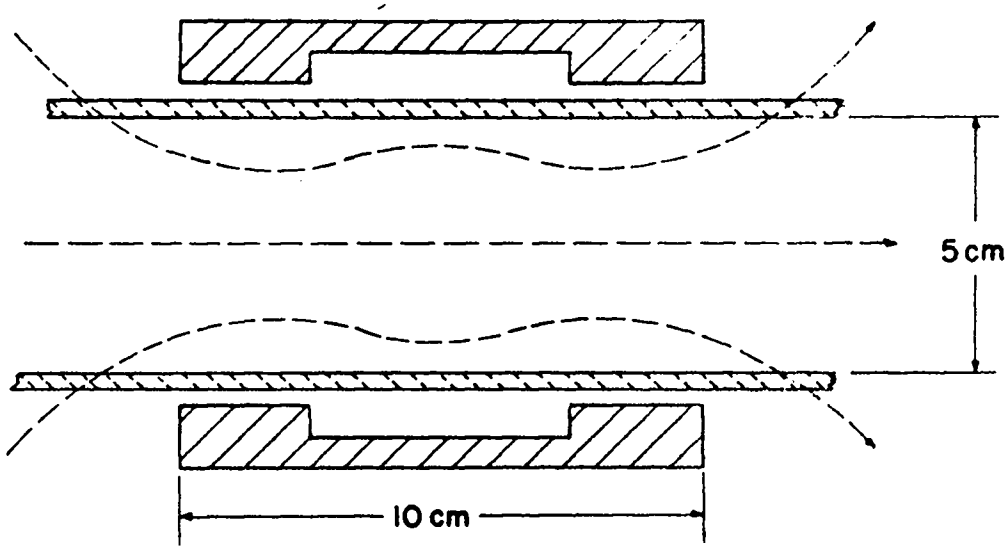

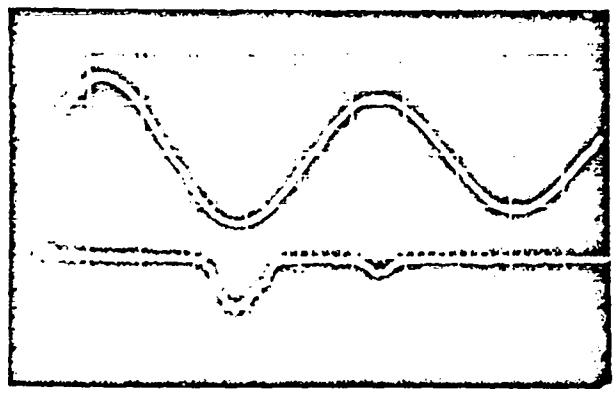

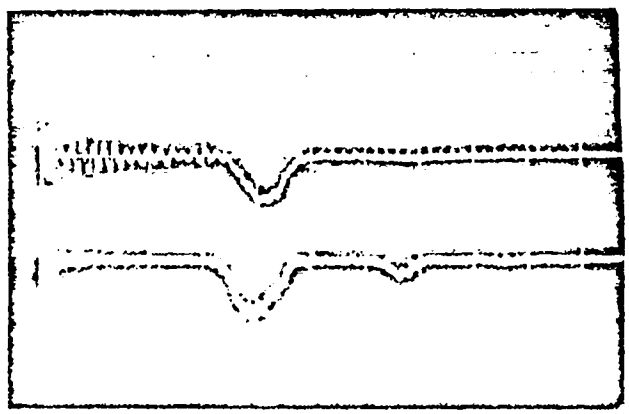

Fig. 2 (a) Gross-sectional drawing of Scylla I compression coil and discharge tube. (b) Oscillograms of compression-coil current (proportional to magnetic field) and the neutron and soft x-ray signals. The horizontal time scale is 1-μsec per division.

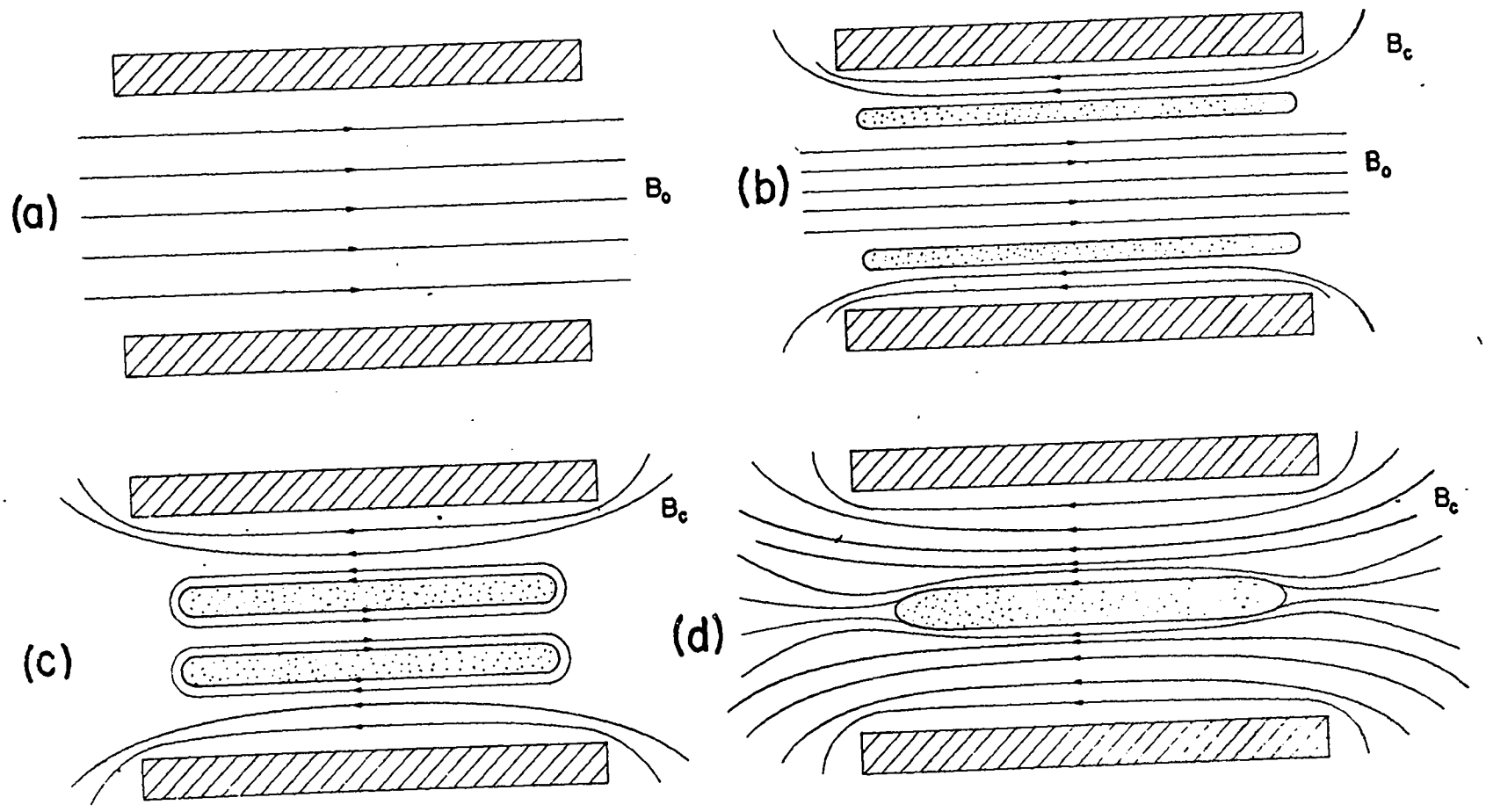

Fig. 3. Reversed trapped field diagrams, illustrating the trapping and annihilation of magnetic field inside the plasma.

half cycle and the shock of the dynamic phase occurs at the beginning of the second half cycle. In the ionization transition from the first to the second half cycle a small amount (~ 4 kG) of first half-cycle field is frozen into the now fully ionized plasma [Fig. 3(b)] to be compressed with it during the early dynamic phase of the second half cycle [Fig. 3(c)]. Thus early in the second half cycle the plasma has a field trapped inside it whose direction is opposite to that of the external field of the coil. The trapped field is then cancelled by a portion of the external field, and the magnetic energy which thereby disappears is converted into plasma energy [Fig. 3(d)]. It is this converted magnetic energy of the trapped field which accounts for most of the ion heating in the Scylla I experiment.

The earliest experiments[3] determined the neutron yield from the $D(d,n)He^3$ reaction in the plasma. Measurements of the neutron energy spectra showed their emission to be isotropic with none of the shifts of mean energy which had earlier characterized neutrons arising from instabilities in Z-pinches. Collimation measurements showed the neutron-emitting plasma to be isolated from the wall with a length of 2-cm and a diameter of 1.5 cm. Magnetic probe measurements showed the trapping of negative field from the first to the second half cycle.

Extensive measurements[4,5,10] were made of the soft x-radiation emitted by the hot plasma. Pinhole photographs of the x-ray emitting region showed it to coincide radially with the neutron emitting region.[4] Measurements of the continuum energy spectrum of the x rays with a Bragg-crystal spectrometer showed it to be of the form

$$dE/d\upsilon \propto \exp[\, -h\upsilon/kT_e\,] \qquad (1)$$

where the electron temperature is 350 eV[5]. Such a form is expected theoretically both for the bremsstrahlung continuum and for the radiative-recombination continuum which arises when free electrons are captured by impurity ions. Line spectra arising from oxygen impurity ions stripped of all but one or two electrons were also measured.[10] Both the continuous spectrum and a portion of the line spectrum are illustrated in Fig. 4. The intensity of the x-ray continuum showed the amount of oxygen contamination to be about 2%,[4] so that its radiation (in the x-ray region)

(a)

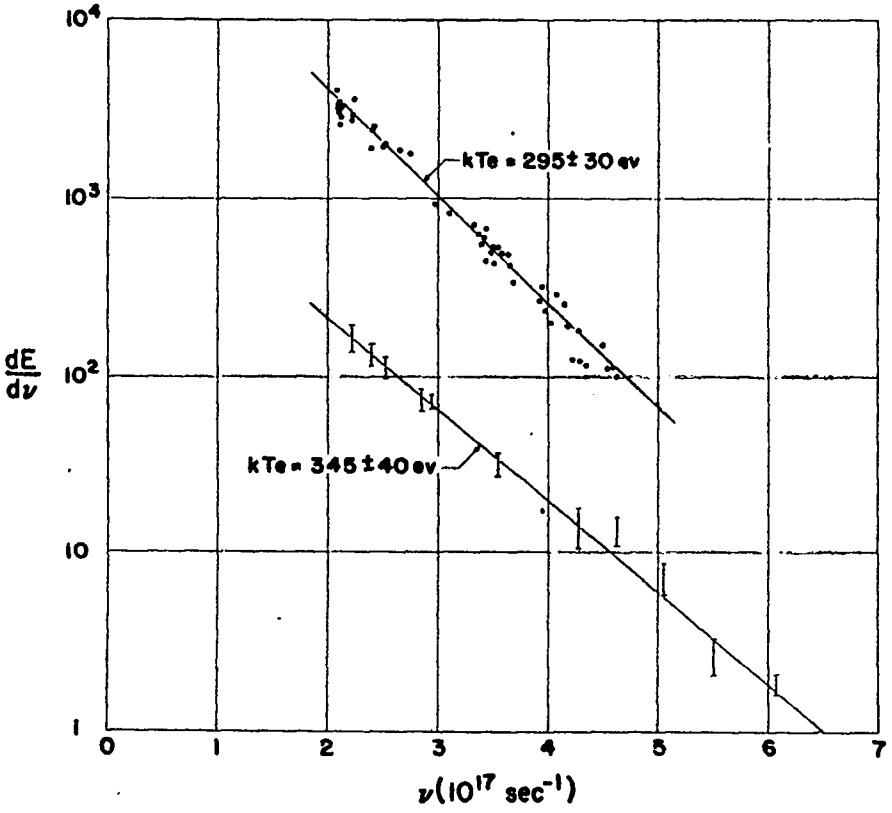

(b)

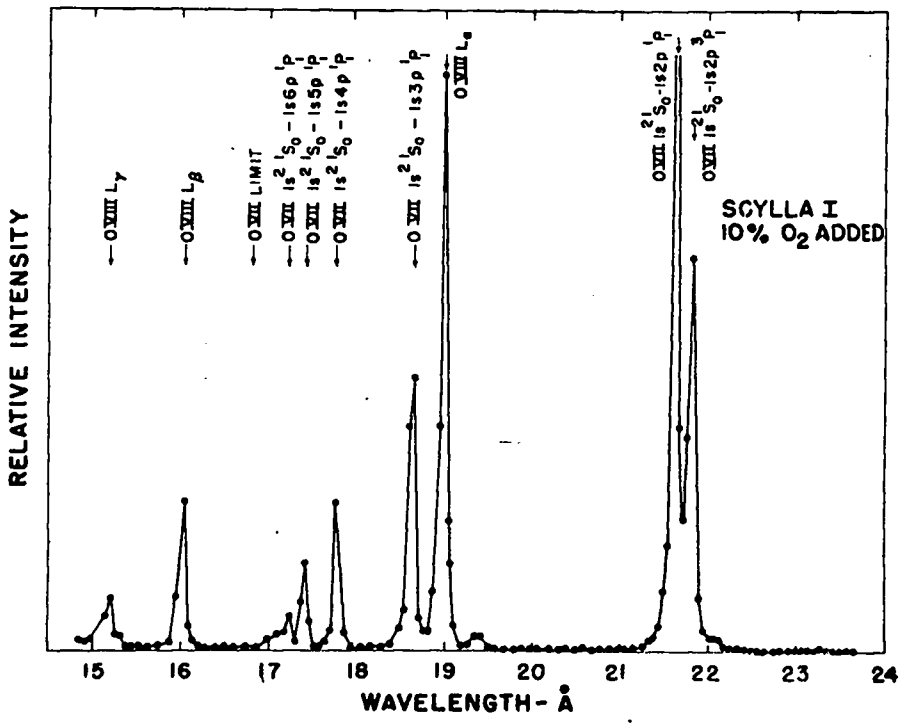

Fig. 4 (a) Continuous soft x-ray emission spectra of Scylla I with (upper curve) and without (lower curve) 10% added oxygen impurity. The logarithmic slope of the emitted energy vs. photon frequency ν determines the electron temperature. (b) A portion of the line spectrum with oxygen impurity added. Lines of HeI-like O VII and of H-like O VIII impurity ions are seen.

was two orders of magnitude in excess of bremsstrahlung. Measurement of the plasma brightness in the visible established the electron density to be 6 x 10^{16} per cm^3.[4]

The apparatus[6] used to determine the deuteron ion energies in the plasma is shown in Fig. 5. The energy spectrum of protons emitted along the axis from D(d,p)T fusion reactions occurring in the plasma was measured by dispersing the protons in a magnetic spectrometer. The proton spectra were Doppler broadened by the motion of the plasma ions. The widths measured from the spectra of Fig. 6 corresponded to plasma deuteron temperatures of 1.3 keV.

It was then possible to check two conditions of the plasma: (a) The plasma pressure $p = n(kT_e + kT_i)$ computed from the measured plasma density and temperatures was found to be equal to that of the external magnetic field B, indicating the condition

$$\beta = p/(B^2/8\pi) = 1.$$

(b) The neutron emission rate per unit volume of plasma,

$$R_n = 1/2\ n^2 \langle\sigma v\rangle$$

could then be computed and compared with the measured rate. (Here $\langle\sigma v\rangle$ is the known product of the fusion cross-section and ion velocity, averaged over a Maxwellian velocity distribution, and is a known function of ion temperature). With measured values of density and deuteron temperature the computed rate coincided with the measured one. Conditions (a) and (b) strongly indicated that the conditions of a thermonuclear plasma had been met: namely that the randomly moving ions which produce the plasma pressure had sufficient energy to produce the observed fusion neutrons. This is contrasted to the spurious situation in which a few very high-energy ions in a relatively cold plasma produce the neutrons and have not enough energy density to account for the plasma pressure.

To obtain a further check on this condition, measurements were made of the magnetic field inside the plasma, which should be small or zero if the ion and electron pressures are indeed equal to the external magnetic pressure. Magnetic probe measurements showed this to be the case early in the compression,[3, 9] but were cast in doubt by the fact that the probe's presence in the plasma disturbed

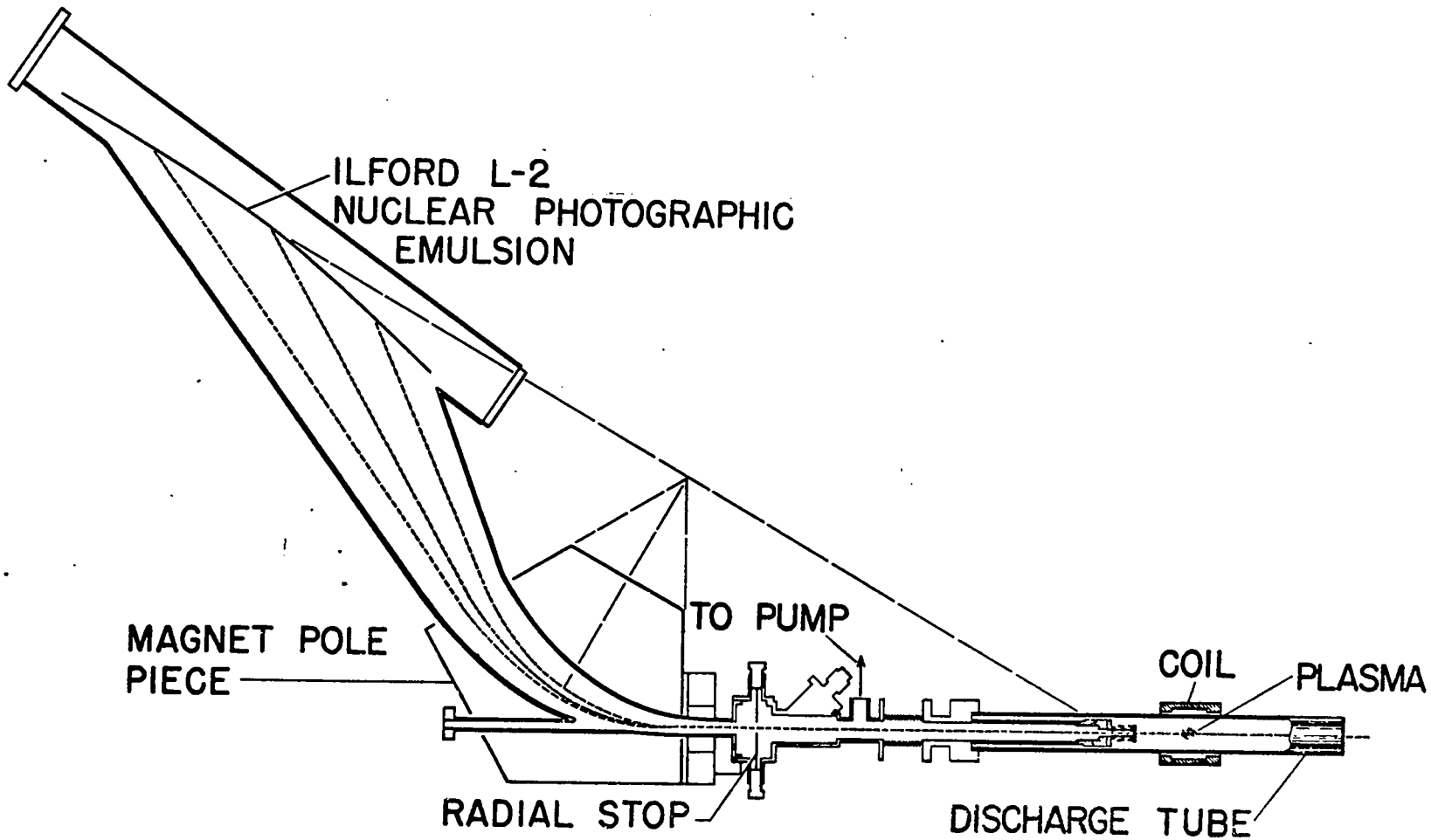

Fig. 5 Diagram of the apparatus for measuring the mean ion energy of Scylla I. The emitting plasma ellipsoid is at the center of the coil.

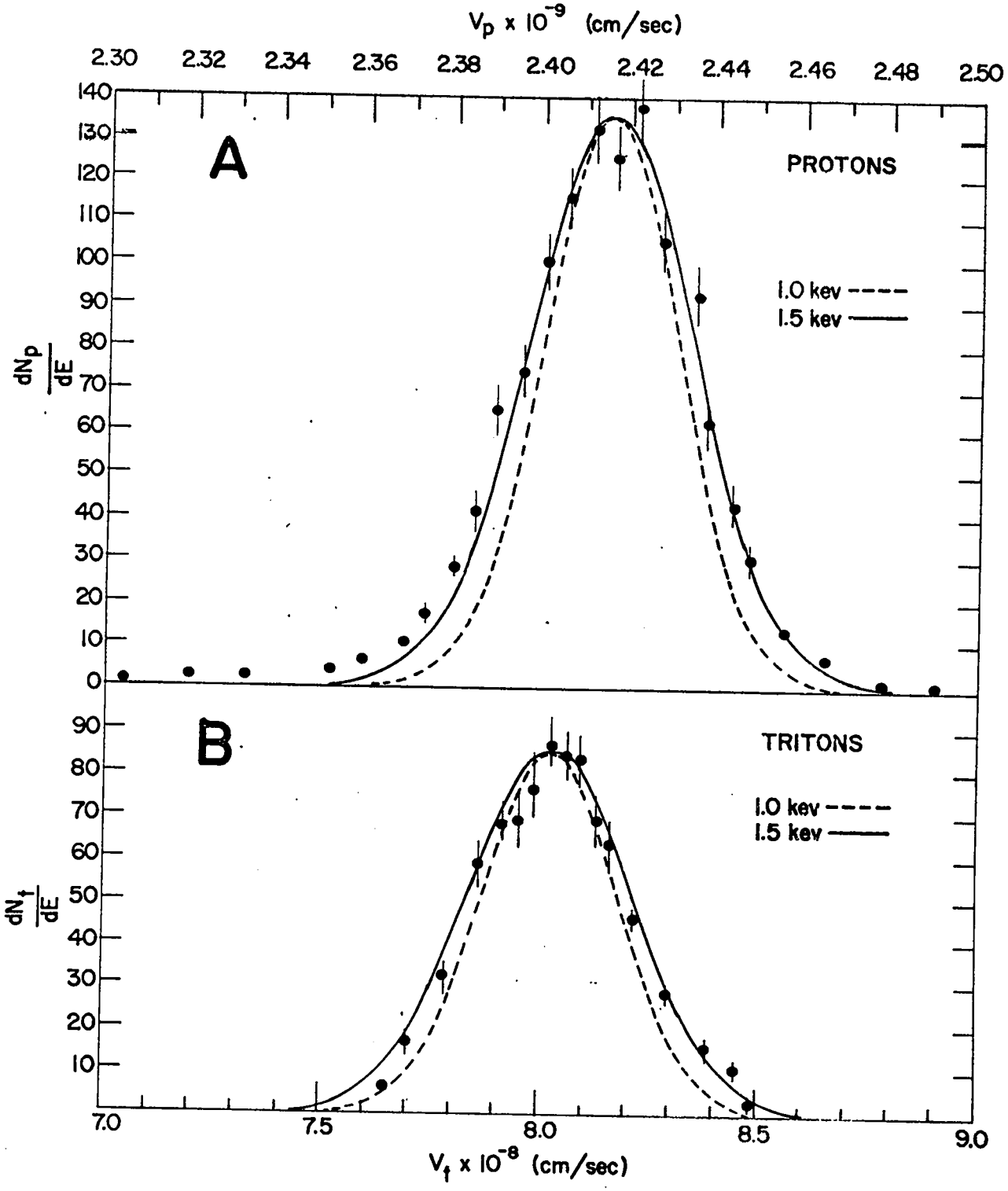

Fig. 6 Spectra of d-d protons and tritons emitted axially from the Scylla I plasma as measured in the arrangement of Fig. 5. Theoretical curves computed for Maxwellian ion velocity distributions of temperatures 1.0 and 1.5 keV are compared with the measured data points.

it near the maximum of the quiescent phase. This question was resolved by measuring the Zeeman splitting of a spectral line from trace carbon impurity ions (CV, a HeI-like ion) during the rise of the compressing magnetic field.[7] The splitting was zero and the internal magnetic field negligibly small. The fact that this condition of $\beta = 1$ persisted throughout most of the compression was proved by magnetic loop measurements[8] which showed the magnetic flux in the plasma to continue undisturbed from its low values at the time of the Zeeman and probe measurements.

Further experiments[9] showed that the θ-pinch behavior just described for the second half cycle could equally well be produced on the first half cycle, provided that the plasma was strongly preionized to have sufficient conductivity to allow the shock of the dynamic phase to form in the first half cycle. The reversed trapped field was applied independently at the beginning of the discharge, and it was verified that neutron emission in the high-pressure regime depended on the presence of negative trapped field.[15] The field mixing was shown to occur during the dynamic phase of the discharge. A proposed mechanism for the field mixing has been discussed in Ref. 16. Only very small neutron emission occurred when there was no trapped field.

The Doppler broadening measurements of deuteron ion energies, discussed above (Figs. 5 and 6) were extended to trace impurity ions by measuring the widths of the soft x-ray and uv spectral lines of C V, O VIII, and Ne IX.[10] The results showed that the temperatures increased linearly with ion mass, corresponding to approximately equal random velocities for each ionic species rather than equal temperatures. The lack of collisional equilibrium thus indicated is believed to be characteristic of plasma in the high density regime whose ion heating arises predominantly from reversed-field annihilation.

C. Scylla III

Scylla III was a larger experiment[11] in which the capacitor energy was increased from 30 to 180 kJ and the coil length from its Scylla I value of 10 cm to as much as 26 cm. The ion and electron temperatures increased to approximately 2 keV and 500 eV respectively. The most important new phenomenon observed was a flute, or interchange, instability of the plasma, which was now

elongated to approximate a cylinder, rather than the short ellipsoid of Scylla I.

The generally accepted model[17] of the flute instability in the low-β limit is illustrated in Fig. 7. Small disturbances of wavelength λ on a horizontal interface under the influence of gravitational acceleration g will grow with e-folding time,

$$\tau = (\lambda/2\pi g)^{\frac{1}{2}}. \qquad (2)$$

In the case of a plasma surrounded by B lines having radius of curvature R the centrifugal acceleration v^2/R of ions running along the B lines drives instabilities in a similar way. For two-fold symmetry their wavelength is $\lambda = \pi r_p$, and the corresponding growth rate is

$$\tau = (r_p R/2v^2)^{\frac{1}{2}} \qquad (3)$$

where r_p is the plasma radius and v the ion thermal velocity. The m = 2 flute shape for a distorted plasma cylinder is shown in the lower-most diagram of Fig. 7.

The Scylla III plasma, when driven to energy densities greater than that of Scylla I showed the m = 2 flute instability with a superimposed rotation of the plasma about the axis.[11] (This instability accounted for the failure of an earlier attempt, called Scylla II, to increase the energy of the Scylla I plasma by applying a stronger field of longer period to its short coil). Figures 8(a) and 8(d) are streak photographs taken from the end of the discharge tube. They show a radial slice of the plasma as a function of time with a characteristic corkscrew appearance, showing the growing magnitude of the instability. The Kerr-cell photographs of 8(b) and 8(c), also viewing end-on, show the elliptical distortion of the plasma.[18]

A calculation of the e-folding time of the instability showed it to be an order of magnitude slower than indicated by the simple, hydromagnetic theory. A plausible explanation of the slower growth rate is the stabilizing effect of the finite ion gyro radius.[19] The criterion for applicability of this effect was closely fitted by the Scylla III plasma. It was also observed

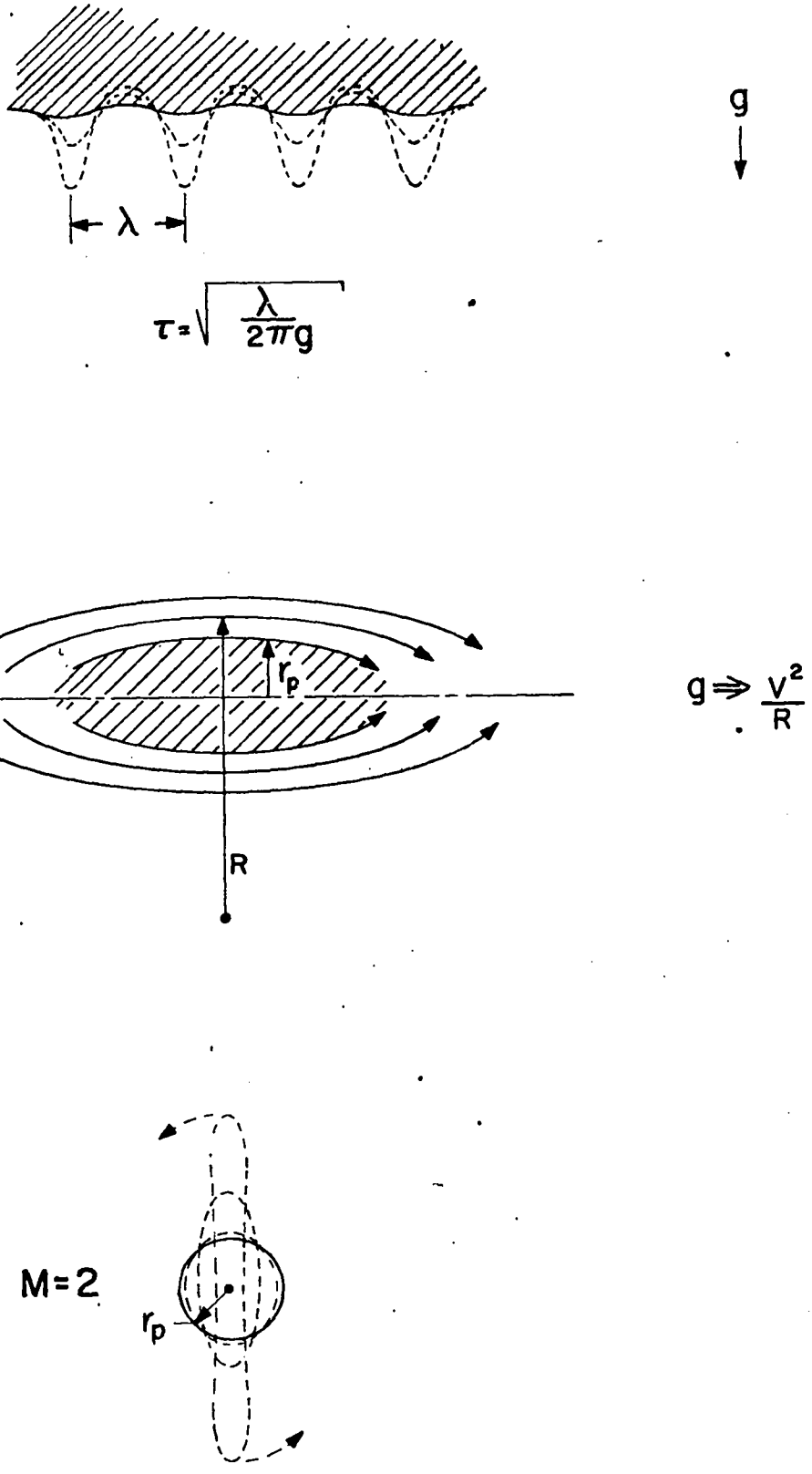

Fig. 7 Model of Rayleigh-Taylor instability (upper diagram) for a plane fluid interface and plasma flute instability (lower diagram) in the presence of curved magnetic lines.

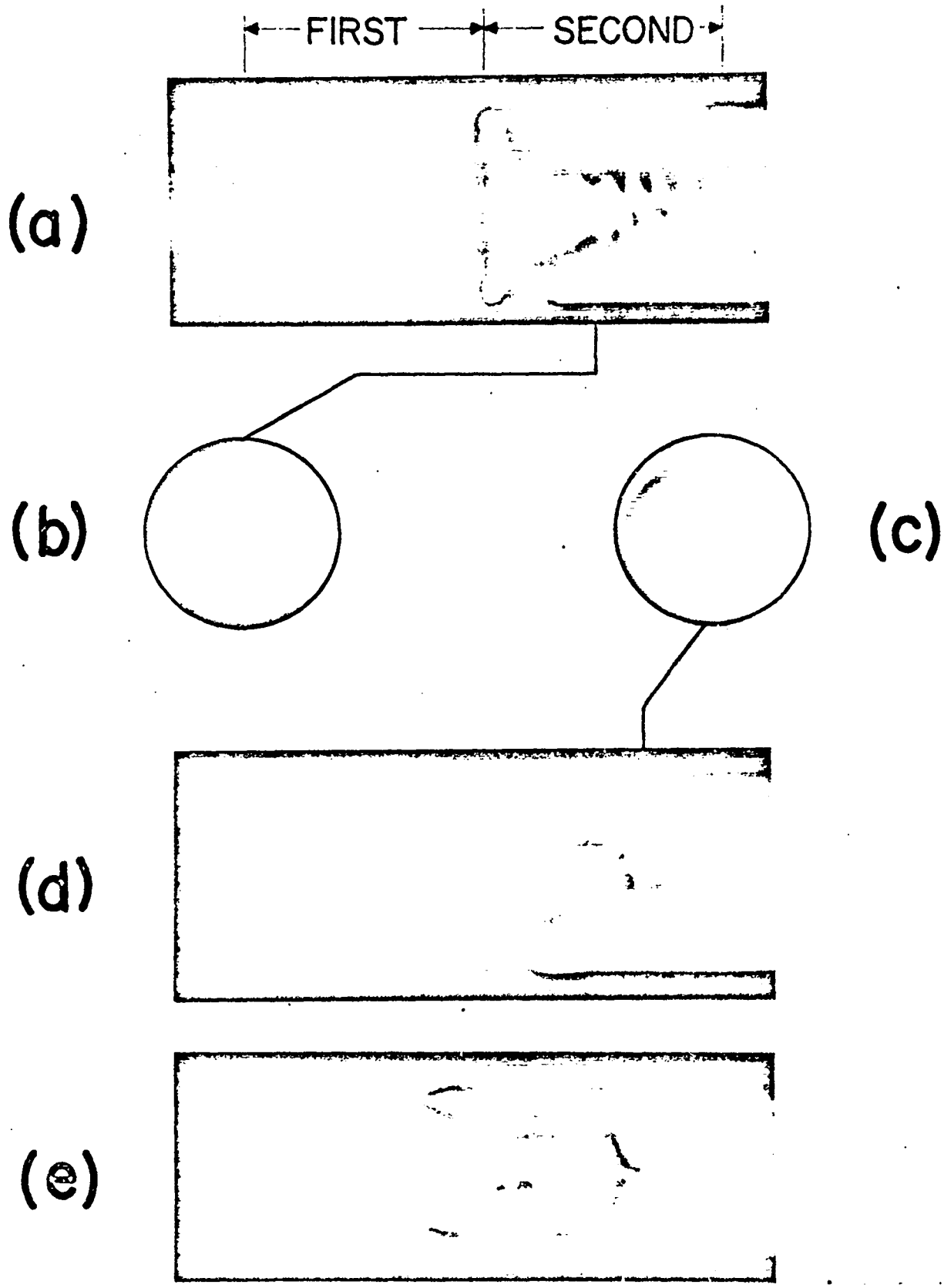

Fig. 8 Photographs of the Scylla III plasma. (a) and (d) are streak-camera, end-on photographs of the rotating flute instability in Scylla III. (b) and (c) are Kerr-cell photographs of the plasma cross sections at the times indicated. The half-cycle duration is 5 μsec.

that the instability became less violent as the coil length was increased, corresponding to increasing R in Eq. (3).

In Ref. 12 the effects on the plasma of the hexapolar magnetic lines from wires parallel to the pinch axis are described. Additional magnetic lines of six-fold symmetry were superimposed on the longitudinal compression field perpendicular to it and convex to the plasma as shown in Fig. 9.[12] This is a particular example of what are now recognized as non-zero minimum, flute-stable, magnetic geometries. It was used in an attempt to stabilize the flute instability of Scylla III. A disadvantage of the particular configuration is that magnetic lines necessarily intersect the discharge tube wall. The observed flute stabilizing effect of the hexapole, Fig. 8(e), was slight but it constrained the plasma strongly to the discharge axis against drifts (like that of Fig. 8(a)) arising from magnetic inhomogeneities due to feed-point asymmetries of the compression coil. Drift of the plasma toward the feed-point due to asymmetry in the current feed had been observed early in the Scylla I experiments and had been corrected by placing a straight section of transmission line leading to the coil. This allowed the current to distribute itself properly to produce a uniform magnetic field in the coil. The drift seen in Fig. 8(a) is probably due to a small residue of feed-point asymmetry. It is remarkable that no deleterious effects on the plasma were observed from the effects of the hexapole magnetic lines intersecting the discharge-tube wall.

D. Scylla IV

1. General Characteristics - Scylla IV, having capacitor energy storage of 3.8 MJ, was built primarily in order to increase the containment time of the plasma by an order of magnitude over its value in the Scylla III experiment. The magnetic half cycle of 50 μsec is long enough that plasma containment should no longer be determined by the time during which field is applied but rather by the intrinsic properties of the plasma.

The apparatus consists of two main capacitor banks, driving a coil of 1-meter length. The primary bank (570 kJ, at 50 kV) drives the dynamic phase of the pinch and provides compression to 100 kG during its 7.4-μsec half period.

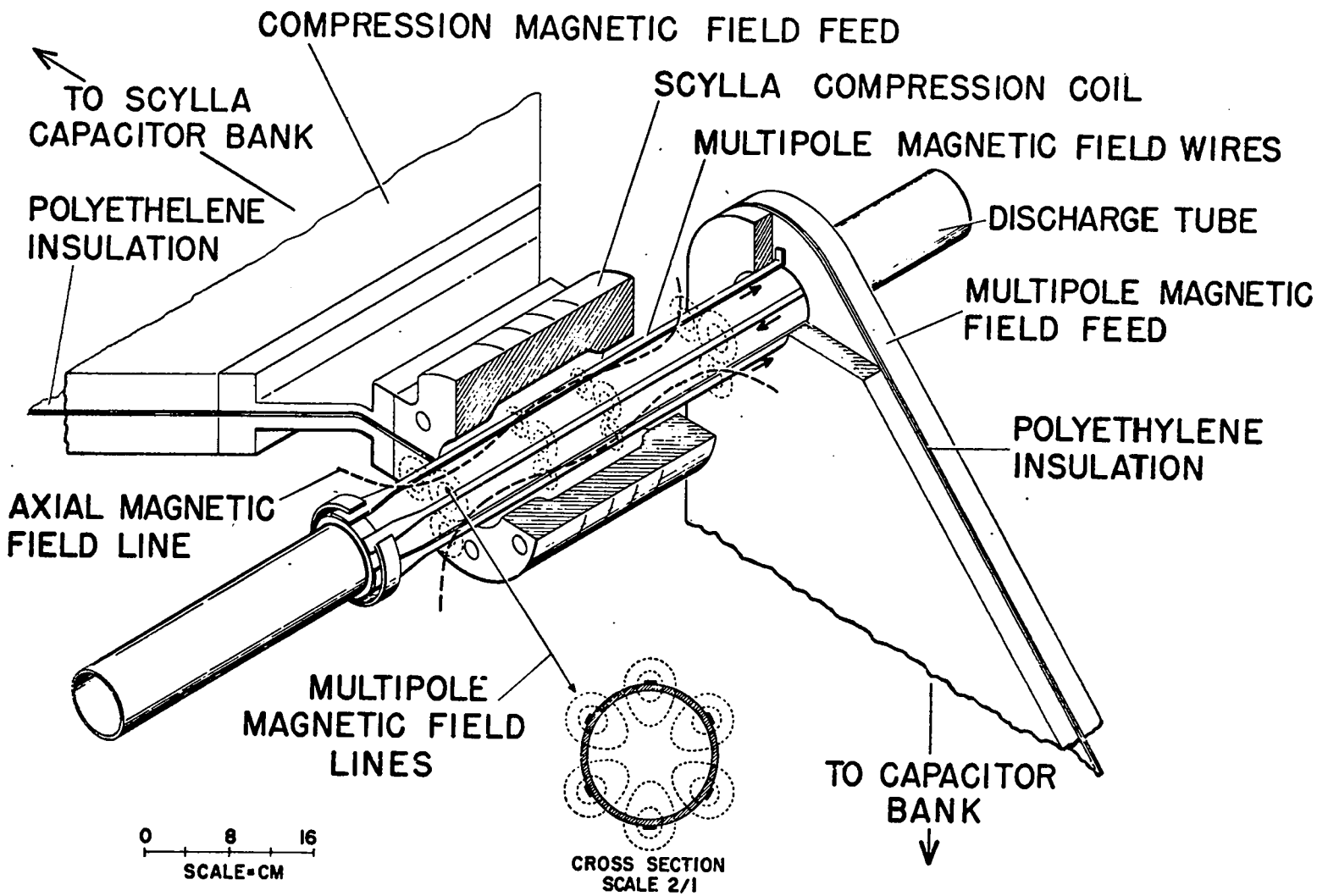

Fig. 9 Diagram of apparatus for applying a hexapolar field to the Scylla III plasma. The six wires parallel to the pinch axis apply magnetic lines, in radial planes, which are convex to the plasma.

The power crowbar (secondary) bank (3.0 MJ, at 20 kV) provides further compression to 200 kG during the quiescent phase, with a 50-μsec half period. A schematic side view of the apparatus is shown in Fig. 10, and a circuit diagram in Fig. 11. The circuit diagram also shows smaller capacitor banks for preionizing the plasma and supplying bias field. The banks are switched in the following order: bias field bank, preionization bank, primary banks, power crowbar bank. The crowbar spark gap provides a short circuit on the compression coil to keep its current from reversing (which otherwise damages discharge tubes by releasing plasma to the wall). A photograph of the front end of the machine is shown in Fig. 12. Plasma experiments[13], [14] have so far been performed without the power crowbar bank of capacitors. The plasma properties so determined will be summarized below.

2. Measurements of Plasma Shape and Stability - When Scylla IV was excited in the high-density regime, it produced plasma having roughly the same properties as the Scylla III plasma (T_e = 1.0 keV, T_i = 2.5 keV, $n \approx 5 \times 10^{16}$ cm^{-3}), except that it showed neither the rotating flute instability nor the slow drift to the tube wall that characterized the smaller experiment.[13] The stability (at least during the 7-μsec half-period) was expected from the trend of the Scylla III data, which indicated that a long plasma would be stable. In addition the plasma showed a sharp radial boundary separating it from the magnetic field. This is illustrated in Fig. 13. The end-on shadowgram and the deflection-mapping photograph both show the refractive effects of the abrupt change of electron density at the surface of the plasma and indicate a boundary thickness of less than 1 mm. This is approximately equal to the ion gyro radius for the cases shown.

3. The Low Density Regime - In the course of the Scylla experiments the "low density" regime discovered by the General Electric group[21] was extensively investigated.[14] By using strongly preionized plasmas at filling pressures as low as 10^{-2} torr (as opposed to $\sim 10^{-1}$ torr in the high density regime) neutron-emitting plasmas are produced without benefit of trapped-reversed-field heating.[22] Such plasmas should present a realization of the ideal theoretical dynamic pinch in which a shock wave in the dynamic phase produces heating through elementary collisional processes, followed by calculable magnetic compression. Comparisons

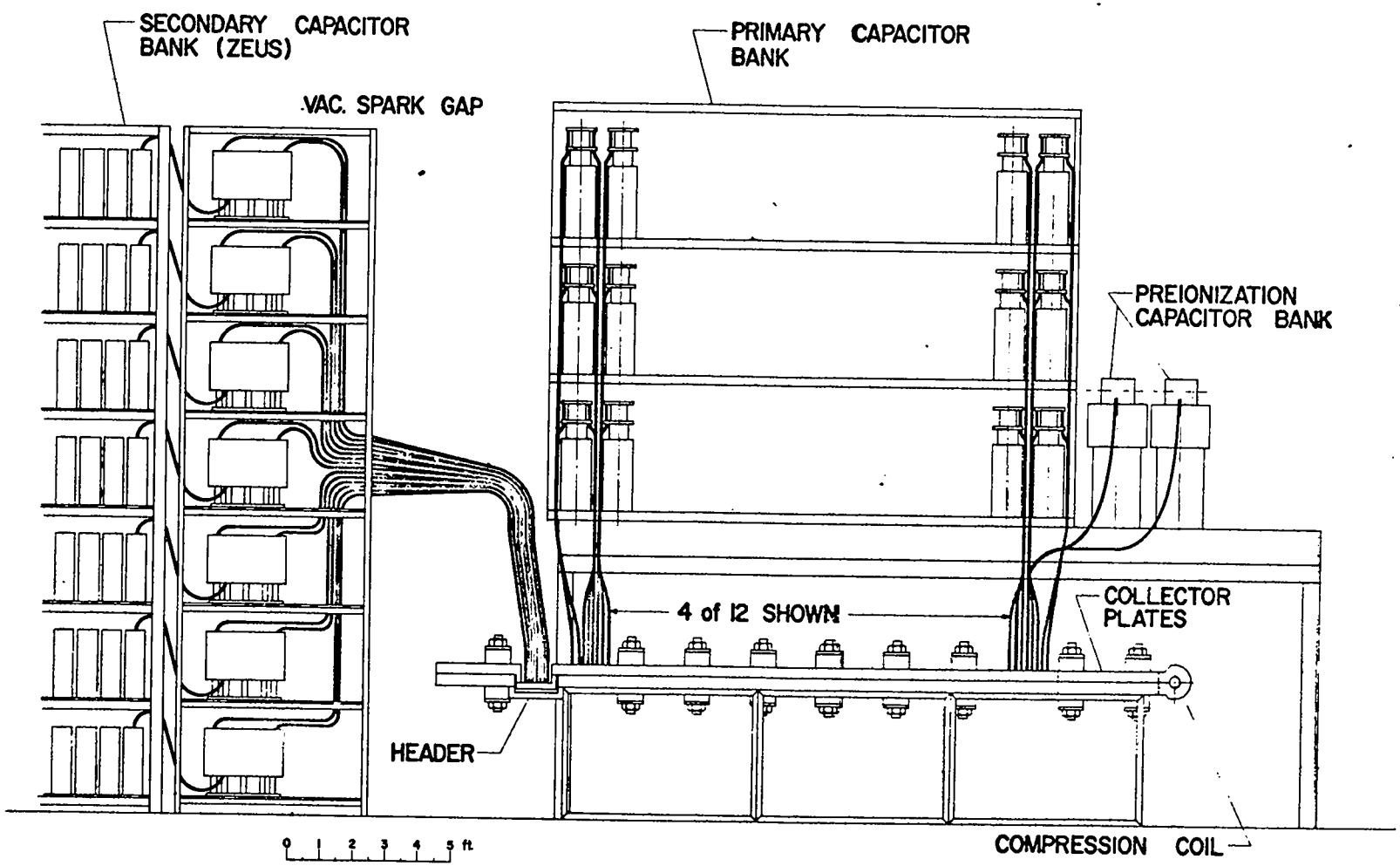

Fig. 10 Side elevation of the Scylla IV experiment. Only the front portion of the secondary (3 MJ) bank is shown. The collector plates are made of 3-in. aluminum alloy.

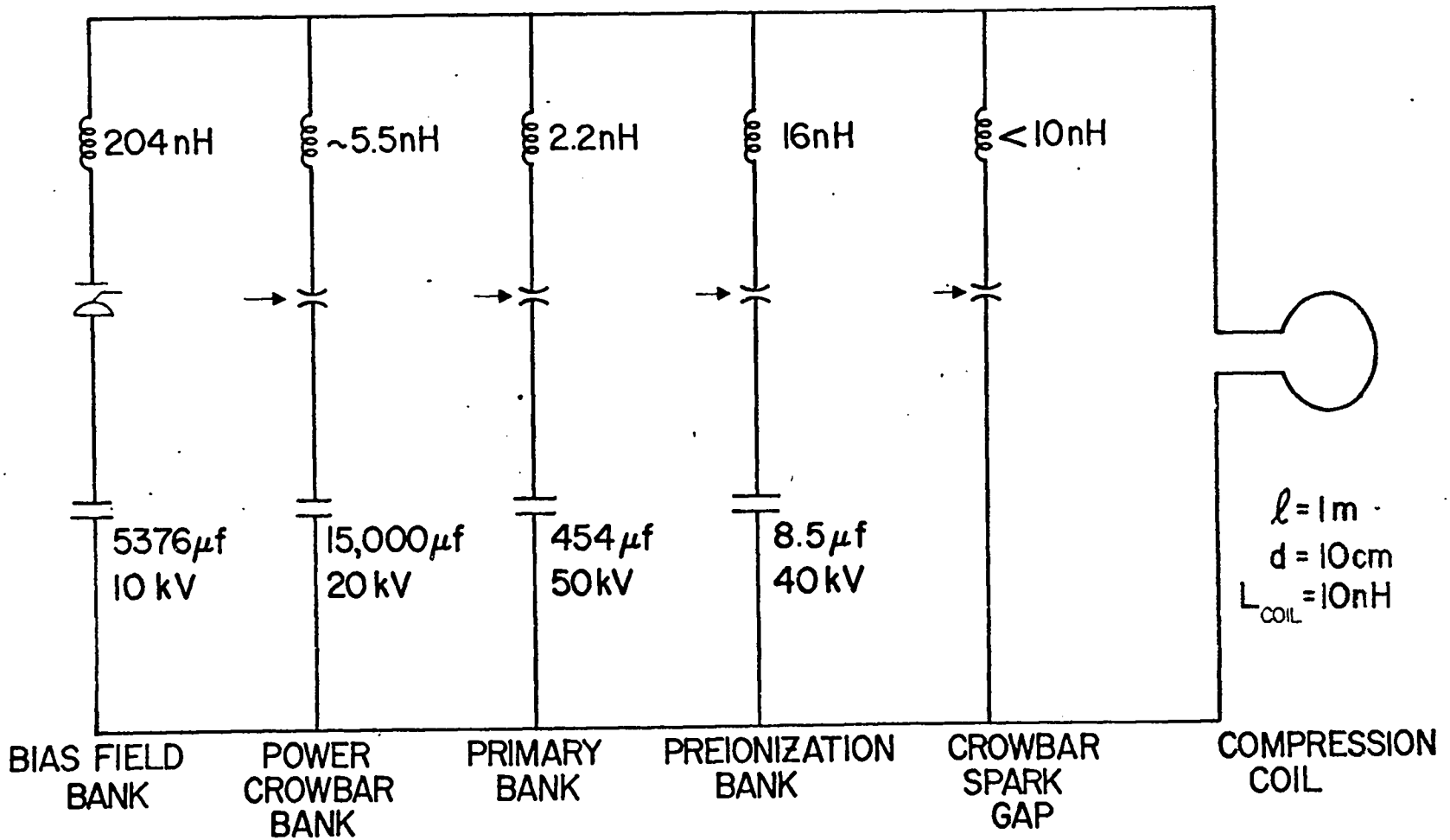

Fig. 11 Schematic circuit diagram of the Scylla IV experiment.

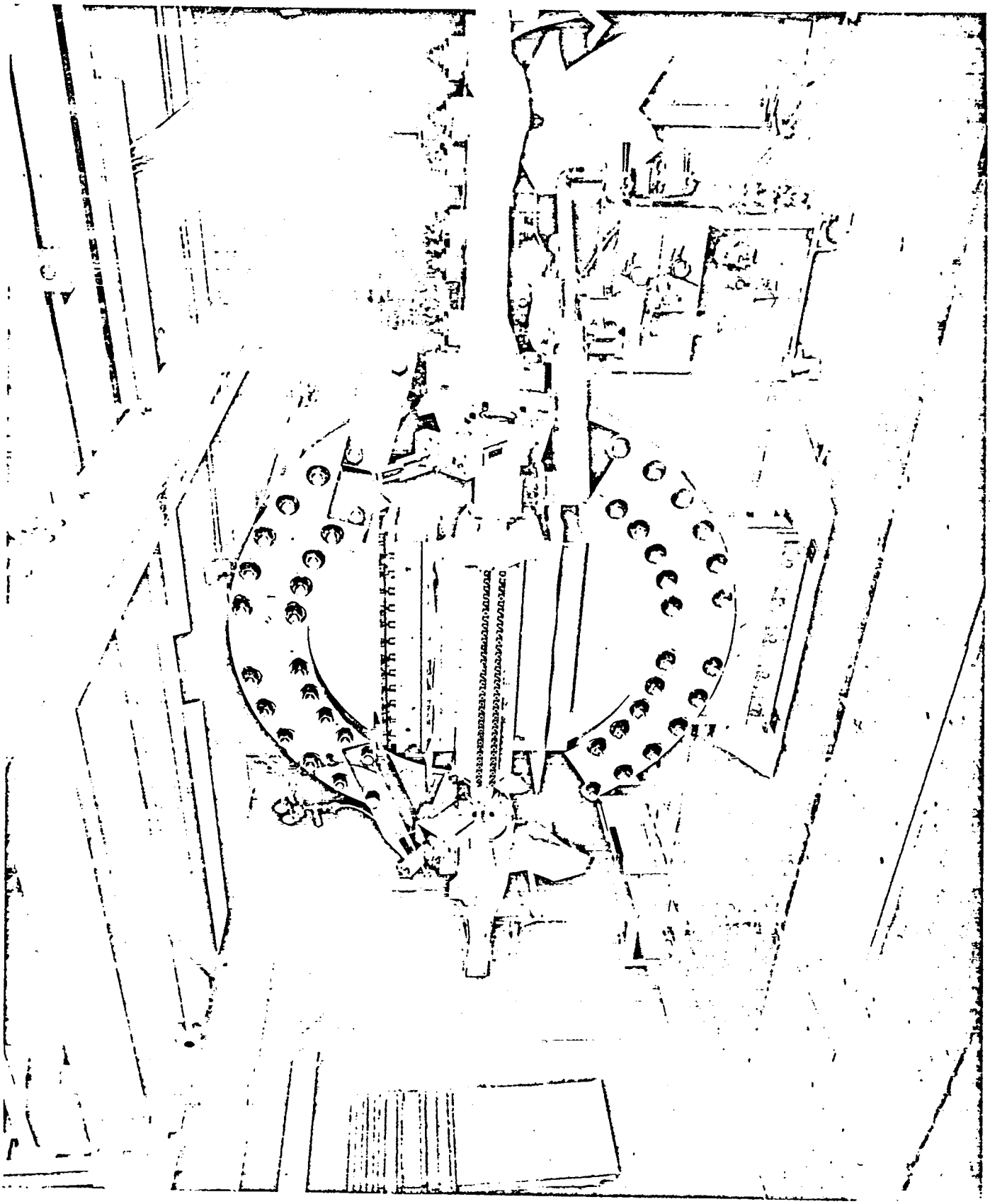

Fig. 12 Front end of Scylla IV. The one-meter aluminum compression coil bolts to the current collector plates which consist of 3-in. thick aluminum alloy, held together by 170 steel bolts (seen in the right rear). The large circular piece is a clamp to balance the 1600 atmospheres of magnetic pressure between the collector plates at the coil feed slot.

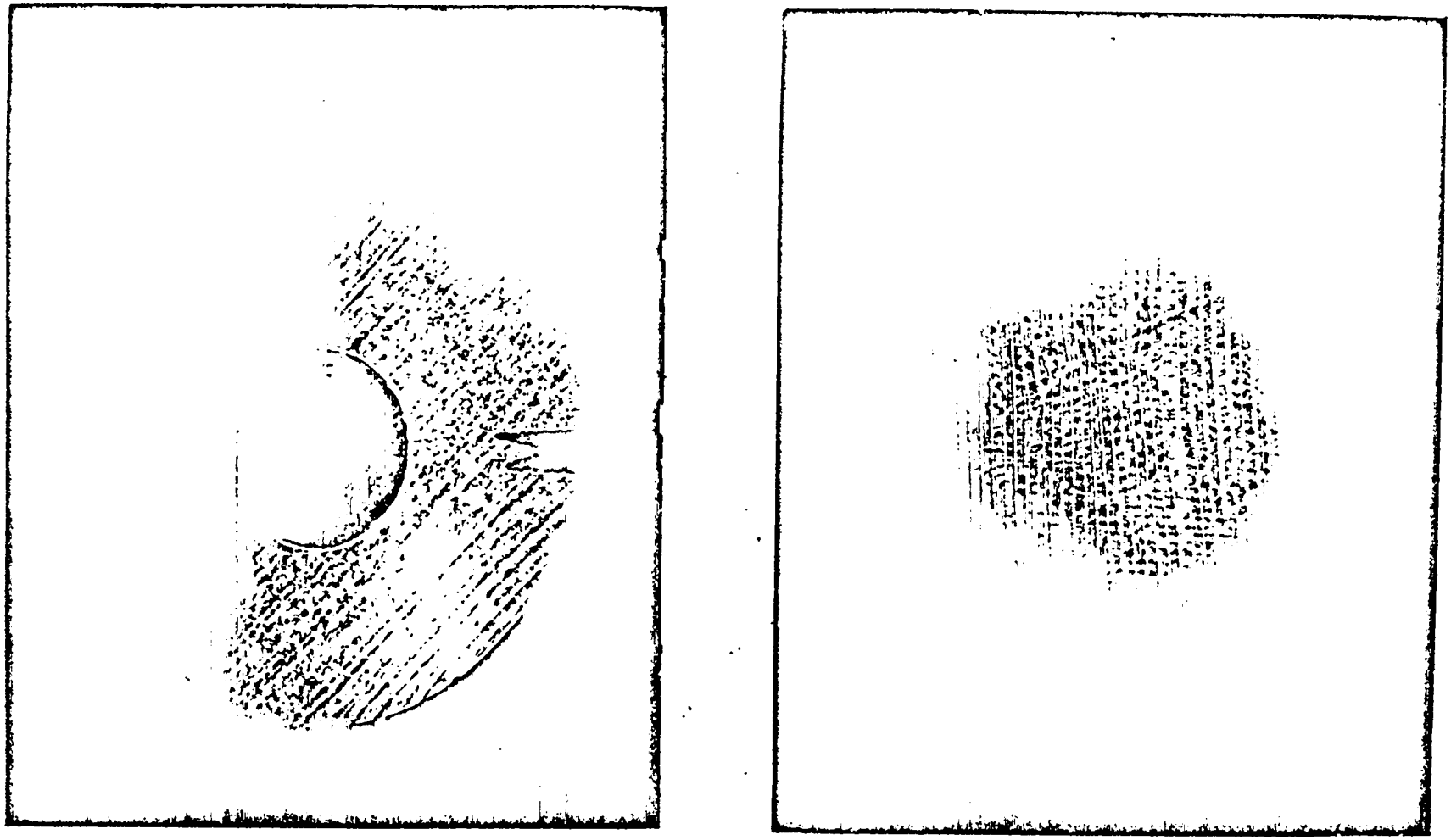

(a) (b)

Fig. 13 (a) A shadowgram of the Scylla IV plasma at peak compression taken in parallel red (ruby laser) light. Regions where the second derivative of electron density gradient is large serve as lenses to focus the rays on the photographic plate, thus showing the boundary of the plasma. (b) The compressed plasma as seen in deflection mapping by means of grid lines ruled on a window between the plasma and a camera. Parallel light is deflected inward by density gradients on the surface of the plasma, producing kinks in the grid lines. One can see the circular plasma outline in the kinks of the grid lines.

of experimental data with theoretical calculations (cf. Section III below) indicate that this is indeed the case. In addition the radiation loss from the plasma in the low density mode has been measured[14] and found to be only about a factor two higher than that of pure deuterium bremsstrahlung, indicating that impurity levels are about 1/50 those of the high density mode. The plasma of the low density regime also appears to be stabler, remaining undistorted under circumstances where the plasma of the high density regime develops 3-fold flutes.

Under the assumption of $\beta = 1$, deuteron temperatures as great as 8 keV have been deduced at filling pressures of 0.01 torr in Scylla IV (see Table II).

4. Plasma Interferometry and End Losses - The technique of optical interferometry, highly developed in the field of aerodynamics, has been used to study the Scylla IV plasma. The index of refraction of the electrons is sufficient to distort a plane wave front of light as it passes along the plasma. In an interferometer the distortion of the wavefront can be made to give a direct measure both of the electron density and the cross sectional shape of the plasma. The index of refraction of a plasma with negligible collisions is

$$N = [1 - \omega_p^2/\omega^2]^{\frac{1}{2}} , \tag{4}$$

where

$$\omega_p = \left(\frac{4\pi n_e e^2}{mc^2} \right)^{\frac{1}{2}} \tag{5}$$

is the electron plasma frequency and ω is the angular frequency of the refracted light. For a plasma of length, L the difference in optical path length between the two paths is

$$\Delta P = (N-1)L/\lambda = (r_e\lambda/2\pi) \int_o^L n_e d\ell . \tag{6}$$

Here r_e = classical electron radius, and λ, the wavelength of light, are constants of the experiment, so that ΔP measures the integral of electron density n_e over the plasma length directly.

Figure 14 shows how measurements of Scylla IV are made with a Mach-Zehnder interferometer.[23] A beam of light from a ruby laser enters the interferometer

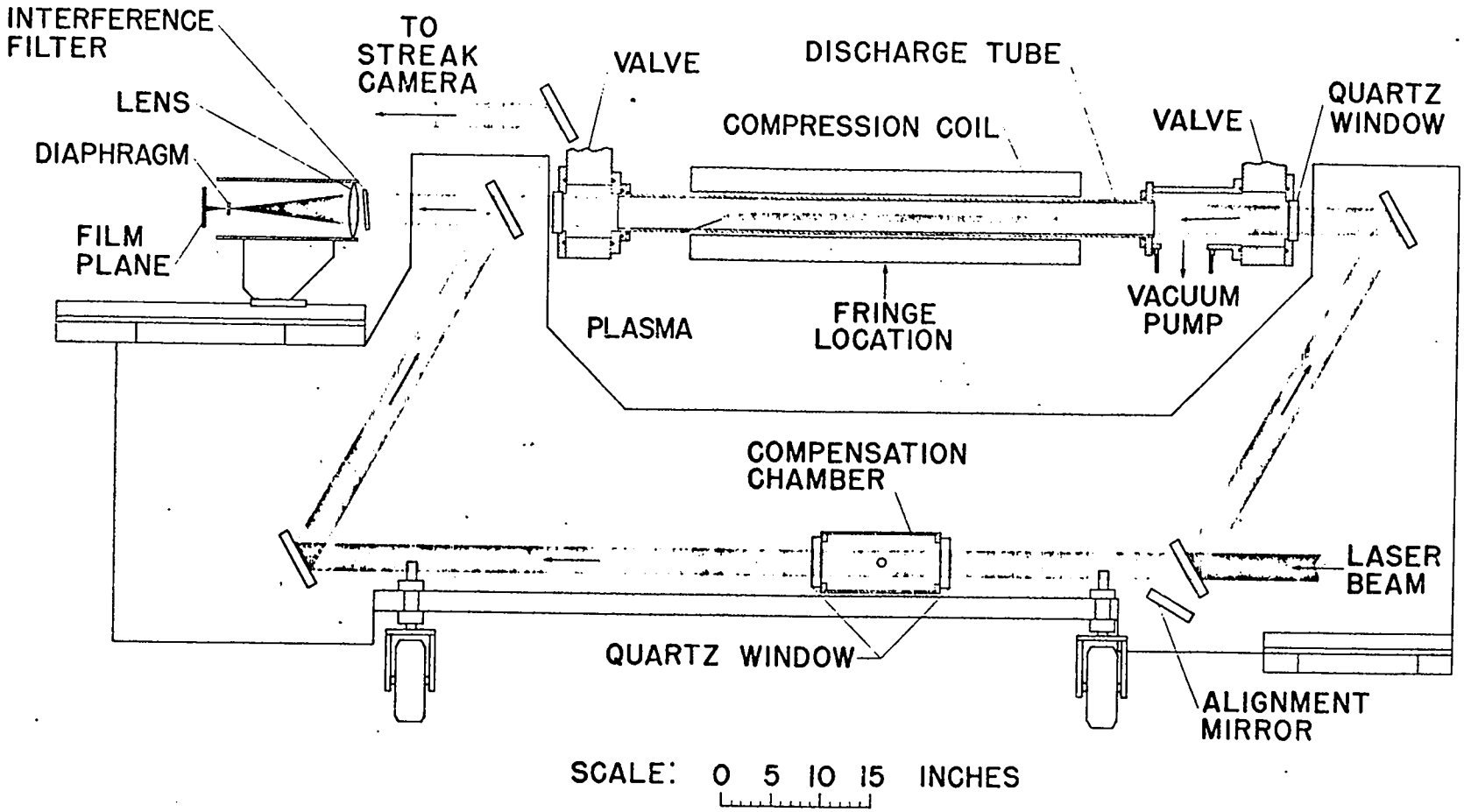

Fig. 14 Diagram of the Scylla IV discharge tube and Mach-Zehnder interferometer used for making plasma density measurements.

at the lower left and is split into two equal beams. The lower beam proceeds undistorted, while the upper beam is again deflected and traverses the plasma. Both beams are then reunited at the final beam splitter and sent into a camera which records the fringes representing interference of the two beams. With no plasma in the θ-pinch discharge tube, the wavefront of the upper beam remains plane, and the mirrors are adjusted to give straight fringes. With plasma a characteristic fringe distortion, analogous to a contour map, is produced.

Typical interferograms are shown in Figs. 15 and 16. The circular outline of the plasma is clearly visible. The interferograms of Fig. 15 depict the high pressure regime of Scylla IV. Figures 15(a) and 15(d) represent the normal plasma configuration of the plasma at peak compression with B_o. Figure 15(c) was taken very early in the discharge and shows the initial shock wave moving inward. Figure 15(b) is an unstable case, deliberately produced by removing the bias magnetic field with high pressure (125 m torr) deuterium filling. The number of fringes increases up to the time of peak compression (3.4 μsec) and then decreases as the magnetic confining field decreases but the area of the plasma remains approximately constant. The decrease of the number of fringes after peak field shows a loss of plasma, which is apparently out the ends of the coil along magnetic field lines.

It is possible to measure the plasma loss rate directly, since a radial integration of the fringes yields the total number of particles in the compressed plasma, independent of any assumption about its length. Extensive measurements in the low density regime[14] show containment (e-folding) times, τ_c, varying from about 2 to 30 μsec, depending on plasma conditions as shown in Table I. The time τ_c characterizes the containment time during the rise of the field. The loss of particles increases during the decay of the magnetic field. Table I also gives estimates of the size of the end holes through which plasma is lost. In the case of a coil without magnetic mirrors the effective hole radius r_E is found to be about equal to one ion gyro-radius r_d in the compression field. This represents a reduction by an order of magnitude of the loss rate from the value it would have if the end holes had radii equal to that of the plasma at its midplane.

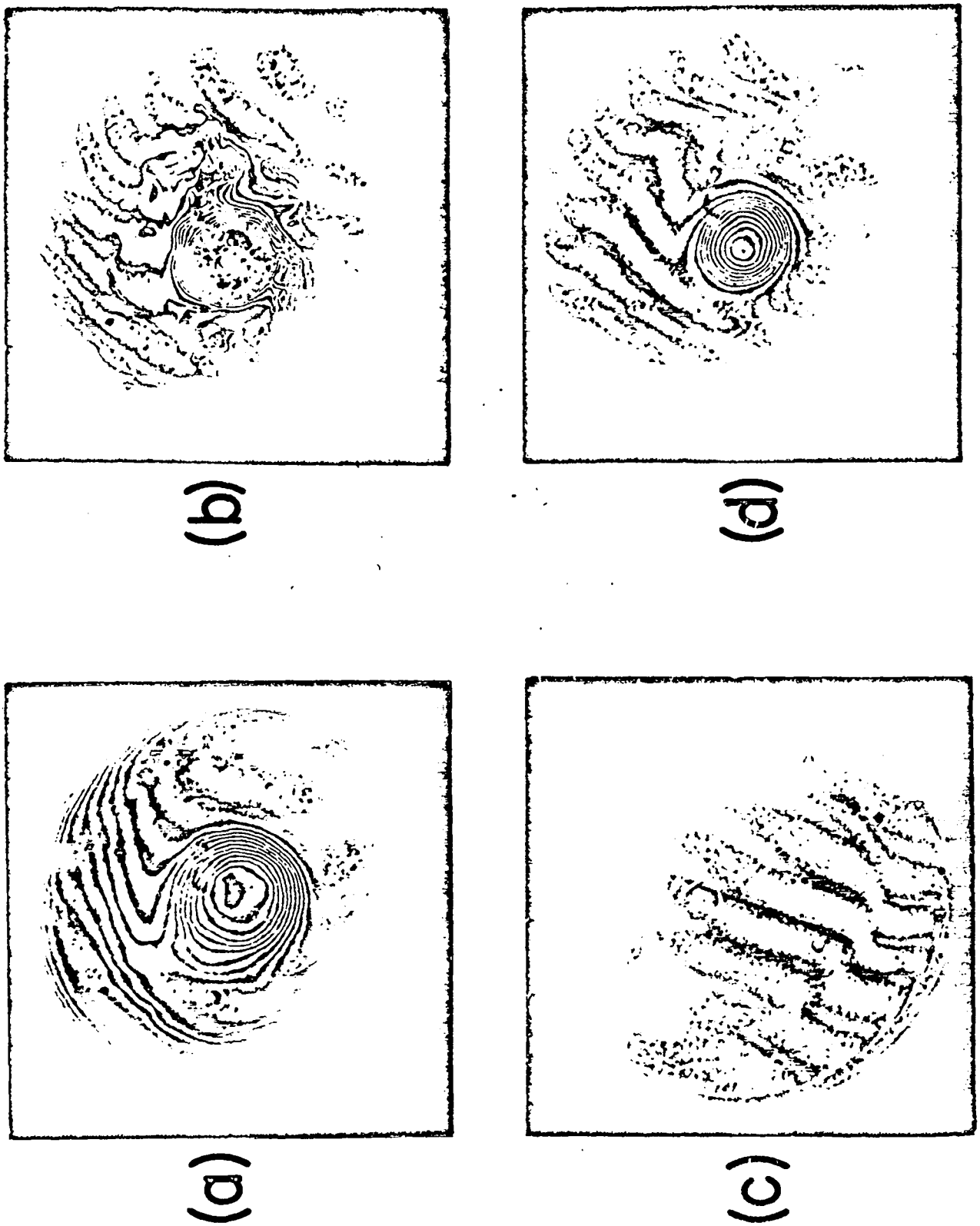

Fig. 15 Mach-Zehnder interferograms taken in the high pressure regime. (a) at 5.0 kG bias magnetic field and (d) at 1.2 kG bias magnetic field are both at peak compression and represent normal hot plasma. (c) was taken very early in the discharge and shows the initial shock wave moving inward. (b) is an unstable case deliberately produced by removing the bias magnetic field with 125 m torr deuterium filling.

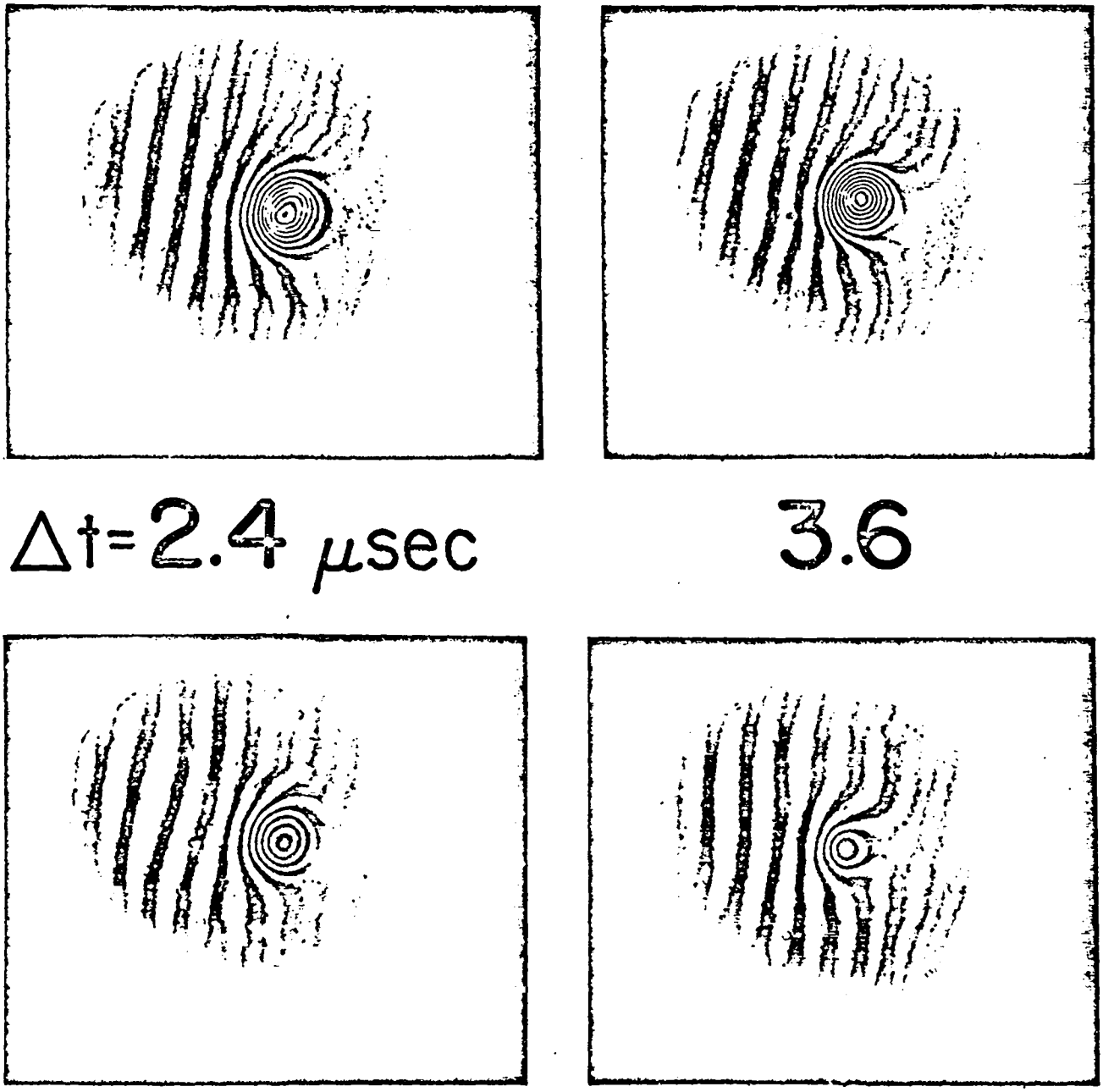

Fig. 16 Interferograms of Scylla IV in the low-pressure regime (25 m torr filling pressure) without bias magnetic field at the times indicated. The peak magnetic field is reached at 3.6 sec. Loss of plasma out the ends of the discharge is indicated by the decreasing number of fringes after peak magnetic field.

TABLE I

Comparison of the Particle Loss Aperture Radius r_E With Deuteron Ion Larmor Radius r_d

P_{D_a} (m torr)	T_d (PB) (keV)	τ_c (μsec)	$\bar{r}_p$ (cm)	r_E (τ_{c1}) (cm)	r_d (B = 75 kG) (cm)	r_E/r_p
50	3.7	29.2	0.57	0.18	0.17	0.32
25	3.8	12.1	0.47	0.22	0.17	0.47
10	8.6	5.9	0.40	0.22	0.24	0.55

T_d = deuteron ion temperature

$\bar{r}_p$ = mean radius of plasma

r_d = ion gyro radius

r_E = radius of end-loss aperture

P_{D_2} = filling pressure of deuterium gas

5. Scylla IV Plasma Properties - The principal plasma parameters of Scylla IV derived from the experimental measurements described here are summarized in Table II. $\bar{d}$ is the mean plasma diameter derived from the interferograms, V is the plasma volume derived from $\bar{d}$ and the measured plasma length of 80 cm with $B_o = 0$ and 70 cm with $B_o < 0$. N_e is the plasma electron density obtained from the interferograms. $\bar{Y}_n$ is the average neutron yield. T_E is the average electron temperature obtained from x-ray absorption measurements. T_D (PB) is the average deuteron ion energy obtained from pressure balance with the magnetic field ($\beta = 1$). T_D (σv) is the deuteron ion energy obtained from the neutron emission, the plasma volume and density assuming a Maxwellian distribution for the ions.

There exists a large discrepancy between the deuteron ion energies obtained from pressure balance and from the neutron emission which can be easily explained. The total confinement time for the plasma, 3 μsec, is barely an ion-ion collision time, so that if the ions were created monoenergetic, there would be insufficient time to develop a Maxwellian tail. Such a plasma requires a higher mean energy to produce the same thermonuclear yield.[24] When the neutron yield is calculated with a monoenergetic ion energy distribution the ion energy required for pressure balance and that required by the neutron yield are in agreement.

6. Summary of the Scylla Experimental Parameters - Table III gives a summary of the electrical and plasma parameters of the three Scylla experiments discussed above. The Scylla IV power crowbar (PCB) shown in the table has not yet been used but is coming into operation at the present writing (January 1965).

TABLE II

Plasma Parameters

P_{D_2} (m torr)	B_o (kG)	$\bar{d}$ (cm)	V (cm^3)	n_e ($\Delta t \sim 3.7$ μsec) (cm^{-3})	$\bar{Y}_n$	T_d (PB) (keV)	$T_d(\sigma v)$ (keV)	T_e (eV)
50	0	1.15	83	5.4×10^{16}	3.0×10^{8}	3.7	1.4	300 ± 30
25	0	0.94	56	4.1×10^{16}	5.8×10^{8}	3.8	2.2	282 ± 31
15	0	0.77	37	2.6×10^{16}	5.6×10^{8}	6.6	3.0	
10	0	0.80	40	2.1×10^{16}	5.5×10^{8}	8.6	3.2	328 ± 56
70	-5.0	1.65	160	5.0×10^{16}	1.4×10^{9}	3.2	1.7	800 ± 200
125	-8.0	1.73	165	5.0×10^{16}	1.5×10^{9}	3.1	1.7	925 ± 100

TABLE III

Summary of Scylla Theta-Pinch Parameter

PARAMETER	SCYLLA I	SCYLLA III	SCYLLA IV	
			Fast Bank	PCB
W	31 kJ	186 kJ	570 kJ	3 MJ
V	85 kV	85 kV	50 kV	20 kV
Coil Length	10 cm	10 - 27 cm	100 cm	
Coil Diameter (ID)	7.5 cm	7.5 cm	10 cm	
V_{Coil}	35 kV	40 - 48 kV	40 kV	13 kV
$\tau/2$	2.7 μsec	4.6 - 5.4 μsec	7.4 μsec	50 μsec
B_{max}	50 kG	100 - 145 kG	90 kG	200 kG
T_e	350 eV	450 - 870 eV	300 - 1200 eV	
T_i	1.3 keV	~ 1.8 keV	2 - 10 keV	
Stability	Stable	Rotational Flute Instability	Stable	

III. NUMERICAL STUDIES OF THE θ-PINCH

It is relatively easy to treat the main features of the θ-pinch theoretically, provided that the differential equations are solved numerically on a digital computer. A complete, "classical," model describes the phenomena in a long, stable θ-pinch. Comparison of the experimental behavior with the computed behavior of the model can clarify the experimental situation in many important respects. Non-classical effects in the experiment, such as ion heating due to field mixing, are then apparent. Generally speaking, the agreement of the theoretical and experimental behavior of the Scylla θ-pinches, especially in the low-density mode, is good.

The ingredients of the "classical" plasma computation are the following:[25-27] A fully ionized plasma is assumed initially to fill a cylinder which is infinitely long in the sense that only the z component of the magnetic field is allowed. The fluid velocity of the plasma has only an r component, called v. A two-fluid model with charge neutrality is used, with ohmic heating confined to the electrons and shock heating to the ions. The numerical solution is that of five partial differential equations for momentum, electron-energy, ion-energy, the mass conservation, and the electromagnetic fields. Heat is exchanged between electrons and ions at an equipartition rate which depends upon the electron temperature. The dependence of the electrical conductivity and the ion and electron thermal conductivities upon their respective temperatures and the magnetic field is also taken into account. These transport coefficients, as well as the viscosity, are those of a fully ionized plasma, to be found in the literature.

The shock heating of the ions is accounted for by the usual Richtmyer-von Neumann formalism which assures satisfaction of the Rankine-Hugoniot conservation equations across the shock front when its physical thickness is of the order of one computer mesh spacing or smaller. In the equations this appears as an additional ion pressure term

$$q_i = {}^{*}A_s \rho (\nabla \cdot v)^2 \qquad \text{if } \partial v/\partial r \leq 0$$

$$q_i = 0 \qquad \text{if } \partial v/\partial r > 0. \tag{7}$$

Here $A_s^{\frac{1}{2}}$ is a constant equal to a few times the computational mesh spacing Δr. At the lower densities encountered in this problem the ion mean free path exceeds the mesh spacing. When this happens the plasma viscosity controls the shock thickness and the corresponding q_i is used in the computation instead of Eq. (7).

By means of the plasma boundary conditions, the voltage and current of the single-turn compression coil (of length ℓ) are fed into the external circuit, which consists of a capacitance C at an initial voltage V_o with a series inductance L_e. This inductance corresponds to the parasitic inductance of the external circuit and of the space (occupied by the discharge tube wall) between the plasma outer radius R and the inside surface of the coil.

The present computation code originated in Europe, [25,26] and was adapted to be used on the Los Alamos IBM-7094 computers.[28] It has since been recoded here[29,30] to change the original system of Eulerian coordinates used in the numerical integration to Lagrangian coordinates and the original explicit time integration scheme for the hydrodynamics to an implicit one. The first change gave a more accurate treatment of the shock and the second a considerable increase in computation speed.

The following experimental properties are accurately predicted by the numerical calculation: (a) the plasma implosion dynamics, (b) the ion temperature, (c) the equality of plasma and magnetic pressure ($\beta = 1$), and (d) the scaling of ion temperature with initial pressure. In particular the computation shows that the observed ion velocities in the reversed-field, high-density regime are too high to be accounted for by classical shock heating and adiabatic compression. The scaling of the computation without trapped field,[29,30] however, adequately accounts for the high ion energies observed in the low-density regime.[14] The computed electron temperatures are found to depend very weakly on the shock of the dynamic phase, corresponding to the observation that they are nearly independent of filling density, but their magnitudes are about a factor three higher than the experimental ones for Scylla IV. The fact that ion temperatures in the experiment are about an order of magnitude higher than electron temperatures is also accounted for by the computation.

The scaling of the computed electron and ion temperatures with initial plasma filling density (corresponding to deuterium pressures of 0.01, 0.025, 0.050, and 0.010 torr for otherwise fixed θ-pinch conditions) appropriate to

Scylla IV is shown in Fig. 17. The high ion energies observed at low filling pressures are adequately accounted for theoretically. At the lower densities the ion-ion mean free path becomes large so that viscosity controls the shock thickness. The discontinuous properties of the shock then disappear quite early in the discharge, giving way to long-range viscous effects. The viscous effects should go in the limit of no collisions to simple adiabatic compression.

IV. LABORATORY ASTROPHYSICS

The vacuum ultraviolet spectrum of Scylla is being studied because of its astrophysical application. The solar spectrum in the extreme ultraviolet[31-33] contains many unidentified lines. A group of lines in the 150-220 Å region is especially strong. In fact, in the extreme ultraviolet their strength is second only to the He-II line at 304 Å, and the desire to identify them has been correspondingly great. The first laboratory clue to their identity came from the emission spectrum of Zeta [34] where a large number of coincidences were observed with the unidentified solar lines. Since it was demonstrated that the lines originated from discharge tube material, and the discharge tube was stainless steel, it seemed probable that many of the unidentified lines were due to iron. Recent work at Los Alamos and at other laboratories[35-37] with iron added to θ-pinch discharges has resulted in an unequivocal identification of the lines as iron lines.

Theta pinch plasma discharges have demonstrated the highest known terrestrial laboratory temperatures and are uniquely able to reproduce the lines of highest excitation in the solar spectrum. In the case of the Scylla I and Scylla III θ-pinches on which the Los Alamos astrophysics experiments are being performed, the character of the hot plasma produced is well known. Of particular importance here is the electron temperature, which has been shown to be 350 eV (4 million degrees K),[5] or considerably more than the temperature of the solar corona.

The technique used with Scylla to excite and observe the spectra of highly ionized atoms is to add small amounts of gaseous impurities to the deuterium filling gas. The spectra observed with and without impurities are compared to

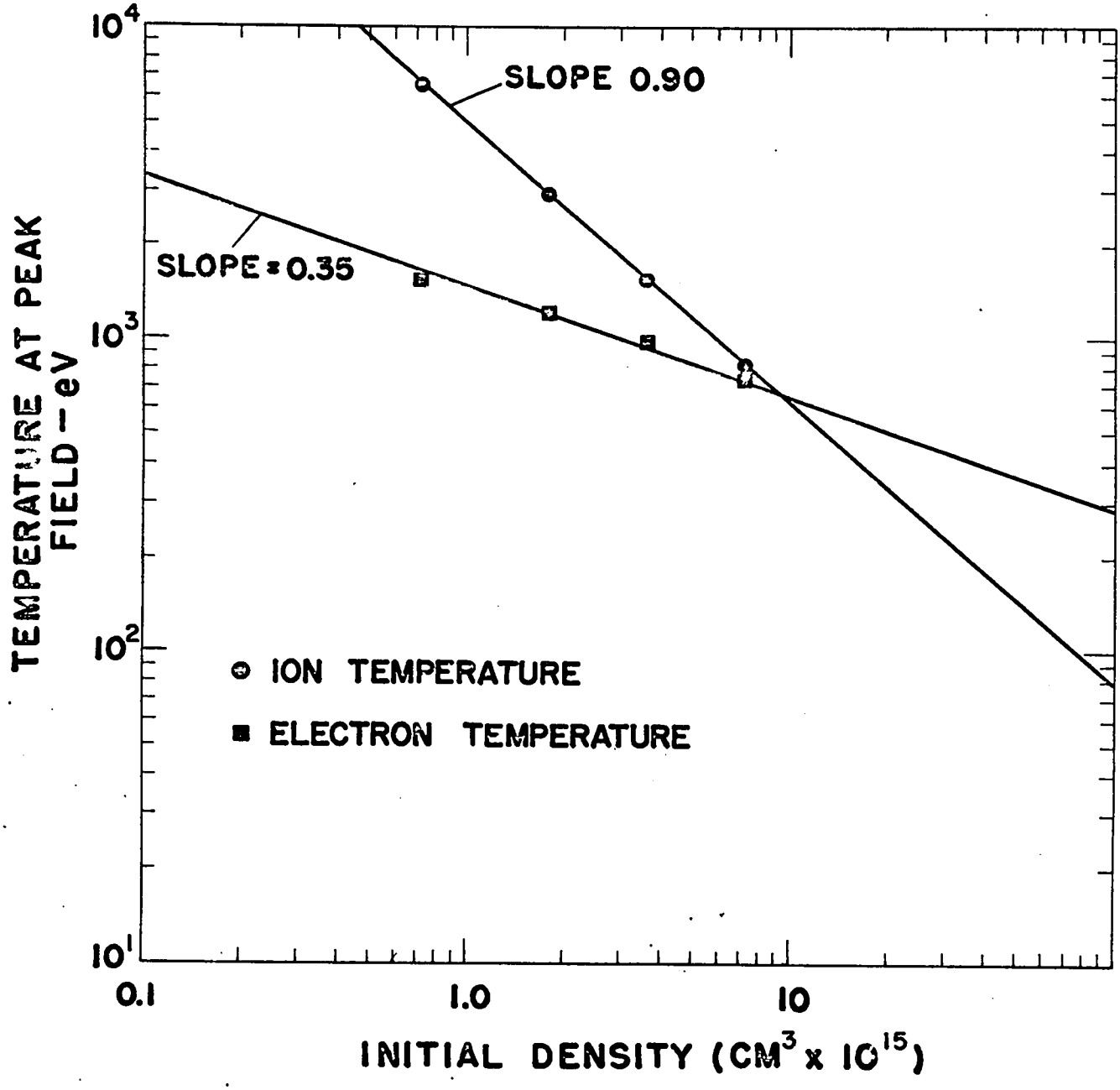

Fig. 17 Graph of ion and electron temperature at peak magnetic compression, as computed by the hydromagnetic code. No bias field was assumed and the parameters of Scylla IV with a one-meter coil were chosen. The curves correspond to Richtmyer-von Neumann shock smearing.

show the presence of new lines. The Scylla discharge is contained in an iron-free ceramic tube so that iron can be independently introduced as vapor of $Fe(CO)_5$ (iron penta-carbonyl), a liquid with a vapor pressure of 30 torr at room temperature. Adding the iron as a gas perturbs the hot plasma less than using solid iron rods or electrodes, as has been done by other laboratories. We believe, therefore, that we have achieved the highest iron excitations.

Figure 18 shows tracings of the spectra in the 150-220 Å region. The top line traces the basic Scylla spectrum. On the second line, with Fe added to Scylla, the locations of some definitely established iron lines are marked with carets. The bottom line shows the solar spectrum observed by H. E. Hinteregger in a rocket flight from White Sands, New Mexico.[31] Several of the prominent iron lines may be observed in the solar spectrum, for example those at 180.41 Å and 195.13 Å.

Unfortunately, the particular ionic species in Fe responsible for most of the observed lines are still unknown, and in fact, presents a considerable mystery since the low lying levels of Fe are known only for species through Fe XV.

The time history of the spectral lines as observed in Scylla is a helpful tool in identifying the ionization state. The more easily excited species are known to burn through quickly,[4] and then to reappear after peak field, while the more highly excited species appear later in the discharge cycle, more nearly centered around peak magnetic field. It is possible in this way, to group the observed lines according to ease of excitation. This is one approach to be used in the identification of iron lines. In addition, theoretical predictions of energy levels and wavelengths, as well as line intensities are being made using a Hartree-Foch method. This technique already has been valuable in eliminating some transitions from consideration as the origin of the observed lines.

The potential for extending the identification of the spectra of many times ionized atoms to other elements is obvious. Neon spectra have already been reported.[38]

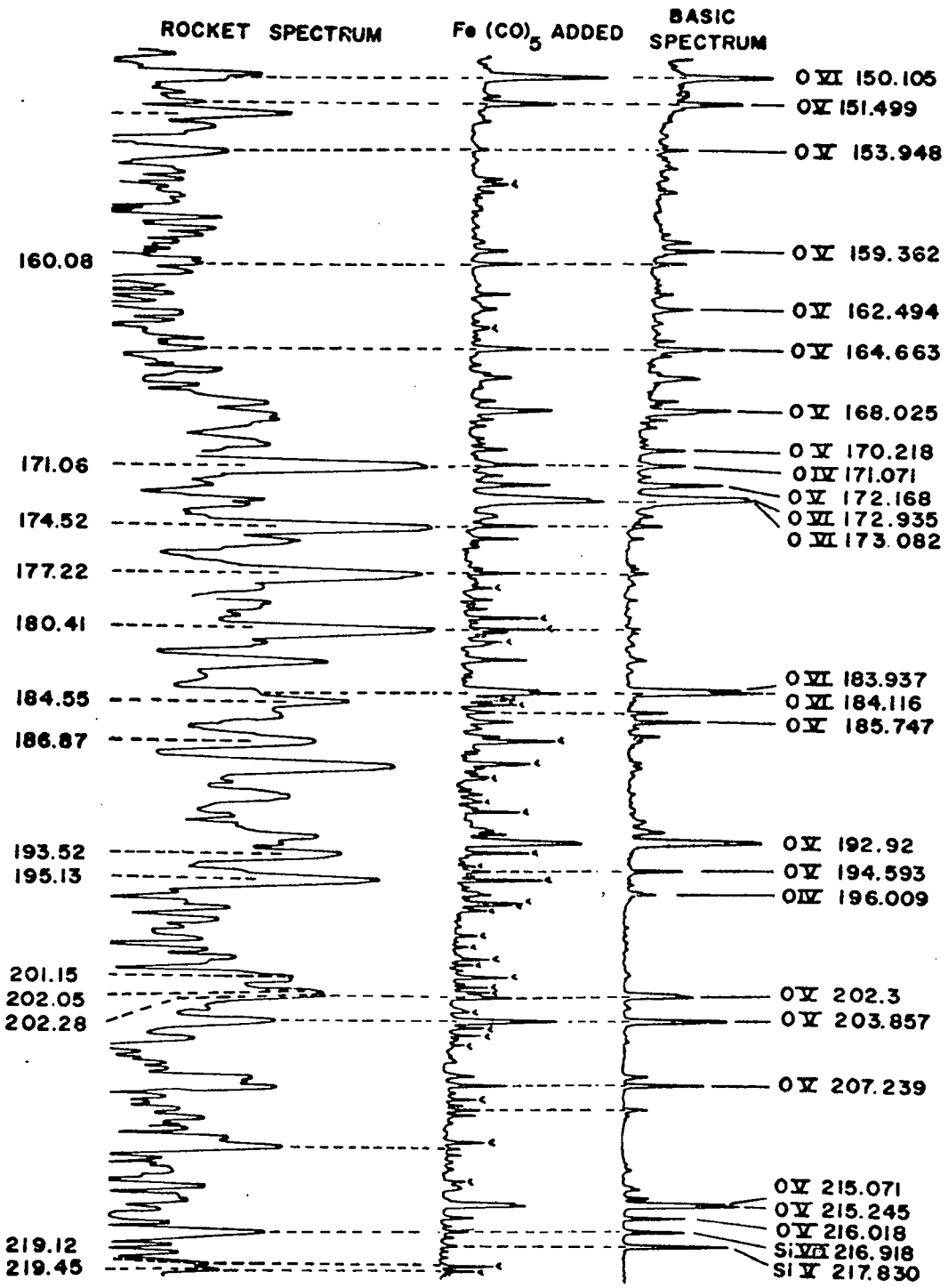

Fig. 18 Grazing-incidence, ultraviolet spectra in the 150-220Å region. The top line traces the basic Scylla I spectrum. On the second line, with Fe added to the discharge gas, the locations of some definitely established ion lines are marked with carets. The bottom line shows the solar spectrum observed by H. E. Hinteregger in a rocket flight from White Sands, New Mexico.

V. THETA-PINCH EXPERIMENTS IN THE UNITED STATES AND EUROPE

Research on θ-pinches is an active field, both in the United States and Europe. The fact that six major research activities exist has been beneficial in allowing corroboration of results from various workers, which is essential to progress in any branch of science. Generally speaking, the Los Alamos Scientific Laboratory and General Electric experiments in the United States have a considerable similarity to each other and are different from the remainder in their use of large voltages to drive the shock of the θ-pinch and the corresponding production of high ion temperatures in the low-pressure regime. The other experiments operate at lower voltages in the high-density regime. The basic phenomena of electron and ion temperatures in the keV range, conditions for plasma stability and drift, and the property of high β at densities in the 10^{16} - 10^{17} cm^{-3} region have been proved out as common features of all the experiments.

A brief summary of other θ-pinch devices and some of the principal experimental methods which have been used to study the plasmas is given in this section. The parameters of present large θ-pinch experiments are listed in Table IV. A general review of earlier devices and associated experiments up through 1961 is given in Ref. 39.

The θ-pinch experiments at the Naval Research Laboratory (NRL) began in 1958 and were first carried out with a 20-kV, 285-kJ capacitor bank which energized single-turn coils with lengths in the range of 10-70 cm and mirror ratios from 1-3.[40] Studies of the continuum radiation yielded electron temperatures up to 2 keV and densities of 7×10^{16}. The observed d-d neutron yields were $\sim 10^5$ per discharge indicating that the ion temperatures were appreciably less than the measured electron temperatures. Streak photography has been used extensively to study the containment and stability of the compressed plasma. Radial plasma oscillations were observed in which the plasma column distorted into an elliptical column and then "fissioned" into a bifilar rotating structure. In the large 20-kV, 2-MJ NRL Pharos experiment with a 180-cm length coil, the compressed plasma column was characterized by a drift toward the coil feed point.[41] The effects of a superimposed radial hexapole field and collector plate feedpoint design on the plasma drift have

been studied rather extensively.[42]

θ-pinch experiments at the General Electric Research Laboratory were first performed in 1959 with a 70-kV, 100-kJ capacitor bank and later with a 60-kV, 380-kJ bank. The latter device is similar to that exhibited by General Electric at the New York World's Fair.[43] Using an axial discharge for preionization in the latter device a high β, neutron-emitting plasma was produced in the absence of reversed bias magnetic fields.[21] A deuteron ion energy measurement has been performed by comparing the experimental ratio of 2.45 MeV neutrons from the D-D reaction to the 14.7 MeV protons from the D-He^3 reaction with the known cross-section energy dependence for the two reactions.[24] The results indicate the following: (1) The mean energy of the reacting ions is approximately 10 keV; (2) The particle velocity distribution is probably more nearly monoenergetic than Maxwellian; and (3) The results rule out accelerated ions interacting with a cold background plasma. In addition a velocity analyzer has been used to analyze the energy spectrum of the deuterons escaping along the axis of the compression coil. Deuteron energies from 1 to 10 keV have been observed.[44] An experiment with a 10-cm diameter, 36-cm length θ-pinch coil with a 2-m radius of curvature in the magnetic field lines showed no observable drift of the plasma with zero and positive trapped fields for times as long as 14 μsec.[45]

In England, θ-pinch experiments have been going on since 1958 in single-turn compression coils which have been energized by either a 30-kV, 45-kJ capacitor bank or a 40-kV, 80-kJ bank.[46] Streak and framing cameras have been used extensively to study the motion and structure of the plasma as a function of the trapped magnetic field. In the cases of appreciable trapped reversed magnetic field, the rotating hydromagnetic flute instability is observed. Experimental studies show that an axial contraction occurs in high density deuterium plasmas with reversed field configurations. A new 40-kV, 1-MJ θ-pinch with a 2-m length, 10-cm diameter coil has been operating since last spring.[47] Experimental studies of the radial plasma drift have been performed as a function of the collector plate feedpoint geometry.

θ-pinch experiments at Julich, Germany, which have been going on since 1959, have concentrated on diagnostic studies of the transient phenomena associated

with the initial hydromagnetic shock implosion and plasma-magnetic field configurations.[48] The initial device was energized by a 25-kV, 5-kJ capacitor bank. The magnetic probe technique has been highly developed and applied to studies of the internal magnetic fields. Extensive spectroscopic studies of the plasma radiations have been performed. A new 20-keV, 600-kJ θ-pinch device is presently coming into operation.[49]

At the Institute for Plasma Physics (Garching, Germany) interferometric and laser scattering experiments have been performed on small θ-pinch devices.[50] A 40-kV, 2.7-MJ θ-pinch device is just coming into operation.

At Frascati, near Rome, the "Cariddi" θ-pinch (114-kV, 145-kJ) has a compression coil made up of six sectors, each driven independently to produce a voltage step-up from the energy storage capacitor bank.[51] The experiments have concentrated on the study of hydromagnetic shock waves produced by the initial implosion. Optical techniques of the shadowgraph type which are capable of measuring density variations in the plasma have been developed.

The Russians at Sukhumi, U.S.S.R., have performed some experiments on θ-pinch type devices.[52] However, they have not made significant contributions to the rapid magnetic compression experiments. It may be that their capacitor technology is not capable of producing the high-voltage, low-inductance capacitors required for θ-pinch type devices.

TABLE IV

Parameters of Theta-Pinch Devices

Parameter	Culham, England	Garching, Germany	General Electric Schenectady, New York	Julich, Germany	Los Alamos Scylla IV Fast Bank	Los Alamos Scylla IV Secondary Bank	NRL Pharos
Voltage (kV)	40	40	60	20	50	20	20
Capacitance (μF)	1340	3330	213	2970	454	15,000	9,800
Energy (MJ)	1.1	2.7	0.4	0.6	0.6	3.0	2.0
Source Inductance (nH)	3	4	30	1.3	2.2	(8)	1.5
Max. Current (MA)	12.9	22	2.8	10.6	9.4	(20)	20
Max. Magnetic Field (kG)	76	220	53	100	93	(200)	120
Half Period (μsec)	12	20	14.5	17	7.4	60	28
Coil Length (cm)	200	100	36	128	100		180
Coil Diameter (cm)	10	10	19	10	10		10.5

VI. ANTICIPATED EXPERIMENTAL PROGRAM FOR (APPROXIMATELY) THE NEXT TWO YEARS

A. Further Measurements with Linear Coils on Scylla IV

1. End Losses - The object of the Scylla IV experiment was to produce plasma temperatures and densities approximating those of the Lawson criterion and to study the problems of instability and end losses.[53] As outlined above, this has been done, using the primary bank of Scylla IV at magnetic fields of 100 kG and a half period of 7.5 μsec. The plasma end losses have emerged as the predominant loss mechanism.

At this writing the power crowbar bank of Scylla IV has been brought into operation, giving a maximum field of 180 kG and a half period of 55 μsec. The major effort for approximately the next year will be to measure the plasma properties at these higher fields and extended times. For the first time Scylla IV plasma containment will be limited not by the duration of the applied magnetic field but rather by the plasma stability and end loss.

With primary bank operation, end loss rates were measured for times shorter than e-folding times. With the longer period of the machine at full energy this limitation will not apply, and we intend to measure end losses as a function of mirror ratio of the compression coil. End losses and instability will be measured in the trapped-reversed field regime as well as the low-density mode.

2. The Sustained Field θ-Pinch - When the feasibility of pulsed reactors using θ-pinches is considered (Sec. VIII), the sustained field θ-pinch[54] emerges as a particularly favorable arrangement. The time history of the applied magnetic field is shown schematically in Fig. 19. An impulse of magnetic field of duration τ and magnitude approximately -B is applied to a coil volume normally filled with a d-c magnetic field B. The plasma is formed on the back-swing of the negative impulse and is then held by the steady field B. The sustained field principle has the advantage that the impulse field, because of its short duration, can be furnished with very little resistive energy loss. The steady field can be furnished by a superconducting coil.

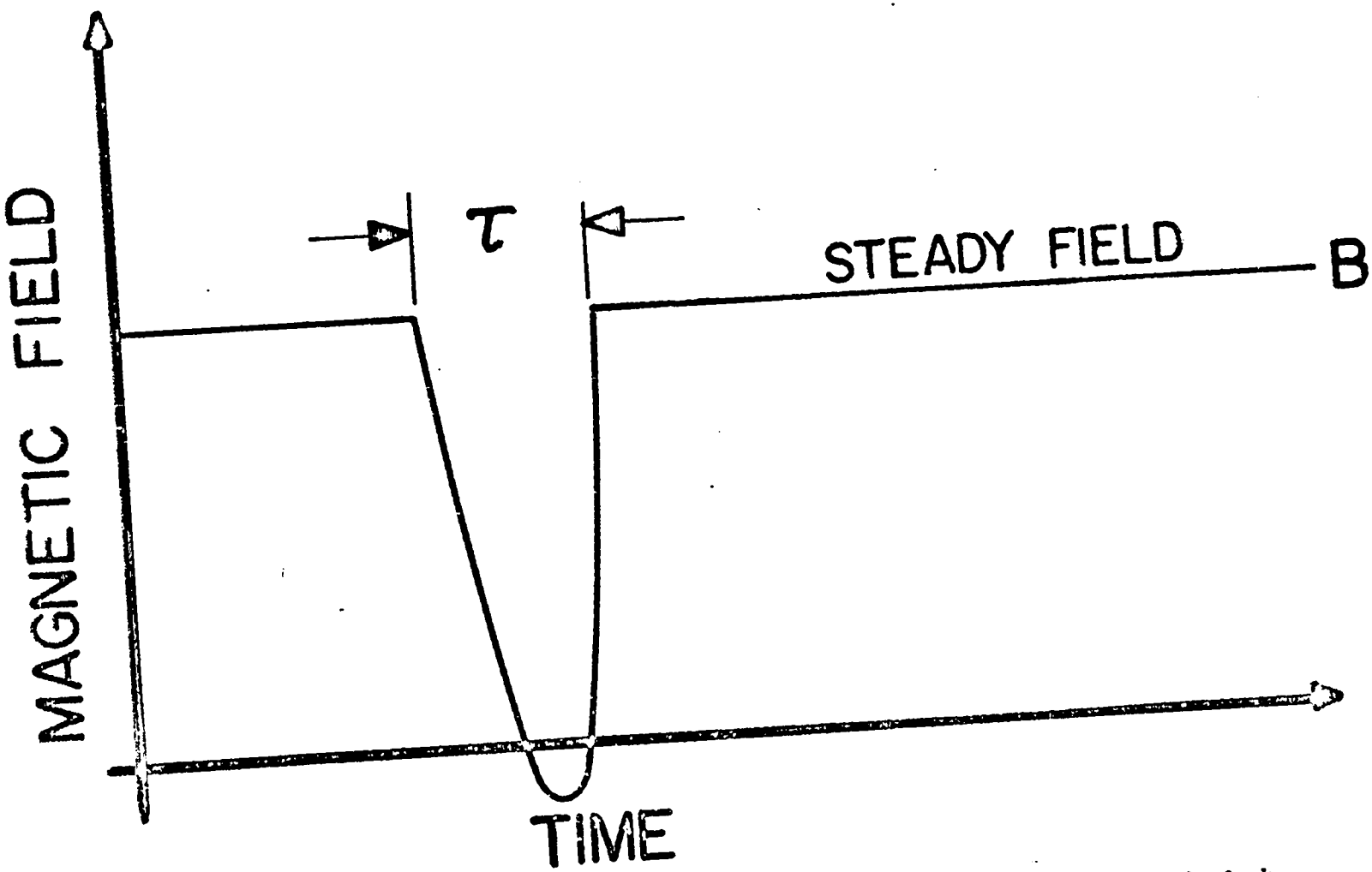

Fig. 19 Time history of the magnetic field in the sustained field θ-pinch. An impulse of magnetic field is superimposed on a steady field B, driving the magnetic field to zero. The plasma is formed on the backswing of magnetic field and sustained by the steady field B.

Scylla IV is ideally adapted to testing the sustained field θ-pinch concept. It is only necessary to rearrange the present time sequence of operations so that the power crowbar capacitor bank is switched on first to furnish a quasi-steady sustained field. At the peak of the power crowbar magnetic field, the primary capacitor bank is switched on to provide the impulsive field. The capacitor banks already have the correct polarity relationship to perform the experiment.

In considering future larger θ-pinch systems it is important to establish whether a typical hot θ-pinch plasma can be generated in the sustained field system. It may be difficult to make a plasma because when the plasma is created at zero B field, the magnetic field is changing slowly (cf Fig. 19) in contrast to the normally large dB/dt in Scylla. We plan to study this system during the next two years.

B. Beginning Toroidal Containment Experiments on Scylla IV

1. Motivation - The primary obstacle to the achievement of long plasma containment in the present Scylla θ-pinch experiments seems to be the plasma end loss, which has approximately predictable magnitude. As the plasma ion temperatures and density approach those appropriate to reactor conditions, it is of primary importance to develop a system which will allow longer containment time. The most promising system is a toroidal one, which will have no end losses.

Experience with longitudinal pinch and Stellarator toroidal systems has shown them to be fraught with difficulties, and it is realized that the subject is not an easy one. However, the θ-pinch offers several novel features and advantages.

First, the θ-pinch provides genuinely hot plasma, a circumstance which circumvents the large collisional effects and plasma resistivity found in other experiments. The diffusion processes for the straight plasma seem to be considerably slower than the "Bohm" processes which are apparently being found in other plasmas.

Secondly, these high-β plasmas have demonstrated interchange instability in the straight case, to the apparent exclusion of microinstabilities during the

time scale of interchange growth. The interchange instability grows much more slowly than simple low-β theory would indicate (cf. Sections II-B and II-C). Therefore it is likely that experiments required to understand how to eliminate the interchange instability will lead to clear-cut experimental answers on this stability problem.

The technique which we expect to use for stabilizing the plasma drift will be that of external stabilizing conductors, energized independently of the main compression field which heats the plasma. In this method the stabilizing field will not interfere with the plasma heating. Experience on Scylla III (Section II-B) with hexapole conductors has already shown that the heating and stabilization functions can be separated in this way.

2. Plasma Drift - In going to a toroidal θ-pinch system, one expects to encounter an outward drift of the plasma, owing to the radial magnetic field gradient. It should be noted that the $\beta \approx 1$ condition provides a considerable difference from the $\beta \ll 1$ case, encountered for example in Stellarators. In the latter case the inward field gradient ∇B induced by the curvature of the lines induces $\nabla B \times \underset{\sim}{B}$ drifts of the ions moving across magnetic field inside the plasma, giving vertical charge separation and hence a vertical electric field $\underset{\sim}{E}$ in which plasma moves outward. The remedy for this drift is the rotational transform[55] which causes magnetic lines to connect the upper and lower parts of the plasma, shorting the E field. In the $\beta \approx 1$ case there is ideally only a plasma pressure unbalance, pushing the plasma outward with net acceleration given approximately by

$$\ddot{R} \approx (B/\pi nM)dB/dr = B^2/8\pi nMR, \qquad (8)$$

where R is the radius of curvature of the lines, n is the number density, and M is the ion mass. The corresponding drift time to the wall

$$\tau_D \approx (2\pi\, nM\, RR_c/B^2)^{\frac{1}{2}} \qquad (9)$$

is shorter by a factor $\approx \beta^{\frac{1}{2}}$ than in the low-β case.

3. Preliminary Experiments to Measure Drift with Curved Magnetic Lines - Our first experiment will be to install a curved compression coil on Scylla IV and to measure the drift at various plasma energies and trapped fields. A relatively large radius of curvature $R \approx 2$ meters will be chosen in order to give manageable values of τ_D. It is important to determine if there are effects such as magnetic line tying to the discharge tube or to the plasma outside the coil ends which affect the drift, making it essentially different than in the true closed toroidal case. An anamolous result has already been reported[56] in which deliberate bending of the lines in a short coil with mirrors failed, under some circumstances, to produce drift. Other experiments,[57] at lower coil voltages, have verified the presence of a drift given by the theory.

4. Projected Experiments on Drift Stabilization - Our approach to drift stabilization presently visualized, is to use asymmetric quadrupole conductors as shown, for example, in the cross-sectional drawing of Fig. 20. The effect of gross drift stabilization is illustrated in Fig. 21. In (a) the inward gradient of magnetic pressure owing to curvature of the lines whose tangents in the Z direction is indicated. In (b) the effect of the x and y fields of a multipole like that in Fig. 20 in reversing the field pressure gradient and providing a minimum is indicated.

The first experiments will be performed in a curved sector coil using curved conductors as shown in Fig. 22. A choice of a large radius of curvature (R = 2 meters) compared to plasma and coil radii keeps the currents in the stabilizing conductors within practicable bounds.

One anticipated effect of any multipole stabilizing field such as that of Figs. 20 and 22 is that magnetic lines intersect the discharge-tube wall. On a short time scale of a few μsec this may not lead to serious plasma leakage or cooling (as is indeed indicated by the Scylla III hexapole experiments, Section II-B). However, in a true toroidal system of long confinement one must expect particles to find their way to the wall along these lines.

The effect of lines intersecting the walls when continuous quadrupole conductors like those of Fig. 20 are applied is shown qualitatively in Fig. 23 (a). Here lines originating at small radii near the plasma surface intersect the discharge tube. This can be avoided by the scheme shown in Fig. 23 (b) where

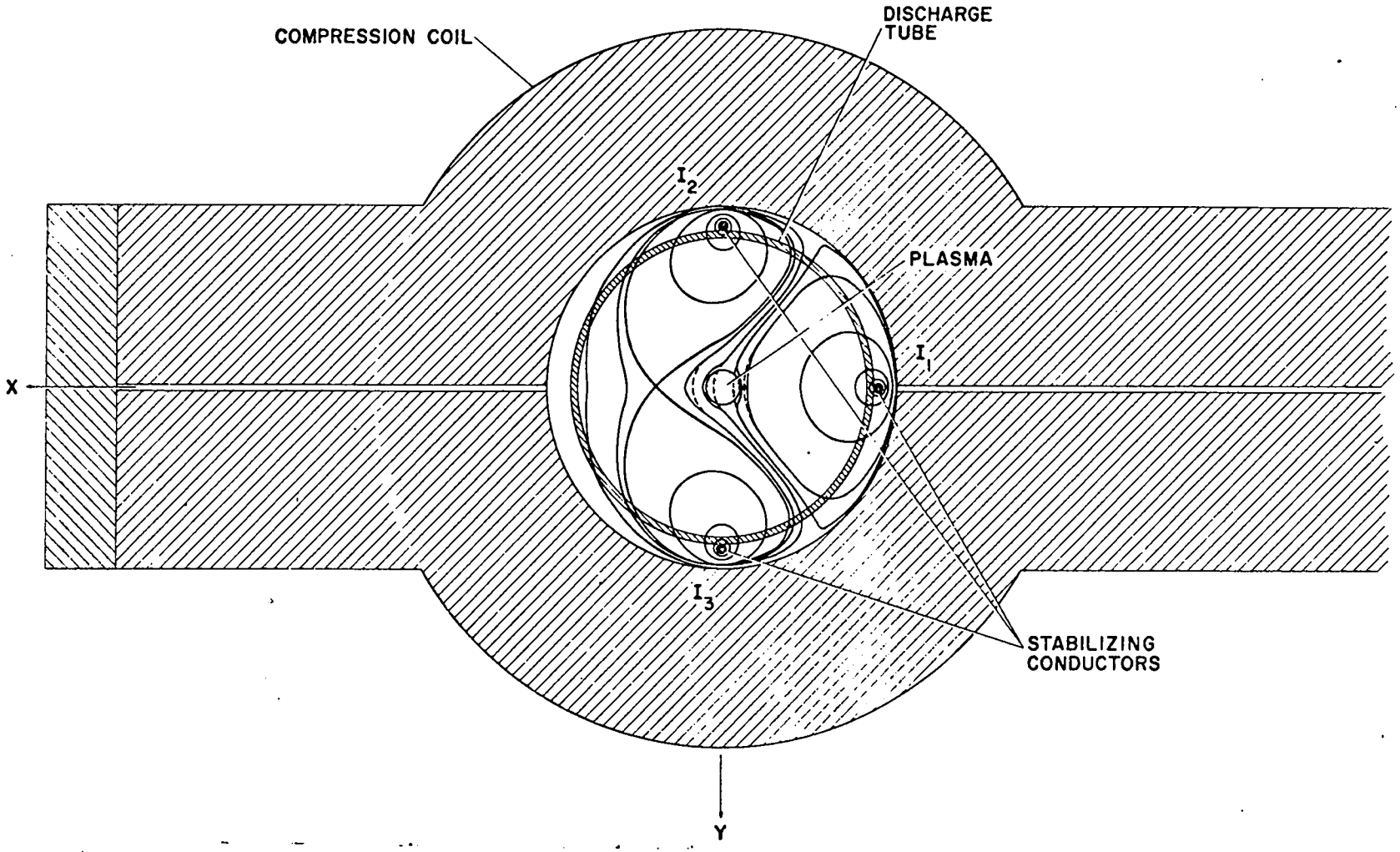

Fig. 20 Cross sectional view of θ-pinch compression coil with three conductors to furnish an asymmetric quadrupole field whose lines are shown. The magnetic lines are indicated by a $\beta = 1$ plasma and qualitatively by the dashed lines in the absence of plasma.

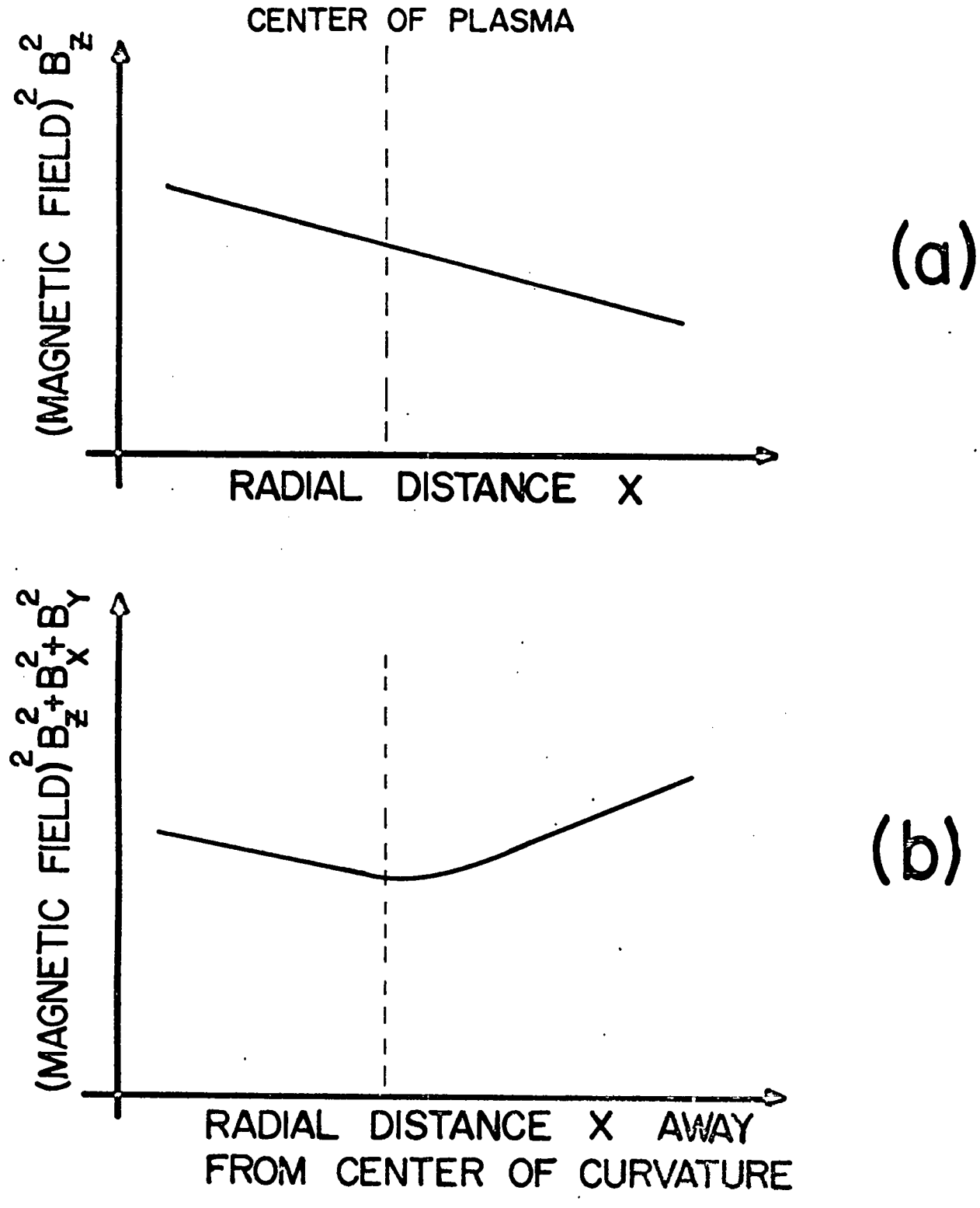

Fig. 21 (a) Magnetic pressure vs radius for curved magnetic lines whose tangent is in the z direction. (b) Magnetic pressure with added x and y components as furnished by the asymmetric quadrupole of Fig. 20.

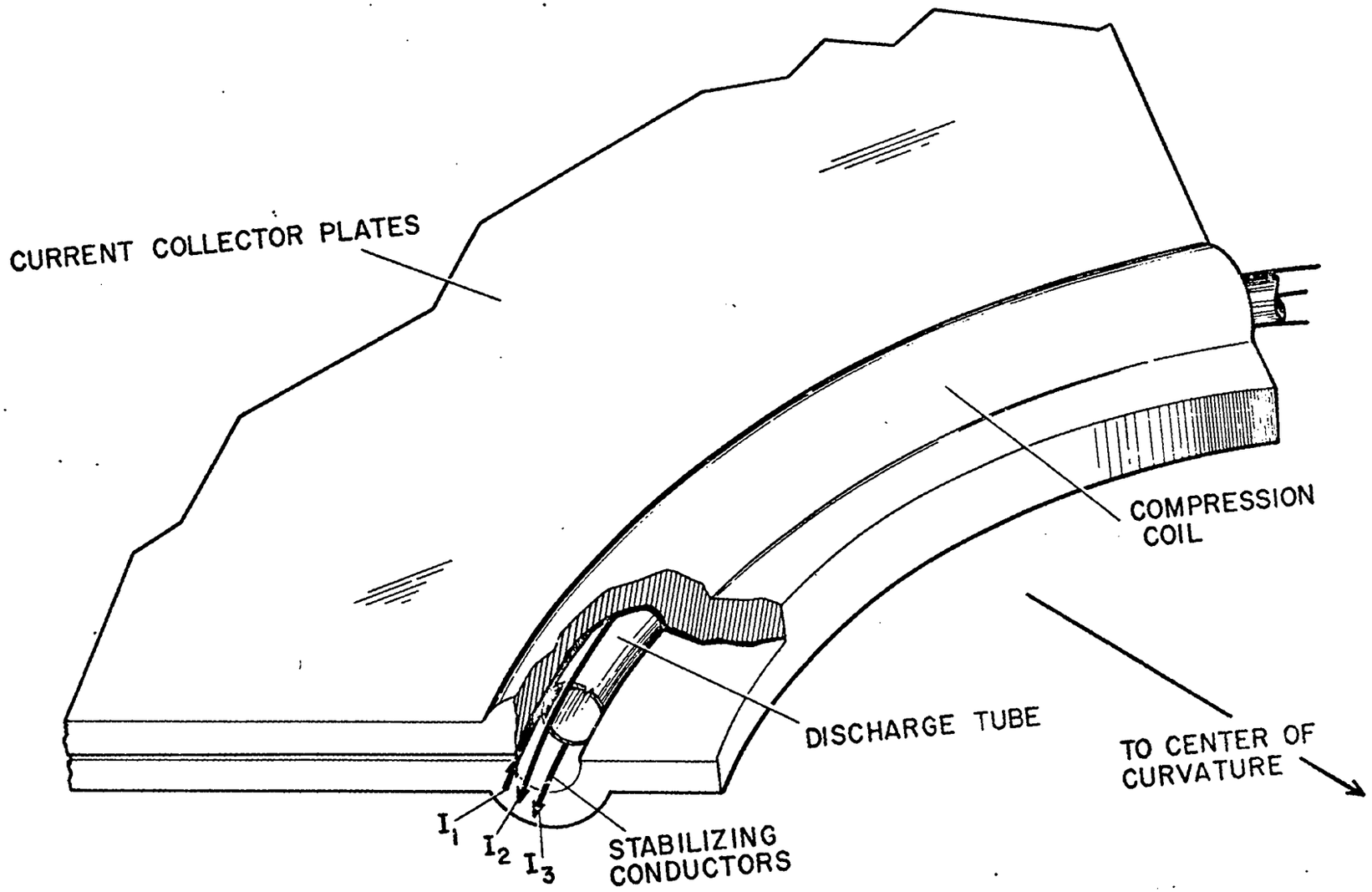

Fig. 22 Schematic view of curved sector coil for a θ-pinch using stabilizing conductors, corresponding to the cross sectional drawing of Fig. 20.

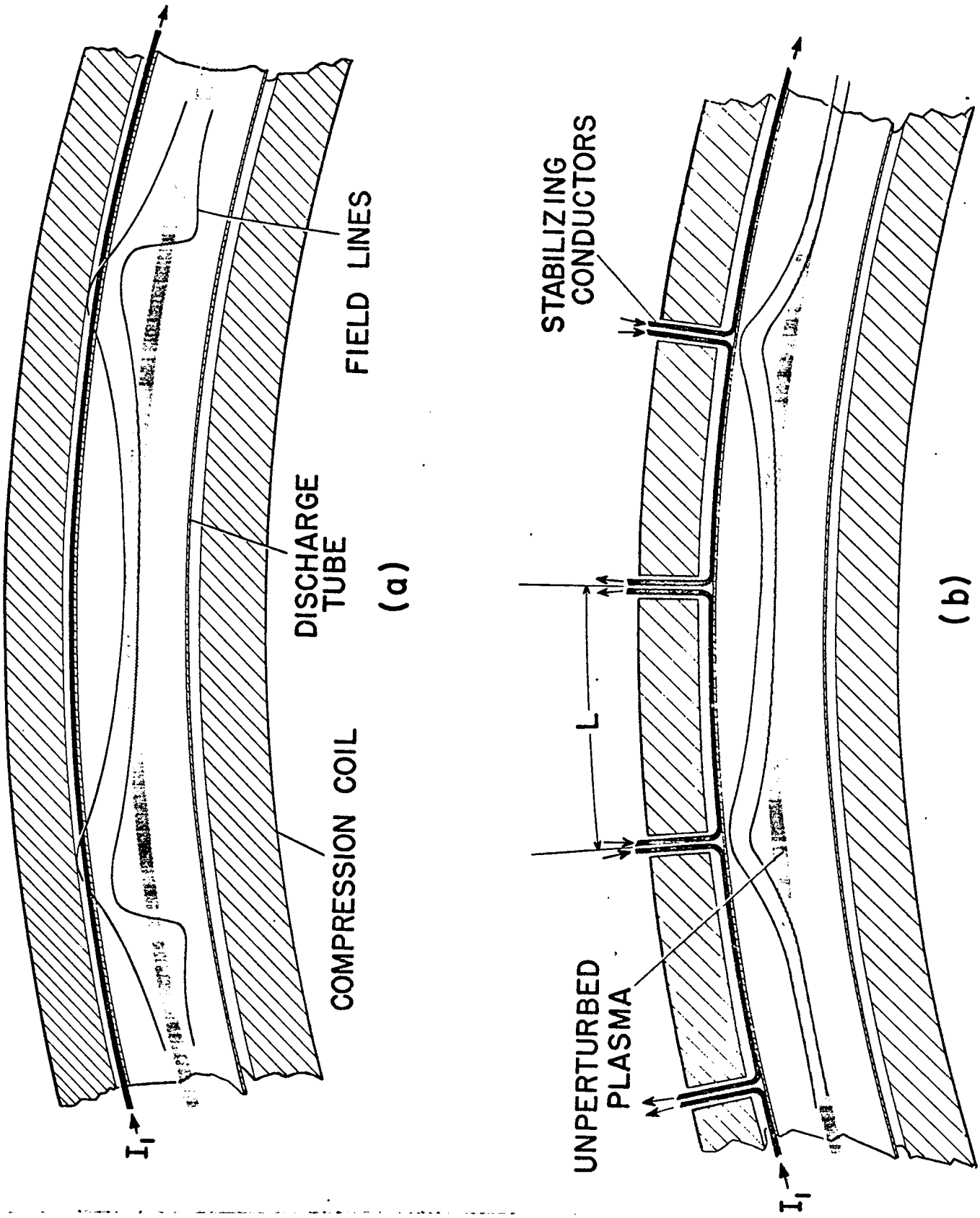

Fig. 23 (a) Qualitative top view of typical magnetic lines from multipole conductors like those of Fig. 20. For continuous conductors the lines pass through the discharge tube. (b) Qualitative view of the magnetic lines when the direction of the current in the multipole conductors is reversed periodically. Lines connecting to a small radius near the surface of the plasma do not intersect the wall.

the conductor currents are reversed periodically with period L so that lines from small radii do not have an opportunity to intersect the wall. Numerical computations to date indicate a length $L \approx 30$ cm, for Scylla IV coil conditions and gross drift stabilization at R = 2 meters.

The lines indicated in Fig. 23 (b) have curvature at their outer excursions near the tube wall which is destabilizing in the same sense as the gross curvature of the B_z lines driving the plasma drift. However it is a prediction of plasma theory[17] that the destabilizing effect of such curvature is not fatal so long as the line integral

$$W = \int d\ell/B \qquad (10)$$

along a magnetic line is a decreasing function of distance (depending also on the gradient of plasma pressure) from the center of the plasma. The alternating-conductor field configuration of Fig. 23 (b) is identical in principal to that proposed by Furth and Rosenbluth[58] who treated the case of a symmetric quadrupole and showed that a stable configuration of magnetic lines exists, provided that the magnitude of B_z is periodically increased (mirrored) and corresponding increases of quadrupole field are made over short z distances. (The latter effects are not indicated in Fig. 23 (b)). Calculations extending the Furth-Rosenbluth result to an asymmetric multipole like that of Fig. 20 are given in Section IX of this report.

It can be seen that the problem of drift stabilization in a toroidal θ-pinch is similar to that of the stabilization of interchange instabilities, which presently occupies a great deal of attention in controlled thermonuclear research. There are as yet no experiments on interchange stabilization in toroidal systems, and we expect our own to provide a meaningful contribution to this field. These experiments may be particularly useful, since they will make use of plasma whose properties are already well determined.

5. Distorted Coil Shapes - It is anticipated that we shall apply stabilization fields by means of external conductors as outlined above in order to preserve the symmetry of the θ-pinch heating process. However at this early stage it is not prudent to exclude the possibility of generating

stabilizing fields by shaping the inner flux-conserving surface of the coil. This mixes the stabilizing field with the main compression field at all times and one runs the risk of upsetting the heating process in the θ-pinch. Figure 23 shows a photograph of a section of a periodic coil in which the stabilizing fields are obtained by shaping the inner surface of the conductor. (The coil shape is like one-half period of a flux surface of the Furth-Rosenbluth model and also like that proposed by Andreoletti[59]). Present plans include machining the inner surface of a θ-pinch coil out of thick aluminum to a shape like the model and driving the coil with the Scylla IV banks. The primary aim of such an experiment would be to see if hot, dense θ-pinch plasma can indeed be formed in such a coil.

C. Light Scattering Measurement of Ion Energies in the Low- and High-Density Regimes

1. Object of the Experiment - A direct measurement of the ion velocity distribution in the low-density regime is called for in order to confirm the ion energies deduced from the $\beta = 1$ condition. Comparison of ion energies deduced from pressure balance ($\beta = 1$) with those derived from neutron yield indicates that the velocity distribution in the low-density regime is more nearly monoenergetic than Maxwellian (cf. Section II C, Table II).

It is also important to measure the difference between the ion velcity distributions generated by trapped-reversed field (as in Scylla I) and those produced in the low-density regime. As discussed in Section II A, the x-ray and nuclear Doppler measurements on Scylla I indicate that the ions are not in collisional equilibrium, at least in the high-pressure regime. The scattering technique to be applied complements these earlier spectroscopic measurements and measures deuteron ion velocities directly, without the intermediary of the fusion reaction. The scattering experiments will be done first on a rebuilt version of the Scylla III machine. After its development the technique will be used on Scylla IV.

2. Experimental and Theoretical Background - Following the original theoretical discussions of plasma correlation effects by Salpeter[60], a number

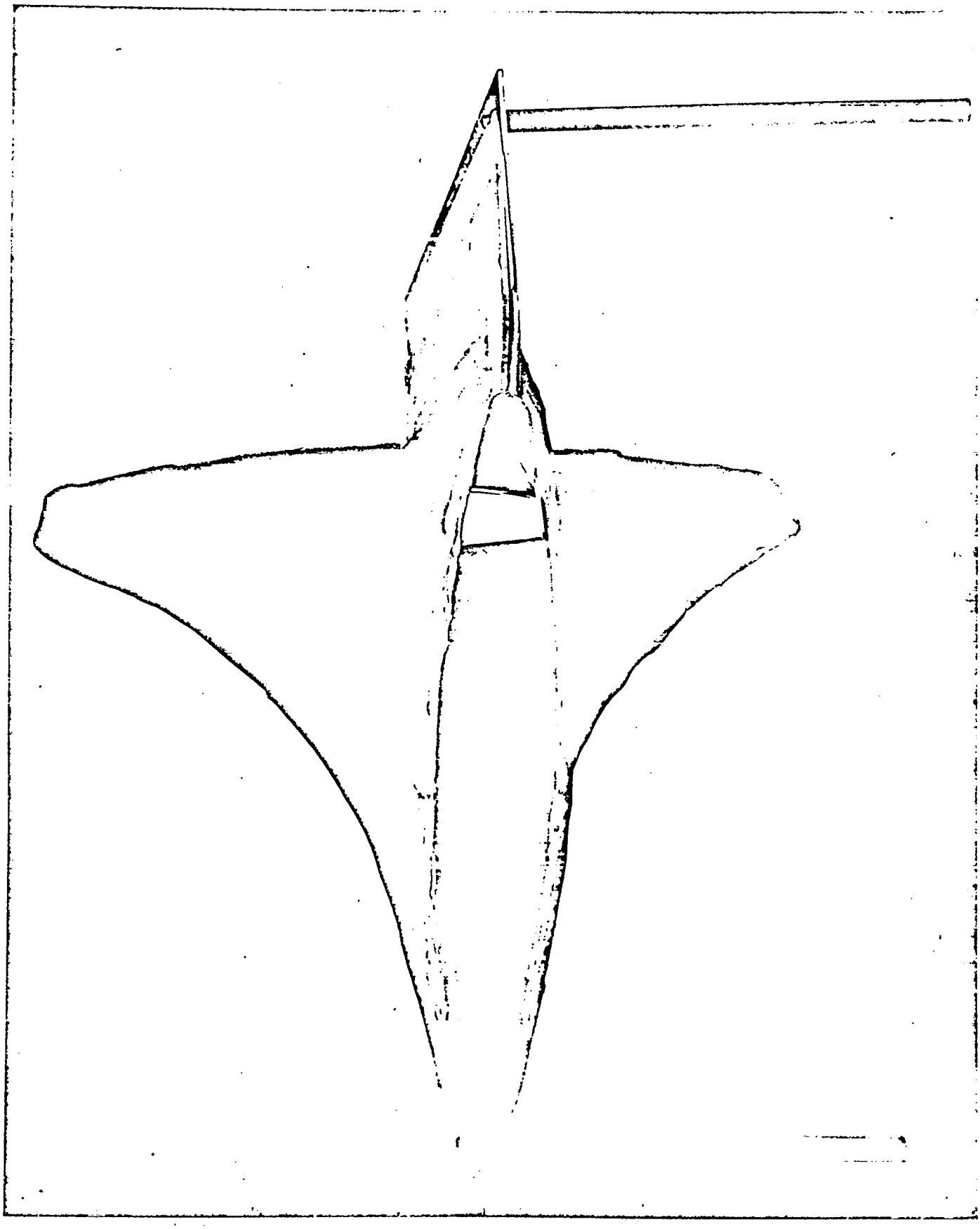

Fig. 24 Photograph of a model section of a periodic θ-pinch compression coil in which stabilization fields are obtained by shaping the inner surface of the conductor.

of scattering experiments at low temperatures ($kT \approx 2eV$) have been performed to measure electron temperatures and densities[61-64]. In this discussion we follow the theoretical work of G. L. Lamb, Jr[65].

Fundamentally one measures the Thompson scattering from plasma electrons and observes the spectrum of the scattered light which, owing to the motion of the electrons, is Doppler broadened. One considers the wave number

$$k = \frac{4\pi}{\lambda_o} \sin \theta_s/2, \tag{11}$$

which is the difference $|\vec{k}_i - \vec{k}_s|$ of the incident and scattered wave numbers. Here $|\vec{k}_i| = 2\pi/\lambda_o = \omega_o/c$; λ_o is the incident (laser) wavelength; and θ_s is the scattering angle. The electron Debye length is

$$L_e = (kT_e/4\pi ne^2)^{\frac{1}{2}} \tag{12}$$

When the parameter

$$\alpha = 1/kL_e = \lambda_o/4\pi L_e \sin \theta_s/2 \tag{13}$$

is much less than unity the electrons scatter independently, and the Doppler broadening is characteristic of the electron thermal velocities v_e. When $\alpha \geq 1$ the electrons scatter cooperatively in such a way that they behave as though all electrons inside a Debye radius of a given ion move with the ion. Then the Doppler broadening of the scattered spectrum is characteristic of the ion thermal velocities v_i. The scattering experiments to be carried out will be done in the $\alpha \geq 1$ regime where cooperative effects dominate so that the Doppler broadening of the scattered light is a measure of ion energy.

According to the Doppler formula, the angular frequency of a photon of incident frequency ω_o is changed by an amount $\Delta\omega$, which for $\beta \ll 1$ is given by

$$\Delta\omega/\omega_o = (\vec{\beta} \cdot \vec{v} - \vec{\beta} \cdot \vec{k}) = \omega_o \beta[\cos \phi - \cos (\phi + \theta_s)]. \tag{14}$$

Where $\vec{v} = \vec{\beta}c$ is the velocity vector of the scattering electron and $\vec{k}$ is the incident photon wave number. θ_s is the photon scattering angle and ϕ the angle between the electron velocity and the scattered-photon direction. For fixed θ_s,

β, and ω_o, $\Delta\omega$ is the maximum when $\phi = (\pi - \theta_s)/2$. Since small scattering angles are necessary in order to obtain cooperative scattering, this means that ion energies transverse to the discharge tube axis are measured. This is another advantage of the scattering technique, since previous spectroscopic methods yielded longitudinal ion velocities.

Figure 25 shows the absolute differential scattering cross sections (calculated from Lamb's report) to be expected at various feasible scattering angles for plasma conditions $kT_i = 4000$ eV, $kT_e = 300$ eV, $n = 3 \times 10^{16}$ cm^{-3}, appropriate to the low-density regime of θ-pinches. In the following a scattering angle $\theta_s = 7^o$ will be assumed for illustration.

3. Experimental Parameters - In order to obtain enough scattered light to give a detectable signal over the bremsstrahlung emission from the plasma a high-power ruby laser is necessary as a source of strong, collimated, incident light. It is proposed to use a 50-MW giant-pulsed laser with an angular spread < 3 milliradians and a wavelength spread $\Delta\lambda < 0.1$ Å.

A preliminary schematic view of the experiment is shown in Fig. 26. Here lens L_1 focuses the laser beam onto the scattering volume; lens L_2 is the scattered-light collector; and lens L_4 provides parallel collimation (to within angular divergence β) into the final monochromator, which is to be composed of three Fabry-Perot etalons in series to provide a response function of good resolution and extremely good rejection of stray laser light outside its pass band.

The 3-etalon Fabry-Perot monochromator is being designed in collaboration with Prof. Julian Mack of the University of Wisconsin. It will have a working diameter of 45 mm at a finesse of about 120, with a free spectral range between interference orders of 8 Å, requiring a narrow plate spacing of 0.30 mm for the etalons.

D. Continuing Diagnostic Measurements

The various techniques of x-ray and uv spectroscopy and of optical and infrared interferometry already developed for θ-pinch measurement will be improved and elaborated. For example, the shock point of the low-density regime

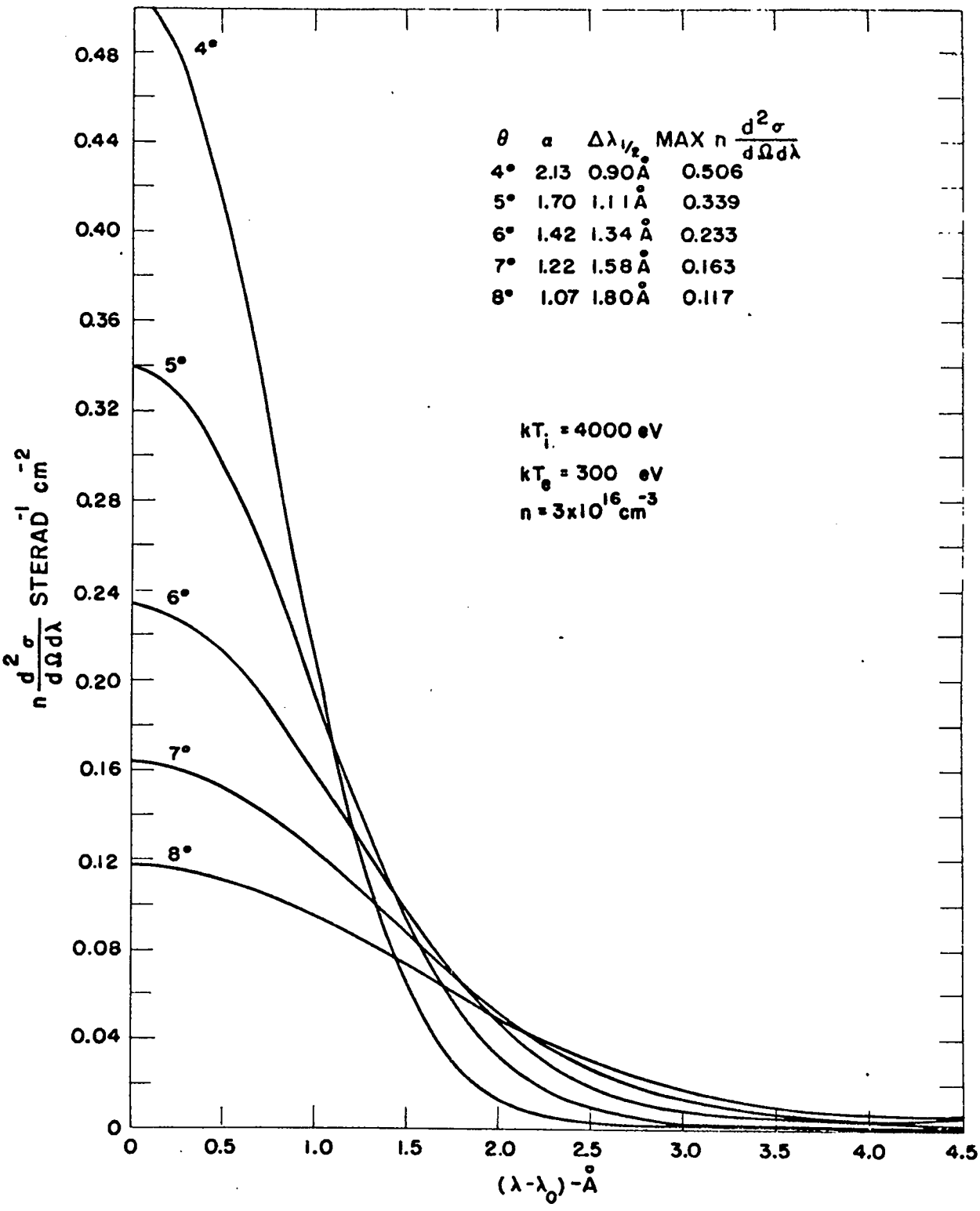

Fig. 25 Absolute differential scattering cross section vs wavelength difference from that of the incident laser beam for assumed Maxwellian distributions of ion and electron velocities at the temperatures and density indicated. The parameter of the curves is the scattering angle θ_s.

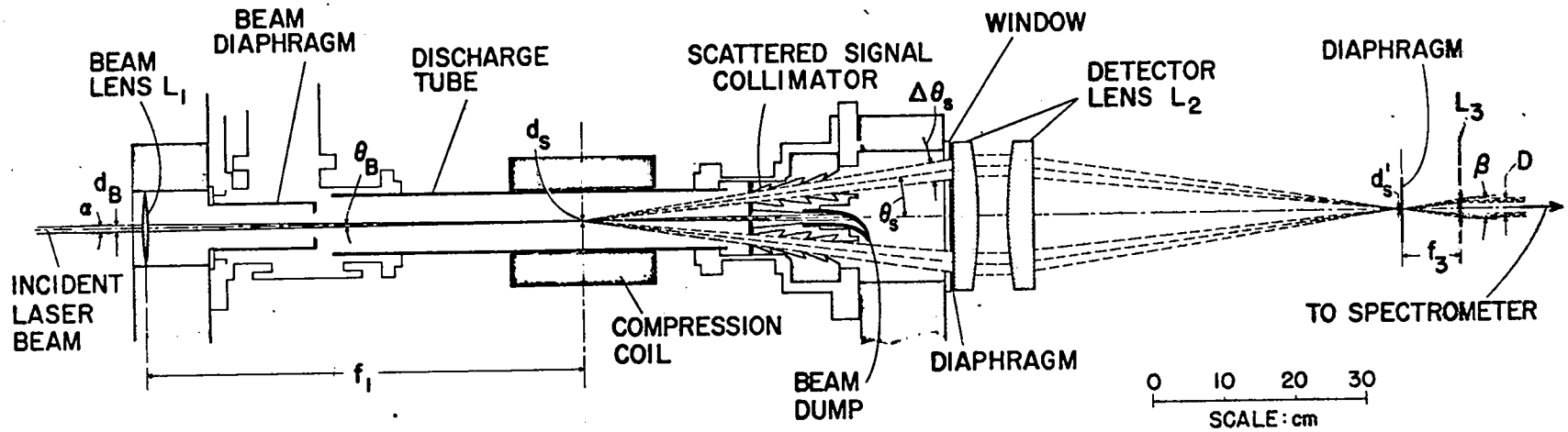

Fig. 26 Schematic view of laser scattering experiment for measuring ion Doppler broadening in Scylla III. θ_s is the scattering angle and d_s' the diameter of a diaphragm that determines the diameter d_s of the scattering volume.

(cf. Section III above) should be examined by means of the Schlieren technique. The magnitude of the magnetic field inside the Scylla IV plasma will be measured by the technique of Faraday rotation of a linearly polarized, infrared, laser beam. The spectroscopic Doppler broadening measurement referred to in Section II A above should be performed in the transverse direction. The increased resolution attainable at grazing incidence with a new spectrograph in the 100 Å region should lead to improved Doppler broadening measurement of impurity ions.

E. Summary of Projected Activities

While the experiments on end losses, the sustained field θ-pinch, ion energy measurement, diagnostics, and toroidal section stabilization are in progress, design of a closed, toroidal θ-pinch, Scylla V, will also be pursued.

VII. ANTICIPATED PROGRAM FOR THE NEXT FIVE YEARS - SCYLLA V

A. Most Favorable θ-Pinch Geometry

As the development of the Scylla θ-pinch concept is extended toward the Lawson criterion and energy breakeven, the most favorable geometry for reaching longer confinement times must be considered. End losses are at present the major factor preventing longer confinement times and are, therefore, one of the principal factors to be considered in choosing a geometry.

1. Linear Geometry - The most straightforward way to deal with end losses would be to increase the length of the confining magnetic field region until the end losses become negligible compared to the total plasma confined. Such a brute-force approach has a good chance of succeeding in principle, but the coil length and capacitor bank energy become prohibitive at the present stage of plasma development. One can estimate by scaling from Scylla IV that a half-kilometer-long coil would be required to reach approximately 3 ms confinement time, and the Lawson criterion. A further drawback to the linear approach for the next Scylla experiment is that it would be little more than a scaled-up version of Scylla IV and would lead to little new knowledge of plasma physics; nor would it allow the development of appreciable new engineering technology.

2. Toroidal Geometry - A toroidal geometry provides a much more attractive solution. The toroid is free of end losses and therefore, the required confinement time can be achieved with much shorter θ-pinch length and much less capacitor energy storage. The major problem of toroidal geometry is the radial outward plasma drift due to the radial magnetic field gradient. The magnitude of the drift unbalance and the means for overcoming it are discussed in Sections VI-B and IX.

The drift problem in closed toroidal geometry and the need for developing stabilization techniques makes it desirable to build a toroidal experiment as soon as possible. As described in Section VI-B above, preliminary

stabilization experiments are planned for Scylla IV. However, such experiments in sectors of toroids cannot provide complete answers to toroidal confinement since end losses will still govern the confinement in any open-ended geometry.

B. Size Required in a Toroidal θ-Pinch

The major diameter required in a toroidal θ-pinch experiment is determined by the requirements of the stabilizing magnetic fields.

As is shown in Section IX, the capacitor energy required to drive the stabilizing conductors is approximately independent of the major radius R. The main bank energy varies as R. Thus the ratio of stabilization-bank energy to main bank energy varies as R^{-1}. Construction of the stabilizing conductors becomes simpler as the period of reversal L of their currents (cf. Fig. 22) becomes larger. From Section IX, L varies approximately as $R^{\frac{1}{2}}$. In general the toroidal perturbation of the θ-pinch problem as presently understood in linear geometry will decrease as R increases.

The above factors all make it desirable to keep the major torus radius as large as possible, but they must be balanced against the energy storage requirement of a large torus. In the design for Scylla IV that follows we have tentatively chosen R = 1.5 and R = 2 meters.

C. Proposal for Scylla V

In line with our belief that θ-pinch pulsed systems constitute a promising and interesting approach to the thermonuclear problem, it is proposed that a new Scylla experiment, Scylla V, be constructed in toroidal geometry. The purpose of this experiment will be to study the toroidal stabilization problem and to achieve long confinement times. The elimination of end losses will allow concentration on the study of plasma stability and purity. Confinement times of about 100 μsec will be possible with the particular design proposed in the next subsection. Further increasing the energy of the power crowbar bank and crowbarring it can lead to magnetic field durations of the order of 1 msec.

D. Conceptual Design of Scylla

1. General Considerations - A preliminary study of θ-pinch toroids having major diameters of 3.0 and 4.0 meters with minor diameters in the range of 10 to 15 cm has been carried out. The deuterium (or D-T mixture) gas will be ionized, "shock" heated, and compressed in the single-turn toroidal coil. Stabilization of the plasma will be provided either by stabilization conductors just inside the compression coil or by appropriate shaping of the flux-conserving inner surface of the compression coil.

The toroidal compression coil will be energized by a fast, high voltage, primary capacitor bank and a slower secondary capacitor bank to extend the magnetic compression field both in time and magnitude. In order to maintain the same initial shock dynamics as in previous Scylla devices, a voltage of 60 kV is chosen for the primary bank which initiates the discharge. The secondary bank (power crowbar) will provide energy storage at a voltage of 10 kV and will be switched onto the compression coil prior to the time of maximum current from the primary bank.

A low energy, fast capacitor bank will be used to inductively preionize the plasma in the coil as in Scylla IV. An additional energy storage capacitor bank will be provided to energize the stabilization conductors.

Inductance and magnetic pressure considerations dictate that the torus be fed by a radial parallel plate transmission line (current collector plates) on its outside perimeter. The conceptual design of the device is indicated in the vertical elevation view of Fig. 27 as well as in the plan views of Figs. 28 and 29. The toroidal compression coil and collector plates will be located on the first floor level, surrounded by the primary capacitor bank. The coaxial cables from the primary bank will feed into the radial collector plate transmission line as indicated in Fig. 27. The secondary capacitor bank will be located in the basement area below the machine and will connect into the collector plates outside the region of the primary bank feed. The preionization capacitor bank will be located over the outer regions of the collector plate system. The energy storage for the stabilization conductors will be located on the basement level.

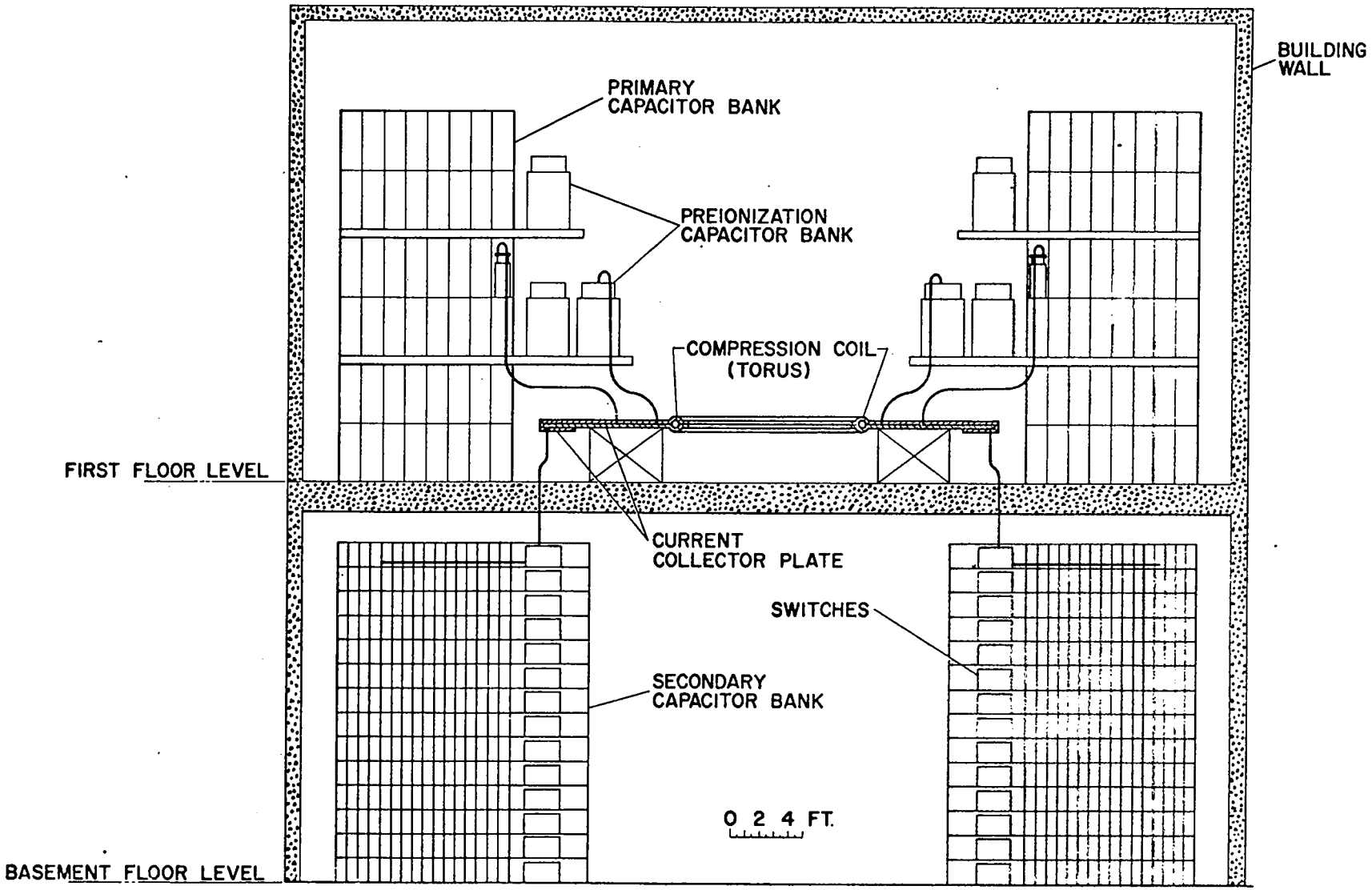

Fig. 27 Elevation of the proposed Scylla V experiment.

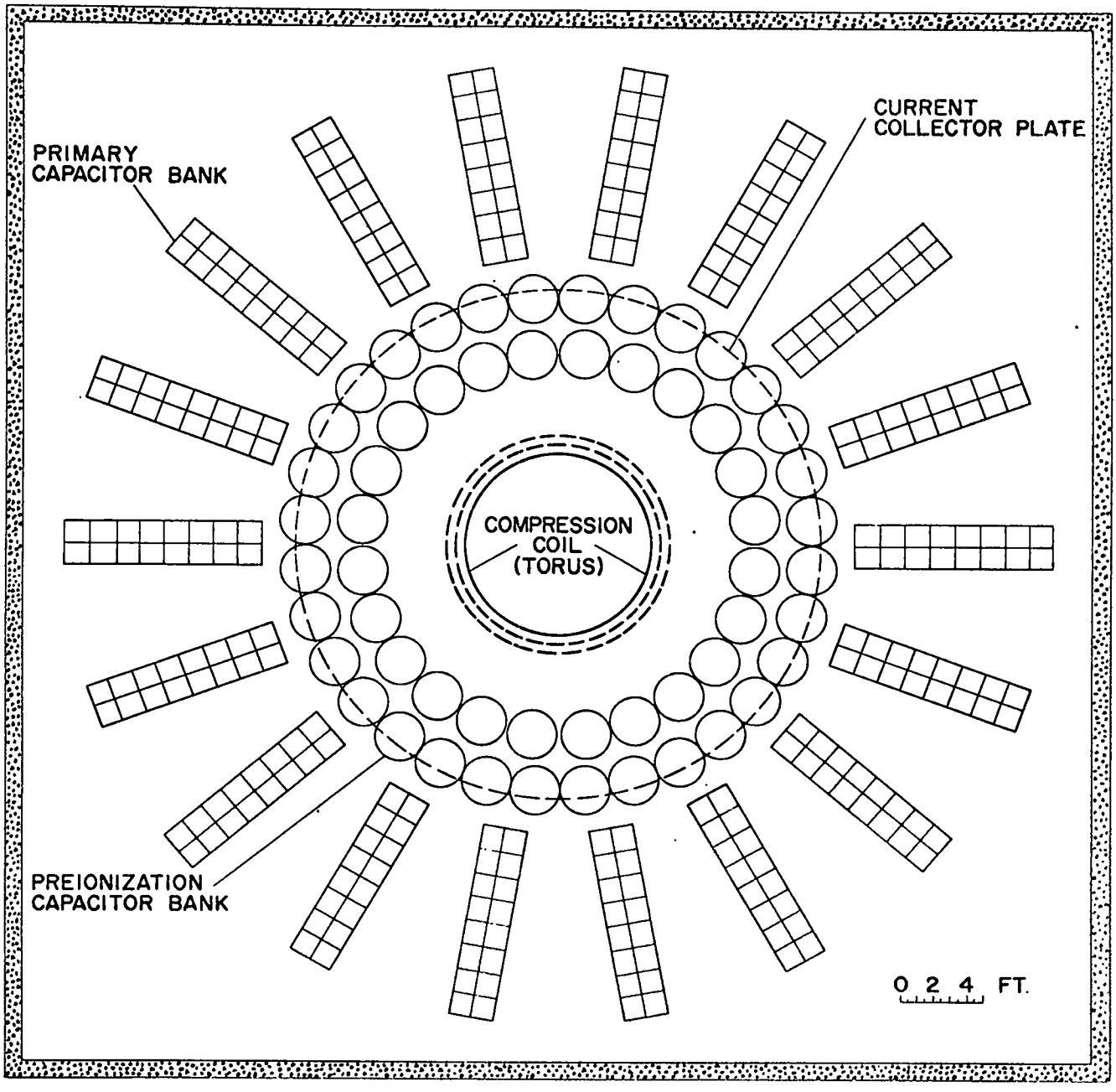

Fig. 28 Main floor plan of the proposed Scylla V experiment.

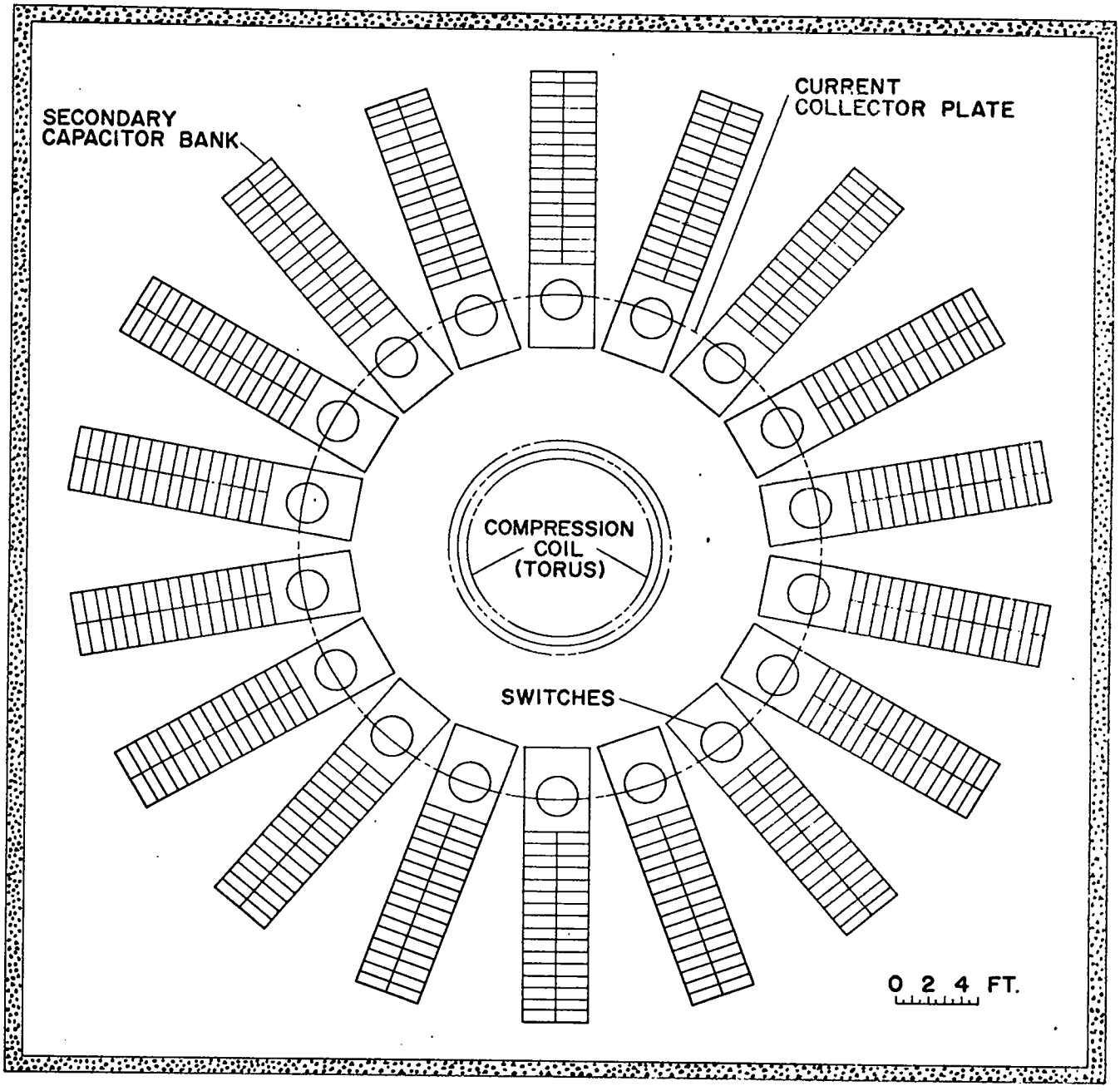

Fig. 29 Basement floor plan of the proposed Scylla V experiment.

2. Electrical Parameters - The circuital form of Ampere's law gives the magnetic field produced in the toroidal coil by a current I,

$$B = \frac{I}{5r} \text{ (G)}, \tag{15}$$

where I is in amperes, and r is the distance from the major axis of the torus in cm.

The inductance L_T of a single-turn torus as obtained from energy considerations is

$$L_T = 4\pi\left[b - (b^2 - a^2)^{\frac{1}{2}}\right] \text{ (nH)}, \tag{16}$$

where b is the major radius and a the minor radius of the torus in cm. If $a \ll b$, the term in the radical can be expanded, and neglecting terms in a^4/b^4 the torus inductance is

$$L_T = 2\pi \frac{a^2}{b} \text{ (nH)}. \tag{17}$$

The ratio λ of source inductance of the capacitor bank and feed to that of the toroidal coil determines the fraction α of the capacitor bank energy W_{cap} and capacitor bank voltage V_{cap} which appears at the coil according to the relation

$$\alpha = \frac{W_c}{W_{cap}} = \frac{V_c}{V_{cap}} = \frac{1}{1+\lambda}; \qquad \lambda = \frac{L_{cap}}{L_T}. \tag{18}$$

Here W_c and V_c are the magnetic energy in the coil and its initial voltage.

It is convenient to express the magnetic field in the compression coil in terms of the capacitor bank energy and the transfer efficiency α by

$$B = 3.58 \times 10^3 \left[\frac{\alpha W_{cap}}{a^2 b}\right]^{\frac{1}{2}} \text{ (kG)}, \tag{19}$$

where W_{cap} is in megajoules.

The maximum azimuthal electric field E_θ produced inside the compression coil is given by

$$E_\theta = \frac{\alpha V_{cap}}{2\pi a}. \tag{20}$$

3. Collector Plate System.- The current collector plates for the Scylla V system will be made of 7.6-cm thick aluminum alloy plate. The outside diameter of the annular collector plate system will be 8 to 12 m, depending on the magnitude of the energy storage. With a primary bank of 5 MJ and a secondary bank of 20 MJ the outside diameter will be 11.5 m. They must be clamped together to withstand magnetic pressures as great as 10,000 psi. Electrically insulated through-bolts will be used to balance the magnetic forces. An identical technique has been used successfully in the Scylla IV device at higher magnetic pressures. Multiple layers of thin Mylar (0.075-mm thickness) built up to a 2-mm thickness will be used for the 60-kV electrical insulation between the plates. Mylar insulation, 1.6-mm thick, has proved reliable in the 50-kV Scylla IV system.

The cables from the primary and secondary banks, as well as from the low energy preionization capacitor bank, will be connected to the collector plates in a minimum inductance arrangement as discussed below. Between the collector plates around each cable two polyethylene insulating hats will be used with thin interleaved sheets of Mylar (Fig. 30). O-ring seals will be made on the cable insulating surface such that air can be evacuated from the system. The entire system will be back-filled with SF_6 electrical insulating gas to a pressure of 40 psi to minimize the voltage creep length required in terminating the cables.

4. Primary Capacitor Bank Parameters - A fundamental problem in the design of θ-pinch devices is that of minimizing the energy storage source inductance while at the same time providing electrical insulation for the required high voltages. As listed in Tables V and VI the inductances of the toroidal coils under consideration are in the range of 0.8 to 2.4 nH. The primary capacitor bank must have an inductance which is small compared to these values. The primary bank inductance can be written as

$$L_{PB} = L\ (\text{capacitors} + \text{switches}) + L\ (\text{cables}) + L\ (\text{collector plates}). \quad (21)$$

The primary bank will use a low inductance capacitor similar to that used in the Scylla IV device with a capacity of 2 μF but with an increased voltage of 60 kV. A four-element spark gap of the type used on Scylla IV will be used on each capacitor. The combined capacitor and gap inductance

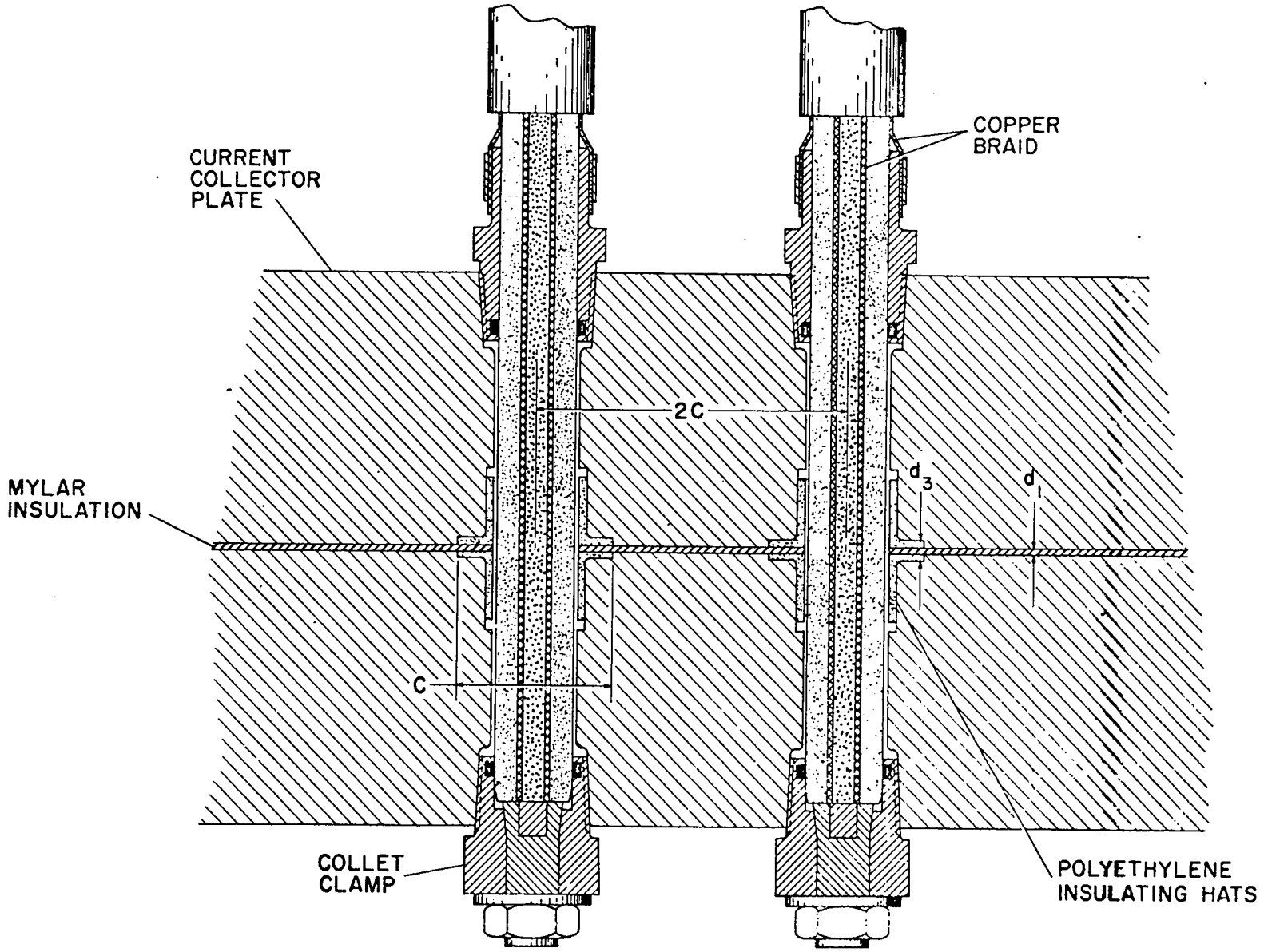

Fig. 30 Detail of the cable feed into the Scylla V collector plate.

has a measured value of 65 nH. Experience from Scylla IV operation has shown that there are no difficulties in firing large numbers of these gaps simultaneously and that they will operate without maintenance for at least 1000 shots.

Inductance considerations indicate it is feasible to use six coaxial cables to connect each capacitor-spark gap unit into the collector plate for primary bank energies less than 6 MJ. As the primary bank energy is increased above 6 MJ, the number of cables should be decreased until their inductance becomes comparable to that of the collector plate. Coaxial cable of the RG 19/14 type with an inductance of 164 nH/m will be used. This cable has been used in Scylla III and is expected to provide reliable operation at 60 kV in Scylla V.

The major inductance problem arises in the collector plate inductance L_{cp}. This inductance is dependent on the manner in which the coaxial cables are distributed and connected into the collector plate system. The collector plate inductance which consists of two parts is given by

$$L_{cp} = 2d_1 \log \frac{r_2}{r_1} + \frac{2\, d_2}{(r_3^2 - r_2^2)^2} \left[r_3^4 \log \frac{r_3}{r_2} - \frac{1}{4} (3r_3^2 - r_2^2)(r_3^2 - r_2^2) \right] \text{(nH)}. \quad (22)$$

Here r_1 is the sum of the major and minor toroidal radii, r_2 is the radial distance to the point in the collector plate at which cables are connected, r_3 is the outside radius of the primary bank cable connections in the collector plate system, d_1 and d_2 are the separation between the parallel collector plates in the region $(r_2 - r_1)$ and $(r_3 - r_2)$, respectively. The first term in Eq. (22) pertains to the region $(r_2 - r_1)$, which does not contain cables and in general has a constant current flow across any closed perimeter path $2\pi r$ with $r_1 \leq r \leq r_2$.

The second term in L_{cp}, Eq. (22), arises from the collector plate area containing the coaxial feed cables. In this region, $(r_3 - r_2)$, the current density which is fed into the plates is a constant, i.e., a uniform distribution of cables. The current flowing across any closed perimeter path $2\pi r$, $r_2 \leq r \leq r_3$, is given by

$$I = I_o \frac{r_3^2 - r^2}{r_3^2 - r_2^2} . \quad (23)$$

The second term in Eq. (22) is obtained from energy considerations which utilize Eq. (23).

Two questions arise in the determination of the collector plate arrangement which gives minimum inductance: (1) What is the optimum value of r_2? (2) Should the cables be close packed or distributed in space to provide lower-inductance current paths? Both analytical and numerical studies of these two problems lead to the following conclusions: (1) The value of r_2 should be a minimum compatible with the toroidal coil current feeds which may be required for different diameter toroids and the auxiliary clamps required to contain the magnetic forces. In the results presented below a conservative value of r_2 has been used. (2) The cables should not be close packed but distributed in space as follows: A minimum inductance design of an individual cable connection into the collector plate, which is compatible with the 60-kV electrical insulation is shown in Fig. 30. It utilizes SF_6 insulation of the voids and requires a square area of C cm (4.4 cm) on a side. The effective plate separation of this area, which takes into account the cable holes in the plate, is 1.38 cm. Numerical studies of the second term in Eq. (22) show that the inductance is minimized if the cables are separated by approximately 2C so there is a region of width C centered between cables having a plate separation 0.2 cm. With this optimum arrangement the effective separation d_2 becomes 0.35 cm rather than the 1.38 in the closed-packed configuration. The optimum width of the region between cables varies slightly with primary bank energy, increasing from 0.9 C at 3 MJ to 1.1 C at 9 MJ. However, the use of 1.0 C times the cable feed width for all cases produces an error of less than 1% in L_{CB} since the minima of the functions L_{CB} vs cable separation are rather flat.

The outer collector plate radius r_3 is a function of the primary bank energy W_{PB} and is determined by the area required to accept the bank cables,

$$r_3^2 = r_2^2 + 2.96 \times 10^3 \, W_{PB}. \tag{24}$$

Here W_{PB} is in MJ and the radii are in cm.

These design considerations give the primary bank inductance as a function of energy storage.

$$L_{PB} = \left[\frac{0.195}{W_{PB}}\right]_{\substack{\text{Capacitor}\\ \text{and}\\ \text{Spark gaps}}} + \left[\frac{0.625}{W_{PB}}\right]_{\text{Cables}} + L_{cp} \quad (\text{nH}). \tag{25}$$

Graphs of the primary bank inductance as a function of W_{PB} and the torus radii are given in Fig. 31. For the indicated torus radii, the minimum source inductance, and thus the maximum transfer efficiency is obtained with a primary bank energy storage of 5 to 6 MJ. As W_{PB} is increased further, L_{PB} does not decrease, owing to the increased collector plate area required to accept the cables. In order to maintain the minimum inductance with W_{PB} in the 6 to 9 MJ region, the number of cables feeding the collector plates from each spark-gap capacitor unit has been reduced from the nominal number of 6.

Tables V and VI present the results of the toroidal θ-pinch study in tabular form. The peak magnetic field B, the maximum azimuthal electrical field E_θ, and the transfer efficiency α, for toroidal coils with indicated radii are given as a function of the primary bank energy storage. It should be noted that in these studies, the electrical resistive losses have been neglected and, to achieve the indicated E_θ and B values, will require that W_{PB} in the tables be increased by approximately 15%.

We assign $E_\theta \approx 1.1$ kV/cm as the minimum value for which acceptable ion energies in the low-density regime can be obtained. Previous Scylla θ-pinches have utilized $E_\theta \approx 1.3$ kV/cm. At these values of E_θ it is concluded that a primary-bank energy storage of 5 MJ at 60 kV would provide an optimum power supply to study the containment and stability problems of the θ-pinch in reasonable toroidal geometry. The corresponding maximum magnetic field is about 70 kG in a torus of 2-meter major radius and 6.25-cm minor radius. The period is about 15 μsec.

5. Secondary Capacitor Bank - The secondary capacitor bank will provide energy storage at 10 kV to extend the magnitude and time duration of the primary bank magnetic compression field. This bank is required to obtain the compression times necessary to study the plasma confinement and stability.

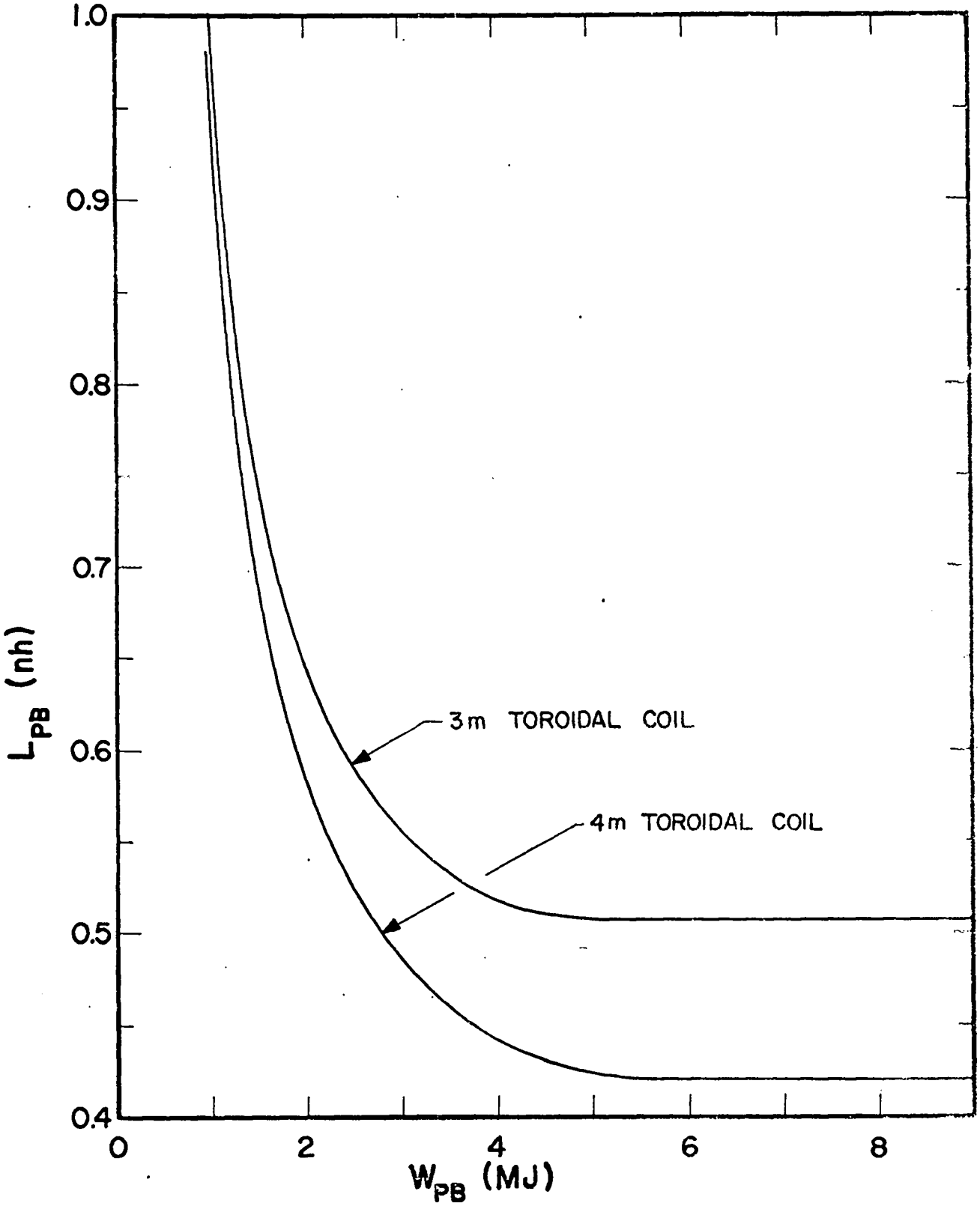

Fig. 31 Inductance of the primary capacitor bank as a function of capacitor energy storage.

TABLE V.. Four-Meter Toroidal Coil Parameters with Primary Capacitor Bank.

a = 5.0 cm

W_{PB} (MJ)	L_{PB} (nH)	L (nH)	α ___	E_θ (kV/cm)	B (kG)	$\tau/2$ (μsec)
1	0.969	1.754	0.448	0.86	33.8	3.1
2	0.587	1.372	0.572	1.09	54.0	3.9
3	0.485	1.270	0.618	1.18	68.7	4.6
4	0.444	1.229	0.638	1.22	80.6	5.2
5	0.427	1.212	0.648	1.24	90.9	5.8
7	0.423	1.208	0.650	1.24	107.7	6.8
9	0.423	1.208	0.650	1.24	122.1	7.7

a = 6.25 cm

W_{PB} (MJ)	L_{PB} (nH)	L (nH)	α ___	E_θ (kV/cm)	B (kG)	$\tau/2$ (μsec)
1	0.966	2.193	0.560	0.86	30.2	3.4
2	0.584	1.811	0.678	1.04	47.0	4.4
3	0.483	1.710	0.718	1.10	59.2	5.3
4	0.441	1.668	0.736	1.12	69.3	6.0
5	0.422	1.649	0.744	1.14	77.9	6.7
7	0.421	1.648	0.744	1.14	92.1	8.0
9	0.421	1.648	0.744	1.14	104.4	8.9

a = 7.5 cm

W_{PB} (MJ)	L_{PB} (nH)	L (nH)	α ___	E_θ (kV/cm)	B (kG)	$\tau/2$ (μsec)
1	0.964	2.731	0.647	0.82	27.1	3.9
2	0.582	2.349	0.752	0.96	41.2	5.1
3	0.480	2.247	0.786	1.00	51.7	6.1
4	0.439	2.206	0.801	1.02	60.3	7.0
5	0.422	2.189	0.807	1.03	67.6	7.8
7	0.418	2.185	0.809	1.03	80.0	9.2
9	0.418	2.185	0.809	1.03	90.8	10.4

TABLE VI . Three-Meter Toroidal Coil Parameters with Primary Capacitor Bank.

a = 5.0 cm

W_{PB} (MJ)	L_{PB} (nH)	L (nH)	α	E_θ (kV/cm)	B (kG)	$\tau/2$ (μsec)
1	1.016	2.063	0.507	0.97	41.5	3.4
2	0.645	1.692	0.619	1.18	64.8	4.3
3	0.554	1.601	0.654	1.25	81.6	5.2
4	0.521	1.568	0.668	1.28	95.3	5.8
5	0.511	1.558	0.672	1.28	106.8	6.5
7	0.511	1.558	0.672	1.28	126.5	7.8
9	0.511	1.558	0.672	1.28	143.2	8.8

a = 6.25 cm

W_{PB} (MJ)	L_{PB} (nH)	L (nH)	α	E_θ (kV/cm)	B (kG)	$\tau/2$ (μsec)
1	1.013	2.649	0.618	0.94	36.6	3.8
2	0.641	2.277	0.718	1.10	55.9	5.0
3	0.552	2.188	0.748	1.14	69.9	6.0
4	0.518	2.154	0.760	1.16	81.3	6.9
5	0.507	2.143	0.763	1.17	91.1	7.7
7	0.507	2.143	0.763	1.17	107.7	9.1
9	0.507	2.143	0.763	1.17	122.1	10.3

a = 7.5 cm

W_{PB} (MJ)	L_{PB} (nH)	L (nH)	α	E_θ (kV/cm)	B (kG)	$\tau/2$ (μsec)
1	1.010	3.366	0.700	0.89	32.6	4.3
2	0.638	2.994	0.787	1.00	48.8	5.7
3	0.548	2.904	0.811	1.03	60.6	6.9
4	0.514	2.870	0.821	1.04	70.4	7.9
5	0.504	2.860	0.824	1.05	78.9	8.9
7	0.504	2.860	0.824	1.05	93.3	10.5
9	0.504	2.860	0.824	1.05	105.8	11.9

The secondary bank will consist of 60-μF, 10-kV capacitors arranged in vertical racks on the basement floor as indicated in Figs. 27 and 29. Each rack will have 12 shelves with 0.1 MJ per shelf. A single vacuum spark gap switch of the multi-electrode type[53] will be used to switch each shelf into the collector plates. This type of vacuum gap is currently being used in a 3-MJ power-crowbar bank on Scylla IV to switch 140 kJ. A single type RG 17/14 coaxial cable will connect each capacitor into the gap. Forty coaxial cables of the RG 19/14 type with average lengths of 6.8 m will be used to connect each spark gap into the collector plate. These cables will connect on the underside of the collector plates through the top collector plate, folded under the plate system as indicated in Fig. 27.

The source inductance of the secondary bank has the following series components: (1) The shelf inductance, which includes capacitors and cables to the vacuum gap, is 3 nH/MJ. (2) The vacuum gap inductances, including the cable connection both in and out, are 2 nH/MJ. (3) The cable inductance from gap to collector plate will be 2.8 nH/MJ. (4) The collector plate inductance is given by

$$L_{SB\text{-}CP} = \frac{0.175}{(r_4^2 - r_3^2)^2}\left[4r_3^4 \log\frac{r_4}{r_3} + (r_4^4 - 4r_3^2 r_4^2 + 3r_3^4)\right] + 0.40 \log\frac{r_4}{r_3} + 0.80 \log\frac{r_3}{r_2} + 0.40 \log\frac{r_2}{r_1}, \quad (26)$$

where r_4 is the outermost radius of the collector plate system and the other r's have been defined previously. This inductance $L_{SB\text{-}CP}$ depends on the magnitude of both the primary and secondary bank energy storages. The secondary bank cables are distributed in the collector plate in a manner similar to those of the primary bank. The total source inductance of the secondary bank is listed in Tables VII and VIII as a function of the secondary bank energy W_{SB} for an assumed primary bank energy of 5 MJ.

Tables VII and VIII present the toroidal coil parameters which result from its energization by the secondary capacitor bank at the indicated energy storages W_{SB}. In the Table, L is the total circuit inductance including that of the toroidal coil, α is the energy and voltage transfer efficiency, B is the maximum magnetic field, $\tau/2$ is the half period, and a

TABLE VII. Four-Meter Toroidal Coil Parameters with Secondary Capacitor Bank.

a = 5.0 cm

W_{SB} (MJ)	L_{SB} (nH)	L (nH)	α ____	B (kG)	$\tau/2$ (μsec)
10	1.314	2.099	0.374	97.6	64.3
15	1.084	1.869	0.420	126.5	74.4
20	0.981	1.766	0.444	150.3	83.6

a = 6.25 cm

W_{SB} (MJ)	L_{SB} (nH)	L (nH)	α ____	B (kG)	$\tau/2$ (μsec)
10	1.312	2.539	0.483	88.8	70.8
15	1.082	2.309	0.532	114.0	82.6
20	0.978	2.205	0.556	134.5	93.3

a = 7.5 cm

W_{SB} (MJ)	L_{SB} (nH)	L (nH)	α ____	B (kG)	$\tau/2$ (μsec)
10	1.314	3.081	0.573	80.6	77.9
15	1.084	2.851	0.620	102.5	91.8
20	0.981	2.748	0.643	120.8	104.0

Table VIII. Three-Meter Toroidal Coil Parameters with Secondary Capacitor Bank

a = 5.0 cm

W_{SB} (MJ)	L_{SB} (nH)	L (nH)	α ___	B (kG)	$\tau/2$ (μsec)
10	1.451	2.498	0.419	119.2	70.2
15	1.223	2.270	0.461	153.3	82.0
20	1.122	2.169	0.483	181.1	92.5

a = 6.25 cm

W_{SB} (MJ)	L_{SB} (nH)	L (nH)	α ___	B (kG)	$\tau/2$ (μsec)
10	1.447	3.083	0.531	107.2	78.0
15	1.220	2.856	0.573	136.7	91.9
20	1.119	2.755	0.594	160.6	104.2

a = 7.5 cm

W_{SB} (MJ)	L_{SB} (nH)	L (nH)	α ___	B (kG)	$\tau/2$ (μsec)
10	1.451	3.807	0.619	96.6	86.7
15	1.223	3.579	0.658	122.1	102.8
20	1.122	3.478	0.677	143.0	116.7

is the minor torus radius. In the calculation of the indicated values, all resistive losses have been neglected. In order to attain the indicated values, the energy storage W_{SB} will have to be increased by approximately 20%.

It is concluded from a study of the secondary bank parameters that a secondary bank energy storage of 15 to 20 MJ is an optimum value for plasma confinement and stability studies in the indicated class of toroidal coils. The magnetic field is approximately 120 kG and the period about 150 μsec.

6. Engineering Aspects of Scylla V - Although a fast primary bank energy storage of 5 MJ and a 20-MJ secondary bank energy storage may appear formidable, the technical problems have been solved in the present Scylla IV device.[53] Essentially all the individual components to be used in Scylla V are presently operational in Scylla IV. It is especially noteworthy that the simultaneous firing of many spark gaps (> 200) in parallel is accomplished without difficulty in the Scylla IV device. Experience with high voltages, large pulsed currents, and the rapid switching of appreciable energies has been obtained during the past seven years with the previous Scylla devices.

E. A Possible Racetrack Experiment

A possible alternative arrangement for a closed geometry experiment is shown in Fig. 32. Two conventional θ-pinch straight sections are joined by U-bends into a racetrack. Plasma lost from either straight section by end loss is guided around the U-bend into the other straight section. The U-bend sections are subject to radial drift and must be stabilized either by stabilizing conductors or shaping of the inside of the coil. Possible advantages of the racetrack geometry are: a) the end coils could be continuously energized and cryogenically cooled if desired. b) The stabilization region is separated from the θ-pinch heating region so that no interactions take place between them. A probable disadvantage is that the U-bends serve to dilute the hot plasma from the θ-pinch region. Cold gas must not be allowed in the U-bends because of its degrading effect on the hot plasma. This would require pulsed injection of the gas filling into the θ-pinch region. This experiment would probably operate at low β, and the plasma properties would be quite different from those of previous θ-pinches.

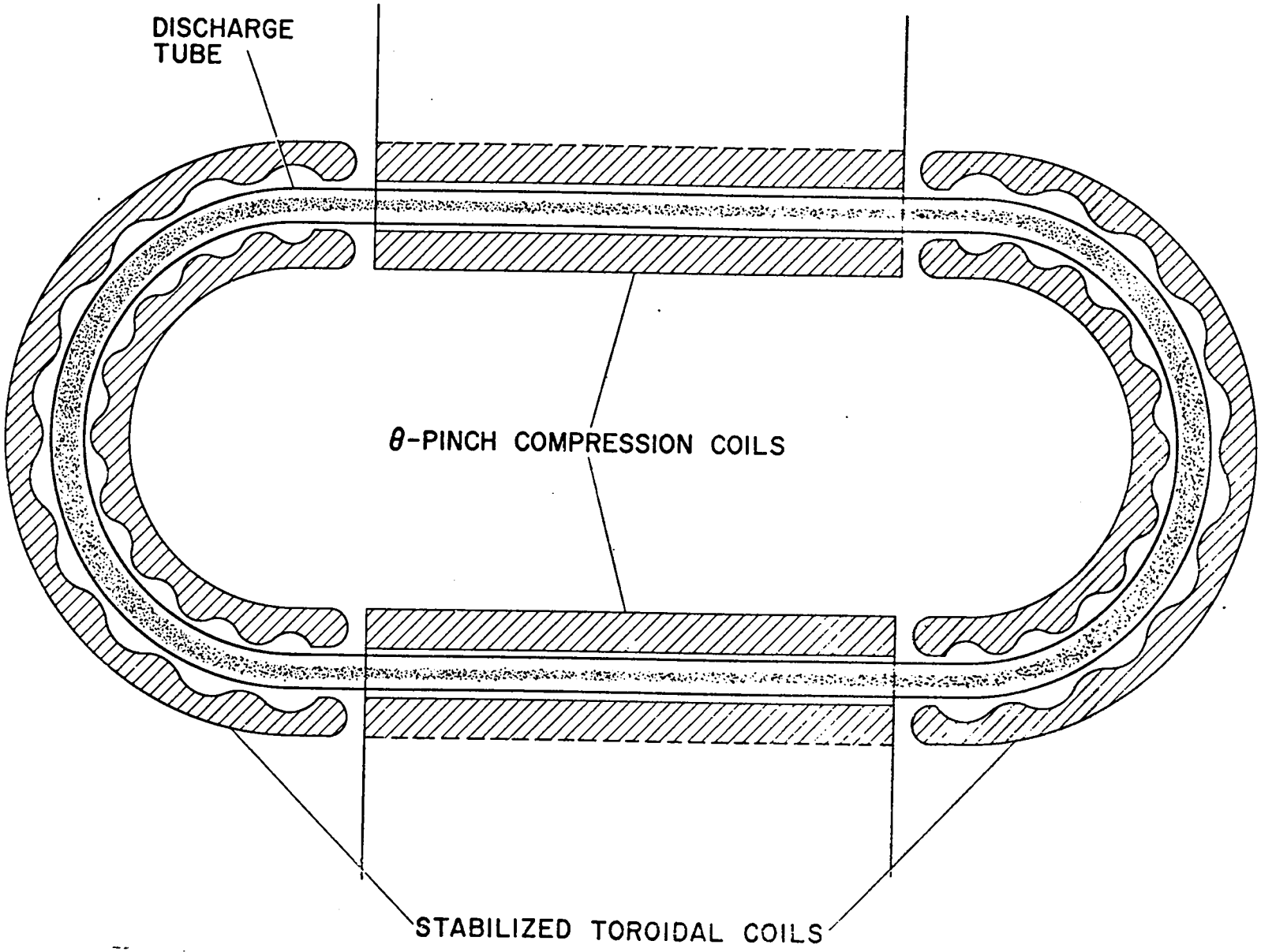

Fig. 32 A possible racetrack geometry for Scylla experiments. Two straight Scylla sections are joined by u-bend guide sections into a closed configuration.

VIII. θ-PINCH SYSTEMS IN RELATION TO PULSED REACTORS

A. Pulsed Systems

θ-pinches of the type discussed here are embryonic forms of pulsed thermonuclear reactors. In such systems the thermonuclear energy produced by the D(t,n) He^4 reaction would be used to overcome losses attendant upon plasma heating and containment and to produce additional useful output energy. In pulsed systems, as opposed to steady-state systems, the plasma is burned for a time τ and then purged. On the next pulse of magnetic field new, cold plasma is heated and burned again.

B. The Lawson Criterion

The minimal conditions of plasma temperature, density, and containment time necessary to achieve a favorable balance between thermonuclear energy production and reactor losses are given by the Lawson Criterion.[66] In this criterion all losses of the system external to the plasma itself are neglected. These would include, for example, electrical joule heating losses incurred in furnishing the magnetic field, refrigeration losses in cooling the magnetic coils, and losses of energy of the fusion reaction products which are not converted to heat or electrical energy output. The energy expenditures considered in the Lawson Criterion are the following irreducible ones:

(1) The energy required to produce each cm^3 of plasma having n/2 deuterons, n/2 tritons and n electrons per cm^3 at a common temperature T:

$$w_p = 3nkT \qquad (27)$$

(2) The energy radiated away as bremsstrahlung during the time τ that plasma is contained and burns:

$$w_B = 4.8 \times 10^{-31} \; n^2 \tau (kT)^{\frac{1}{2}} \qquad (28)$$

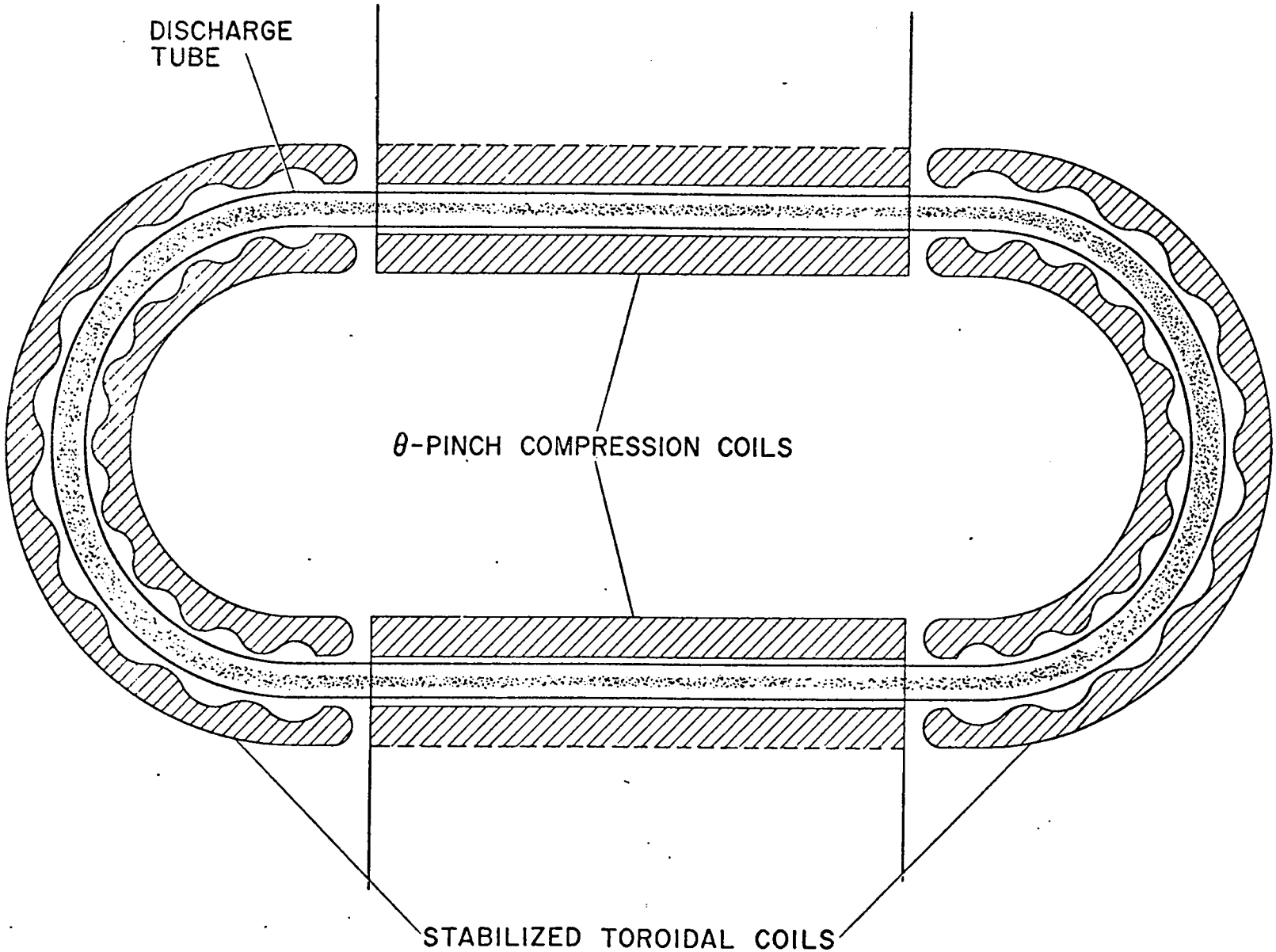

Fig. 32 A possible racetrack geometry for Scylla experiments. Two straight Scylla sections are joined by u-bend guide sections into a closed configuration.

LASL-AEC-OFFICIAL

Here w_B is in joules per cm^3, and kT is in keV. (The Gaunt factor of bremsstrahlung theory has been taken as unity).

It should be remarked that another radiative loss is that of electron-cyclotron radiation.[67] In $\beta = 1$ plasmas such as are being considered here, this radiation arises only from the surface layer separating plasma from magnetic field. At the temperatures appropriate to pulsed reactors this radiation is small compared to bremsstrahlung.

(3) The thermonuclear energy produced by each cm^3 of plasma is given by

$$w_T = \tfrac{1}{4}\, n^2\, Q\overline{\sigma v}\tau \ , \qquad (29)$$

where Q is the energy released per D-T fusion reaction (17.6 MeV), plus that released in the moderating blanket in producing a triton, and $\overline{\sigma v}$ (T) is the fusion cross section averaged over all relative velocities for binary collisions between deuterons and tritons having a Maxwellian velocity distribution at the same temperature T. The function $\overline{\sigma v}$ vs kT for a deuterium-tritium mixture is shown in Fig. 33.

In the Lawson Criterion w_T, as well as w_p and w_B themselves, is considered as a source of thermal energy, and it is assumed that this energy is converted to useful output at a thermal efficiency ϵ. Then the minimal condition for useful energy production is given by

$$\epsilon\,(w_T + w_p + w_B) \geq w_p + w_B \ . \qquad (30)$$

Substituting for these quantities gives

$$\tfrac{1}{4}\, Q\overline{\sigma v}(n\tau) \geq \frac{1-\epsilon}{\epsilon}\ \left[3kT + 4.8\times10^{-31}(kT)^{\frac{1}{2}}\, n\tau\right] \qquad (31)$$

For $kT \gtrsim 5$ keV, the bremsstrahlung term can be neglected, giving for the Lawson Criterion

$$n\tau \gtrsim 12\ \frac{1-\epsilon}{\epsilon}\ kT/Q\overline{\sigma v} \ . \qquad (32)$$

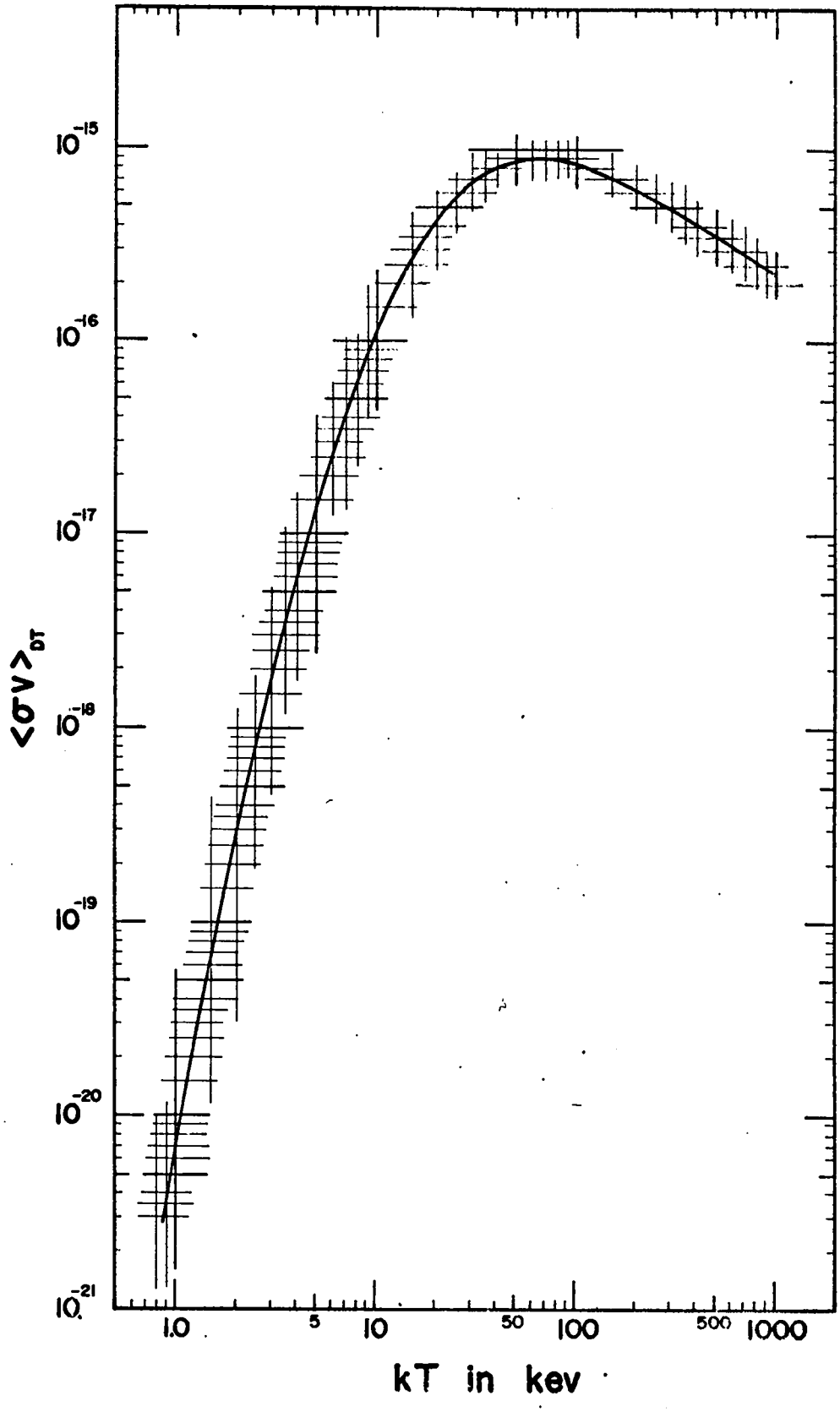

Fig. 33 The nuclear cross section for fusion reactions between deuterons and tritons averaged over a Maxwell distribution of velocities as a function of temperature.

A graph of the Lawson Criterion (including bremsstrahlung) for $\epsilon = \frac{1}{3}$ and Q = 17.6 MeV is given in Fig. 34. In this plot of $n\tau$ vs kT the region above the curve represents net energy gain per unit volume of plasma. At the minimum near kT = 25 keV the value of $n\tau$ is about 7×10^{13} cm^{-3} sec. This accounts for the often-quoted figure $n\tau \approx 10^{14}$ as the goal of containment experiments.

For $\beta = 1$ the pressure balance equation is

$$2nkT = B^2/8\pi. \tag{33}$$

Hence at the minimum of the Lawson curve (kT = 25 keV)

$$\tau = 1.41 \times 10^8/B^2, \text{ (sec)} \tag{34}$$

where B is in gauss. The maximum value of B set by the strength and melting of conductors is approximately 500 kG. Therefore the minimum value of containment time for satisfaction of the Lawson Criterion is approximately 0.5 millisecond. A more practical upper limit on B is 250 kG; then $\tau \approx 2$ ms.

C. Conditions for Net Power Production in a Pulsed Reactor

When one attempts to extend these considerations to determine plasma conditions sufficient for a net-power-producing reactor the situation becomes less definite, since a particular model must be assumed in order to evaluate actual energy losses. One must not lose sight of the fact that the thermonuclear reactor problem is basically one of plasma physics and that the materials technology which is eventually necessary for its solution will probably need to be developed to accommodate the exigencies of the plasma solution. Therefore in considering feasibility of an eventual reactor system it is premature to specify in terms of the present state of the art such things as energy sources for furnishing the magnetic field, and heat exchange systems for conversion of thermonuclear heat to useful output. For example, at the large stored energies which are eventually necessary, magnetic energy storage, using cryogenic conductors or superconductors, is probably the most appropriate. Even the magnitude of the magnetic fields which can eventually be used in superconducting systems is

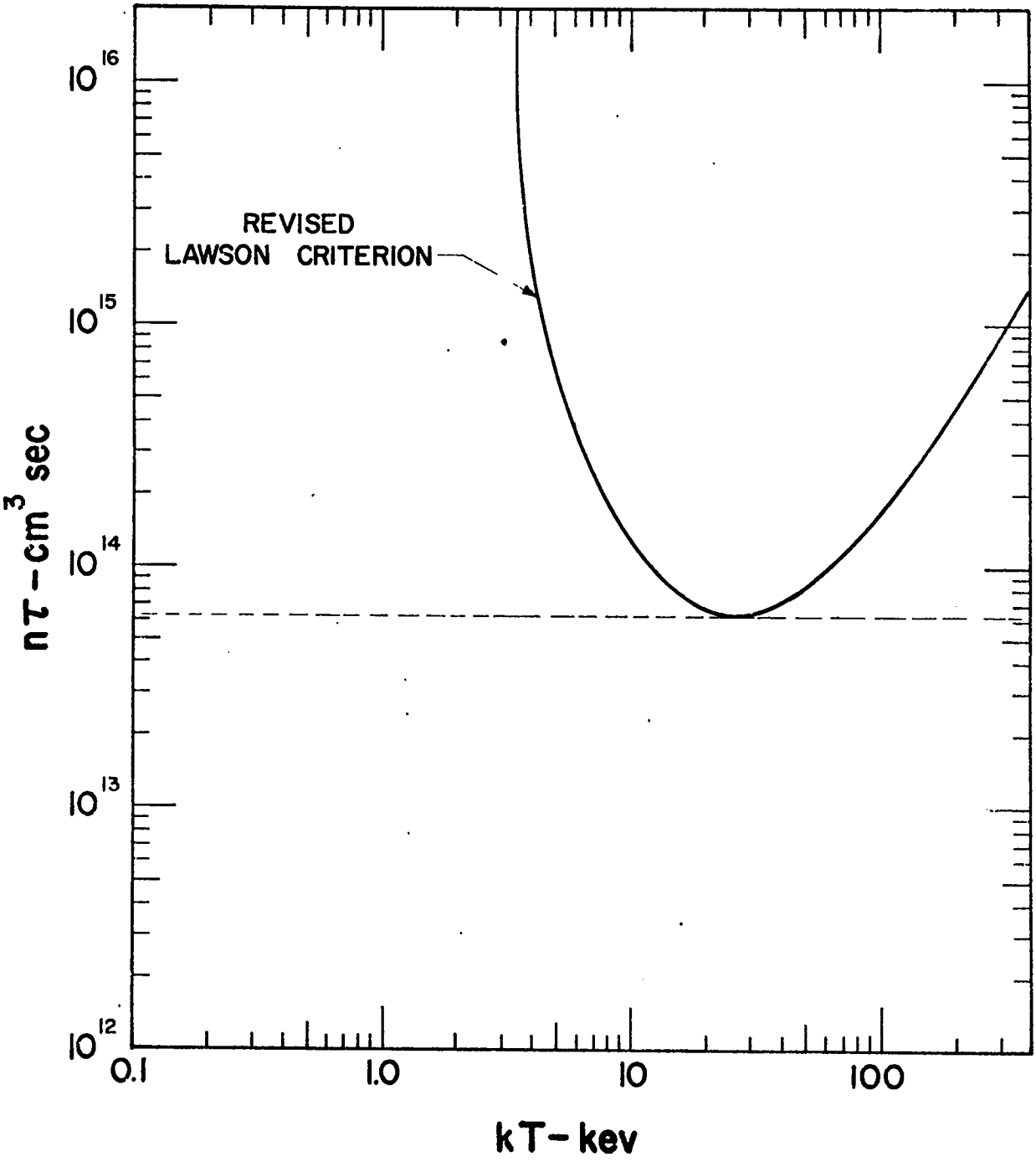

Fig. 34 The Lawson criterion for the minimum product of density and confinement time to produce useful thermonuclear energy vs temperature.

presently unknown.

However, there are a number of basic elements which must comprise an eventual thermonuclear reactor and which determine its losses when certain assumptions are made:

(1) The thermonuclear energy is emitted predominately as kinetic energy of 14-MeV neutrons. This must be converted to heat in a moderating blanket outside the plasma. For reasonable thermal efficiency the blanket should simultaneously act as a heat-exchange coolant at a temperature in excess of 200°C. The same blanket must also breed sufficient tritium to maintain a positive tritium budget against reprocessing losses.

(2) For a given $n\tau$ a fraction

$$f = \tfrac{1}{2}\, n\tau\, \overline{\sigma v} \tag{35}$$

of the D-T is burned up. Assuming the energy of the α-particles to be retained and thermalized in the plasma, which also expands against constant magnetic field B, one can calculate the work ΔW done against the magnetic field. This represents electrical work done on the electrical energy source that furnishes the magnetic field and can be more than sufficient to make up the joule heating loss W_E, allowing the electrical system to be energetically self sufficient.

(3) The coil which furnishes the magnetic field is commonly conceived of as a hard superconductor when steady-state reactors are considered, and it is assumed to be placed outside the moderating blanket in order that heat deposited in it by the neutrons need not be removed by the refrigerator which maintains the temperature of the coil. In a pulsed reactor it may or may not be necessary to furnish the magnetic energy filling the volume of the blanket. However, in the models considered below the pulsed coil is placed inside the blanket. The energy deposition by neutrons in the coil then becomes a major factor in the energy balance, and its treatment largely controls the materials technology. It is also prudent to choose an inexpensive coil material which can be replaced when radiation damage becomes excessive.

In a separate report[68] a feasibility study of a pulsed reactor is given. Two basic models are chosen: The first uses a hot beryllium copper or cryogenic aluminum coil inside the neutron blanket. All of the magnetic field is furnished by this coil, so that none permeates the neutron blanket. The second model is that of the sustained field θ-pinch described in Sec. VI-A and Fig. 18. A pulsed, hot Be-Cu coil lies inside a steady field which can be furnished by a super conductor placed outside the neutron blanket. In two of the cases, (the pulsed, aluminum cryogenic coil and the copper coil of the sustained-field θ-pinch) the pulsed electrical circuit is underdamped: in the first case because the resistivity of the Al is very low and in the second because of the very short duration τ of the magnetic impulse used to form the hot plasma. In the third case of the hot Be-Cu coil the circuit is overdamped. The advantage of the hot Be-Cu coil is that no refrigeration losses are incurred and it is more efficient even though the resistivity is two orders of magnitude higher than that of Al, cooled to liquid H_2 temperatures.

In both the Al and Cu cases, there is sufficient heat generated during the reactor pulse by electrical joule heating, bremsstrahlung, and nuclear reactions from the 14-MeV neutrons to drive the temperature far above its initial value, if one relied only upon the thermal conductivity and heat capacity of the coil material itself to accommodate the heat. It is possible, however, to remove this heat by flowing supercritical H_2O or liquid H_2 through coolant channels so that the temperature excursion stays within modest bounds.

D. Principal Energy Losses and Energy Balance in a Pulsed Reactor

The electrical loss W_E is that which takes place within one skin depth of the inner surface of the coil and feed slot as an assumed sinusoidal impulse of magnetic field is pulsed into and out of the coil from the energy source. The electrical loss per cm length of coil is given by

$$W_E = 5.3 \times 10^{-4} \, \eta^{\frac{1}{2}} \, \tau^{\frac{1}{2}} B^2 \, R_c \ (\text{w/cm}), \tag{36}$$

where η is the resistivity of the conductor in ohm-cm, B is the maximum

magnetic field, τ its half period, and R_c the coil inner radius. This energy loss is proportional to the stored magnetic energy per unit length

$$W_M = R_c^2 \, B^2/8, \tag{37}$$

which is in turn proportional to the plasma energy

$$W_p = 3\pi \, R_p^2 \, nkT \tag{38}$$

per unit length of coil (R_p is the plasma radius).

The bremsstrahlung energy loss deposited in the surface of the coil or discharge tube per unit length is of about the same magnitude as the electrical energy loss. It is given in terms of Eq. (28) by

$$W_B = \pi R_p^2 \, w_B. \tag{39}$$

A major source of energy loss is the heating of the conductor by 14-MeV neutrons. Each deposits an average energy E in charged particles and γ rays at a collision rate determined by the total cross section σ_T. This energy deposition per unit time is proportional to the thermonuclear power production and is given by

$$P_N = \Delta R_c \, n_c (\sigma_T E) \, P_T/Q, \tag{40}$$

where

$$P_T = \pi/4 \, R_p^2 \, n^2 \, Q \, \overline{\sigma v} \tag{41}$$

is the thermonuclear power production per unit length of reactor, n_c is the number density of conductor atoms and ΔR_c is the coil thickness.

The simplest criterion for determining ΔR_c is that it be sufficient for the coil to support the internal magnetic pressure $B^2/8\pi$ in tension (or the external magnetic pressure in compression in the sustained field case). However, the price of large R_c is correspondingly large nuclear heating. In the two cases with hot Cu coils this price can be paid, since the nuclear energy deposition occurs at a high temperature, at least twice the temperature of the neutron-blanket heat exchanger. However, in the cryogenic case this heat is deposited in the H_2 cryogen at low temperature and the refrigeration losses are prohibitive for such large ΔR_c. In this case ΔR_c must be chosen small, so that the coil is not self supporting. Then the magnetic pressure is

primarily counter balanced by transmitting it through the blanket to a heavy outer support cylinder. Owing to the compressibility of the blanket fluid, it would also be necessary to apply a pulse of hydraulic pressure to coincide with that of the magnetic field.

For both the hot and cryogenic coils, one must take into account the power P_p (per cm length) necessary to pump the coolant. A fraction 0.2 of the pump power is assumed to be deposited in the coolant itself. Furthermore, the pumps must run continuously, so that P_p must be multiplied by a duty factor ξ with respect to the impulsive losses. Here ξ is the ratio of the period 2τ of the magnetic wave to the effective time τ_T during which D-T reactions take place.

The overall energy balance for the cases of the hot copper coils is written as follows:

$$\epsilon P_T \tau_T + \Delta W + 0.2\epsilon\xi P_p \tau_T = (1 - \epsilon)(W_E + P_N \tau_T + P_B \tau_T + W_p) + \xi P_p \tau_T \, . \qquad (42)$$

Here ΔW is the work done by the plasma in expanding outward against the magnetic field, as mentioned above.

In the case of the cryogenic Al coil

$$\epsilon P_T \tau_T + \Delta W = (1/\epsilon_R)(W_E + P_N \tau_T + P_B \tau_T + 0.2\ \xi\ P_p \tau_T) + \xi\, P_p \tau_T \, . \qquad (43)$$

(Here, at the long pulse times involved, it is assumed that the plasma can be purged without having to remove its heat from the cryogenic coil). The quantity ϵ_R is the refrigeration efficiency given by

$$\epsilon_R = T_C \eta_R / [T_h - T_C (1-\eta_R)], \qquad (44)$$

where T_C is the cryogen temperature, T_h is room temperature and η_R is the efficiency of the refrigerator with respect to an ideal, Carnot heat engine.

F. Summary of Plasma Conditions at Reactor Energy Balance

By far the most favorable energy balance is that for the sustained-field θ-pinch. For R_c = 10 cm, R_p = 5 cm, ϵ = 0.4, B = 200 kG, the times τ_T derived from Eq. (42) are scarcely larger than those of the Lawson Criterion, i.e., about 5 milliseconds. In this case the small refrigeration loss to maintain the outer superconducting coil is probably comparable to the other terms in Eq. (42) and

should be included.

The second most favorable case is that of the hot Cu-Be coil of sufficient thickness to support the magnetic pressure. For the same parameters given above an energy balance occurs at $\tau_T \approx 25$ milliseconds. The plasma density is determined independently from the pressure balance condition (33) and is 3×10^{16} at B = 200 kG.

The least favorable case is that of the cryogenic aluminum coil, owing to refrigeration losses. Energy balance is difficult to obtain and is possible only for τ's of the order of one second.

Choosing the case of the hot copper coil as probably the most practical, since it allows greater choice of the method of plasma heating than the sustained-field θ-pinch, the following plasma conditions are sufficient for overall energy balance:

$$kT \approx 15 \text{ keV}$$

$$n \approx 3 \times 10^{16} \text{ cm}^{-3}$$

$$\tau_T \approx 0.03 \text{ sec}$$

$$n\tau_T \approx 10^{15} \text{ cm}^{-3} \text{ sec}.$$

Thus an $n\tau$ value approximately ten times that of the Lawson Criterion is indicated. All of these quantities are sensitive functions of the peak magnetic field B, and both τ and $n\tau$ decrease rapidly as B is raised.

IX. STABILITY OF AN ASYMMETRIC MULTIPOLE

A. Field Configuration and Drift Stabilization

We consider the magnetic field inside the volume of a torus of minor radius ρ and major radius R. The field is to be a superposition of a longitudinal, "B_z"-field, in general modulated in the z-direction, with a tranverse quadrupole field set up by three longitudinal current-carrying wires located at distances a from the center as shown in Fig. 35(a), and carrying currents I, I, -2I respectively. The wall is considered to be perfectly conducting.

We first calculate the magnetic scalar potential χ for the transverse quadrupole field in the neighborhood of its null. The null point distance b is calculated taking into account the effect of the image currents in the conducting wall:

$$\frac{b}{a^2 + b^2} - \frac{1}{a + b} = \frac{b}{\rho^4/a^2 + b^2} - \frac{1}{\rho^2/a + b} . \tag{45}$$

The solution of this equation, reducible to a general quartic in b, is greatly simplified by setting $\rho = a + \Delta$, assuming $\Delta/a \ll 1$, and expanding to first order in Δ/a. Letting $\gamma = a/b$, Eq. (45) becomes, to first order in Δ/a

$$\frac{2\gamma^2}{(\gamma^2 + 1)^2} = \frac{\gamma}{(\gamma + 1)^2} . \tag{46}$$

The physical conditions for the desired solution of this quartic equation are that γ be real, and $\gamma > 1$ in order that the field null fall within the torus. Then the desired solution is unique and is found to be

$$\gamma \approx 2.89, \text{ and } b = a/\gamma.$$

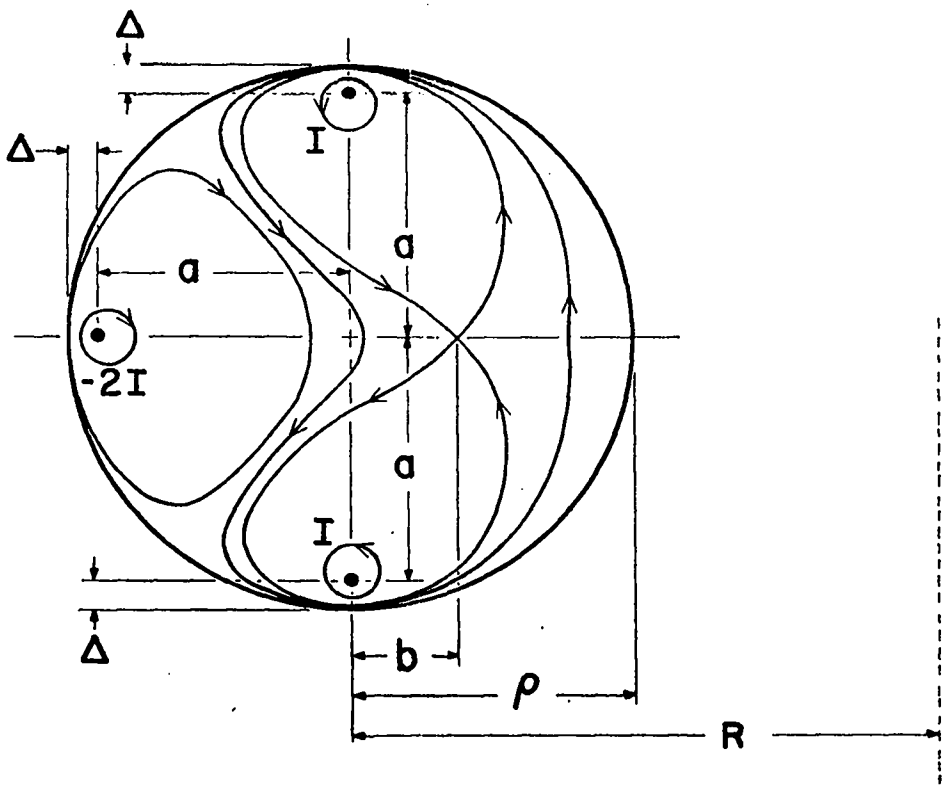

(a)

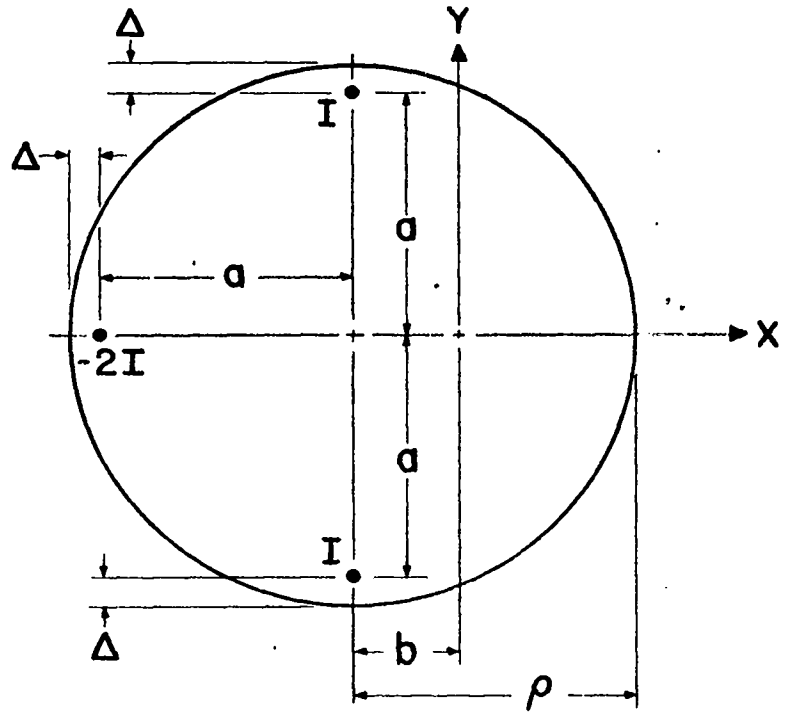

(b)

Fig. 35 Configuration of multipole conductors for stabilization of a toroidal θ-pinch. (a) shows the position of the bars and the magnetic field-line configuration. (b) shows the change of coordinates for calculating the scalar potential.

To calculate the scalar potential χ, we adopt a coordinate system centered at the null point, and oriented as shown in Fig. 35(b). The scalar potential describing the quadrupole field is then given by

$$\chi_Q(x,y) = 2I\Big[\tan^{-1}\Big(\frac{y - a}{x + b}\Big) + \tan^{-1}\Big(\frac{y + a}{x + b}\Big) - 2\tan^{-1}\Big(\frac{y}{x + a + b}\Big) - \tan^{-1}\Big(\frac{y - \rho^2/a}{x + b}\Big) - \tan^{-1}\Big(\frac{y + \rho^2/a}{x + b}\Big) + 2\tan^{-1}\Big(\frac{y}{x + \rho^2/a + b}\Big)\Big] + \text{const.} \tag{47}$$

The quadrupole field is given by $\vec{B}_Q = \vec{\nabla}\chi_Q$. We expand χ to second order in x and y, i.e., we shall find the field in the neighborhood of the null point.

$$\chi_{Q.P.}(x,y) \cong 4I\Big\{ y\Big[\frac{b}{a^2 + b^2} - \frac{1}{a + b} - \frac{b}{\rho^4/a^2 + b^2} + \frac{1}{\rho^2/a + b} \Big] + xy\Big[\frac{1}{(a + b)^2} + \frac{a^2 - b^2}{(a^2 + b^2)^2} - \frac{1}{(\rho^2/a + b)^2} - \frac{\rho^4/a^2 - b^2}{(\rho^4/a^2 + b^2)^2} \Big] \tag{48}$$

We again expand to first order in Δ/a, and note that the term linear in y vanishes because of Eq. (46), as is to be expected since we are expanding about a field null. The result is

$$\chi_Q(x,y) = \frac{16I\Delta}{a^3}\Big[\frac{1}{(1 + 1/\gamma)^3} + \frac{1 - 3/\gamma^2}{(1 + 1/\gamma^2)^3} \Big] + \text{higher order terms}. \tag{49}$$

To this scalar potential we add the potential due to a toroidally longitudinal B_z-field, modulated in z. The toroidal z-coordinate is to be taken positive in the direction pointing out of the plane of Fig. 35(b), i.e., the current I is positive when flowing in the positive z direction.

The total scalar potential has the form

$$\chi(x,y,z) = \int^{z} dz' f(z')\left(1 + \frac{x}{R}\right) - \tfrac{1}{4}(x^2 + y^2)f'(z) + gxy$$

$$- \frac{1}{6R} f'(z)x^3 + \ldots . \qquad (50)$$

Here it is assumed that R is large compared to all other transverse dimensions; f is the B_z field on the z-axis, expressible in terms of the ab-ampere-turns per centimeter $\mathcal{N}/L$ of the winding setting up the B_z-field. For constant f we have

$$f = 4\pi \frac{\mathcal{N}}{L} \; ; \; L = 2\pi R. \qquad (51)$$

Since f is modulated in z, the more general relationship is

$$f = 4\pi \frac{d(\mathcal{N})}{dz} ,$$

$$g = \frac{16I\Delta}{a^3}\left[\frac{1}{(1 + 1/\gamma)^3} + \frac{1 - 3/\gamma^2}{(1 + 1/\gamma^2)^3}\right] . \qquad (52)$$

The toroidal B_z-field, in the absence of the quadrupole field, could not be used for plasma confinement purposes because it provides no equilibrium configuration; $|B|^2$ decreases uniformly toward the outside of the torus, and there results a corresponding outward drift of the plasma. The addition of the quadrupole field, however, permits us to establish an equilibrium configuration by allowing $|B|^2$ to achieve a minimum within the toroidal volume. We first establish a criterion for the existence of such an equilibrium configuration, and then examine the magnetohydrodynamic stability of this equilibrium.

We neglect terms higher than quadratic in x, y in Eq. (50) and find

$$B^2(x,0,z) = \left|\vec{\nabla}\chi\right|^2_{y=0}$$

$$= \left[\tfrac{1}{4}(f')^2 + g^2\right]\left\{x + \frac{f^3}{R\left[\tfrac{1}{4}(f')^2 + g^2\right]}\right\} + f^2 - \frac{f^4}{R^2}\,\frac{1}{\left[\tfrac{1}{4}(f')^2 + g^2\right]}. \qquad (53)$$

In calculating $B_x = \frac{\partial\chi}{\partial x}$ from Eq. (50) care must be taken to account for the curvature of the toroidal z-axis; this provides a term cancelling the term proportional to $\frac{1}{R}$, produced by straightforward differentiation with respect to x. B^2 is seen to have a parabolic minimum, and a reasonable criterion for achieving equilibrium is to demand that the minimum fall in the neighborhood of the center of the toroidal volume. This condition is expressed by the relation

$$\left(\frac{\partial N}{8I}\right)^2 \frac{a^5}{R^3\,\Delta^2}\,\gamma\left[\frac{1}{(1+1/\gamma)^3} + \frac{1-3/\gamma^2}{(1+1/\gamma^2)^3}\right]^{-2} = 1. \qquad (54)$$

In deriving criterion 54 we used an approximate field expression, valid for $\frac{x}{a}, \frac{y}{a} \ll 1$ to compute the field at x = -b, the coordinate of the toroidal axis. This produces no material error, however; in fact, we might have chosen the B^2 minimum point to lie somewhere between the center of the tube and the null point of the quadrupole field and still have satisfied the $\frac{x}{a} \ll 1$ condition.

B. Magnetohydrodynamic Stability

To discuss the magnetohydrodynamic stability of the equilibrium we find it convenient to introduce a new coordinate system, whose origin coincides with that of the above coordinate system, but whose axes are rotated by 45°. In terms of the new coordinates x', y', where

$$x = \frac{1}{\sqrt{2}}(x' - y')$$

$$y = \frac{1}{\sqrt{2}}(x' + y'), \qquad (55)$$

the scalar potential has the form

$$\chi(x',y',z) = \int^{z} dz' f(z')\left[1 + \frac{x' - y'}{R\sqrt{2}}\right] - \tfrac{1}{4}(x'^2 + y'^2)f'(z) + \tfrac{1}{2} g(x'^2 - y'^2) + \ldots . \quad (56)$$

Except for a small additional term proportional to $\frac{1}{R}$, this is precisely the field configuration whose stability has been studied by H. P. Furth and M. N. Rosenbluth,[58] for the case of periodic modulation of f and g. The criteria for marginal stability, expressed by these authors in terms of minimum modulation parameters, are independent of our equilibrium criterion, so that both equilibrium and magnetohydrodynamic stability are obtainable by proper choice of f, f', and g. For large R, i.e., $\frac{a}{R} \ll 1$, the toroidal curvature has negligible influence upon the stability criterion of Ref. 58.

C. Choice of Experimental Parameters

The currents in the stabilizing windings may be derived from when $\mathcal{J}N$ is expressed in terms of B, the maximum compression field of the θ pinch:

$$\mathcal{J}N = RB/2 \quad (57)$$

$$I^2 = \frac{B_o^2 a^5 \gamma}{(16\Delta)^2 R}\left[\frac{1}{(1 + 1/\gamma)^3} + \frac{1 - 3/\gamma^2}{(1 + 1/\gamma^2)^3}\right]^{-2} . \quad (58)$$

For the choice a = 5 cm, Δ = 0.5cm, R = 200 cm, B = 100 kG, (γ = 2.89), one derives 2I = 1.8 MA. A measurement gives L $\approx$ 0.4 μH/m for the inductance of the wires. Therefore for R = 2m, the capacitor bank energy to drive the stabilizing conductors is 8 MJ. As was shown in Sec. VIID above, the total bank energy to drive such a toroidal θ-pinch is about 15 MJ.

A rough idea of the parameters involved in a set of stabilizing conductors can be derived from Fig. 2 of Ref. 58, where the authors give various quantities as functions of the quadrupole strength parameter

$$\alpha \approx gL/B. \tag{59}$$

Here L is approximately the period defined in Fig. 23. Substituting (52) and (58) into (59), gives

$$\alpha = 1.7\ L/(aR)^{\frac{1}{2}}. \tag{60}$$

For L = 30 cm, $\alpha = 1.6$. In addition we assume it possible by shaping the θ-pinch coil to derive a mirror ratio M = 1.4. This gives for the excursion of the flux lines $Q \approx 9$. This figure is to be identified with the ratio of the discharge tube inner diameter to plasma diameter, which is about 8 in the present experiments. The ratio λ of the length of region over which the field is increased to MB to the period L is about 0.05.

We conclude that a θ-pinch, which is a long narrow object, is well adapted to this type of stabilization experiment. It remains to be seen to what extent interchange instability occurs in the torus and what stabilization parameters are actually necessary.

BIBLIOGRAPHY OF PRINCIPAL SCYLLA PUBLICATIONS

1. W. C. Elmore, E. M. Little, and W. E. Quinn, Neutrons of Possible Thermonuclear Origin, Phys. Rev. Letters 1, 32 (1958).

2. K. Boyer, W. C. Elmore, E. M. Little, and W. E. Quinn, Neutrons from Plasma Compressed by an Axial Magnetic Field (Scylla), Proc. of the Second United National International Conference on the Peaceful Uses of Atomic Energy (United Nations, Geneva, 1958) Vol. 32, p. 337.

3. K. Boyer, W. C. Elmore, E. M. Little, W. E. Quinn, and J. L. Tuck, Studies of Plasma Heated in a Fast-Rising Axial Magnetic Field (Scylla), Phys. Rev. 119, 831 (1960).

4. F. C. Jahoda, E. M. Little, W. E. Quinn, G. A. Sawyer, and T. F. Stratton, Continuum Radiation in the X-Ray and Visible Regions from a Magnetically Compressed Plasma (Scylla), Phys. Rev. 119, 843 (1960).

5. A. J. Bearden, F. L. Ribe, G. A. Sawyer, and T. F. Stratton, X-Ray Continuum and Line Spectra from Highly Stripped Atoms in a Magnetically Compressed Plasma, Phys. Rev. Letters 6, 257 (1961).

6. D. E. Nagle, W. E. Quinn, F. L. Ribe and W. B. Riesenfeld, Velocity Spectrum of Protons and Tritons from the d-d Reaction in Scylla, Phys. Rev. 119, 857 (1960).

7. F. C. Jahoda, F. L. Ribe, and G. A. Sawyer, Zeeman-Effect Magnetic Field Measurement of a High-Temperature Plasma, Phys. Rev. 131, 24 (1963).

8. F. C. Jahoda and G. A. Sawyer, Pickup Coil Measurement of the Plasma Magnetic Field in the Scylla I Theta Pinch, Phys. Fluids 6, 1195 (1963).

9. E. M. Little, W. E. Quinn, and F. L. Ribe, Effects of Ionization and Magnetic Initial Conditions on a Magnetically Compressed Plasma (Scylla), Phys. Fluids 4, 711 (1961).

10. G. A. Sawyer, A. J. Bearden, I. Henins, F. C. Jahoda, and F. L. Ribe, X-Ray Crystal Spectroscopy of a Theta Pinch Plasma in the Region 15-25 Å, Phys. Rev. 131, 1891 (1963).

11. E. M. Little, W. E. Quinn, F. L. Ribe, and G. A. Sawyer, Studies of Stability and Heating in the Scylla Magnetic Compression Experiment Nuclear Fusion - 1962 Supplement, Part 2, p. 497.

12. E. M. Little and W. E. Quinn, Effects of Added Hexapole Magnetic Fields and Preionization in Theta Pinch Experiments, Phys. Fluids 6, 875 (1963).

13. F. C. Jahoda, E. M. Little, W. E. Quinn, F. L. Ribe, and G. A. Sawyer, Plasma Experiments with a 570-kJ Theta Pinch, J. Appl. Phys, 35, 2351 (1964). 2351 (1964).

14. E. M. Little, W. E. Quinn, and G. A. Sawyer, Plasma End Losses in the "Low Pressure" Regime of a Theta Pinch, Phys. Fluids, (1965) (To be published).

REFERENCES

15. The correlation between reversed trapped field and neutron emission was first reported by A. C. Kolb, C. B. Dobbie, and H. R. Griem Phys. Rev. Letters 3, 5 (1959).

16. R. C. Mjolsness, F. L. Ribe, and W. B. Riesenfeld, Phys. Fluids 4, 730 (1960).

17. M. N. Rosenbluth and C. L. Longmire, Ann. Phys. 1, 120 (1957).

18. A better illustration of this effect is to be found in H. A. B. Bodin, and A. A. Newton, Phys. Fluids 6, 1338 (1963).

19. M. N. Rosenbluth, N. A. Krall and N. Rostocker, Nuclear Fusion - 1962 Supplement, Part 1, p. 143.

20. M. S. Ioffe, Nuclear Fusion - 1962 Supplement, Part 3, p. 1045.

21. L. M. Goldman, H. C. Pollock, J. A. Reynolds and W. F. Westendorp, Phys. Rev. Letters 9, 361 (1962).

22. Neutron-producing plasmas without trapped reversed field were first produced at Los Alamos in Scylla III, when it was preionized by injecting plasma into it with a coaxial gun cf. E. M. Little, J. Marshall, W. E. Quinn, and T. F. Stratton 4, 1570 (1961).

23. W. M. Borkenhagen, F. L. Ribe, and G. A. Sawyer, Los Alamos Scientific Laboratory Report LAMS-2940 (1963).

24. L. M. Goldman, R. W. Kilb, and H. C. Pollock, Phys. Fluids 7, 1005 (1964).

25. K. Hain, G. Hain, K. V. Roberts, S. J. Roberts, and W. Koppendorfer, Z. Naturforschg 15a, 1039 (1960).

26. K. Hain and A. C. Kolb, Nuclear Fusion - 1962 Supplement, Part 2, 561 (1962).

27. T. A. Oliphant, Jr., Los Alamos Scientific Laboratory Report, LAMS-2944 (December, 1963).

28. F. L. Ribe, R. M. Gilmer, H. C. Hoyt, G. Hain, and K. Hain, Los Alamos Scientific Laboratory Report, LAMS-2911 (July, 1963).

29. T. A. Oliphant and F. L. Ribe, Los Alamos Scientific Laboratory Report, LA-3202-MS (October 20, 1964), p. 105.

30. T. A. Oliphant and F. L. Ribe, Bull. Am. Phys. Soc. Sec. II 10, 224 (1965).

31. H. E. Hinteregger, L. A. Hall, and W. Schweizer, Astrophys. J. 140, 319 (1964).

32. W. E. Behring, W. M. Neupert, and J. C. Lindsay, Proc. Third International Space Science Symposium (Washington, D. C. 1962) p. 814.

33. R. Tousey, W. E. Austin, J. D. Purcell, and V. G. Widing, Proc. Third International Space Science Symposium (Washington, D. C. 1962) p. 772.

34. B. C. Fawcett, A. H. Gabriel, W. G. Griffin, B. B. Jones, and R. Wilson, Nature 200, 1303 (1963).

35. L. L. House, W. A. Deutschman, and G. A. Sawyer, Astrophys. J. 140, 814 (1964).

36. R. C. Elton, A. C. Kolb, W. E. Austin, R. Tousey, and K. G. Widing, Astrophys. J. 140, 389 (1964).

37. B. C. Fawcett, and A. H. Gabriel, Culham Laboratories Report CLM-P56, Culham Laboratory, Abingdon, Berkshire, England (1964).

38. L. L. House, and G. A. Sawyer, Astrophys. J. 139, 775 (1964).

39. W. E. Quinn, Progress in Nuclear Energy (Pergamon Press, London, 1963), Series XI, Vol. 2, p. 166.

40. H. R. Griem, A. C. Kolb, W. H. Lupton, and D. T. Phillips, Nucl. Fusion, Supplement, Part 2, (1962) p. 543.

41. A. C. Kolb, H. R. Griem, W. H. Lupton, D. T. Phillips, S. A. Ramsden, E. A. McLean, W. R. Faust, and M. Swartz, Nuclear Fusion, Supplement, Part 2, (1962) p. 553.

42. E. Hintz, A. C. Kolb, W. H. Lupton, and H. R. Griem, Phys. Fluids 7, 153 (1964).

A. C. Kolb, E. Hintz, and P. C. Thonemon, Bull. Am. Phys. Soc. Ser. II, 10, 224 (1965).

43. General Electric Research Laboratory Bulletin, Summer, 1964.

44. R. L. Bingham and L. M. Goldman, Bull. Am. Phys. Soc. Ser. II, 10, 224 (1965).

45. L. M. Goldman and H. Hurwitz, Jr., Bull. Am. Phys. Soc, Ser. II, 10, 216 (1965).

46. H. A. B. Bodin, T. S. Green, G. B. F. Niblett, N. J. Peacock, J. M. P. Quinn, J. A. Reynolds, and J. B. Taylor, Nucl. Fusion, Supplement, Part 2, (1962), 511 and 521.

47. G. B. F. Niblett, J. A. Reynolds, E. E. Aldrige, and M. Keilhacker, Bull. Am. Phys. Soc., Ser. II, 10, 216 (1965).

48. H. Beerwald, P. Bogen, T. El-Khalafawy, H. Fay, E. Hintz, and H. Kever, Nucl. Fusion, Supplement, Part 2, 1962, 595, 601, and 607.

49. H. L. Jordan, Nucl. Fusion, Supplement, Part 2, (1962), 589.

50. F. P. Küpper, Z. Naturforschg, 18A, 895 (1963).
E. Fünfer, K. Hain, H. Herold, P. Igenbergs, and F. P. Küpper, Z. Naturforschg, 17A, 976 (1962).

51. J. E. Allen, C. Bartoli, B. Brunelli, J. A. Nation, B. Rumi, and R. Toschi, Nucl. Fusion, Supplement, Part 2, (1962), 621.

52. I. F. Kvartskhava, K. N. Kervalidze, Yu. S. Gvaladze, and B. N. Kapanadze, Nucl. Fusion, Supplement, Part 2, 533 (1962).

53. E. L. Kemp, T. M. Putnam, W. E. Quinn, and F. L. Ribe, Los Alamos Scientific Laboratory Report LAMS-2609 (October 11, 1961).

54. W. F. Westendorp and H. Hurwitz, Jr., General Electric Research Laboratory Report 63-RL-(3254E) (Revised, Nov. 1963).

55. L. Spitzer, Jr., Phys. Fluids 1, 253 (1958).

56. L. M. Goldman and H. Hurwitz, Jr., Bull. Am. Phys. Soc. Series II, Vol. 10, 216 (1965).

57. E. Hintz, A. C. Kolb, W. H. Lupton, and H. K. Griem, Phys. Fluids 7, 153 (1964).

58. H. P. Furth and M. N. Rosenbluth, Phys. Fluids 7, 764 (1964).

59. J. Andreoletti, C. R. Acad. Sc. Paris, 257, 1235 (1963).

60. E. E. Salpeter, Phys. Rev. 122, 1663 (1961).

61. E. Fünfer, B. Kronast, and H. J. Kunze, Phys. Rev. Letters 5, 125 (1963).

62. H. J. Kunze, A. Eberhagen, and E. Fünfer, Phys. Letters 13, 38 (1964).

63. W. E. R. Davies and S. A. Ramsden, Phys. Letters 8, 179 (1964).

64. A. W. DaSilva, D. E. Evans, and M. J. Forrest, Nature 203, 1321 (1964).

65. G. L. Lamb, Jr., Los Alamos Scientific Laboratory Report LA-2715 (October 13, 1962).

66. J. D. Lawson, Proc. Phys. Soc. (London), B70, 6 (1957).

67. W. B. Riesenfeld, Progress in Nuclear Energy (Pergamon Press, London, 1963) Series XI, Vol. 2, p. 247.

68. F. L. Ribe, Los Alamos Scientific Laboratory Report, LA

PRESENT PROGRAM

HYDROMAGNETIC GUN DEVELOPMENT
GUN PLASMA INJECTION STUDIES*

FUTURE PROGRAM

CAULKED CUSP MACHINE

D. A. Baker, J. E. Hammel, I. Henins, E. L. Kemp,
John Marshall, and J. L. Tuck

* Work performed under the auspices of the U. S. Atomic Energy Commission

CONTENTS

I. PRESENT PROGRAM

A. Hydromagnetic Plasma Gun Development

An obvious way of charging a thermonuclear reactor is to accelerate a puff of plasma to high velocity, trap it in the containment field of the reactor and allow the energy of translation to degrade into thermal energy. In principle it should be possible to accelerate a plasma to almost any particle energy by, for example, applying $\vec{j} \times \vec{B}$ forces over a long acceleration path. There are possible advantages in this indirect method of heating a plasma in that: (1) The plasma may be at low temperature while it is accelerated so that boiling of impurities from walls might be reduced. (2) The high speed plasma can be removed from the region where it is generated, where presumably the pressure is high, to a highly evacuated containment region. (3) Large quantities of plasma can in principle be handled, there being very little of the intensity limitation caused by space charge in charged particle beams.

There has been a program for the development of hydromagnetic plasma guns at Los Alamos since 1957. In all of the acceleration methods which have been tried the plasma has been derived from a burst of gas admitted to an initially evacuated system by a fast mechanical valve. First tried were electrodeless discharges where the plasma was accelerated by magnetic mirror fields, either simply time varying as in a θ-pinch or moving in space as well (a moving magnetic piston). These methods were attractive a priori because, there being no electrodes, there could be no contamination by electrode material. Such guns have been abandoned here in favor of coaxial guns, but have been developed further elsewhere in the world. Under some conditions they may be preferable, but the yield of fast plasma is so much larger from a coaxial gun of comparable input energy that it has appeared more attractive.

The coaxial gun in its present local form (Fig. 1), generates and accelerates plasma between copper electrodes of 3.18 and 8.25-cm diameter. The electrodes are 50-cm long and the gas inlet is through an annular slot in the center electrode 20 cm from the muzzle. It is driven by a 30-μF capacitor bank at 21 kV which is switched by ignitrons so as to provide a source inductance at the gun terminals of about 10nH. A fast valve driven by thermal expansion admits about 1 cm^3 atm. of deuterium gas through a labyrinth designed to prevent plasma damage to the dry Viton O-ring which seals the inlet plenum. The terminal insulator is a pierced Pyrex disk protected from direct radiation from the discharge by a copper baffle. The end of the central electrode is approximately hemispherical. These perhaps boring details are given to emphasize the fact that a minor change in any of these parameters would probably make a major change in gun behavior. Additional important parameters are the following: delay between gas admission and firing time, steepness of the front of the admitted gas, cleanliness of the vacuum, and recent history of the gun such as when it was fired and with what gas. The present parameters are the result of an extensive series of experiments designed to optimize the cleanliness and yield of thermonuclear plasma. Enough parameters are involved here that a systematic search through them is a very difficult job and the present gun design is certainly not the best possible.

The mechanism of gun operation can be thought of very simply as the $\vec{j} \times \vec{B}$ interaction of a radial plasma current with the $B = \frac{2i}{r}$ magnetic field of the current along the center electrode which feeds the discharge. In actual fact it is much more complicated than this, involving critical breakdown conditions, motion of a current front along the barrel through the gas filling so as to leave energy stored both in kinetic energy of plasma and magnetic field, and finally utilization of some of this stored energy to produce a jet of fast plasma from the tip of the center electrode. These mechanisms are not thoroughly understood. Given leisure for the job they would certainly offer rewarding subjects for study.

The fast plasma jet contains about 5×10^{17} deuterons of approximately 10 keV kinetic energy. They appear to be emitted in a hollow cone of something

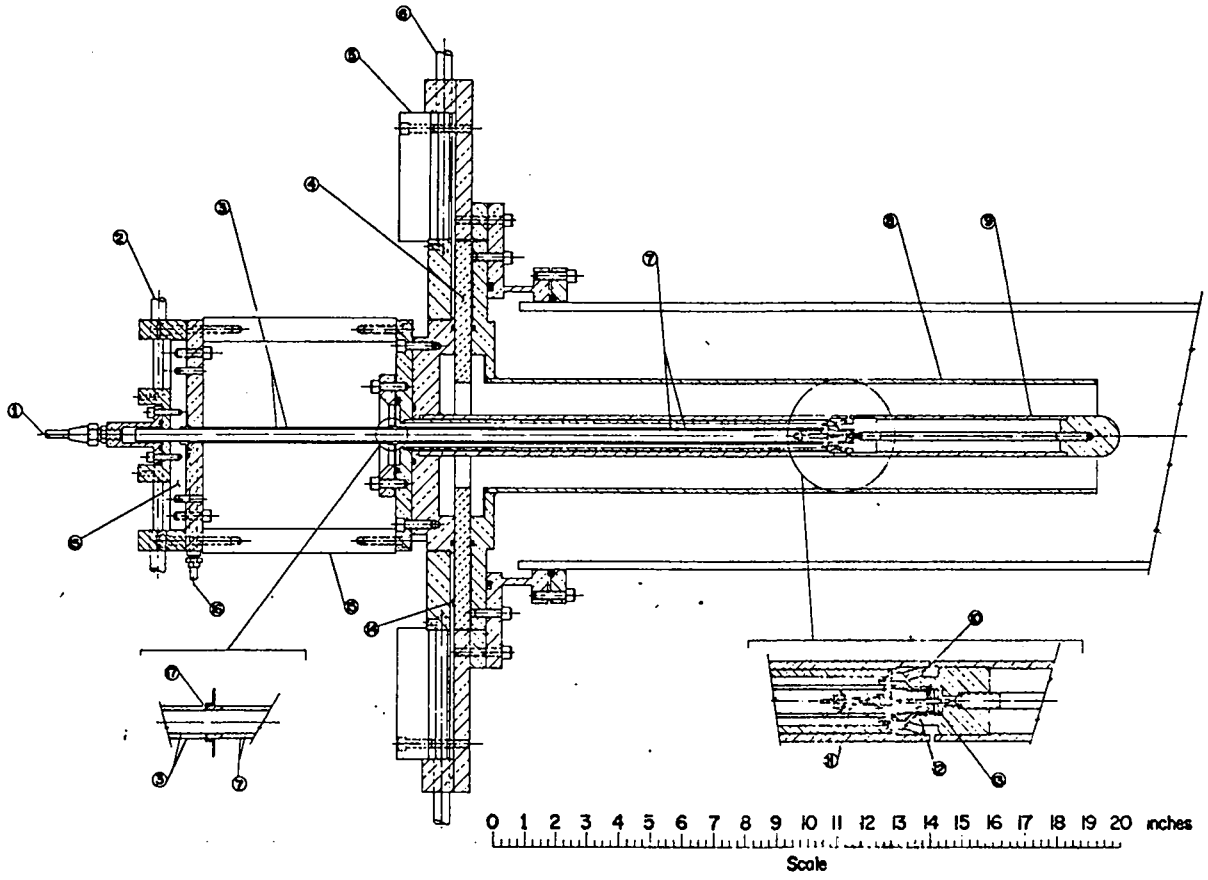

Fig. 1. Plasma Gun Design With Fast Thermal Expansion Valve. (1) Gas inlet. (2) Sixteen REX-4 cables to valve driver capacitor bank. (3) Driver section. (4) One-half in. thick glass insulator. (5) Lucite clamping ring. (6) Twenty-four B.I.C.C. Type 20 cables to gun capacitor bank. (7) Sonic line. (8) Outer electrode. (9) Inner electrode. (10) Gas outlet holes (15 holes, 1/8-in. diam). (11) Valve spring. (12) Valve plenum. (13) Teflon bumper washer. (14) Polyethylene insulation. (15) Phenolic insulator. (16) Cooling air inlet. (17) Small holes for air outlet.

like 10^{o} half width. This is about 1% of the injected gas. The fast deuterium plasma is followed by a slower plasma (~ 100 eV, 10^{7} cm/sec) containing most of the rest of the admitted gas. The properties of the plasma have been deduced from a large variety of experiments including calorimetry, diamagnetism, spectroscopy, particle analysis, neutron emission, and others. It is hoped in the future to study further empirically the effects of changes in electrode configuration and other gun parameters. In addition measurements will be made which it is hoped will shed some light on the important phenomena which appear to produce the fast plasma at the gun muzzle. Hopefully a better understanding of these phenomena will allow improvement of gun performance. Most of the recent efforts in this program have been directed toward the study and elimination of plasma impurities. During approximately the last year a serious contamination of the fast plasma with high speed multiply ionized carbon impurities was observed and apparently has been cured by the rigorous exclusion of all sources of oil and grease from the vacuum system and the protection of what organic materials remained from decomposition by the plasma. It is planned during the coming year to study the impurities further by particle analysis in a large cleanly pumped metal tank. At present the impurities are dominated by secondary plasma ions generated when the fast plasma interacts with the glass walls of the system.

B. Axial Injection

A large part of the experimental work which has been carried out in the hydromagnetic gun program has dealt with injection of gun plasma along magnetic field lines into either magnetic guide fields or containment geometries. Unfortunately axial injection of containment geometries implies an open geometry, for instance a mirror machine, and the trend at the moment is toward closed geometries. Still axial guide fields might prove useful between gun and containment region, and at least they provide a means of keeping gun plasma substantially off the walls of a system so that there is some hope of studying primary gun plasma rather than secondary plasma derived from wall evaporation.

A series of experimental programs has been conducted in the past few years including such things as the collision of two gun plasmas impinging on each other from opposite ends of the same guide field, gun injection of one of the Scylla θ-pinches, and gun injection of a more or less static mirror machine. These programs had a variety of motivations most of which included to some degree the desire to produce a hot plasma suitable for charging a reactor. From them a great deal has been learned about gun plasmas, of which perhaps the most important single thing is that they are extremely difficult to diagnose reliably. Probes inserted into a high energy streaming gun plasma are subject to an enormous rate of deposition of surface energy. This usually results in evaporation of the surface of the probe, generation of a local secondary plasma of high energy density but relatively low particle energy, and completely false results. The same thing happens with the slits of a particle analyzer so that to achieve reliable results one must back off to large distances where the energy flux is low. The net result of the energy flux difficulty is that all diagnostics must be done from outside the plasma or at least with no ordinary material probes. Such measurements tend to average the effects from a reasonably large plasma volume so that the experimenter must be careful not to accept too smooth and simple a picture of what is going on inside.

A brief summary of what appears to be happening in the injection of gun plasma into axial guide fields might be as follows: The generation of the fast plasma is partly in the guide field itself, so that it is impossible to separate the phenomena of plasma acceleration from those of field penetration. Intense electric fields are generated in the region around the injection point, some of these having to do with the different magnetic ballistic properties of the electrons and ions, the ions in general being able to penetrate the field farther, and consequently producing a positive space charge sheath on the outside of the plasma. Inductive effects in the gun, however, are fundamentally responsible for the acceleration of the ions and can do this only through electric fields. This implies an electric field in the direction of ion acceleration so that out in front of the gun there is a high negative potential

driven effectively through a very low impedance since an ion current of the order of 10^5 A is accelerated by some 10 kV. Wall effects are extremely important in the penetration of the fast plasma into the field and under some conditions all the electrons in the plasma that have penetrated the field originate at the wall (Ashby, Culham, 1963). Under some wall conditions the fast plasma is confined to a relatively smooth cylindrical volume of approximately the same diameter as the outer gun electrode. With the wall pulled back away from the gun muzzle the plasma shreds badly on entering the field but appears cleaner in that it does not evaporate large quantities of glass as it does with the glass wall closer around the gun muzzle.

The fast injected plasma is throughly mixed with magnetic field although in general it has substantial diamagnetism, the particle energy density close to the muzzle exceeding the field energy density. The diamagnetic effects up to a meter or so away from the gun are large enough so that plasma effects on the field allow self trapping of the plasma behind a magnetic mirror in a manner apparently similar to Tuck's "Entropy Trapping" proposal. Single particle trapping is well known to be impossible in a d.c. magnetic field. The dynamics of the fast plasma have been studied in guide fields by observation of the diamagnetism of the plasma as it moves along the field and by allowing the plasma to strike various instruments and targets. It is hoped next to apply the Jahoda, Baker and Hammel modification of the Ashby and Jephcott gas laser interferometer technique to studying the plasma density along a guide field as a function of time and distance.

The slow gun plasma which follows the fast is roughly one hundred times as dense and is clearly not desirable as a diluent of the fast plasma in a reactor experiment. It appears to behave hydromagnetically in its interaction with the field, under some conditions (relatively low guide fields), extending as a field free arm of plasma into the guide field, but then acting as a zero β slow dense plasma stream scattering source in the guide field. Measurements of these phenomena are particularly difficult because of the previous passage of high energy plasma, and it is hoped that laser interferometry will add considerable information.

C. Transverse Injection

This program was originally undertaken in an attempt to inject gun plasma into a transverse field, and then to accelerate it to higher particle energies by the application of an orthogonal electric field, so as to produce an $(\vec{E} \times \vec{B})/B^2$ plasma drift. Difficulty was encountered in the attempt to accelerate the plasma to higher velocities but a very interesting and potentially useful behavior was found in that the plasma entered the transverse field easily and could be controlled subsequently by allowing self-generated depolarizing currents to be drawn along field lines to conducting surfaces.

The gun plasma, upon encountering the transverse magnetic field, is subject to a $\vec{v} \times \vec{B}$ Lorentz force which polarizes the jet of plasma, leaving space charges on the surfaces parallel to the field. These space charges produce an electric field normal to the plasma velocity and to the magnetic field just sufficient to provide an $\frac{E}{B}$ plasma drift speed equal to the initial speed of the gun plasma. The plasma jet continues to drift across the field, probably with a loss of surface plasma from the space charge region, until it hits something or goes out the other side of the field, except when it comes to a set of field lines leading to a conducting surface capable of discharging the polarization charge. When this happens a current flows along the field lines from the electrically-charged surface of the plasma to the depolarizing conductor, along the conductor to the field lines leading back to the oppositely charged plasma surface, and then along these field lines to the plasma. Currents of the order of 10^4 A are observed passing through a Rogowsky loop around the depolarizing conductor or around the bundle of field lines between it and the polarized plasma surface. Clearly a current of this magnitude isn't carried in a vacuum but depends on the presence of a plasma for space charge neutralization. The currents which flow can be thought of as neutralizing the space charges which allow the plasma to drift across the field or as applying $\vec{j} \times \vec{B}$ forces to the plasma so as to stop it.

The transverse injection process provides an automatic mechanism for the separation of fast plasma from the slower undesirable plasma following it

out of a gun. A separation is possible because of the delay in current buildup in the inductance associated with the depolarization current loop. A burst of plasma which moves past a short depolarization conductor can pass beyond the short-circuited field lines before the current builds up enough to decelerate it appreciably. On the other hand, slower plasma following immediately behind spends a longer time in the short-circuited region and even finds a certain amount of current already built up by the fast plasma.

If plasma is injected across a field which reverses its direction on the other side of a field null, there is an opportunity for the plasma to depolarize itself, since if the plasma is to keep moving the polarization must reverse its direction where the field reverses. If the field lines on one side of the null connect by a reasonably short vacuum path to those on the other side, it becomes possible for the plasma polarization on the exit side to be overwhelmed by currents derived from the polarization of the entering plasma. This stops the plasma in the field null region and would appear to offer an ideal mechanism for the trapping of gun plasma in bridged cusp field null devices. This effect has been observed here and is planned as the method of injection of the Caulked Cusp machine discussed below. Ohkawa at General Atomic and Kerst at Wisconsin are using it to inject their toroidal octufilar experiments.

A short linear section model of the Caulked Cusp machine is under construction with which it is planned to replace the present mirror coil arrangement in the Transverse Injection experiment.

1. Closed Field Geometry Reactors- In the various injection studies carried out with coaxial guns it has become more and more obvious that if there are field lines leading from the plasma to a wall, plasma will follow the lines and bombard the wall. Also it has become obvious that if this happens, large amounts of gas will be evolved. The approximate figures for the high energy plasma yield from the present coaxial gun (5×10^{17} deuterons at 10 keV) correspond to 800 J of particle energy. The plasma is produced in somewhat less than a microsecond, so these figures correspond to an instantaneous power level of about 1000 MW. A power this large absorbed by

a solid surface, even over a rather large area, overloads the heat absorption capacity of the surface so that material is evaporated. The wall vapor spoils the vacuum in the system, and that part of it which is ionized by the incident plasma produces a secondary plasma to confuse measurements.

What might appear to be a barely adequate thermonuclear reactor plasma ($n = 10^{15}/cm^3$, $T = 20$ keV) would have a particle power flux of several thousand megawatts per cm^2. Even a very small fraction of this, allowed to scatter out of a containment region along field lines, would produce a flood of gas from any wall. There appears then to be a great advantage in closed field geometries for reactors in which no field lines lead directly from the contained plasma to any material wall.

II. FUTURE PROGRAM

A. Caulked Cusp Machine

It has been understood for a long time that stability against fluting can be realized in a magnetic containment device by arranging it so that the field lines are convex toward the plasma. This is equivalent to the statement that the magnetic field increases its strength in the outward direction. Unfortunately, field lines which are everywhere convex inward imply cusps which lead lines out from the containment region so that an open geometry results. It is impossible to make a closed field geometry where the lines are convex inward along their entire lengths. An increase of field strength in every outward direction implies a minimum somewhere in the containment region, and this minimum can be of a zero or non-zero nature. Zero and non-zero minima are separately interesting in containment devices and it is plain that, strong statements by enthusiasts for one or the other notwithstanding, both types of containment deserve investigation.

The type of flute stable containment device with a field zero inside has a longer history than the type with a non-zero field minimum, simply because the field itself is easier to visualize. However, even so it has not yet had a fair test. The main reason for this is that a field zero implies non-adiabatic containment of individual particles in the very center

of the flute stable containment region. The ions passing near the field zero fail to conserve their orbital magnetic moments and this has the effect of scattering particles so that their pitch angle changes relative to the field lines in the cusps. Only a few passes close to the field zero are required for most of the particles to leak out. Experiments with non-zero field minimum devices do not suffer from this difficulty, hence the work of Ioffe which has demonstrated an improvement of stability of plasma confinement in an open field geometry when the field is made to increase in the outward direction.

The experimental difficulty of cusp leakiness induced by non-adiabatic ion scattering near a field null is similar in a way to the scattering difficulty which might be expected in an actual reactor. Ion-ion collisions are the very essence of a reactor, and there are many more Coulomb collisions than collisions leading to a fusion reaction. Consequently an open geometry reactor will certainly lose a large fraction of its plasma through its mirrors whether or not it is capable of adiabatic containment. In a closed field geometry particles scattered out in this way return along the same lines to the machine, and so are not lost. Consequently a field zero does no harm in this case. It appears then that closed field geometry machines, if they are possible at all, have strong advantages over open geometry machines. A machine with a field zero inside requires closed field geometry from the beginning, but in a sense so does any machine if it is to be investigated under reactor conditions.

It should be noted that high plasma density machines are to some extent excluded from the considerations immediately above. Such machines, if of open field geometry, would certainly leak particles. However, by going to large plasma containment volumes it might well be possible to make a reactor by offsetting the higher reaction rate against the leak rate.

Considerable attention has been given recently to closed field geometry flute stable systems with no field zeros inside. Particularly interesting proposals have been made by Furth and Rosenbluth. Some of these systems have shear stabilization in addition to $\int \frac{d\ell}{B}$ stabilization. The standard criterion for $\int \frac{d\ell}{B}$ stability is that the line integral should decrease as it is taken over closed field lines farther and farther from the plasma. It appears to be

a valid criterion for flute stability provided the plasma is isotropic in its distribution function, would remain so after a fluting perturbation (most unlikely), is a zero beta plasma so that line integrals calculated along vacuum fields apply to the real case and so that balooning modes are impossible, and provided the line integrals can really be closed. These conditions are not all of the conditions which can be thought of, so that clearly theory and experiment are going to have to advance together to determine whether any field geometry is actually capable of the confinement of a reactor plasma for sufficient time to make a reactor. Experiments are needed particularly with closed field geometries both with and without internal field zeros. It has been suggested that the type of experiment to look for is one which allows comparison in the same apparatus of $\int \frac{d\ell}{B}$ stable systems with variable shear. This sounds very attractive in theory but in practice, when the moment of truth arrives, when one has to design the machine that will do this, one finds that other things are changed in the experiment besides the amount of shear, and that the experiment, already difficult, becomes even more so.

The proposal for a flute stable closed field geometry containment field was first made by Tuck in 1957. Similar proposals were made independently by Braginsky and Kadomtsev in the U.S.S.R. Tuck's proposal, the "Caulked Picket Fence," used a conducting ring or series of rings inside of and coaxial with a pulsed solenoid and opposing by flux conservation the field of the solenoid. A toroidal quadrufilar null is formed inside the ring concentric with it. Two of the leaky field surfaces leading from the null bridge the ring and return, so as to bring escaping particles back. The other two pass along the solenoid where they may connect to other ring nulls or, if the solenoid is bent into a torus, they can return to the other side of the same null. This would effectively stop all leaks along lines. The Caulked Picket Fence diagram reproduced here from Glasstone and Lovberg is for a case where the ring current is larger than would be induced in a perfect conductor. This would imply a more complicated magnetic history than simple pulsing on of the solenoid current. Also the field in the diagram could not be generated with uniform current density in the solenoid.

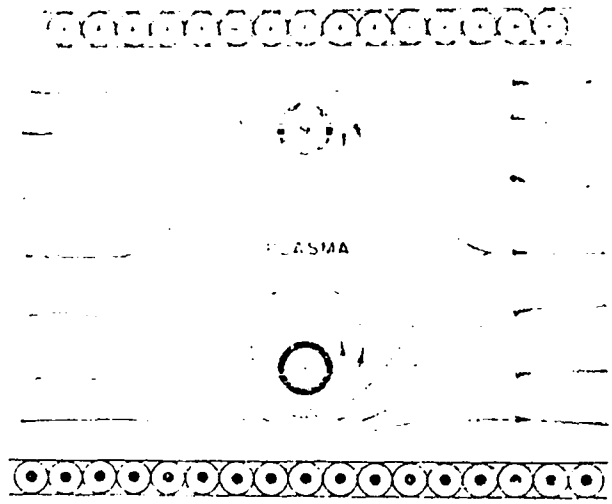

Fig. 11-9. The caulked picket fence.

Experimental work is needed to establish whether configurations of this sort are capable of containing a reactor plasma. Actual work has been done and is still in progress under Kerst at Wisconsin and Ohkawa at General Atomic on what they call toroidal octupoles. The properties of these systems are similar to the Caulked Picket Fence except that the field lines are normal to the toroidal direction. The programs of these workers are quite similar in that both groups are studying machines with cusp lines bridged over four internal conducting rings. The rings are in the corners of a toroidal outer vessel of approximately square cross-section and are driven inductively by currents in the wall of the outer vessel. These currents originate in a capacitor bank, and both Kerst and Ohkawa use rather modest stored energies. This of course simplifies the engineering of the machines, but it limits the particle energies which can be contained. As a result the plasma energies are quite low and this, by reducing the energy with which the plasma can bombard a surface, makes it possible to hang the ring conductors on supports. In addition, because of reduced charge exchange cross sections accompanying the low plasma temperatures as well as smaller particle velocities, the vacuum requirements are quite modest. On the other hand, because of the low plasma energies, there are a number of important diagnostic techniques which cannot be applied.

Plans are being made here to build a caulked field null machine capable of working at high plasma particle energy and energy density. There are several reasons for doing this. The most important is that in practice plasmas appear to be cleverer than people. If it is desired to investigate the behavior of reactor-type plasmas, experiments had better be performed with plasmas as nearly like reactor plasmas as possible. With large plasma energy a different set of experimental phenomena is found from that at low energy. Certainly if fusion reactors ever exist they will involve large plasma energies, and there is good reason for experimenters to keep their feet wet in this particular puddle. Another reason is that the larger variety of diagnostic techniques accompanying high plasma energy will make interpretation of injection and containment experiments easier. With a machine designed for high energy it is always possible to turn down the field and the plasma energy to study it at low energy. The reverse, however, is not true. Finally we have at Los Alamos a source of high-energy plasmas in our coaxial guns and we appear to have a usable injection mechanism in the cross-field injection experiments of Baker and Hammel.

1. Machine Design - A machine with large plasma energy density is not easy to build in the octufile configuration. The reason is that the octufile in its simple form is not in mechanical equilibrium. A magnetic force drives each of the rings toward the field zero in the torus. The radial component of this force can be supported by tensile or compressive strength of the ring (Fig. 2), but the only way of supporting the axial component of the force is directly with support rods. At large particle energy and therefore large magnetic field, or large dimensions, or both, the forces are larger, and with large plasma energy densities the support rods are intolerable. One can dream of systems with shaped walls so that the rings would be supported axially by the field itself, but these appear more complicated than would be desirable for a start.

A toroidal quadrufilar machine has the advantage of mechanical equilibrium, in the absence of gravity at least, although it has the disadvantage of smaller $\int \frac{d\ell}{B}$ stability than the octufile. It is shown in principle in Fig. 3 with floating conducting rings carrying current in one toroidal direction, the current inductively driven by an oppositely directed primary current in the outer torus. Mechanical forces are a bursting hoop stress in the inner ring and a compressive hoop stress in the outer. A field of this type can be shown

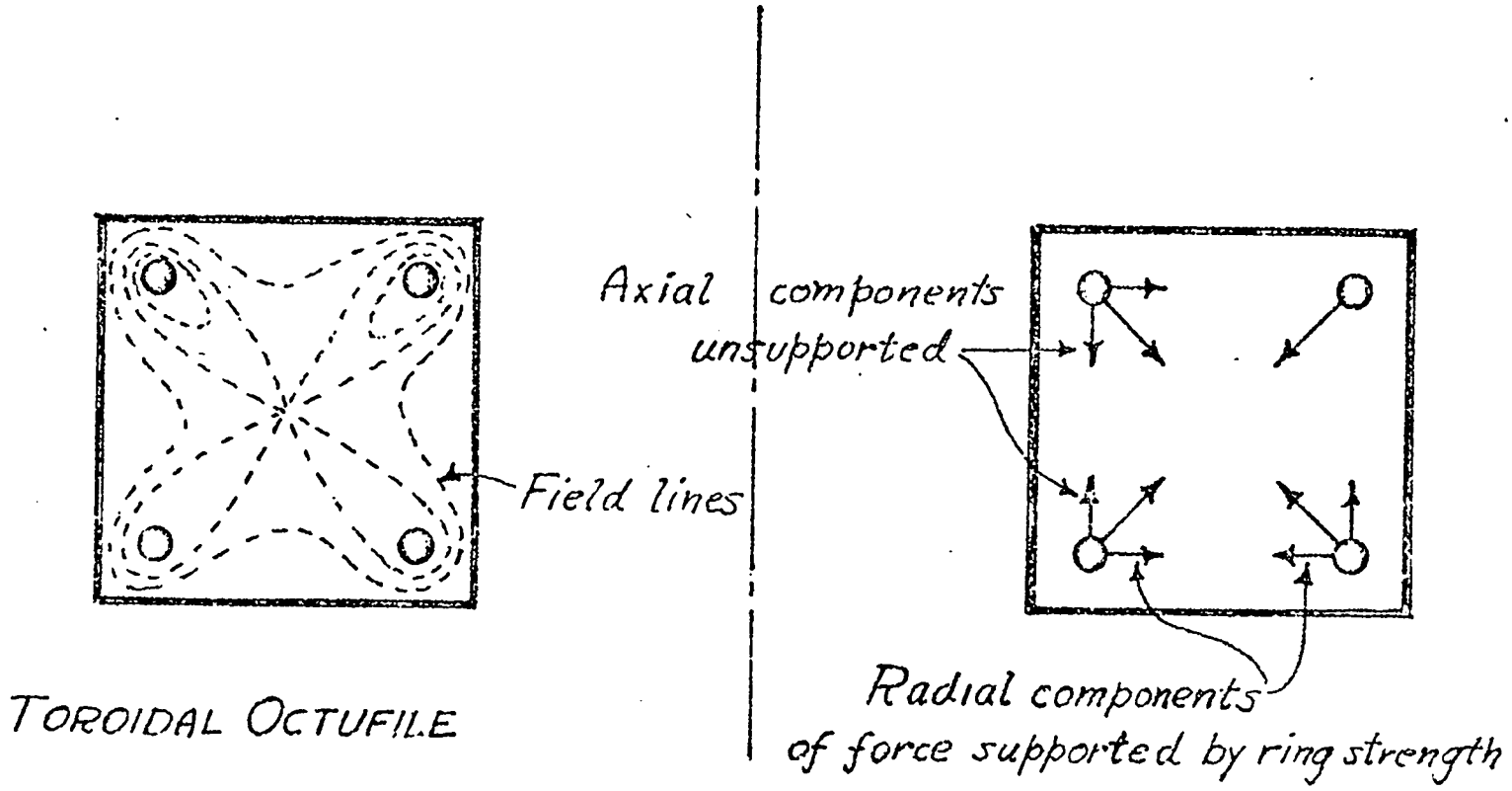

FIG. 2 Toroidal Octufile Configuration

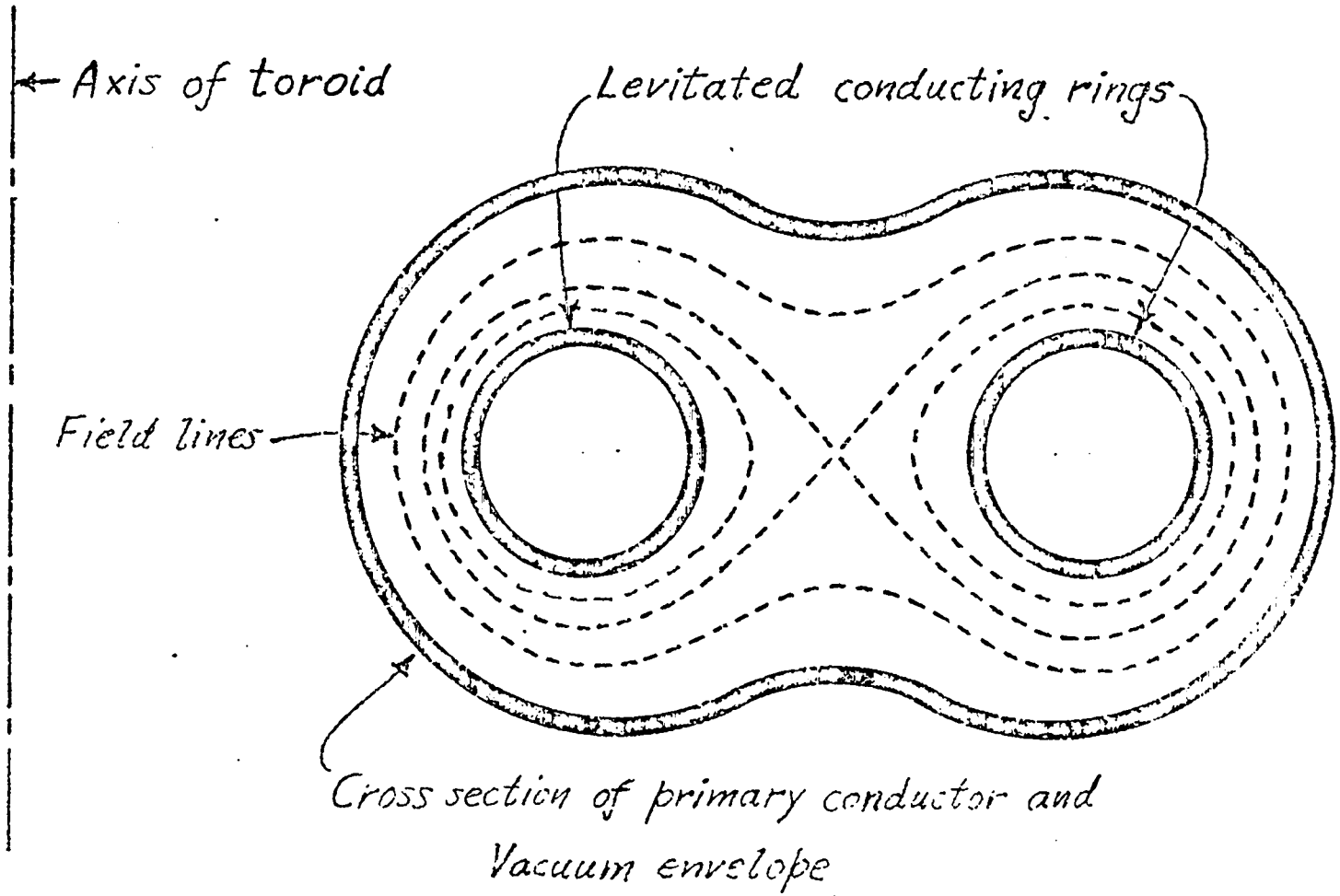

FIG. 3 Toroidal Quadrufile Configuration

always to have some region near the separatrix (the field surface which connects to the null) inside of which $\int \frac{d\ell}{B}$ stability is formally achieved. This follows since the favorable portion of the line integral, the part in the region where the lines are concave inward, can be made overwhelmingly large by integrating along a line close to the field null so that the denominator contains a small value of B. A flute stable machine with a field of this shape can always be constructed in principle by scaling the field and/or the linear dimensions so that particles of the desired energy can be contained inside the calculated last stable line of the field. In principle the containment field could be achieved by scaling either the field strength or the linear size of the machine. In practice there is usually some maximum field strength which can be allowed, either because of mechanical strength, enhanced loss of flux through soaking into conductors, or plasma injection considerations.

2. Field Computation - A computing machine field computation effort is in progress with the object of arriving at a field shape capable of presumably flute stable plasma confinement of 10-keV deuteron plasmas with the minimum practicable field energy. A workable machine code for this purpose to calculate shapes, strengths, and the appropriate integrals of toroidal bridged quadrufilar fields has been adapted from the octufile relaxation code of R. A. Dory developed for Kerst at Wisconsin. Examples of fields computed here by this code are given in Figs. 4 and 5. Other computation methods are in various stages of development, particularly by Ralph Lewis and Emory Stovall of this laboratory. The effort will continue until a satisfactory field is worked out. It is assumed from the meager experimental information available that five deuteron gyro radii of containment field should be provided between the separatrix and any material wall. For 10-keV deuterons this amounts to 10^5 G cm. The method at present is first to assume a set of boundary flux surfaces. These might be thought of as the surfaces of two perfectly conducting, coplanar, coaxial floating rings inside of a perfectly conducting doughnut. A solution of Laplace's equation is now found by the computer code where the net flux passing between the rings is zero, and both the rings and the doughnut are flux surfaces of the field. The strength of the computed field is next scaled to have a maximum value in the injection region of 10 kG or a maximum in the bridge

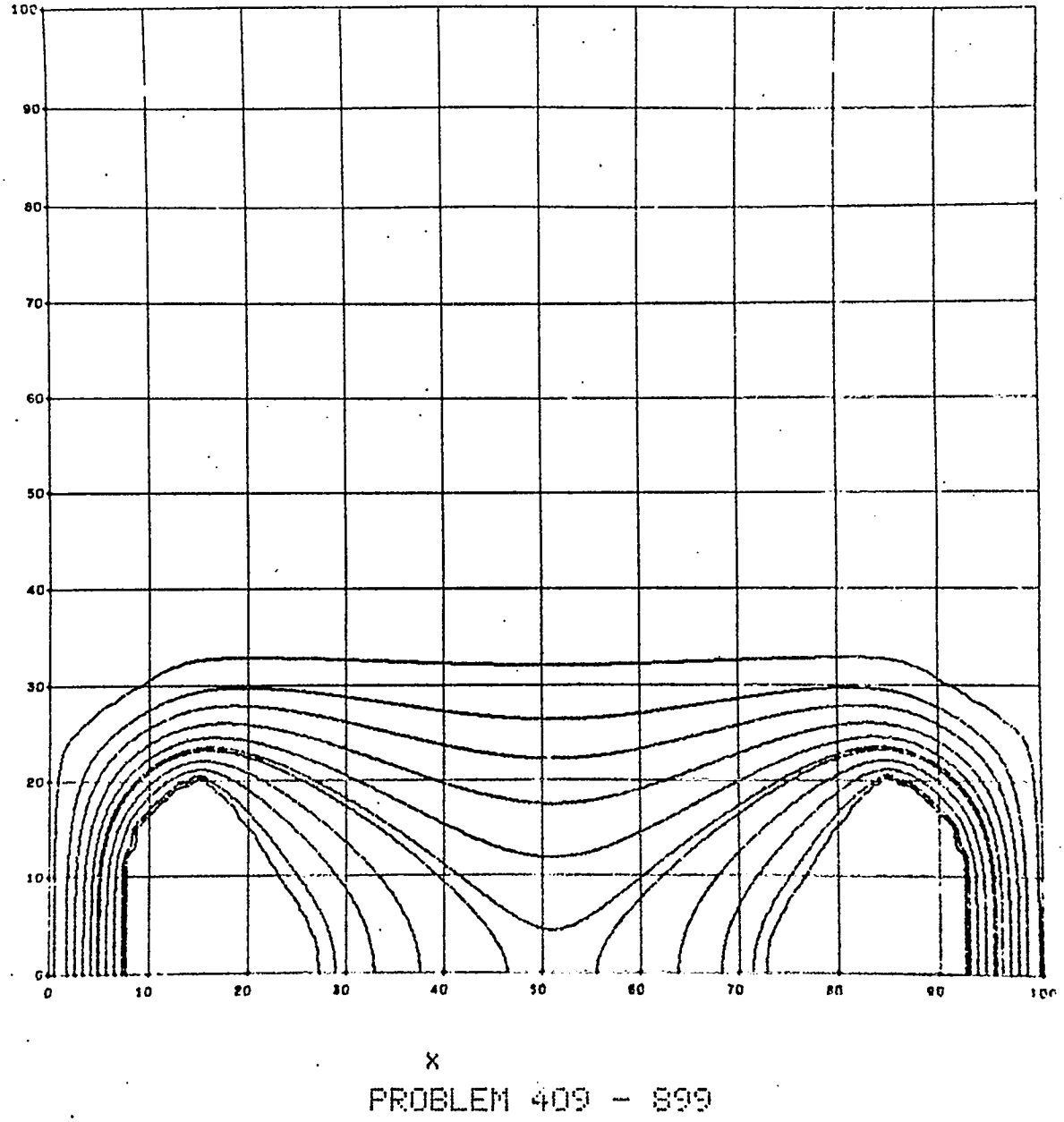

FIG. 4 Dory Code Field Plot (Example 1)

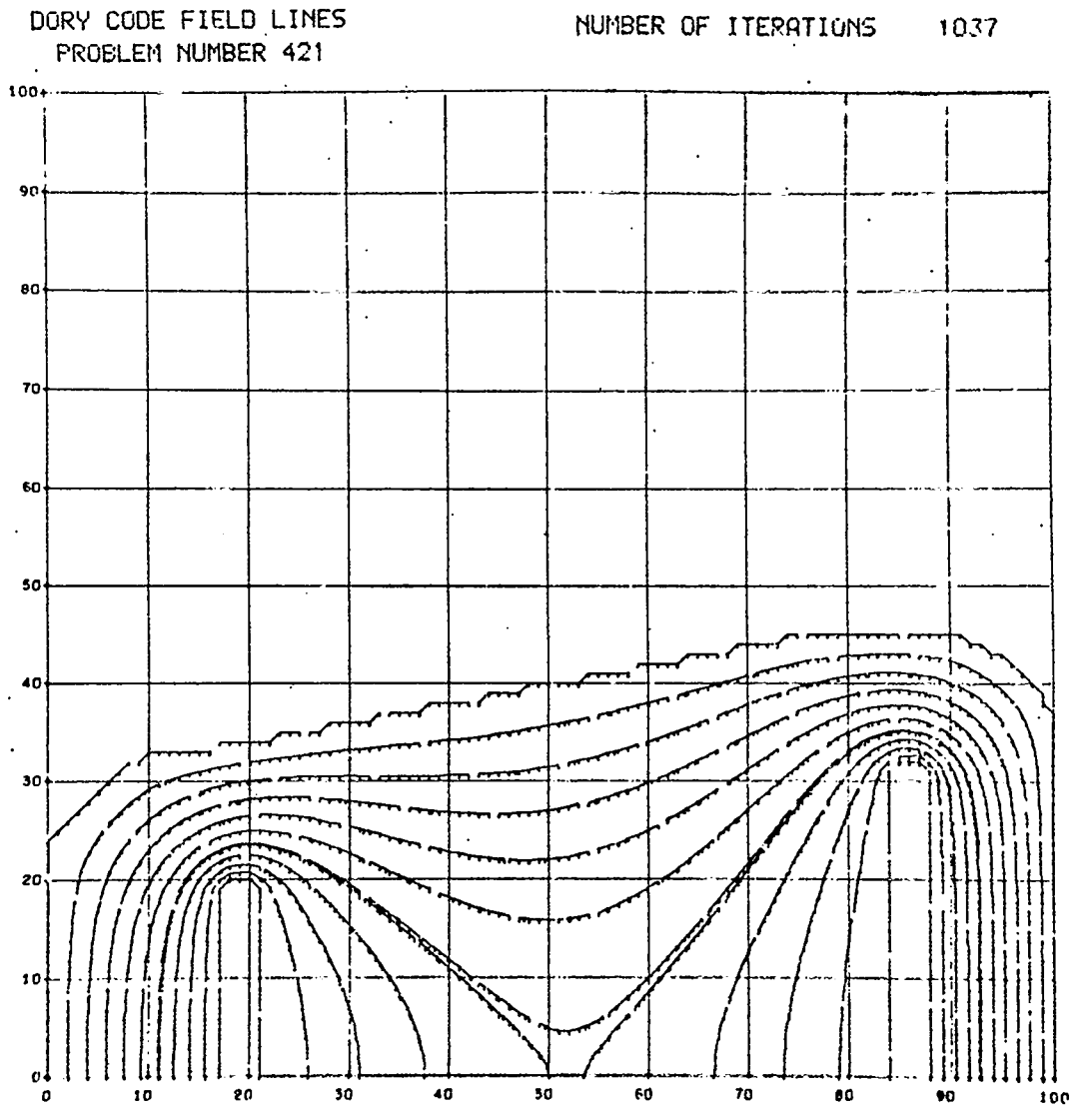

FIG. 5 Dory Code Field Plot (Example 2)

regions of 50 kG. The linear dimensions of the machine are then scaled to provide the assumed 10^5 G cm containment blanket in the outer bridge (the weakest point). An approximation, based on the observed fact that the shapes of the field lines depend very little on changes of the toroidal aspect ratio of the field, is used to adjust the size of the hole in the doughnut so that the necessary flux can be passed through it in a ferromagnetic core. The laminated iron core is necessary in order to drive the rings inductively without excessive lost energy and stray field in the primary circuit. Figure 6 shows the closest approach to a reasonable field shape calculated so far. This particular field is still unsatisfactory in that it has excessive strengths at the corners of the rings, and that there is a mirror region in the bridge fields inside the separatrix. Some increase of field energy will almost certainly be required to rectify these shortcomings, but since the energy in this case within the stable containment region is a little less than 5 MJ, it is reasonably certain that the stored energy required to generate the field of the actual machine can be made less than 10 MJ.

There has not as yet been found any orderly way of attacking this problem because of the practically infinite number of parameters involved in arbitrary boundary shapes. After a formally satisfactory field is found it has to be inspected carefully to determine whether this actual field can be generated and held without ruinous distortion using actual materials of finite conductivity. One of the major problems is the soaking of fields into conductors. This involves solution of the transient skin effect, and this should rightly be done for the particular surface shapes and field shapes finally employed. During the search this is not practical of course, but a working understanding of the effects involved has been attempted by solving for the soakage in a coaxial geometry with a hollow cylindrical inner conductor. The field is assumed to rise sinusoidally for a quarter-period and then to be perfectly crowbarred. With a 10-msec quarter period, the effective skin depth in copper at room temperature is about one cm. This means that a large amount of flux can soak into the ring surface at high field regions and thus become unavailable for containment. There are various conceivable tricks for minimizing these effects, some of them even less practicable than others. The reason why they have to be considered at all is that the amount of energy required to be stored (in a capacitor bank presumably) is larger than has ever been transferred from one capacitor bank before.

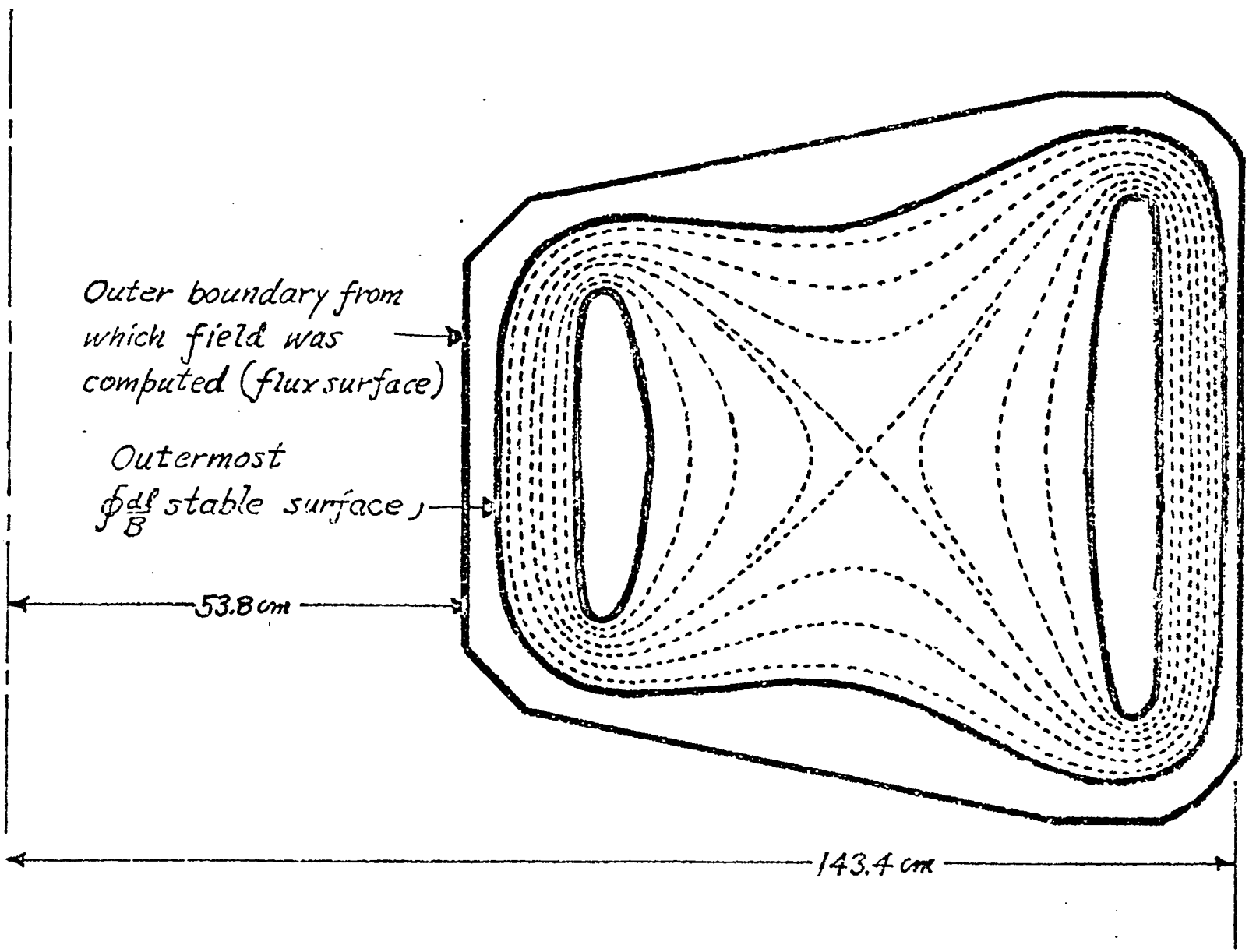

FIG. 6 Present Least Energy Quadrufile Field

3. Levitation - The inner rings of the machine will have to be capable of being levitated during the interesting experimental time of a shot. This has been done before, by Colgate and Furth, for instance, in the Levitron hard-core toroidal pinch machine, but in this machine the problem is harder in that larger weights, longer pin pulling distances, and probably longer levitation times are required. Plans at present are to drive the entire doughnut into a free fall trajectory with cams, pull the ring supports pneumatically through bellows, allow the entire assembly to fall freely with no ring supports for from 10 to 30 msec, reinsert the supports and decelerate with cams. A model levitation machine is in detailed design for testing.

4. Liner and Coil Structure - The machine will have a resistive metal liner so as to avoid a number of very serious problems which would exist if there were a metallic liner with a feed gap. These problems center around the electric fields and consequent crossed field plasma drifts which would be found around such a feed point. The difficulty could, in principle, be avoided with an insulating liner, but a ceramic or glass liner of this size and form appears impracticable. The liner can be formed out of pie sections of thin stainless steel of about the size of truck fenders, welded together, and with a hand-smoothed gasket surface inside and outside in the median plane. The metal liner will be backed up and supported against atmospheric pressure by a fiberglass, epoxy resin, and copper coil structure made up of a large number of sub coil units having equal numbers of turns, as nearly as possible equal in resistance, and a distribution of current conductors calculated so as to bound the field in the doughnut.(Fig. 7). The sub-coil units will be connected in parallel to an extent which it is hoped will allow redistribution of current in case of imperfect centering of the rings, so as to provide sufficient mechanical stability. This problem has not yet been seriously investigated but certainly it must be before construction starts. The problem of course is that a pair of rings such as the floating conductors, carrying currents in the same direction and isolated from other conductors would be expected to be subject to a pinch instability, the two rings approaching one another on one side of the axis, and separating on the other. A perfectly conducting outer wall would be expected to reduce this instability by providing image

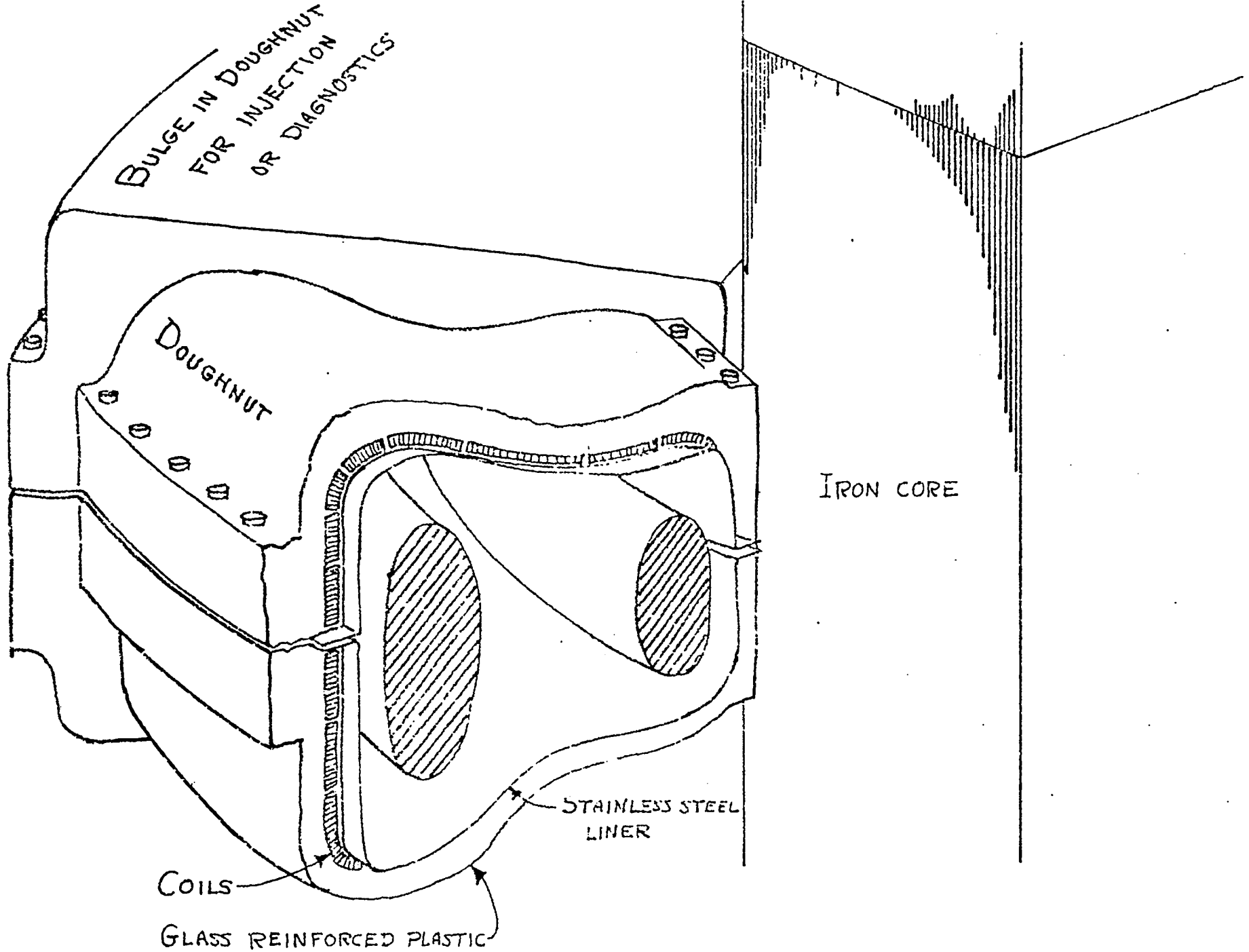

FIG. 7 Conceptual Toroidal Quadrupole Machine (Cut away)

currents which would repel a ring if it approached the wall closely. Unfortunately the outer wall cannot be considered to be perfectly conducting on the scale of this experiment, particularly since the resistive liner enforces a long field rise time to prevent excessive energy loss in the short circuited resistive turn which it represents in the electrical circuit. The skin effect field soaking to be expected on this time scale (~ 10 msec rise time) could represent a serious distortion of the field with time, since more flux would be expected to soak in in high field regions than in low. This distortion can be largely eliminated by the use of a wound coil of many relatively small conductors. For various electrotechnical reasons ten kilovolts is a reasonable voltage for the energy storage device for this machine. Ten kilovolts and 10-msec rise implies a reasonably large number of turns in the coil (something like 25 to 50).

5. Vacuum System - All of these magnetic and mechanical problems have to be solved under clean vacuum conditions. Appreciable amounts of hydrocarbons on the walls have been observed to interfere with gun operation and if any reasonable containment time is to be achieved the vacuum will have to be a rather good one. It is planned to pump the system primarily by a combination of ion pumping and titanium sublimation. The vacuum problem is alleviated in a negative sort of way by the likelihood that the high energy deuterons will combine with wall oxygen to produce lightly bound wall water. This problem is rather hard to lick at the moment, and the total pressure will probably be no better than about 10^{-8} torr.

6. Injection Port - At the injection position there must be a hole in the doughnut and in the current winding outside the doughnut. Since in most places the current conductors will be laid as close as possible to the last stable flux surface so as to conserve field energy, this poses a considerable difficulty in field distortion, particularly as the injection hole will probably have to be a rather large one. A way of getting around this problem appears to be offered by the arrangement sketched in Fig. 8. Using this trick of bulging the doughnut in one place and filling the bulge with an extension of the same field, the winding can be pulled back far enough from the field so that

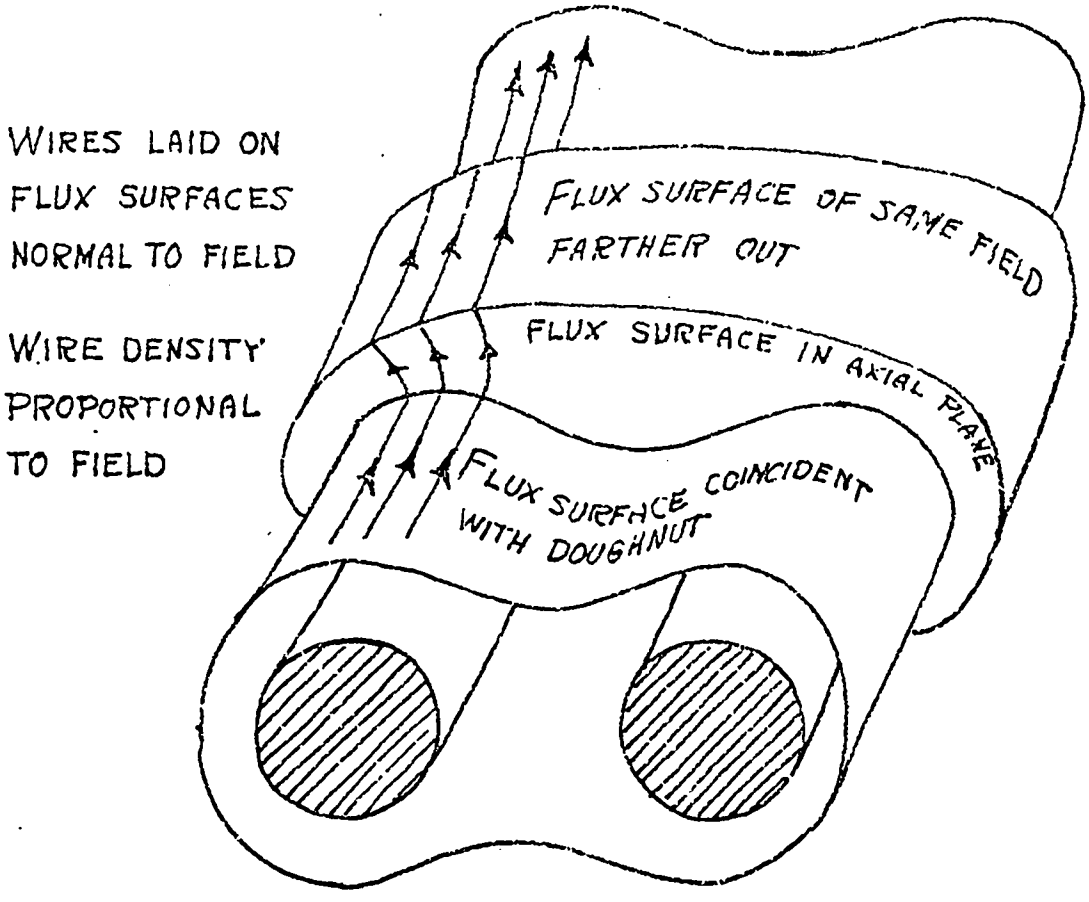

FIG. 8 Field Extension in Injection Region

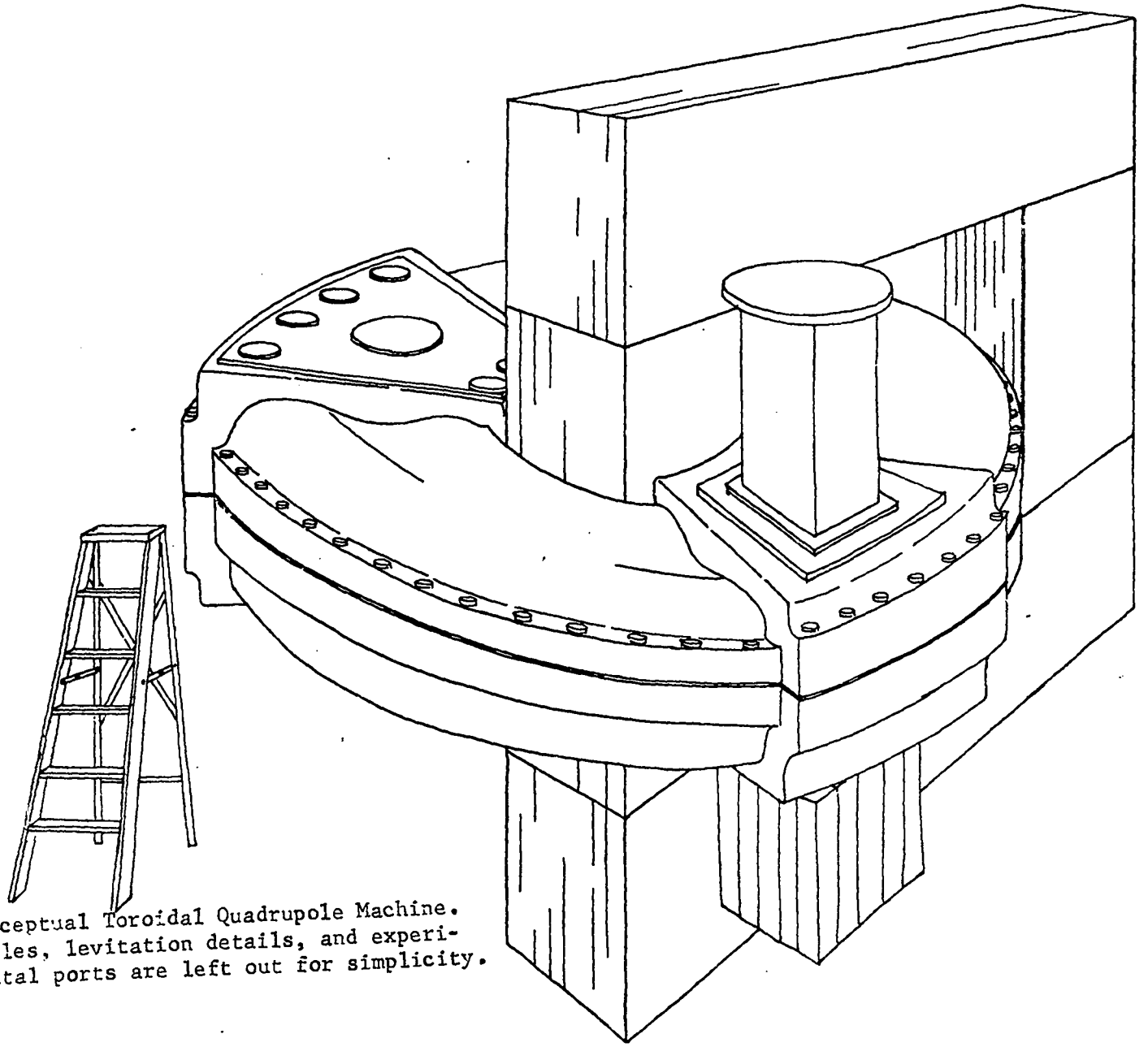

FIG. 9. Conceptual Toroidal Quadrupole Machine. Cables, levitation details, and experimental ports are left out for simplicity.

local perturbations such as spreading the wires apart to pass around an injection hole won't seriously distort the containment field.

It is most likely that some sort of guide field will be placed between the gun muzzle and the containment field. Whatever this is, it need not last as long as the containment field and therefore can be isolated from the containment field region by metal flux guiding surfaces. The guide field region will probably have to be experimented with after the containment field is constructed and in operation. A massive metal flange will provide both magnetic isolation and a convenient attachment point.

7. Laminated Iron Core - The desired field in the Caulked Cusp machine will all be in the space between the coil windings and the floating rings. However, the coil by itself also produces a field which threads through the hole in the doughnut, and makes a dipole field at large distances. These two fields can be considered as being produced by parallel inductive circuits, one on the inside surface of the coil, and one on the outside. The outside circuit is parasitic in the sense that it produces a field unwanted in the machine. An iron core, threaded through the hole in the doughnut and returning on the outside, can be considered as increasing the inductance of the outer parasitic inductor without affecting the inner one. With no iron core, the two inductances, in this case, would each be of the order of one microhenry. Approximately half of the energy fed to the machine terminals would appear in the parasitic field. With an iron core the parasitic energy can be made negligible. Of course the core must not be allowed to saturate.

In the pulse approximation the resistance of either of the floating rings can be considered to be zero. Thus during a pulse the flux threading the inner ring cannot change. Containment field has to be generated, however, in the inner bridge, and this produces a flux change through the inner ring. The iron core then must be capable of handling this flux without saturating. The amount of flux change which can be carried by an iron core in a pulse can be doubled by back-biasing the core so that its flux is reversed during the pulse. Since this can make the hole in the doughnut smaller, the perimeter can be reduced and less flux is required. In principle, then the amount of iron required for the core can be reduced by more than a factor two by back biasing.

In practice back biasing introduces difficulties. Since the flux is reversed in the relatively short field rise time of a shot, a large voltage is induced in the bias winding, and this must not be allowed to drive current through the bias supply, both because of the large overload which it would produce there, and because of interference with machine operation. The standard method of handling this difficulty is a choke in the bias supply line. The choke, however, is a monster, and fortunately one is not necessary in this machine since the bias current can be transferred from the winding to the floating rings just before a shot by simply opening the bias circuit (first with a resistor-capacitor combination across the switch to reduce arcing). There is still possibility of an accident however, if for instance the capacitor bank driving the machine should fire prematurely while the bias supply is still connected. Prefires of this kind are quite probable with capacitor banks and may be even more probable with a very large bank. It should be possible to protect the system while the bank is being charged by short circuiting the machine terminals with a mechanical switch, the switch to be opened just before current is transferred to the rings from the bias winding. A fault in the short interval remaining could be handled by explosively triggered dielectric switching, which is likely to be unpleasant and require rebuilding the switch, but which can prevent much worse damage. The long L/R time constant of the rings on the core, ($\sim$ 100 sec) which makes possible the transfer of current from the bias winding to the rings, also makes impossible fast pulse biasing of the core. If it were possible, pulse biasing would be convenient because then the bias field would be forced to be parallel to the core laminations, a condition which does not necessarily apply to a d.c. field. Only the component of the bias field parallel to the laminations can be reversed during a pulse. With a rectangular assembly of the iron core in elevation and cross-section, it is possible to make sure that the bias field is parallel to the laminations provided the laminations lie in planes parallel to the plane of the assembly, and provided the bias winding is applied to the surface of the core in exactly the right pattern. The pattern incidentally is different for different values of the bias. With a non-rectangular cross-section of the core, as for instance, if an attempt is made to fill the non-rectangular hole in the doughnut completely with iron, perfect parallelism of bias field with laminations is possible only with a toroidal core and bias winding. This is likely to be more expensive

than a rectangular assembly, and to have other practical difficulties, so it is not planned at present.

The core will be made of ordinary 60-cycle laminations of silicon steel. Theoretically this may not be the optimum material in this application, but for economy and reliability it is usually important to allow industry to fabricate things in their accustomed way.

7. Energy Storage and Switching - The large amount of stored energy required for the Caulked Cusp machine is a major cause of worry. To our knowledge no one has yet operated a capacitor bank at this level of energy storage. Capacitor bnaks which nominally approach this size exist as for example the Zeus bank here at Los Alamos which is rated at 6 MJ. On the other hand the Zeus bank has never been connected all in parallel to the same load, and it is a rare capacitor bank which is operated at full voltage more than occasionally. The reason for all this diffidence is that the probability of electrical failures goes up proportional to the number of components employed, and that for a large bank an electrical failure can be most spectacular.

Capacitor banks, however, are well established in our local technology, and in principle we know how to safeguard against the worst accidents by more or less elaborate systems designed to dump bank energy in a safe place in case of a fault. Certainly our first experiments with this machine will be driven by capacitor energy storage from banks of a size covered by our experience.

However, for a field energy of ten megajoules, or for conceivably larger energies to come in the future, it may be that an alternate energy storage scheme may be better. One can think of a number of ways of storing energy which might become more convenient than capacitor banks at large energy levels. The method among these which looks most attractive for the requirements of a machine of this kind is inductive energy storage. In principle one simply charges a storage inductor by building a large current up in it from a d.c. source, and then opens a switch in series, forcing the current to transfer into the desired load. Unfortunately it is notoriously difficult to open a switch in series with an inductor because of the arc which forms across the switch contacts. In the simple system just described it can be shown that, in driving an inductive load such as we will have here, only one-fourth of the

energy initially stored can be transferred to the load inductor. Half of the energy goes into the arc across the switch contacts and the remaining quarter is still in the storage inductor. The arc can be replaced by a resistor capable of dissipating this amount of energy less spectacularly. Electrolytic resistors are cheap and eminently suitable. But still a 40 megajoule inductor, if it is to be charged by a reasonable power supply, is a large piece of hardware. Its L/R time constant, if it is to be charged by a 2 megawatt supply, must be at least 40 seconds, and more than 100 tons of copper would be required. In addition to this a switch would be required to open something like a quarter of a million amperes at ten kilovolts. It is quite possible that a switch of this sort could be developed. There have been several ideas here as to how it could be done, but this looks like a separate research project in its own right, and we are short of personnel.

Several ingenious methods have been suggested elsewhere for making inductive energy storage practicable. Notable is the work of H. C. Early and collaborators at Michigan and the suggestions of Furth and of Simon and Bronner of Princeton. For various reasons we consider these solutions to be unsuitable for our application.

One method for transferring inductively stored energy, however, appears simple enough so that it might be applied here, and to offer a chance that it might markedly increase the reliability of the system. This is to connect a large capacitor bank across the switch so as to keep the voltage near zero as the switch is opened. Switch 2 would be closed just before Switch 1

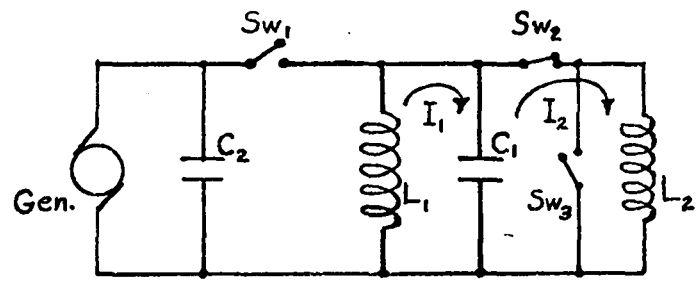

is opened to connect the load to the supply. For a 10 megajoule energy transfer the main capacitor C_1 would have to be capable of storing 5 megajoules on a pulse basis. C_2 would be a small capacitor capable of absorbing the

inductively stored energy in the generator circuit. The normal cabling of a 5 megajoule bank has so many leads in parallel that the inductance would be negligible in a case like this. The time history of the energy transfer assuming L_1 and L_2 equal would be as follows:

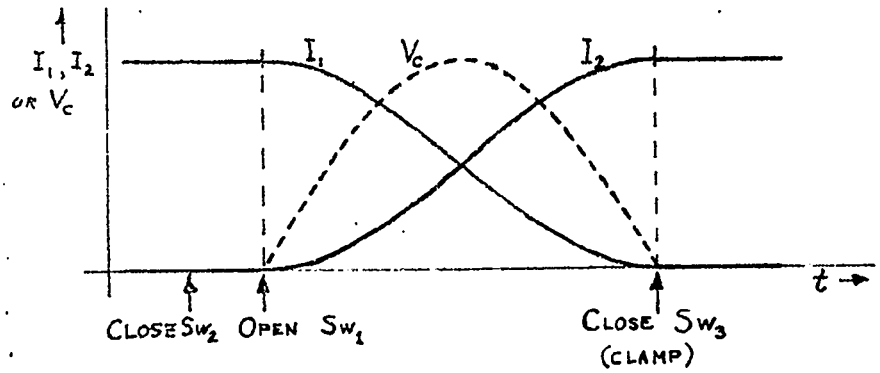

At the half-way time the current in each inductor is half the initial current in the storage inductor. Thus each inductor contains one-fourth of the energy and therefore the capacitor contains one-half.

This energy transfer scheme will be studied in detail in the near future, and if it looks sufficiently promising an attempt will be made to develop the necessary mechanical switching. In any case a mechanical clamp switch will be needed to back up ignitron clamps.

8. Diagnostics - The purpose of the Caulked Cusp experiment is to investigate the possiblity of using field geometries of this general sort, or sharing certain properties with it, for the containment of a thermonuclear reactor plasma. It is somewhat unlikely of course that the machine itself as it is projected will be satisfactory as a long time plasma container and that it will be possible to inject plasma satisfactorily exactly as planned. Accordingly the entire exercise becomes purposeless unless plasma behavior in both

the injection and containment phases can be studied in detail. Experience in Sherwood has been that diagnostics are mostly developed on the experiment itself and are not planned in advance. Frequently the diagnostics planned in advance are not useful for some unforeseen reason. It is highly important to provide access to the machine for any diagnostic technique which might be thought to be applicable. Certainly some diagnostic methods not yet thought of will be applicable through the same ports and others will not.

Unfortunately the large amount of field energy required for the experiment forces the design toward a tight fit between the field excitation windings and the containment region. Otherwise it would be possible to leave gaps between coils for ad lib. diagnostic ports to be added later. As it is a large number of small ports will have to be incorporated in the original coil design. Most diagnostics in use at the present time can be done through rather small holes. For those which require large holes the bulge around the injection azimuth and a similar one on the other side of the machine should provide reasonable access.

Diagnostics will be aimed at: (1) understanding the injection process including the initial penetration of gun plasma and trapping in the machine, (2) spreading of plasma around the machine, (3) containment and loss of plasma and of plasma energy. Methods of diagnostics will include whatever is applicable of methods used in the past plus useful future developments. A partial list of methods previously used in the laboratory which are likely to be useful in this experiment follows:

1. Optical
   a) Infrared laser interferometry
   b) Visible and uv spectroscopy
   c) Visible photography
   d) Microwave interferometry
2. Magnetic
   a) Probes
   b) Diamagnetic pickup coils outside containment region.
3. Electrostatic
   a) Probes
   b) Capacitive pickup

4.	Particles	a) d-d neutrons
		b) d-d protons and tritons
5.	Thermal	a) Calorimetry on targets
		b) Energy loss through radiation and particle flux.

In addition there are many more diagnostic techniques which don't look particularly useful to begin with but which may turn out to be possible or useful later. There are also techniques in use elsewhere which have not been used as yet in this laboratory. Particularly important is the observation of charge exchange neutrals. Molecular beam probes may also be useful.

CONTENTS

I. DENSE PLASMA FOCUS EXPERIMENT*

The creation of a dense deuterium plasma focus or foci beyond the end of the inner electrode of a coaxial electrode geometry is an outgrowth of the hydromagnetic gun work[1] performed in 1960. Since then, this dynamical mode has been studied in more detail; the results are in publication.[2] These results resemble those reported by Petrov[3] and Filippov[4] using a metal wall pinch tube apparatus.

In this work it is shown that the current sheath is established at the breech in a quasi-stable configuration which progresses toward the end of the center electrode due to the $\vec{j} \times \vec{B}$ force. The sheath moves through a uniform gas distribution of pressures ~ 2-4 torr. At the end of the center electrode, most of the condenser energy is stored behind the sheath and, as the sheath leaves the end of the electrode, this energy is rapidly converted into plasma energy by the pinch effect forces which produce the dense plasma focus. The focusing action of the current sheath is not an unnatural phenomenon. It is a well-known theorem that an unconstrained current circuit will move in such a way to maximize its inductance -- in this case the final current position is on axis. A schematic of the electrode geometry is shown in Fig. 1. The plasma produced in this manner has many interesting properties.

Soft x-ray pinhole images of the dense plasma shown in Fig. 2(a), (b), (c), and (d) were taken in a perpendicular direction to the discharge axis in the region of the end of the electrode for various pinhole diameters and for similar neutron yields (~ 5×10^{10}/burst). Copper and tungsten center electrodes were used as indicated. Such measurements show that the volume of plasma is extremely small (1-5 mm^3) and approximately centered on axis at 1.5-2 cm in front of the electrode. The blackening of the x-ray film increases with neutron production.

A dual soft x-ray spectrometer is utilized to record the ratio of soft x-ray intensity from the dense plasma through separate channels of different absorber material or thickness. Such measurement, assuming the plasma emits pure deuterium bremsstrahlung, yields the electron temperature

* This work was performed under the auspices of the U. S. Atomic Energy Commission.

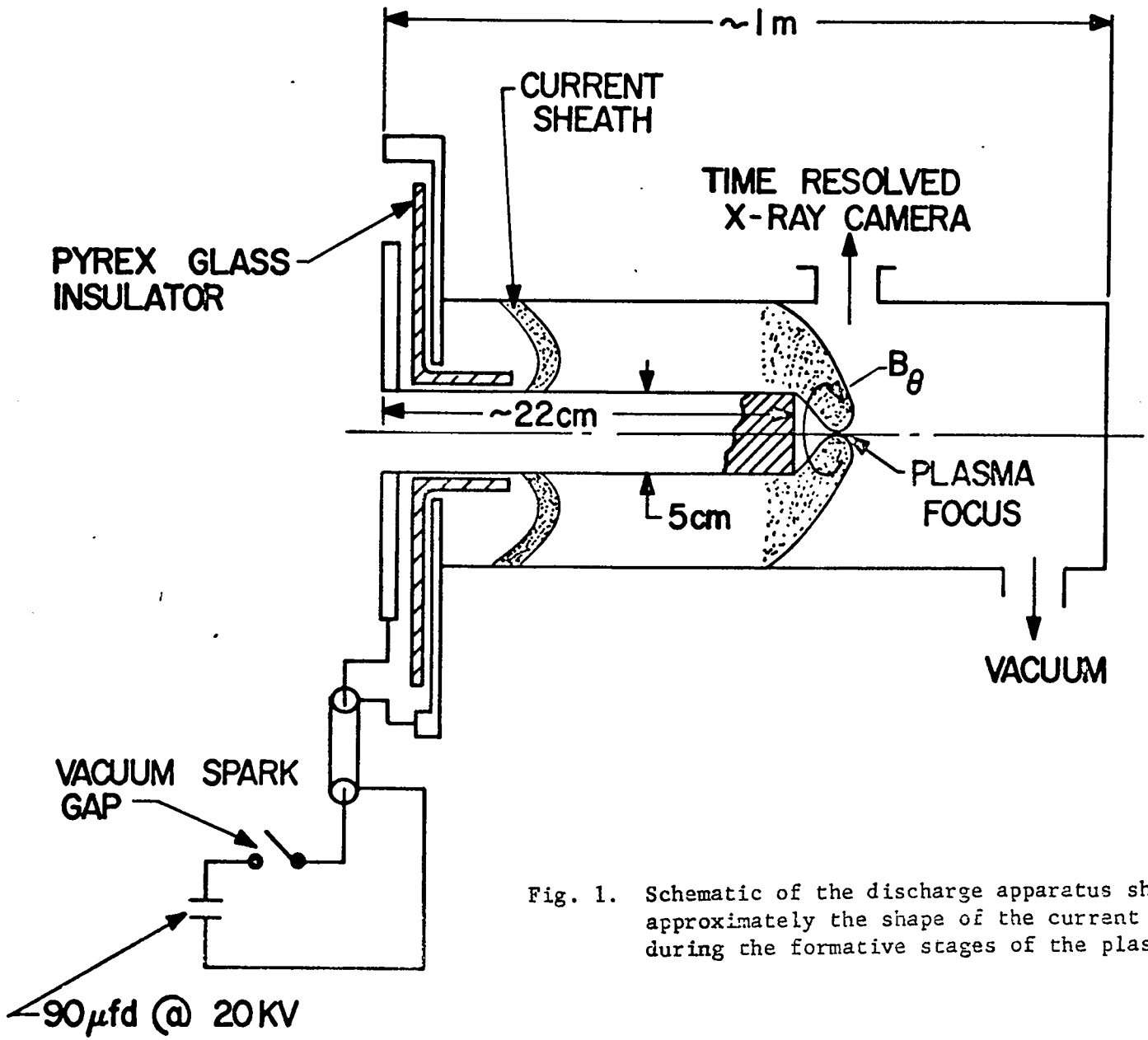

Fig. 1. Schematic of the discharge apparatus showing approximately the shape of the current sheath during the formative stages of the plasma focus.

Soft X Ray - Positive Voltage

Al Abs. 3.14 mg/cm^2

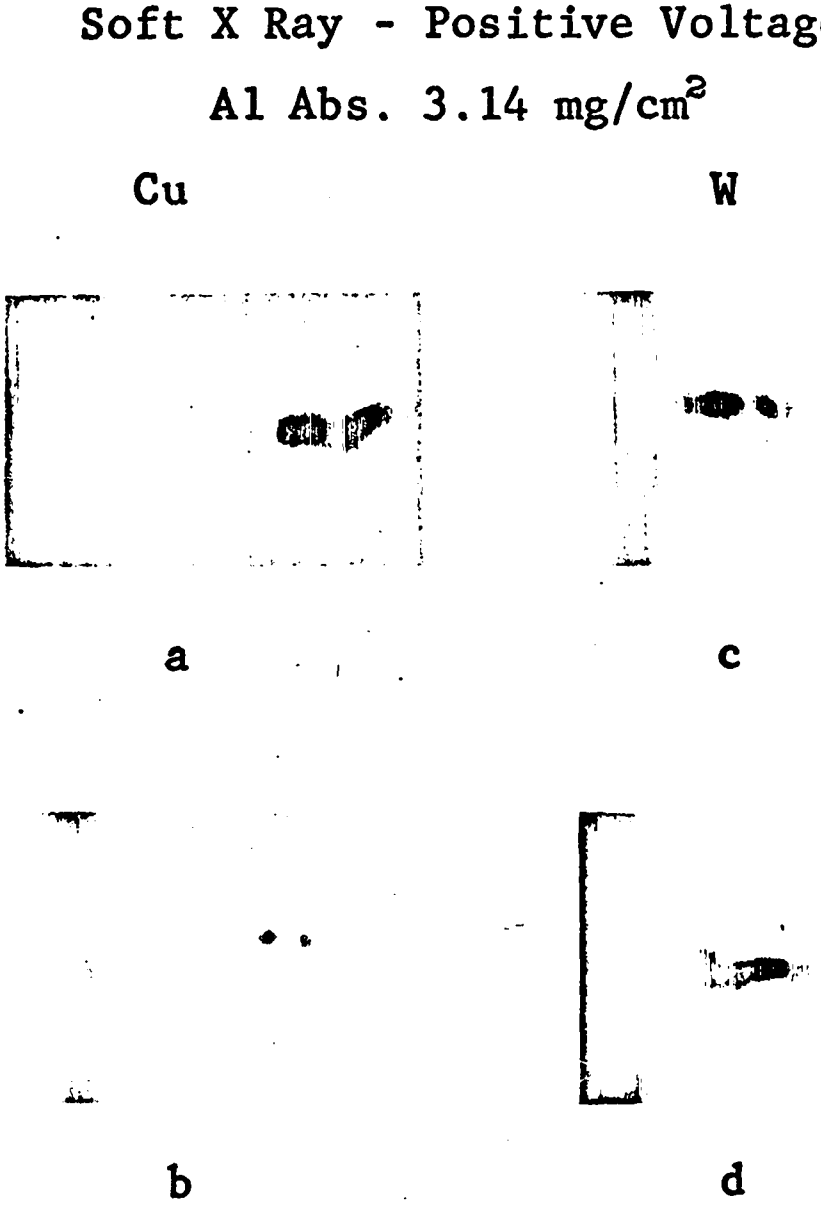

Pinhole Diam	Neutrons
a - 0.9 mm	3×10^{10}
b - 0.45 mm	5×10^{10}
c - 0.625 mm	2×10^{10}
d - 0.625 mm	7×10^{10}

Fig. 2. Pinhole images of the dense plasma foci in the light of soft x rays for a copper (a,b) and tungsten (c,d) electrode for several neutron yields and pinhole sizes. The face of the 5-cm diam center electrode is ~ 2.5 cm to the left of center in each photograph.

as a function of time. Figure 3 shows a typical example of the time dependence of the electron temperature which ranges from 0.5-7 keV and an associated neutron pulse (dN/dt). An average T_e of 5 keV lasts for $\sim$ 0.4 μsec. These observations clearly point out that the electron temperature is delayed relative to neutron production. This is as expected because if the mechanism is an electromagnetic compression mechanism (pinch effect) the ions are preferentially heated at first and the electrons can only be heated by collisional impacts with hot ions. The ion-ion and electron-electron relaxation times are extremely rapid; thus we are initially dealing with an ion and electron thermal distribution at different temperatures. On the basis of the radial collapse time, and further adiabatic compression of the hot ions, deuteron temperatures could easily exceed 10 keV. In fact one can show qualitatively at least that in order for the electrons to be heated to a final temperature $T_e \sim 5$ keV through a collision of a hot ion with a cold electron, the initial deuterium ion temperature $T_i > T_e$. The time dependent x-ray signal shows the formation of several hot spots which correlate with the multiple foci x-ray images. Neutron yields are usually largest when multiple foci are observed.

Neutron production depends to first order on the energy of the condenser bank. The largest yields observed are $\sim 10^{11}$/burst, for a burst time of $\sim$ 0.2-0.3 μsec. It should be remarked that the absolute neutron calibration of the silver-activated detectors is difficult because corrections for neutron back-scattering from close-in hydrogenous material, the aging of the Geiger counters and high neutron yield carry-over from shot-to-shot can easily account for errors of a factor of 2 or better. A systematic study of these effects is being pursued.

Neutron production from the dense plasma appears to be spatially isotropic. Measurements of the yield ratio, upstream to downstream of the plasma focus, gives $\sim 1 \pm 5\%$. The uncertainty of $\sim 5\%$ leads to a center of mass (c.m.) velocity of $\leq 2 \times 10^7$ cm/sec. This is found to be the case for either a positive or negative center electrode.

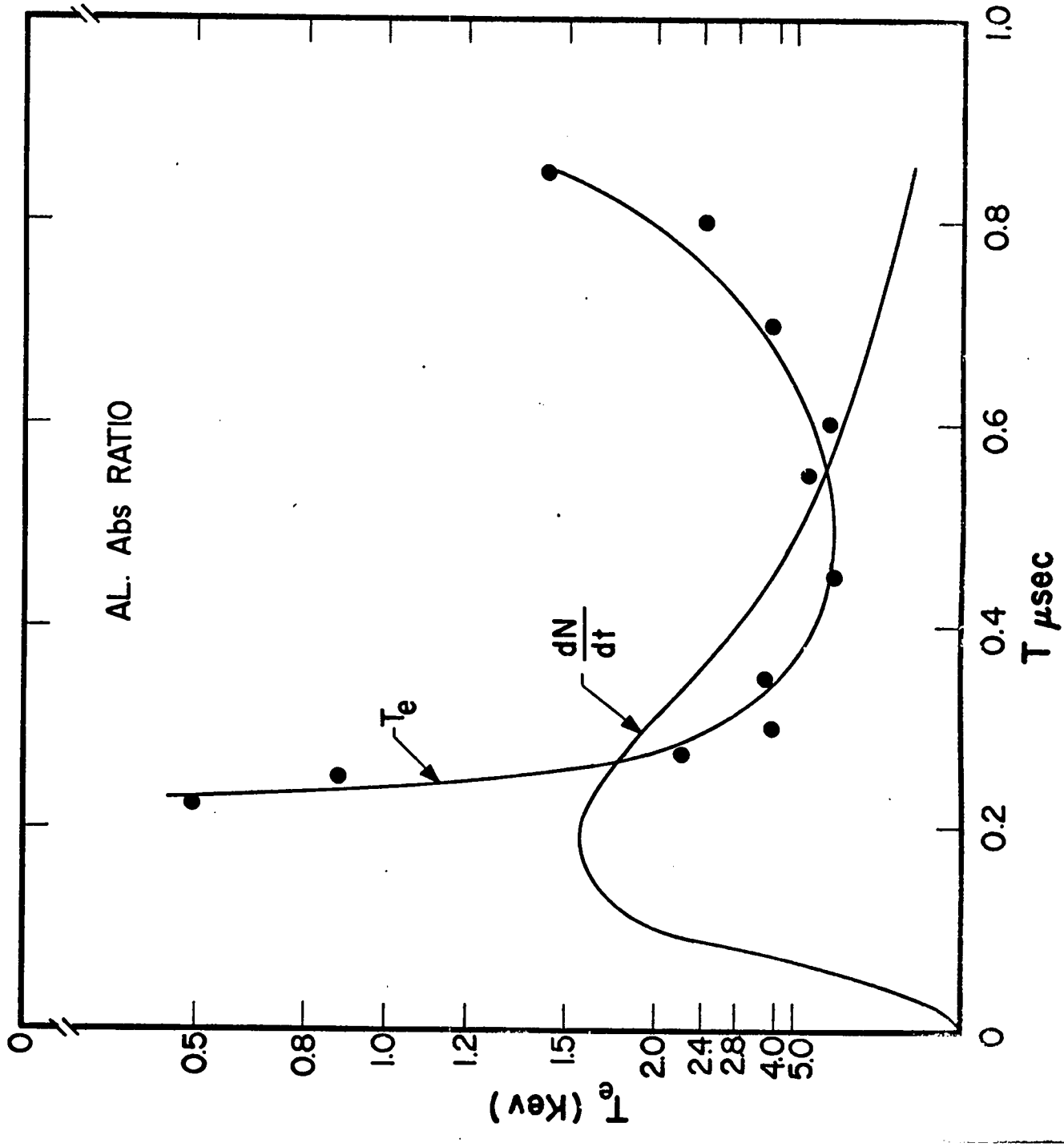

Fig. 3. A simultaneous measurement of neutron production (dN/dt) and electron temperature (T_e) as a function of time. Actually the ratio of soft x-ray transmission through two different absorption channels (6.25 and 3.14 mg/cm^2 of Al), with the assumption of pure deuterium bremsstrahlung, gives T_e.

The uncertainty of ~ 5% is more than likely due to statistics since such a calculated c.m. velocity would lead to a smearing of the x-ray pinhole photographs and also to the time dependent soft x-ray signals. Neither is observed.

Magnetic probe analyses of the dynamics of the current sheath show good agreement with the "snow plow" "M" theory, especially for that portion of the sheath near the surface of the center electrode. Furthermore, the use of small axial magnetic fields in the region of the plasma focus are shown to be compressed by the symmetrical collapse of the current sheath as it leaves the end of the center electrode. This latter measurement is difficult to refute since neutron yields were measured as the axial probe sampled the compressed field. When the probe was eventually placed in the region of the focus, the probe was destroyed and neutron yield was absent.

An analysis of the rate of change of current (di/dt) and the voltage at the breech (V) shows that the inductance of the discharge increases approximately linearly between the breech and end of the center electrode; then as the current collapses, a large change in inductance is observed to occur in ~ 0.1 μsec. The inductance subsequently continues to increase in a less rapid manner. This analysis is made for a particular discharge and strongly shows that a majority of the current participates in the dense plasma formation and that no subsidiary breakdown occurs in the accelerator section. Oscilloscope traces (sweep speed 0.5 μsec/cm) are shown in Fig. 4, reading from top to bottom, of (1) the total current and (2) breech voltage -- the third and fourth trace are di/dt and breech voltage, respectively, for a separate discharge. The large inductive change occurs near peak current. Similar conclusions were obtained from magnetic probe measurements in the annulus along the length of the accelerator.

If it is assumed that the plasma is a collision-dominated plasma and further that a least deuteron temperature of ~ 5 keV is due only to the sheath implosion and not increased due to any subsequent adiabatic

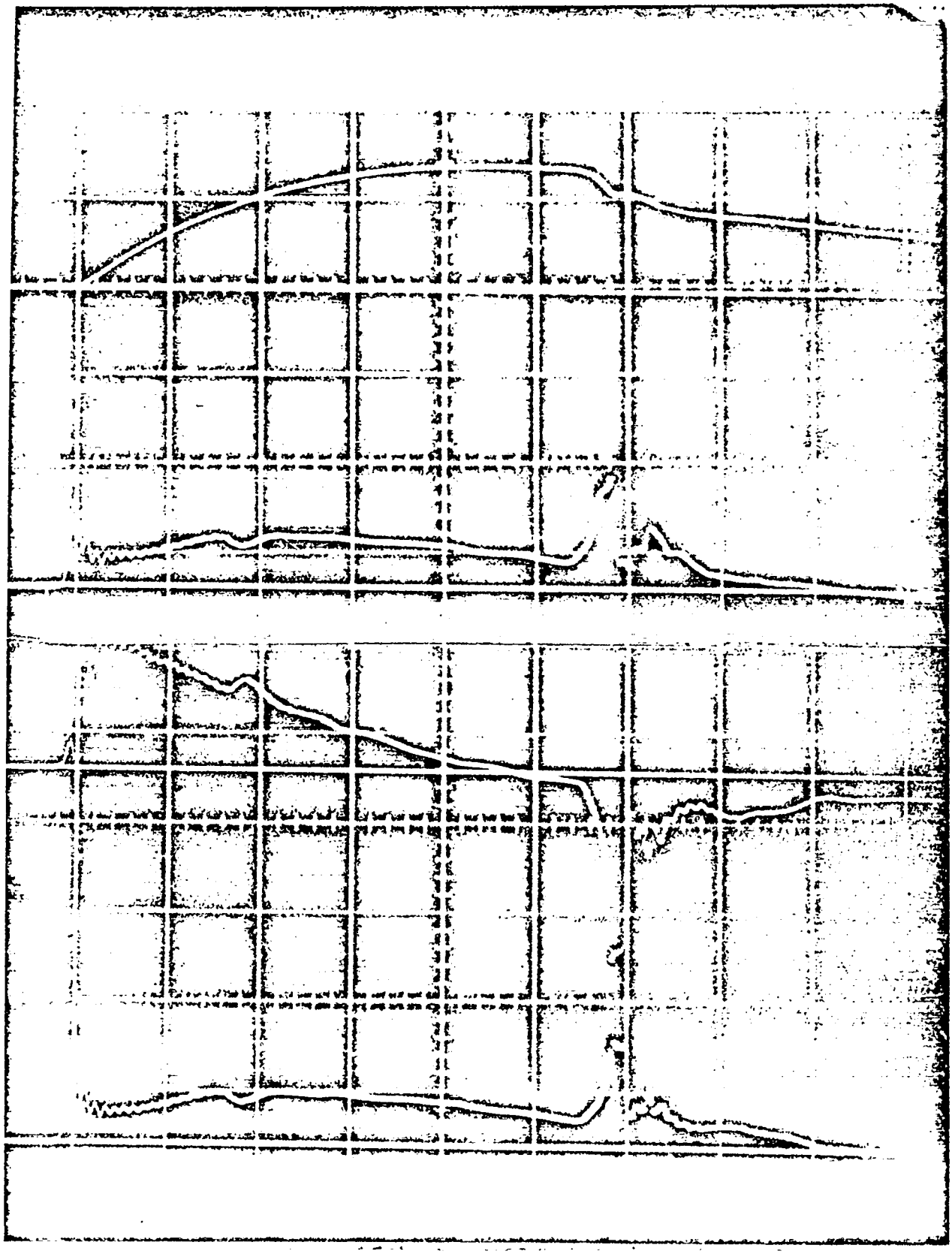

Fig. 4. Oscilloscope traces, reading from top to bottom, show a simultaneous measurement of total current and breech voltage and also di/dt and breech voltage for a separate discharge. Sweep speed 0.5/μsec/cm. An analysis of the third and fourth trace leads to the inductance $L_D(t)$ of the discharge

compression, then a calculation, based on a thermonuclear plasma, yields a final particle density of 2-3 $\times 10^{19}$/cc. A time duration of 0.25 μsec, volume of $\sim$ 1 mm^3 and neutron yield of 10^{10}/burst were used in the above calculation. Since maximum electron temperatures of $\sim$ 5-7 keV are observed, the deuteron temperature must be > 5 keV initially in order that the electrons become heated to $\sim$ 5 keV. For neutron yields of $\sim 10^{11}$/burst, either a deuteron temperature of $\sim$ 10 keV or a slightly higher density is sufficient to account for the yield. In any case, it is not difficult to obtain internal consistency with a thermonuclear neutron yield calculation. A further check on the internal consistency can be made using the Bennett pinch relation, i.e., $I^2 = 200\,\pi r^2 nkT$. For $T_e \approx T_i = 5$ keV, $r = 0.05$ cm, a current of $I \sim 7 \times 10^5$ A is required in order for the plasma pressure to be balanced by the magnetic pressure. At 20 kV, peak current is $\sim 8 \times 10^5$ A.

One may ask, can these neutrons be caused by an acceleration process. We dispel immediately the process of an m = 0 "necking off" instability first proposed for the Columbus pinches, with the following comments: (1) it is shown experimentally that the reversal of the center electrode voltage does not affect the isotropy of the neutron distribution and (2) to obtain a neutron yield of $\sim 4 \times 10^{16}$/sec would require $\sim 10^8$ A of deuteron current at an energy of 10 keV striking a target of 5×10^{18} deuteron/cm^2. Only 8×10^5 A of electron current are available in the experiment.

To test the hypothesis of a collision-dominated thermal plasma it is planned to perform a deuterium-tritium experiment. Since the $\langle \sigma v \rangle_{DT}$ cross section at temperatures of $\sim$ 5 keV is $\sim 100 \times \langle \sigma_{DD} v \rangle$, neutron yields for a 50% mixture of D-T would be some 50 times larger. Since it is next to impossible to measure the ion temperature, a comparison between D-D and D-T would be extremely useful. There is also a second reason for the D-T experiment, namely, to test another hypothesis that the larger Larmor radius of the tritium ion will increase the plasma lifetime according to the finite orbit stabilization theory. It appears

to date that no satisfactory theory, including the hydromagnetic instability theory, can account for the long lifetime of the plasma focus. However, it appears that the finite orbit theory is a good contender and a simple calculation shows that the plasma with properties mentioned previously is stable. It is in this connection that the use of tritium may enhance the lifetime and give possibly the first test of the finite orbit stabilization theory in dense plasmas.

Our immediate objective in the plasma focus experiment is to measure the plasma electron density by the well-known Schlieren and interferometric technique. The Schlieren technique detects deviations of parallel light due to refractivity gradients in the plasma; in the limit of small deviations $\epsilon \cong L/n \nabla n$ where L is the path length and ∇n is the refractivity gradient averaged along the light path. For an electron gas $n-1 = -4.46 \times 10^{-14} \lambda^2 N_e$ where λ is the wavelength of light and N_e the electron density. The Schlieren technique is suitable for detecting rapid density changes, however, the interpretation in terms of electron density depends on plasma shape. The Mach-Zehnder interferometer will eventually replace the Schlieren technique and yield a less ambiguous electron density.

Scaling of the dense plasma focus is being undertaken with the view of increasing the available condenser energy from 18 kJ to $\frac{1}{4}$ MJ. The neutron data, to date, show an approximate linear relationship with energy. If this relationship continues, neutron yields of $\sim 7 \times 10^{11}$/burst can be expected for the D-D reaction. An increase in the final plasma density is also expected since larger initial gas densities are required at higher energies in order to meet the experimental condition that the current sheath arrive at the breech end of a given electrode structure at peak current time. It is a curious fact that the maximum average current sheath velocity in the annulus between two coaxial cylindrical electrodes is limited to values $\leq 1.5 \times 10^7$ cm/sec. Thus larger $\vec{j} \times \vec{B}$ forces, due to the larger currents must be offset by larger initial gas densities.

REFERENCES

1. J. W. Mather, Phys. Fluids Suppl. 7, 528 (1964).
2. J. W. Mather, Phys. Fluids 8, 366 (1965).
3. D. P. Petrov, N. V. Filippov, T. I. Filippova and V. A. Khrabrob Plasma Physics and the Problems of Controlled Thermonuclear Reactions (Pergamon Press, London, 1960), Vol. IV.
4. N. V. Filippov, T. I. Filippova and V. P. Vinogradov, Nucl. Fusion Suppl., Pt 2, 577 (1962).

II. CAULKED STUFFED NONZERO ABSOLUTE MINIMUM B (NZAM) EXPERIMENT

The caulked stuffed nonzero absolute minimum B geometry encompasses a superposition of three magnetic fields: (1) a dc axial field provided by coils external to the vacuum tank, (2) a pulsed B_θ field, generated by current conductors through the axial stuffer tube, and (3) the field due to an azimuthal current conductor suspended in the midplane of the device providing closed magnetic field lines about this coil. A schematic of the geometry is shown in Fig. 1 and a typical field plot is shown in Fig. 2. The combined fields produce a minimum B region encircling the stuffer current conductor. Part of the minimum B region is closed on itself through a bridged region between the wall of the vacuum tank (acting like a flux conserver) and the azimuthal conductor. The remainder of the minimum B region is connected by open field lines (in the sense that field lines intersect the wall at a distance from the NZAM region), however, large mirror fields will be encountered by the escaping plasma from the NZAM region. The lines of constant B form closed nested surfaces about the minimum region. The construction of this device is nearly completed. The method of filling the minimum B region with plasma that is currently being studied entails the $\vec{E} \times \vec{B}/B^2$ rotational heating technique in which a radial electric field is impressed between the central stuffer current conductor and the azimuthal current conductor. This electric field, crossed into the axial magnetic field $\vec{E} \times \vec{B}/B^2$, produces an azimuthal drift of the plasma (ions and electrons), $v_o = E_r/B_z$. This technique of heating, rather than plasma injection into the minimum region, creates a hot plasma within the confining field region. This experiment has set about with the main objective to study the confinement of a hot plasma in a minimum B field geometry. Such questions as to (1) the stability of the plasma in the

*This work was performed under the auspices of the U. S. Atomic Energy Commission.

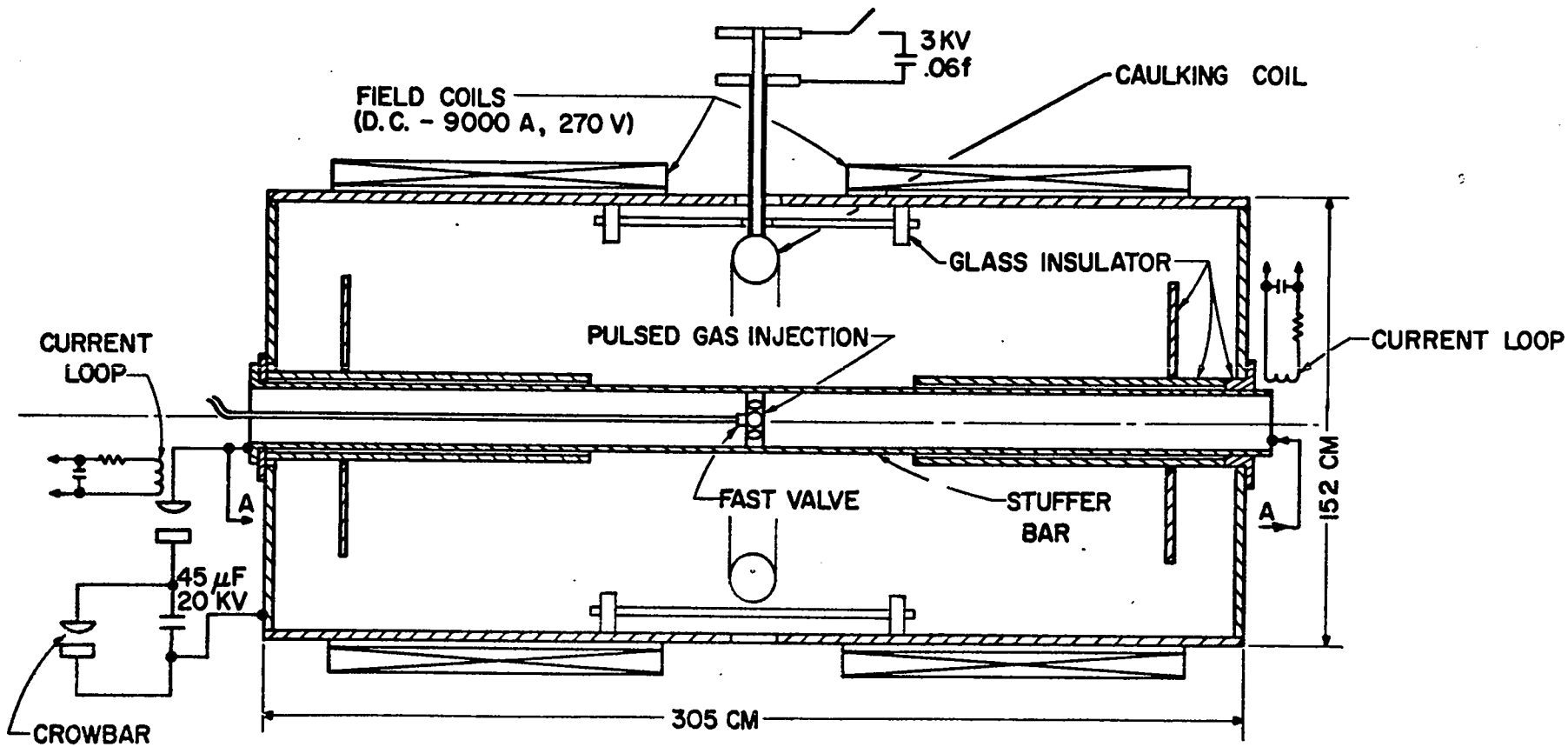

CAULKED STUFFED CUSP GEOMETRY

Fig. 1

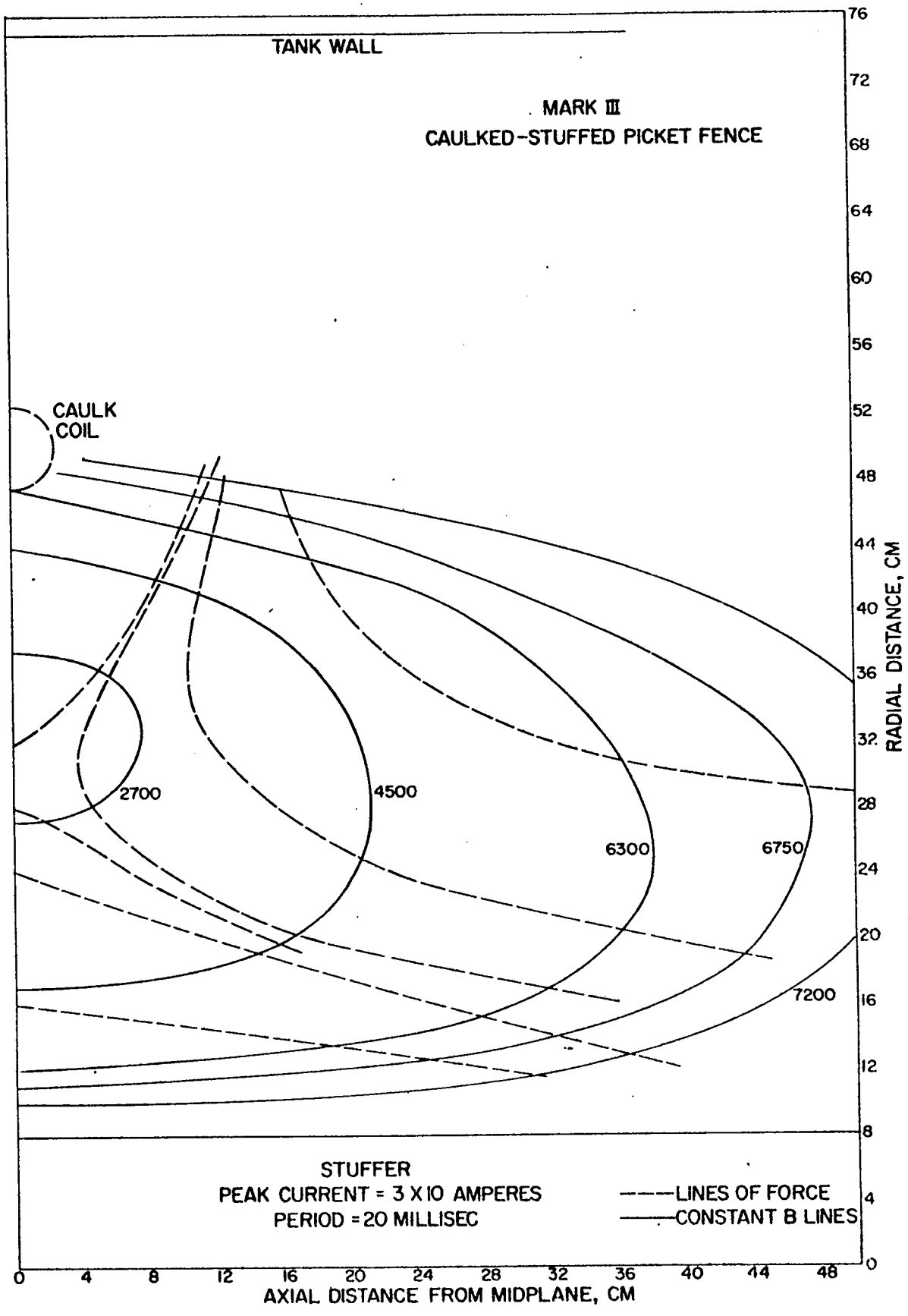
TANK WALL
MARK III
CAULKED-STUFFED PICKET FENCE
CAULK COIL
2700
4500
6300
6750
7200
STUFFER
PEAK CURRENT = 3 X 10 AMPERES
PERIOD = 20 MILLISEC
LINES OF FORCE
CONSTANT B LINES
RADIAL DISTANCE, CM
AXIAL DISTANCE FROM MIDPLANE, CM
0
4
8
12
16
20
24
28
32
36
40
44
48
52
56
60
64
68
72
76

Fig. 2

unfavorable B curvature region of the bridge, (2) the axial drift of the plasma away from the minimum B region during the heating pulse, (3) the effect of the large mirror field region on confinement, and (4) electric drift along B lines (during the heating phase).

The spatial extent of the minimum B region, on the basis of a preliminary field plot, shows a region of ~ 75 X 50 cm in cross section which encircles the stuffer current conductor. This problem is currently being coded to determine lines of magnetic force and contours of constant $|B|$.

The plasma will be examined using the following diagnostics: (1) plasma density will be measured using the He-Ne laser densitometer, (2) neutral particle detectors will sample the energetic hot ions through charge exchange using a gas exchange cell and magnetic and electrostatic analyzers, (3) spectroscopy, using the Doppler shift of the D_β or He^{II} (used as a trace element) lines to detect the rotational velocity, (4) electrostatic and magnetic probes will be used to measure the extent of the plasma during the heating stage. These measurements will be correlated with other parameters such as applied voltage, field magnitude, and injected gas pressure. Once the plasma is put into rotation, the radial electric field is removed. At this time most of the energy is in Larmor energy and the question of stability and confinement can be assessed.

A high vacuum tank (14,000 liter) has been placed into operation. A vacuum of 3×10^{-10} torr has been reached using cryogenic, sublimation and VacIon pumping. External field coils will provide a dc magnetic field of ~ 12 kg over several meters in length. The caulking field coil is completed which, in conjunction with the dc field and the stuffer conductor, will provide a minimum B (NZAM) magnetic field system.

The objective set forth in the above depends by and large on the generation of a hot plasma. Experimental work has been and is currently proceeding to study the generation of a hot plasma using the $\vec{E} \times \vec{B}$

rotational heating technique. At present this heating is studied in ordinary mirror field geometry by applying a radial electric field between a cylindrical conductor and the stuffer current conductor. Gas is injected through a series of radial ports located in the stuffer conductor.

The main results to date show that a plasma is indeed set into rotation. Doppler shift measurements of the He^{II} line in this case correspond to v_θ velocities of $\sim 2.2 \times 10^7$cm/sec. The results at times of 8 and 15 μsec are shown in Fig. 3. For deuterons, this would correspond to a rotational energy of ~ 500 eV. As expected the results are very sensitive to the applied radial electric field, gas pressure, and the axial magnetic field. Wall contamination is a major problem. A change in wall material from aluminum to copper is planned. Plasma density measurements using a laser densitometer are in progress.

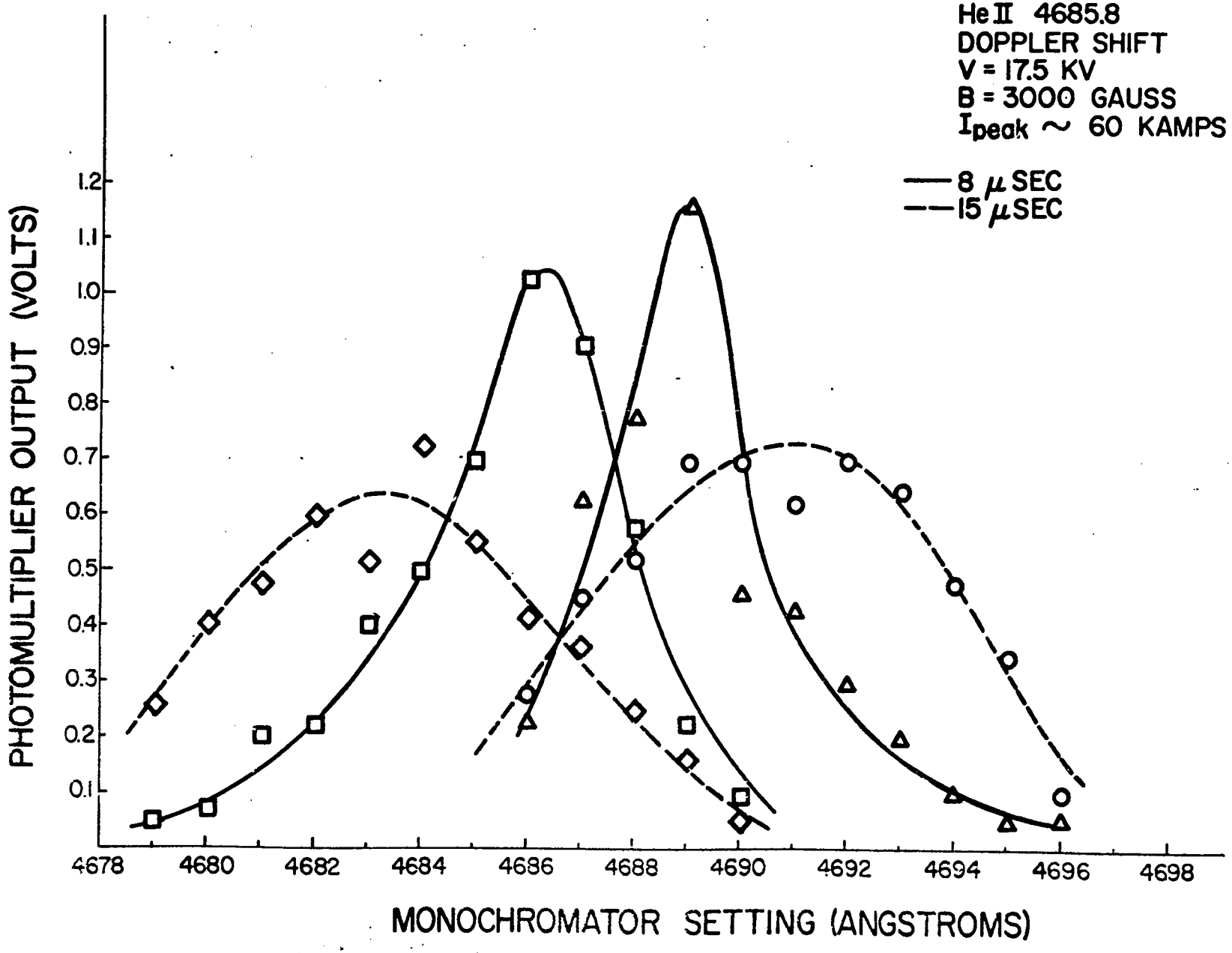
He II 4685.8
DOPPLER SHIFT
V = 17.5 KV
B = 3000 GAUSS
Ipeak ~ 60 KAMPS
8 μSEC
15 μSEC
PHOTOMULTIPLIER OUTPUT (VOLTS)
1.2
1.1
1.0
0.9
0.8
0.7
0.6
0.5
0.4
0.3
0.2
0.1
4678
4680
4682
4684
4686
4688
4690
4692
4694
4696
4698
MONOCHROMATOR SETTING (ANGSTROMS)

Fig. 3

III. BEAM-PLASMA EXPERIMENT*

The object of the beam-plasma experiment is to generate rapidly a high density plasma with a high ion temperature inside a magnetic trap by passing a very large electron current parallel to the magnetic field lines through a pre-existing neutral gas. This approach is an alternative to injecting a plasma from outside the trap. Reports in the Russian literature[1-3] indicate that it is possible to generate high ion temperatures if the electron beam density is sufficiently high. The beam currents used in these Russian experiments are far higher than any current which could be realized by a space charge limited electron gun at the low voltages used. The electron currents quoted range up to 40 A at 2 kV which would require a perveance of 500 micropervs if Child's law applied, which is 100 times larger than the perveance of the best vacuum diode. Increasing the accelerating voltage to draw more current is not acceptable since this increases the electron beam velocity which must match the phase velocity of some wave in the plasma if an interaction is to occur.

The Russian workers have reported the production of a plasma with an ion temperature of about 1 keV, an ion density of $7.5 \times 10^{10} cm^{-3}$, and a volume of $7.5 \times 10^{3} cm^{3}$ which was generated by an electron beam of 12 A at 1100 V. Note that the plasma ion energy is about equal to the beam electron energy. The plasma density seems to have been limited by the beam current, but it is not clear why a larger beam current was not used. It seems likely that it may have been the capacity of the pumps to handle the continuous gas flow. We hope to overcome this difficulty by using a pulsed gas feed. It

---

* This work was performed under the auspices of the U. S. Atomic Energy Commission.

[1] M. V. Nezlin, JETP 14, 723-727 (1962).

[2] M. V. Nezlin and A. M. Solntsev, JETP 18, 576-582 (1964).

[3] M. V. Nezlin, JETP 19, 26-30 (1964).

is also not clear why the accelerating potential was not raised above 1100 V. It may be that the violent spontaneous interaction on which their experiment depended becomes weaker as the electron beam velocity is increased. If so, we hope that we may be able to overcome this by premodulating the electron beam current at the natural frequency of this weakened interaction so that the power coupled to the plasma ions would still be sufficient to beat them. The frequency required would be of the order of megacycles.

The experimental apparatus consists of a 30-cm-diam stainless steel high vacuum vessel ~ 2 m long. Axial field coils can be positioned to obtain a reasonably uniform axial magnetic field along the tube. The electron gun components are being installed. The first experiments will entail the study of the properties of the electron gun, with reference to current magnitude spatial extent, and beam divergence.

IV. "SLINGSHOT" ACCELERATOR*

A new type of plasma accelerator proposed by J. W. Mather and J. A. Phillips has been constructed which in principle should allow one to produce a relatively clean plasma and also eject this plasma into a magnetic confinement system. This accelerator consists of two concentric drive coils which produce in essence a quadrupolar magnetic field in the annular region between the inner and outer single turn coils and a second coil located adjacent to the drive coils at one end, the purpose of which is to generate a magnetic field that will unbalance the axial magnetic field and thus produce an axial thrust on the plasma. With this coil arrangement closed field lines will be obtained that encircle the two drive coils and the ejection coil to form a magnetic field "slingshot" configuration. The experimental arrangement encompasses three main parts, (1) the generation of a plasma ring discharge in the annulus similar to a toroidal pinch discharge, (2) the ejection of the plasma ring current by the field imbalance due to the ejection coil, and (3) the radial compression or focusing of the ejected plasma ring by shaping the outer drive coil. It is expected that the main attributes of this type of accelerator are (1) a cleaner plasma than that obtained from coaxial guns, (2) large axial velocities, and (3) higher plasma densities than can be obtained from theta pinch guns (conical or straight).

A small "slingshot" accelerator is now being studied which consists of a 12.5-cm inner and 27.5-cm outer diameter coil system with a length of 7.5 cm. A 45-μF, 20-kV capacitor bank produces peak currents of ~ 450 kA with a rise time of 3.0 μsec. Preliminary measurements show that (1) a magnetic field zero exists approximately centered in the annulus region between the drive coils before a plasma is generated and (2) with argon or helium gas filling, a plasma ring discharge is observed to collapse in

* This work was performed under the auspices of the U. S. Atomic Energy Commission.

radius to the equilibrium radius. From end-on integrated light photographs, the plasma ring appears centrally located and grossly stable. For helium pressures of $\sim$ 0.1 torr, the ring discharge is observed to exhibit irregularities which suggest a m = o (necking off) instability. At higher pressures, the plasma ring becomes more stable. Generally, the boundary of the ring discharge appears more stable on the inner side and less so on the outer periphery. Time dependent light photographs and magnetic field distributions will be obtained to determine if trapped magnetic fields are present. Trapped fields will inhibit the ejection of the plasma ring. The ejection coil will consist of a 17.5-cm diam single turn coil located at one end. The rise time of the ejection field will be $\sim$ 0.1-0.3 μsec.

V. PULSED FIELD CALCULATIONS*

In order to design an experiment like the caulked, stuffed cusp experiment (a nonzero absolute minimum field (NZAM) configuration) or the toroidal, caulked cusp experiment properly, it is necessary to determine the shape and dimensions of the apparatus, as well as electrical operating conditions, such that the desired magnetic field configuration is achieved within the experimental volume, and such that it is feasible to obtain and operate the apparatus. With the caulked, stuffed cusp experiment it is also required to provide an appropriate electric field for the $\vec{E} \times \vec{B}$ heating phase. The magnetic field in the caulked, stuffed cusp experiment consists of two parts: a component whose period is long compared with the time required for field to penetrate the metal walls of the apparatus plus a component whose period is shorter than the time required for much penetration. It is a useful approximation to consider the first component to be static and to consider the second component not to penetrate the walls of the apparatus at all. Likewise, it is useful to consider the magnetic field in the toroidal, caulked cusp experiment not to penetrate the walls of the apparatus at all. Computation of static magnetic fields presents no difficulty if the current sources are known. On the other hand, if the magnetic field does not penetrate the metal walls which bound the experimental volume, then eddy currents are induced in the walls and those eddy currents render computation of the magnetic field appreciably more difficult. In the two experiments being considered, there is nearly complete symmetry about an axis. In that case, computation of a magnetic field which does not penetrate the metal walls can be reduced to solving a boundary value problem for the so-called stream function $\psi = rA_\theta$, where r is distance from the axis of symmetry and A_θ is the azimuthal component of the vector potential; the other components of the vector potential are zero. The equation satisfied by ψ within the

* This work was performed under the auspices of the U. S. Atomic Energy Commission.

experimental volume is

$$\frac{\partial^2 \psi}{\partial r^2} + \frac{\partial^2 \psi}{\partial z^2} - \frac{1}{r}\frac{\partial \psi}{\partial r} = 0,$$

where z is distance along the axis of symmetry. The boundary conditions are that ψ assume constant values on the metal walls. This equation is very similar to the equation for the electrostatic scalar potential, φ, in such a geometry. That equation is

$$\frac{\partial^2 \varphi}{\partial r^2} + \frac{\partial^2 \varphi}{\partial z^2} + \frac{1}{r}\frac{\partial \varphi}{\partial r} = 0,$$

and the boundary conditions are that φ assume constant values of the metal boundaries. Thus, the fast vacuum magnetic fields in the two experiments, as well as the electric field for the $\vec{E} \times \vec{B}$ heating can be approximated by solving

$$\frac{\partial^2 f}{\partial r^2} + \frac{\partial^2 f}{\partial z^2} + c\,\frac{1}{r}\frac{\partial f}{\partial f} = 0,$$

where $f = \psi$ if $c = -1$, and $f = \varphi$ if $c = +1$.

The usual method of solving this equation is to approximate the equation by a difference equation which is then solved by standard relaxation techniques over a mesh of points. This procedure has been applied to the toroidal, caulked cusp geometry. However, there are two basic objections to this method which are related to the rather arbitrary shapes of boundaries being considered here and to the fact that the region over which the equation is to be solved is not simply-connected. The first objection is the very slow rate of convergence of the standard relaxation techniques when applied to these geometries, a fact which renders obtaining a solution very costly even with high speed computers. The second objection

to the usual difference approximation is the necessity of determining the extent to which the results obtained fail to satisfy the original differential equation. This difficulty is always present if a difference approximation is used, although it can be considerably reduced if irregular meshes can be introduced.

Two new approaches for obtaining numerical solutions of the differential equation have been devised. One of these is a method of solving the difference equation over a possible irregular mesh, which does not involve repeated iterations. This method shows promise of being an advantageous technique in using the difference approximation with complex boundaries.

The second new method of solving the differential equation does not involve a difference approximation. With this method, an exact analytic solution of the differential equation is obtained in the region of interest, and this exact solution is made to approximate the boundaries. This approach has the advantage that the results obtained always represent a physical situation -- because an exact solution of Maxwell's equations is achieved -- and that electric and magnetic fields can be obtained by exact differentiation of the potentials. Furthermore, it has been demonstrated by application to the caulked, stuffed cusp and toroidal, caulked cusp geometries that the boundaries can be satisfactorily approximated, and that the computing time involved for a given trial is short. It is necessary to use some intuition when applying this method. However, with experience, a small number of trials can suffice to obtain a satisfactory fit to the boundaries. A computer code is now available for determining contours of constant field intensity and $\int d\ell/B$ along field lines.